Investigation of genetic modifiers of *C9orf72* toxicity in *Drosophila* and iPSC neuron models

Ashling Giblin

A thesis submitted in partial fulfilment of the requirements for the degree of Doctor of Philosophy from University College London

Department of Genetics, Evolution and Environment
UCL

November 2023

Declaration

I, Ashling Giblin confirm that the work presented in this thesis is my own. Where information and data has been derived from collaborators and other sources, I confirm that this has been indicated in the thesis.

Acknowledgements

Firstly, thank you to my supervisors, Professor Dame Linda Partridge and Professor Adrian Isaacs, for giving me the opportunity to undertake a PhD in both of your labs. It has been a privilege to work with two outstanding scientists, whose enthusiasm, guidance, and support throughout this journey has been instrumental to my development as a researcher.

This research would not have been possible without the support of Clive and Mary, and Alzheimer's Research UK, I am deeply appreciative for your generosity.

My sincere gratitude to Teresa, Magda, Nathan, Alex H and Enric for being scientific role models, and for teaching me everything I know about *Drosophila*. Thank you for your valued friendship and for sharing your wisdom on science and life. Thank you, Rachel, for your patience and kindness in teaching me iPSC culture. Thank you to all members of the IHA for creating such a warm and welcoming environment in which to do science, and the Isaacs lab for a supportive and fun workplace.

Thanks to Alex C, who has been a scientific teammate for much of the journey. I am proud of what we have achieved by working together and I am excited to see what this research will develop into.

Special thanks to all the collaborators to this project, whose technical expertise, scientific insight, provision of samples and experimental contributions have been invaluable.

A huge thanks to Aoife, Ger, Mirjam, Sharifah, Eimear and Sinead for your wonderful friendship and support during this past four years.

I have been fortunate to have had excellent teachers along the way who inspired me to pursue my passion for science, particularly James. Thank you to the excellent lecturers of Biomedical Science, University of Galway, especially Eilis, Maura, David and Derek for encouraging me to dream big and pursue a PhD in neuroscience.

Thank you to my brother Darragh, and my parents, Nora and Padraig, who have been my biggest cheerleaders since day one. Growing up on a farm sparked my scientific curiosity, while my creativity originates from you, Mum. Your work ethic and sacrifices have been a huge motivation for me to get to where I am today.

Thank you, Martin, for constantly supporting me throughout the highs and lows of this journey. You're the reason I weathered the storms. I am incredibly lucky to have you by my side and I look forward to our next chapter.

Publications produced during the Ph.D. project

The publications listed below were published (or are in the process of publication) during the timeframe of this Ph.D. project, although the data from these publications may not be represented in this thesis.

- **Giblin, A.*,** Cammack, A.*, Mikheenko, A., Blomberg, N., Carcolé, M., Coneys, R., van der Kaant, Coyne, A., R., Giera, M., Partridge, L., Isaacs, A.M. Neuronal polyunsaturated fatty acids are protective in *C9orf72* ALS/FTD. *In preparation.*

- **Giblin, A.,** Isaacs, A.M., Partridge, L. Trpgamma over-expression rescues survival, motor and sleep deficits in *C9orf72* ALS/FTD *Drosophila*. *In preparation.*

- Milioto, C., Carcolé, M., **Giblin, A**., Coneys, R., Attrebi, O., Ahmed, M., Harris, S.S., Il Lee, B., Yang, M., Ellingford, R.A., Nirujogi, R.S., Biggs, D., Salomonsson, S., Zanovello. M., De Oliveira, P., Katona, E., Glaria, I., Mikheenko, A., Geary, B., Udine, E., Vaizoglu, D., Anoar, S., 3, Jotangiya, K., Crowley, G., Smeeth, D.M., Adams, M.L., Niccoli, T., Rademakers, R., van Blitterswijk, M., Devoy, A., Hong, S., Partridge, Linda., Coyne, A.N., Fratta, P., Alessi, D.R., Davies, B., Busche, M.A., Greensmith, L., Fisher, E.M.C., Isaacs, A.M. (2023). PolyGR and polyPR knock-in mice reveal a conserved neuroprotective extracellular matrix signature in *C9orf72* ALS/FTD neurons. *Accepted at Nature Neuroscience*.

- Xu, D., Vincent, A., González-Gutiérrez, A., Aleyakpo, B., Anoar, S., **Giblin, A.**, Atilano, M.A.., Adams, M., Shen, D., Thoeng, A., Tsintzas, E., Maeland, M., Isaacs, A.M., Sierralta, J., Niccoli, T. (2023) A monocarboxylate transporter rescues frontotemporal dementia and Alzheimer's disease models. *PLOS Genetics 19(9): e1010893.*

- Morón-Oset, J., Fischer, L.K.S., Carcolé, M., **Giblin, A**., Zhang, P., Isaacs, A.M., Grönke, S., Partridge, L. (2023). Protein tags affect toxicity of *C9orf72* DPRs. *Life Science Alliance, 6(9): e202201739.*

Abstract

A GGGGCC repeat expansion mutation in the *C9orf72* gene is the most common genetic cause of both ALS and FTD. However, the key downstream effector pathways mediating neuronal loss are still unclear. The aims of this thesis were to reveal novel insights into the pathogenesis of *C9orf72* ALS/FTD using $(G_4C_2)_{36}$ *Drosophila* models, to identify protective genes and pathways for further investigation.

First, I investigated the protective effects of *odd* and *bowl,* previously identified in a genetic overexpression screen for suppressors of $(G_4C_2)_{36}$ toxicity. Novel transgenic *Drosophila* expressing the human orthologs of *odd* and *bowl*, *OSR1* and *OSR2,* extended C9 fly survival when overexpressed in adult neurons. The extent of survival benefit varied between the genes tested; *odd* and *OSR2* produced greater survival extensions than *bowl* or *OSR1*, attributable to *odd* and *OSR2* decreasing DPR levels.

Next, I characterised *Trpγ*, as a modifier of C9 toxicity. *Trpγ* was upregulated at an early timepoint in C9 flies. Furthermore, *Trpγ* orthologs *TRPC4* and *TRPC5*, were upregulated in patient-derived iPS motor neurons, while *TRPC4* was downregulated in C9ALS post-mortem cortical neurons. Overexpression of *Trpγ* improved multiple neurodegenerative phenotypes in C9 flies, in part by reducing levels of toxic poly(GR), suggesting that early upregulation of *Trpγ* is a protective response.

Lastly, I performed RNA sequencing on C9 fly heads at a pre-degeneration timepoint to identify early dysregulated pathways and found downregulation of fatty acid synthesis and desaturation pathway genes. Remarkably, this signature was conserved in a transcriptomic dataset of human ALS spinal cord. Lipidomic analyses of C9ALS/FTD iPSC-neurons and FTD post-mortem brains revealed a striking loss of highly unsaturated phospholipids. Desaturase overexpression was

sufficient to extend survival in C9 flies and protect against excitotoxicity in C9 iPSC-derived motor neurons, implicating altered neuronal phospholipid saturation as a novel pathway in C9ALS/FTD pathogenesis.

Impact statement

Amyotrophic lateral sclerosis (ALS) and frontotemporal dementia (FTD) are two devastating neurodegenerative diseases, for which there are currently no effective disease modifying treatments. ALS affects the upper and lower motor neurons, leading to motor impairments and eventual paralysis, while FTD affects the frontal and temporal lobes of the brain impacting behaviour and language. The lifetime risk of ALS is 1 in 350 for males, and 1 in 400 for females, with an average age of onset of 64 years and average survival after symptom onset of 30 months. FTD is the second most common form of early-onset dementia, with a disease duration of approximately 8 years. These diseases present a substantial burden to affected individuals and their caregivers, as well as substantial socioeconomic costs. Therefore, there is an urgent need for therapeutics that effectively delay disease progression and provide a greater quality of life to patients.

In 2011, a repeat expansion of GGGGCC in the first intron of the *C9orf72* gene was discovered to be the most common genetic cause of both ALS and FTD. The repeat DNA undergoes bidirectional transcription to produce sense and antisense repeat RNA, which can undergo repeat associated non-AUG (RAN) translation, to produce five different dipeptide repeat proteins, of which poly(PR) and poly(GR) have been experimentally shown to be the most toxic. Significant progress has been made in understanding the mechanisms of toxicity associated with the *C9orf72* mutation. However, the key downstream effector pathways mediating neuronal loss are still unclear. This work aimed to utilise *Drosophila* models of C9ALS/FTD to reveal novel protective pathways for further validation in patient cells and tissues, thus enabling the development of much needed therapies for these devastating diseases.

Trpγ, a gene that encodes a TRPC ion channel was identified as a genetic modifier of toxicity in a *Drosophila* model of C9ALS/FTD, extending survival and ameliorating motor impairments by decreasing toxic poly(GR) levels, when expressed in neurons. *Trpγ,* and its human homologs *TRPC4* and *TRPC5* were

found to be transcriptionally dysregulated in C9 *Drosophila*, patient iPSC neurons and post-mortem brains. Riluzole, the first approved drug for ALS, can activate TRPC5 channels, and therefore further experiments investigating the potential of TRPC4 and TRPC5 expression and activity, to modify *C9orf72* repeat toxicity in mammalian models are warranted.

In this work, unbiased transcriptomic analysis identified genes belonging to the fatty acid synthesis and desaturation pathway as downregulated in a *Drosophila* model of C9ALS/FTD, and in human post-mortem ALS spinal cord. Furthermore, a pronounced loss of specific polyunsaturated fatty acids (PUFAs) from phospholipids was found in C9ALS/FTD iPSC neurons and FTD frontal cortex tissue. Neuronal overexpression of desaturation genes could prevent C9-associated neurodegeneration in *Drosophila and* protect against excitotoxicity in C9 iPSC-derived motor neurons. Multiple studies have previously implicated altered lipid metabolism, particularly involving PUFAs in ALS and FTD. However, until this study, it was yet to be determined if PUFA-containing lipids were altered in ALS/FTD neurons and whether this contributes directly to neuronal loss. The results presented here are the first to directly implicate neuronal PUFA metabolism in C9ALS/FTD pathogenesis and suggest that modulating neuronal PUFA metabolism is a potent approach for ameliorating C9-associated neurodegeneration.

Additionally, similar transcriptomic and lipidomic profiles were observed between non-C9ALS and C9ALS, and non-C9FTD and C9FTD respectively; suggesting that phospholipid PUFA dysregulation may be a converging pathway among *C9orf72* and non-*C9orf72* ALS and FTD, expanding the potential utility of our findings. This opens up further research avenues to explore neuronal PUFA metabolism in non-C9 ALS and FTD, and to test whether modulating neuronal PUFA metabolism may also prevent neurodegeneration in sporadic ALS and other genetic forms of ALS and FTD.

The data from this study has formed the basis for two successful grant applications to further investigate the mechanisms underlying PUFA

dysregulation and the mechanisms by which desaturases rescue neurodegeneration.

Table of Contents

List of Figures

List of tables

Abbreviations

AA	Arachidonic acid
aa	Amino acid
ACC	Acetyl-CoA carboxylase
AcCoAS	Acetyl-Coenzyme A synthetase
ADIPOR2	Adiponectin receptor 2
ALA	Alpha-linolenic acid
ALS	Amyotrophic lateral sclerosis
ANG	Angiogenin
ANOVA	Analysis of variance
ASO	Antisense oligonucleotide
bp	Base pair
BSA	Bovine serum albumin
C9	C9orf72
C9orf72	Chromosome 9 open reading frame 72
C9ALS	*C9orf72* mutation-associated ALS
C9FTD	*C9orf72* mutation-associated FTD
C9ALS/FTD	*C9orf72* mutation-associated ALS and/or FTD
CNS	Central nervous system
COX	Cyclooxygenase
CSF	Cerebrospinal fluid
daGS	Daughterless-gene-switch
Desat1	Desaturase 1
DIV	Days in vitro
DG	Diglyceride, or diacylglycerol
DHA	Docosahexaenoic acid
DMEM	Dulbecco's modified eagle medium
DMSO	Dimethyl sulfoxide
DPR	Dipeptide repeat protein
DTT	Dithiothreitol
ECL	Electrochemiluminescence
EDTA	Ethylenediaminetetraacetic acid

elavGS	Elav-gene-switch
ER	Endoplasmic reticulum
FA	Fatty acid
FASN	Fatty acid synthase
FAT-1	Omega-3 fatty acid desaturase fat-1
FAT-2	Delta(12) fatty acid desaturase fat-2
FDR	False discovery rate
FTD	Frontotemporal dementia
FTLD	Frontotemporal lobar degeneration
FUS	Fused in Sarcoma/Translocated in Sarcoma
GFP	Green fluorescent protein
GMR	Glass multiple reporter
GO	Gene ontology
GRN	Progranulin
GWAS	Genome wide association study
HPLC	High performance liquid chromatography
HRP	Horseradish peroxidase
iPSC	Induced pluripotent stem cell
iPSN	Induced pluripotent stem cell-derived neuron
KIF5A	Kinesin family member 5A
LB	Lysogeny broth
LC-MS/MS	Liquid chromatography tandem-mass spectrometry
LOX	Lipoxygenase
LV	Lentivirus
MAPT	Microtubule associated protein tau
MN	Motor neuron
MSD	Meso scale discovery
NEK-1	NIMA Related Kinase 1
NFV-PPA	Non-fluent variant of primary progressive aphasia
OPTN	Optineurin
PBS	Phosphate buffered saline
PCR	Polymerase chain reaction
PI	Propidium iodide

Poly(AP)	poly-alanine-proline
Poly(GA)	poly-glycine-alanine
Poly(GP)	poly-glycine-proline
Poly(GR)	poly-glycine-arginine
Poly(PR)	poly-proline-arginine
PPARγ	Peroxisome proliferator-activated receptor gamma
PUFA	Polyunsaturated fatty acid
PVDF	Polyvinylidene fluoride
p62	p62 protein (SQSTM1 gene product)
RAN	Repeat-associated non-ATG initiated
RBP	RNA binding protein
RIPA buffer	Radioimmunoprecipitation assay buffer
RO	RNA-only
ROCK	Rho-associated protein kinase
RT-qPCR	Reverse Transcription-quantitative Polymerase Chain Reaction
RU	RU486, Mifepristone
RU486	Mifepristone
SCD	Stearoyl-CoA Desaturase
S.D.	Standard deviation
SDS	Sodium dodecyl sulphate
SNP	Single nucleotide polymorphism
SOD1	Superoxide Dismutase 1
SODA	Simple Omics Data Analysi
SREBP1	Sterol regulatory element-binding protein 1
SV-PPA	Semantic variant of primary progressive aphasia
SYA	Sugar-yeast-agar *Drosophila* medium
TARDBP	TDP-43
TBK1	TANK-binding kinase 1
TBS	Tris buffered saline
TDP-43	TAR DNA-binding protein 43 (TARDBP gene product)
TG	Triglyceride, or triacylglycerol

TRPC	Transient receptor potential cation channel, subfamily C
UAS	Upstream activation sequence
UPS	Ubiquitin proteasome system
UTR	Untranslated region
VCP	Valosin-containing protein

Chapter 1. Introduction

1.1 Introduction to ALS and FTD

Amyotrophic lateral sclerosis (ALS) is a rapidly progressive neurodegenerative disorder that affects the upper and lower motor neurons, resulting in voluntary muscle denervation (Mead *et al.*, 2023). Clinical presentation is varied, with approximately 75% of patients presenting with limb-onset, with muscle weakness, spasticity, fasciculations and wasting; while bulbar-onset is seen in 25% of patients, characterised by spastic dysarthria, tongue wasting and difficulty speaking (Kiernan *et al.*, 2011). The lifetime risk of ALS is 1 in 350 for males and 1 in 400 for females (Ryan *et al.*, 2019), with a mean age of onset of 58-63 years (Kiernan *et al.*, 2011). The average survival after symptom onset is 30 months, with patients invariably succumbing to neuromuscular respiratory failure (Masrori and Van Damme, 2020; Westeneng *et al.*, 2018).

Frontotemporal dementia (FTD) is the second most common form of early-onset dementia (Young *et al.*, 2017). FTD is a progressive neurodegenerative disorder that affects the frontal and temporal cortex and can be divided into three major subtypes. Firstly, behavioural variant frontotemporal dementia which is characterised by disinhibition, apathy, lack of empathy and stereotyped behaviours. Semantic variant of primary progressive aphasia (SV-PPA) presents with impaired individual word comprehension (anomia) but retained grammar and fluency of speech as well as issues with object recognition. Non-fluent variant of primary progressive aphasia (NFV-PPA) is characterised by laboured agrammatical and halting speech (Boeve *et al.*, 2022). FTD has a prevalence of 3-26 per 100,000 in the UK population, with disease onset typically between 45 to 64 years of age, and a disease duration of approximately 8 years (Bang, Spina and Miller, 2015).

1.1.2 ALS and FTD are part of the same disease spectrum

It is now well established that ALS and FTD represent two ends of a neurodegenerative disease continuum, with overlapping clinical, pathological and genetic features (Strong *et al.*, 2017; Ling, Polymenidou and Cleveland, 2013; van Langenhove, van der Zee and van Broeckhoven, 2012).

1.1.2.1 Clinical overlap of ALS and FTD

Approximately 40-50% of ALS patients have cognitive impairment, with 15% meeting diagnostic criteria for FTD (Phukan *et al.*, 2012; Ringholz *et al.*, 2005). Similarly, 15% of FTD patients meet the criteria for an ALS diagnosis (Lomen-Hoerth, Anderson and Miller, 2002).

1.1.2.2 Pathological overlap of ALS and FTD

Pathologically, ALS and FTD are related by the fact that they share pathological proteinaceous inclusions. Ubiquitinated inclusions of phosphorylated TDP-43, are found in the neurons of 97% of ALS and 45% of FTD cases (Arai *et al.*, 2006; Neumann *et al.*, 2006). Furthermore, fused in sarcoma (FUS) neuronal cytoplasmic and intranuclear inclusions are found in approximately 10% of FTD patients and 1% of ALS patients (Urwin *et al.*, 2010; Vance *et al.*, 2009; Kwiatkowski *et al.*, 2009; Neumann *et al.*, 2009). Additionally, tau inclusions are found in 45% of FTD patients, but not ALS while SOD1 inclusions are found in 2% of ALS cases but not FTD cases (Ling, Polymenidou and Cleveland, 2013) (Figure 1.1).

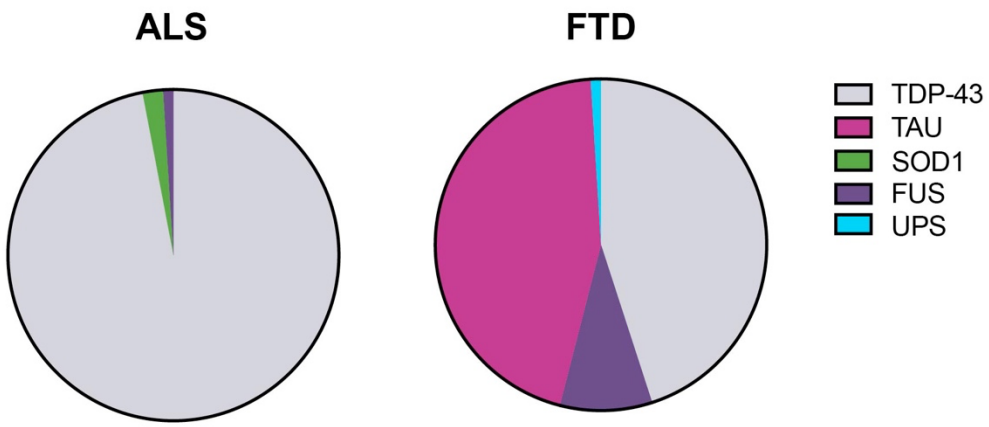

Figure 1.1 Pathological protein inclusions in ALS and FTD.
In ALS, the major protein inclusions are TDP-43, present in 97%, SOD1 in 2% and FUS in less than 1% of cases. In FTD, TDP-43 and TAU are each found in 45% of cases, FUS in 9% and ubiquitin-proteasome system (UPS) related inclusions found in 1%. Figure adapted from (Ling, Polymenidou and Cleveland, 2013) and produced using GraphPad Prism and Adobe Illustrator.

1.1.2.3 Genetic overlap of ALS and FTD

10% of ALS cases are familial, with 90% thought to be sporadic. Among familial ALS cases, mutations in superoxide dismutase 1 (*SOD1*) were the first described, and account for 20% of cases (Rosen *et al.*, 1993). Other mutations that cause familial ALS include those in NIMA Related Kinase 1 (*NEK1*), kinesin family member 5A (*KIF5A*), and optineurin (*OPTN*) (Nicolas *et al.*, 2018; Brenner *et al.*, 2016; Maruyama *et al.*, 2010). Up to half of FTD cases have a genetic component, with mutations in microtubule-associated protein tau (*MAPT*) and progranulin (*GRN*) each responsible for approximately 20% of inherited FTD cases (van Langenhove, van der Zee and van Broeckhoven, 2012; Baker *et al.*, 2006; Cruts *et al.*, 2006; Hutton *et al.*, 1998). Additionally mutations in *CHMP2B* are a rare cause of FTD (Skibinski *et al.*, 2005). Mutations in *FUS* and *TDP-43* can lead to both ALS and FTD (Lagier-Tourenne, Polymenidou and Cleveland, 2010; Mackenzie, Rademakers and Neumann, 2010; Kwiatkowski *et al.*, 2009; Vance *et al.*, 2009; Sreedharan *et al.*, 2008; Kabashi *et al.*, 2008; Van Deerlin *et al.*, 2008). Additionally, mutations in *C9orf72* (see below), valosin-containing protein (*VCP*) (Johnson *et al.*, 2010; Watts *et al.*, 2007), ubiquilin-2 (*UBQLN2*) (Deng *et al.*, 2011), TANK-binding kinase 1 (*TBK1*) (Freischmidt *et al.*, 2015;

Gijselinck *et al.*, 2015) or p62/sequestosome (*SQSTM1*) (Rubino *et al.*, 2012) can cause either ALS or FTD (Figure 1.2).

These disease-causing mutations are tolerated for decades before patients present with symptoms, suggesting that ageing and resulting loss of cellular homeostasis lowers the threshold of tolerance to these toxic mutations.

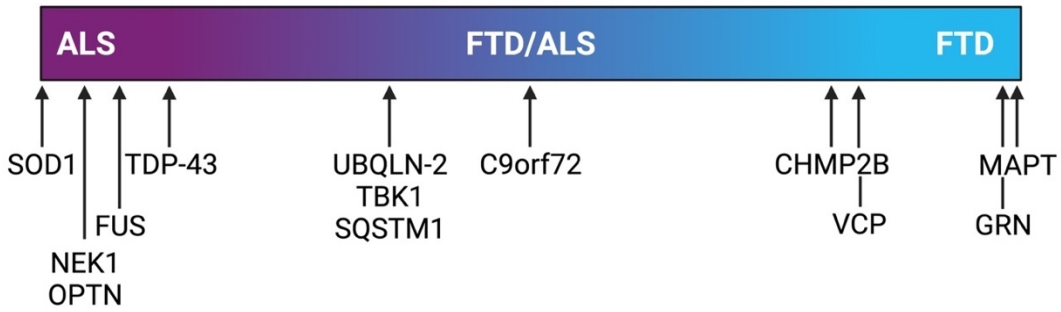

Figure 1.2 Diagram highlighting some of the major genetic mutations causing either ALS, FTD or both ALS and FTD.
Figure adapted from (Ling, Polymenidou and Cleveland, 2013) and produced using BioRender.

1.2 *C9orf72* ALS and FTD

In 2011, it was discovered that a hexanucleotide repeat expansion of GGGGCC in the chromosome 9, open reading frame 72 (*C9orf72*) gene is the most common genetic cause of both ALS and FTD in European and North American populations (Woollacott and Mead, 2014; Majounie *et al.*, 2012; DeJesus-Hernandez *et al.*, 2011; Renton *et al.*, 2011). Typically, patients can carry hundreds to thousands of these repeats, with an arbitrary pathological threshold of 30 repeats used in studies (Suh *et al.*, 2015; van Blitterswijk *et al.*, 2013). Somatic instability and mosaicism of this mutation occurs, with longer repeats found in the CNS versus blood, and different repeat lengths in different brain regions (Gijselinck *et al.*, 2016; Nordin *et al.*, 2015; Fratta *et al.*, 2015; Beck *et al.*, 2013). *C9orf72* has three main transcript variants, with the mutation located in the first intron of variants 1 and 3 and in the promoter region of variant 2. Variant 1 produces a short 222 amino acid C9ORF72 protein, while variants 2 and 3 produce a longer C9ORF72

protein of 481 amino acids (Figure 1.3) (Balendra and Isaacs, 2018; Todd and Petrucelli, 2016).

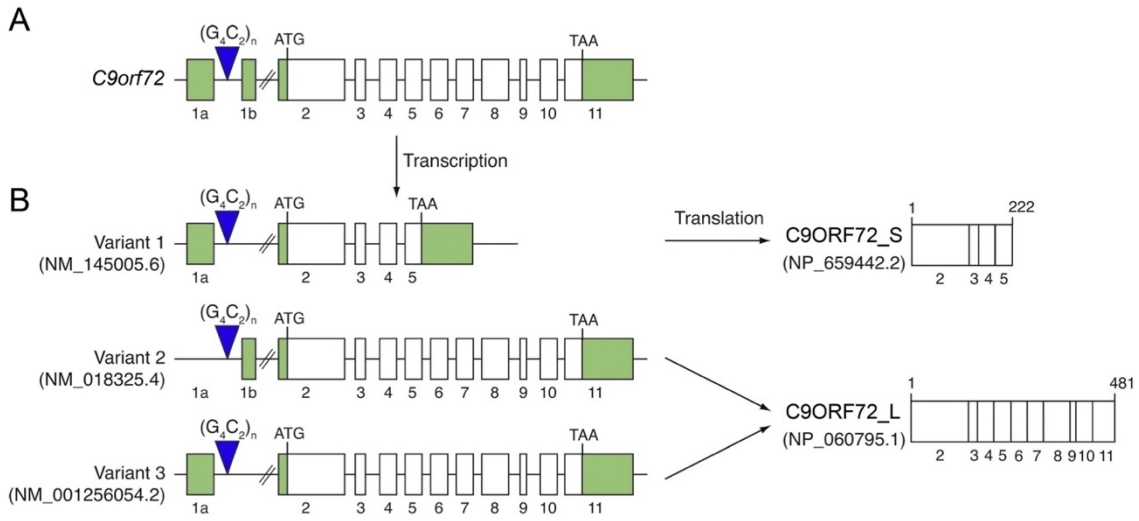

Figure 1.3 *C9orf72* gene structure and location of hexanucleotide repeat expansions.
A. *C9orf72* gene structure (note: length of introns not to scale). The GGGGCC repeat expansion is indicated by the blue arrow. B. *C9orf72* has three pre-mRNA transcript variants. The G_4C_2 repeats are located within the first intron of variants 1 and 3, and within the promoter region of variant 2. Variants 2 and 3 encode the long (481 amino acid) protein isoform C9ORF72-L, containing the coding sequence from exons 2-11, whereas variant 1 produces the short (222 amino acid) isoform C9ORF72-S containing coding sequence from exons 2-5. Coding regions are shown in white, while non-coding regions are shown in green. NCBI transcript and protein accession numbers are shown. Figure adapted from (Todd and Petrucelli, 2016).

1.2.1 Proposed mechanisms of toxicity in *C9orf72* ALS/FTD

There are three proposed non-mutually exclusive mechanisms of toxicity associated with the *C9orf72* mutation, which may act synergistically (Zhu *et al.*, 2020) (Figure 1.4). These include toxic gain of function from the transcribed sense and antisense RNA, toxic gain of function from the translated dipeptide-repeat proteins and loss of function of C9ORF72 protein (Figure 1.4).

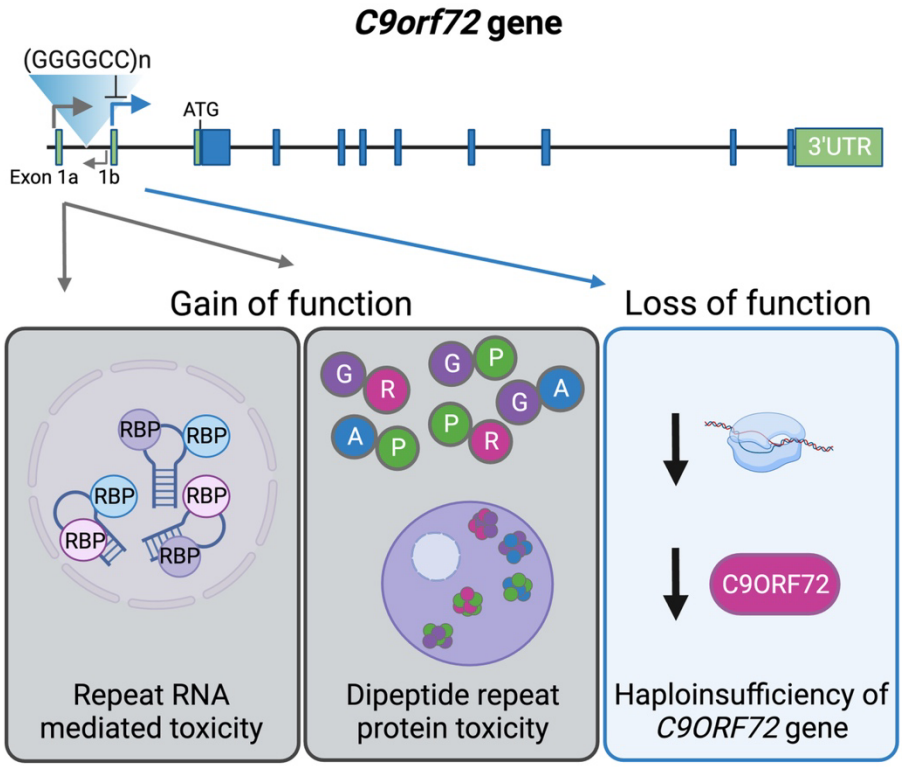

Figure 1.4 Proposed mechanisms of toxicity of *C9orf72* hexanucleotide repeat expansion.
Gain of function mechanisms include repeat RNA mediated toxicity and dipeptide repeat protein toxicity, loss of function toxicity may occur though haploinsufficiency of the C9ORF72 protein. Figure adapted from (Ling, Polymenidou and Cleveland, 2013) and produced using BioRender.

1.2.1.1 *C9orf72* haploinsufficiency

As previously mentioned, *C9orf72* has three transcript variants (Figure 1.3). Variant 2 is normally expressed at higher levels than variants 1 or 3 in the CNS (Rizzu *et al.*, 2016; Tran *et al.*, 2015). The expanded repeats are in the promoter region of variant 2, and therefore can decrease expression of this variant (Balendra and Isaacs, 2018; Rizzu *et al.*, 2016; Tran *et al.*, 2015). Transcript variants 1 and 3 harbour the repeat expansion in intron 1, which is retained in the mature RNA that can form RNA foci and be RAN translated to produce DPRs. Sense and antisense transcripts containing intron 1 are increased in C9ALS/FTD brains (Zu *et al.*, 2013; Mori *et al.*, 2013), while reduced levels of mature, spliced *C9orf72* mRNA are reported in *C9orf72* patient brain, spinal cord, blood lymphocytes and iPSC-derived neurons (Tran *et al.*, 2015; Waite *et al.*, 2014;

Belzil *et al.*, 2013; Donnelly *et al.*, 2013; DeJesus-Hernandez *et al.*, 2011; Renton *et al.*, 2011). Reduced C9ORF72 protein levels have been reported in frontal cortex (Xiao *et al.*, 2015; Waite *et al.*, 2014) and cerebellum (Frick *et al.*, 2018). Of note, increased levels of transcript variant 1 in the frontal cortex and cerebellum associated with increased survival, therefore loss of function may contribute to disease pathogenesis (van Blitterswijk *et al.*, 2013).

C9ORF72 is homologous and structurally related to the DENN (Differentially expressed in normal and neoplasmic cells) guanine nucleotide exchange factors proteins, which activate Rab proteins, important for vesicular trafficking (Levine *et al.*, 2013). The C9ORF72-L isoform has a role in autophagy induction (Sellier *et al.*, 2016; Gijselinck *et al.*, 2012), while patient iPSC derived neurons have basal autophagy impairments and a heightened sensitivity to autophagy blockade (Aoki *et al.*, 2017; Webster *et al.*, 2016; Almeida *et al.*, 2013). C9ORF72 localises to lysosomes and plays a role in endolysosomal trafficking (Amick, Roczniak-Ferguson and Ferguson, 2016; Farg *et al.*, 2014). *C9orf72* conditional knockout, *C9orf72* heterozygous mice and transient loss of function mouse models fail to recapitulate motor or behavioural phenotypes or neurodegeneration seen in human ALS/FTD. Only *C9orf72* homozygous mutant mice show behavioural and survival phenotypes related to immune cell dysfunction but do not display neurodegeneration (Atanasio *et al.*, 2016; Burberry *et al.*, 2016; O'Rourke *et al.*, 2016). *C9orf72* loss of function is not sufficient to drive toxicity but haploinsufficiency likely acts synergistically, with gain of function mechanisms to exacerbate toxicity (Zhu *et al.*, 2020).

1.2.1.2 RNA-mediated toxicity

The GGGGCC repeat DNA undergoes bidirectional transcription to produce sense and antisense repeat RNA that can form sense and antisense RNA aggregates or foci (Mizielinska *et al.*, 2013; Gendron *et al.*, 2013). The guanine-rich GGGGCC sequence can form stable DNA and RNA G-quadruplex secondary structures as well as RNA-DNA hybrid (R-loop) or hairpin structures (Haeusler *et al.*, 2014; Fratta *et al.*, 2012). These RNA foci are capable of binding and sequestering RNA binding proteins, which could lead to neurotoxicity (Cooper-

Knock *et al.*, 2014; Lee *et al.*, 2013; Wojciechowska and Krzyzosiak, 2011). Intranuclear RNA foci are found in various human brain regions and spinal cord and in patient-derived cells (DeJesus-Hernandez *et al.*, 2017; Lagier-Tourenne *et al.*, 2013; Mizielinska *et al.*, 2013; DeJesus-Hernandez *et al.*, 2011). Colocalisation of sense and antisense RNA foci with the RNA binding proteins SRSF2, hnRNP A1, hnRNP F, ALYREF has been demonstrated in Purkinje neurons of the cerebellum of *C9orf72* ALS cases, with direct interaction confirmed by UV crosslinking assays (Cooper-Knock *et al.*, 2015). In that study, only antisense RNA foci correlated with TDP-43 mislocalisation in *C9orf72* ALS patient motor neurons (Cooper-Knock *et al.*, 2015), a finding that has recently been corroborated (Aladesuyi Arogundade *et al.*, 2019). A more recent study using BaseScope reported a correlation of sense RNA foci with TDP-43 aggregation in spinal motor neurons but not in motor cortex neurons or glia (Mehta *et al.*, 2020). Repeat RNA has been shown to affect the nuclear pore, initiating a POM121-mediated reduction in nucleoporins, and neuronal cell death (Coyne *et al.*, 2020).

1.2.1.3 DPR-mediated toxicity

The GGGGCC repeat expansion RNA can undergo an unconventional form of translation, called repeat associated non-AUG (RAN) translation, which is thought to be dependent on RNA secondary structure (Zu *et al.*, 2011). RAN translation also occurs in other repeat expansion neurological disorders including fragile X-associated tremor ataxia syndrome, myotonic dystrophy type 2, spinocerebellar ataxia, Fuchs endothelial corneal dystrophy and Huntington disease (Cleary, Pattamatta and Ranum, 2018). Expanded RNA in *C9orf72* ALS/FTD, is RAN translated in all three reading frames to produce dipeptide repeat proteins (Ash *et al.*, 2013). RAN translated DPRs produced from the sense strand include poly-glycine arginine (poly(GR)), poly-glycine proline (poly(GP)) and poly-glycine alanine (poly(GA)), while DPRs produced from the antisense strand include poly-glycine proline (poly(GP)), poly-proline arginine (poly(PR)) and poly-proline alanine (poly(PA)) (Figure 1.5) (Ash *et al.*, 2013; Mori *et al.*, 2013; Gendron *et al.*, 2013; Zu *et al.*, 2013). DPR abundance is highest in cortical, hippocampal, and cerebellar regions (Saberi *et al.*, 2018; Mackenzie *et al.*, 2015;

Schludi *et al.*, 2015; Mackenzie *et al.*, 2013; Zu *et al.*, 2013; Ash *et al.*, 2013; Mann *et al.*, 2013). DPRs are mostly found as perinuclear cytoplasmic aggregates, and occasionally as dendritic aggregates, while poly(GP) and poly(GA) also show diffuse cytoplasmic staining, whereas poly(PR) and poly(PA) are rarely detected in post-mortem brain tissue (Saberi *et al.*, 2018). Only poly(GR) has been shown to co-localise with phosphorylated TDP-43 (Saberi *et al.*, 2018). The above studies relied on immunohistochemical methods to detect insoluble DPR aggregates, however, soluble and insoluble DPRs can be detected by MSD immunoassays, with poly(GA) found to be more insoluble while poly(GP) is mostly soluble (Quaegebeur *et al.*, 2020; Gendron *et al.*, 2015). Soluble DPRs are less abundant in clinically affected brain regions, most abundant in the clinically unaffected cerebellum, and poly(GR) and poly(GP) solubility correlates with disease severity (Quaegebeur *et al.*, 2020). Overall, there is a lack of clear spatial correlation of DPR inclusions with neurodegeneration in post-mortem brain tissue.

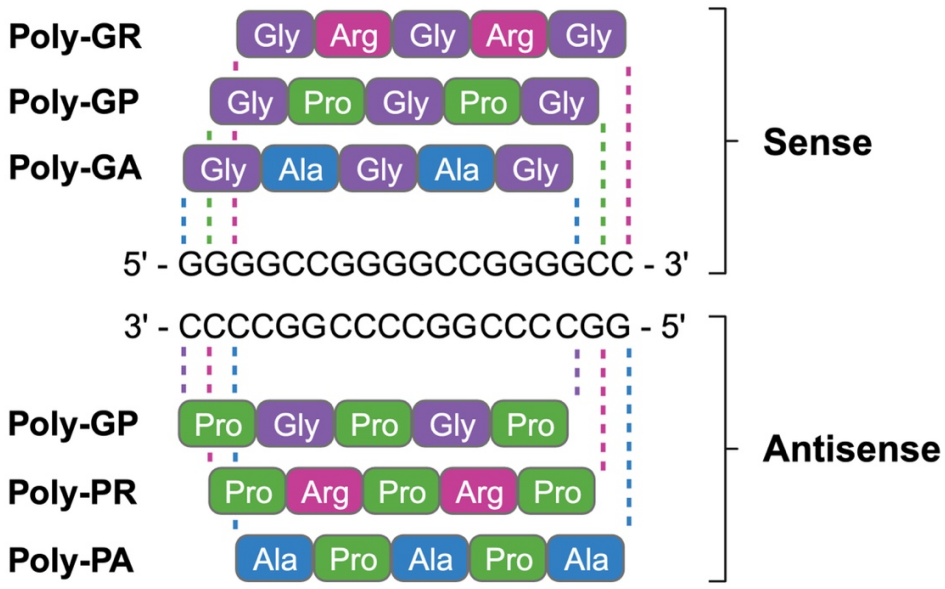

Figure 1.5 Dipeptide repeat proteins produced from the GGGGCC sequence by RAN translation.
RAN translation of the GGGGCC expanded repeats occurs in all three reading frames to produce dipeptide repeat proteins (DPRs). DPRs produced from the sense strand include poly-glycine arginine (poly(GR)), poly-glycine proline (poly(GP)) and poly-glycine alanine (poly(GA)), while DPRs produced from the

antisense strand include poly-glycine proline (poly(GP)), poly-proline arginine (poly(PR)) and poly-proline alanine (poly(PA)). Figure adapted from (Balendra and Isaacs, 2018) and produced using BioRender.

Drosophila do not possess a *C9orf72* ortholog, and therefore have proven useful for dissecting the relative toxic contributions of gain of function mechanisms, independent of *C9orf72* haploinsufficiency. DPRs rather than repeat RNA have been shown to cause neurotoxicity in *Drosophila* models (Moens *et al.*, 2018; Mizielinska *et al.*, 2014). Overexpression of 36 GGGGCC repeats in *Drosophila* eyes or adult neurons led to neurodegeneration (Mizielinska *et al.*, 2014). However, blocking translation of the repeats into DPRs, by interrupting the sequence with stop codons in each reading frame, prevented neurodegeneration, demonstrating that it is the production of DPRs that causes toxicity in this model (Mizielinska *et al.*, 2014) (Figure 1.6). Also, by exploiting codon-degeneracy, Mizielinska et al. generated protein-only models, individually expressing the five DPRs in an ATG-dependent manner, via non-GGGGCC RNA sequences and concluded that the basic glycine-arginine (GR) and proline-arginine (PR) DPRs are primarily responsible for toxicity, with glycine-alanine yielding a mild, length dependent toxic phenotype (Mizielinska *et al.*, 2014) (Figure 1.7). *Drosophila* neuronally expressing sense or antisense RNA, but not DPRs, at similar lengths to those found in patients, do not develop neurodegeneration, despite the production of RNA foci and RNA binding protein sequestration (Moens *et al.*, 2018). Additionally, a *Drosophila* model ubiquitously overexpressing 160 intronic GGGGCC repeats, in which the G_4C_2 sequence was spliced out to form RNA foci but not DPRs also showed no evidence of neurodegeneration (Tran *et al.*, 2015). DPRs have been shown to be neurotoxic in multiple disease models despite the fact that DPRs do not correlate well with neurodegeneration in ALS/FTD post-mortem brains (Moens, Partridge and Isaacs, 2017).

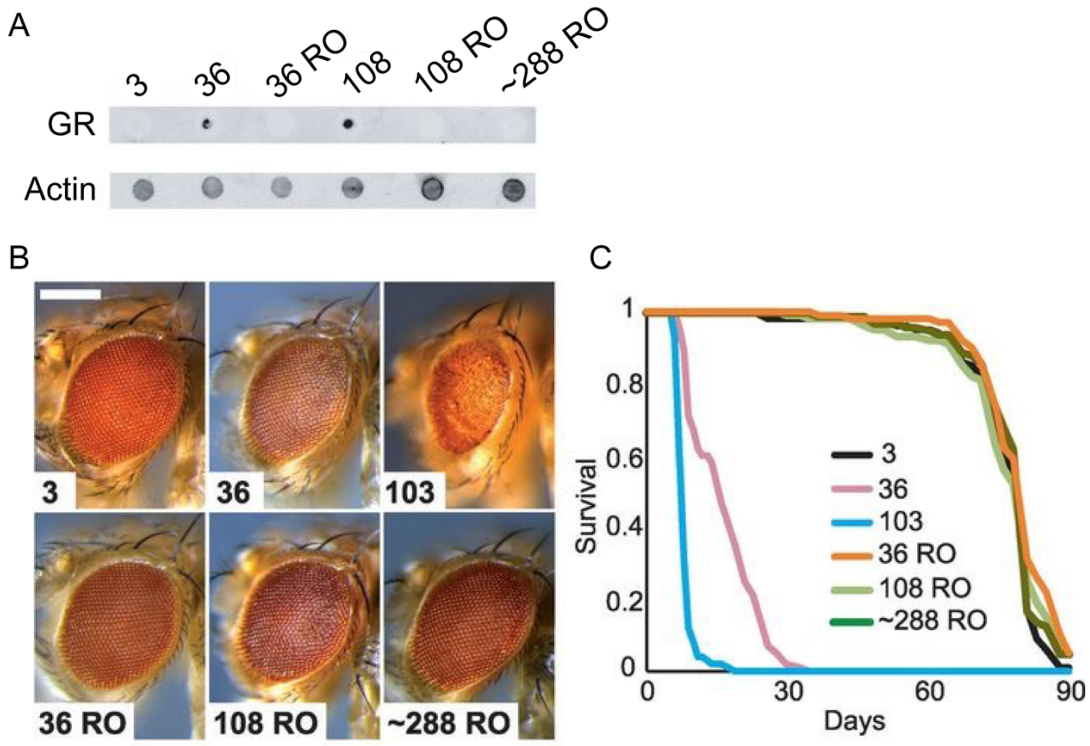

Figure 1.6 GGGGCC expanded repeats promote neurodegeneration through dipeptide repeat proteins.
A. Dot blot confirming the production of poly(GR) by both $(G_4C_2)_{36}$ and $(G_4C_2)_{103}$ pure repeat flies, but not by $(G_4C_2)_3$ flies or RNA-only (RO) flies. B. Eye toxicity was observed with $(G_4C_2)_{36}$ and $(G_4C_2)_{103}$ pure repeats, while $(G_4C_2)_3$ pure repeats and 36, 108 or 288 RO repeats had no effect. C. Expression of $(G_4C_2)_{36}$ and $(G_4C_2)_{103}$ in adult neurons reduced survival, while $(G_4C_2)_3$ and RO repeats had no effect. Figure adapted from (Mizielinska *et al.*, 2014).

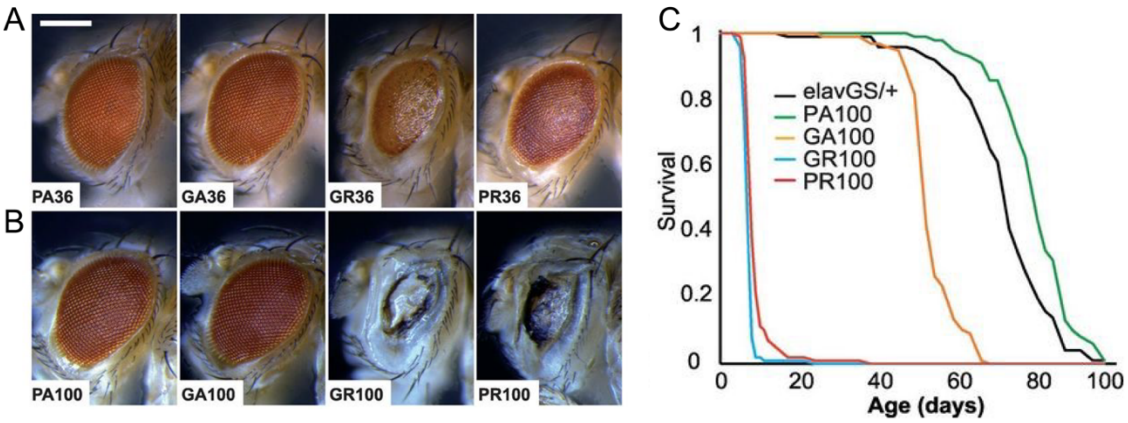

Figure 1.7. Arginine-containing DPRs are most toxic in *Drosophila*.
A. Expressing $(GR)_{36}$ or $(PR)_{36}$ in *Drosophila* eyes lead to a rough eye phenotype. B. There is a length-dependent toxicity of poly(GR) and poly(PR) on the rough eye phenotype, with $(GR)_{100}$ and $(PR)_{100}$ more toxic than $(GR)_{36}$ and $(PR)_{36}$. C. Expression of $(GR)_{100}$ and $(PR)_{100}$ in adult neurons dramatically reduced survival,

while $(GA)_{100}$ produced a late-onset survival deficit. Neuronal expression of $(PA)_{100}$ or elavGS driver alone had no effect on survival. Figure adapted from (Mizielinska *et al.*, 2014).

1.2.1.4 Pathways implicated in C9ALS/FTD

Many cellular processes have been associated with toxicity downstream of *C9orf72* expansions. Cell autonomous pathways include defective RNA processing, translation inhibition, DNA damage, autophagy and lysosomal dysfunction, impaired ubiquitin proteasome system, altered liquid-liquid phase separation, endoplasmic reticulum stress, nucleocytoplasmic transport dysfunction, impaired axonal and vesicular transport, mitochondrial dysfunction, hyper and hypoexcitability, glutamate excitotoxicity, neuronal branching defects and altered growth cone dynamics (Figure 1.6) (Balendra and Isaacs, 2018). Non-neuronal cells of the CNS, including microglia, astrocytes and oligodendrocytes, have also been implicated in ALS/FTD, with both protective and toxic involvement, particularly in relation to neuroinflammation (Vahsen *et al.*, 2021; Guttenplan *et al.*, 2020; Balendra and Isaacs, 2018). Despite the large number of cellular pathways implicated in C9ALS/FTD, the molecular mechanisms driving neuronal loss are unclear. Dissecting the causative versus consequential and correlative pathways in this cascade, in a temporal manner will be crucial to intervene in this downstream neurodegeneration.

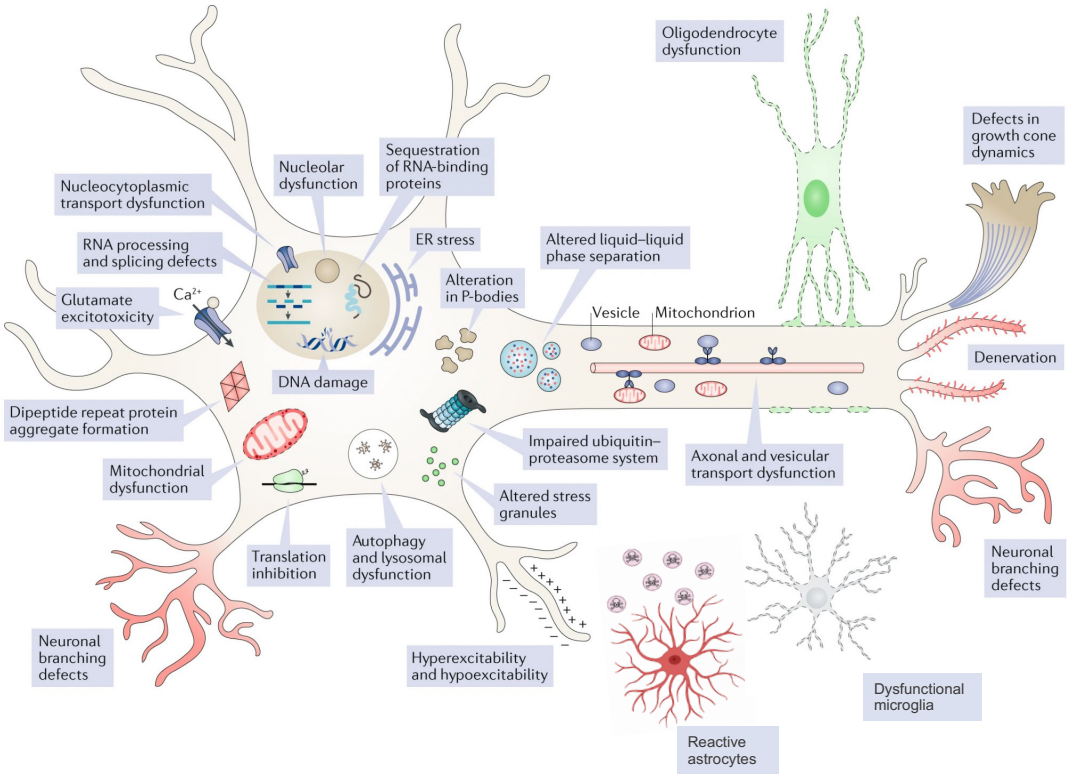

Figure 1.8. Cellular pathways implicated in C9ALS/FTD.
Figure adapted from (Balendra and Isaacs, 2018).

1.3 *Drosophila* as a model for neurodegenerative disease

Drosophila are a useful model for biological research given their short lifespan, low maintenance costs, ability to generate large populations and their genetic tractability (Piper and Partridge, 2018). *Drosophila* and human genomes share 60% homology, while 75% of genes that cause disease in humans have a functional homolog in *Drosophila* (Ugur, Chen and Bellen, 2016; Reiter *et al.*, 2001). The low genetic redundancy of the *Drosophila* genome simplifies the study of complex human diseases (Anoar, Woodling and Niccoli, 2021). *Drosophila* have a complex nervous system, and display complex behaviours including sleep, learning and memory, which are impacted by ageing and the expression of toxic genes, making *Drosophila* a useful model for neurodegenerative research (Anoar, Woodling and Niccoli, 2021; Chan and Bonini, 2000).

The GAL4/UAS (upstream activating sequence) system is widely used to control the expression of genes of interest in *Drosophila* (Brand and Perrimon, 1993).

The yeast-derived transcriptional activator GAL4, is under the control of a tissue specific promoter, and the line carrying these elements is called the 'driver'. When GAL4 binds to UAS, transcription of the downstream gene of interest occurs. The Gal4-Geneswitch iteration of this system, has a progesterone inducible element fused to the DNA binding domain of GAL4. Transcriptional activation only occurs upon feeding with the RU486 drug, allowing the expression of toxic constructs to be limited to adult tissues (Osterwalder *et al.*, 2001). Using this system to overexpress G_4C_2 repeats specifically in adult neurons, the Partridge and Isaacs labs demonstrated DPR mediated toxicity with reduced lifespan and neurodegeneration (Mizielinska *et al.*, 2014) (Figure 1.6).

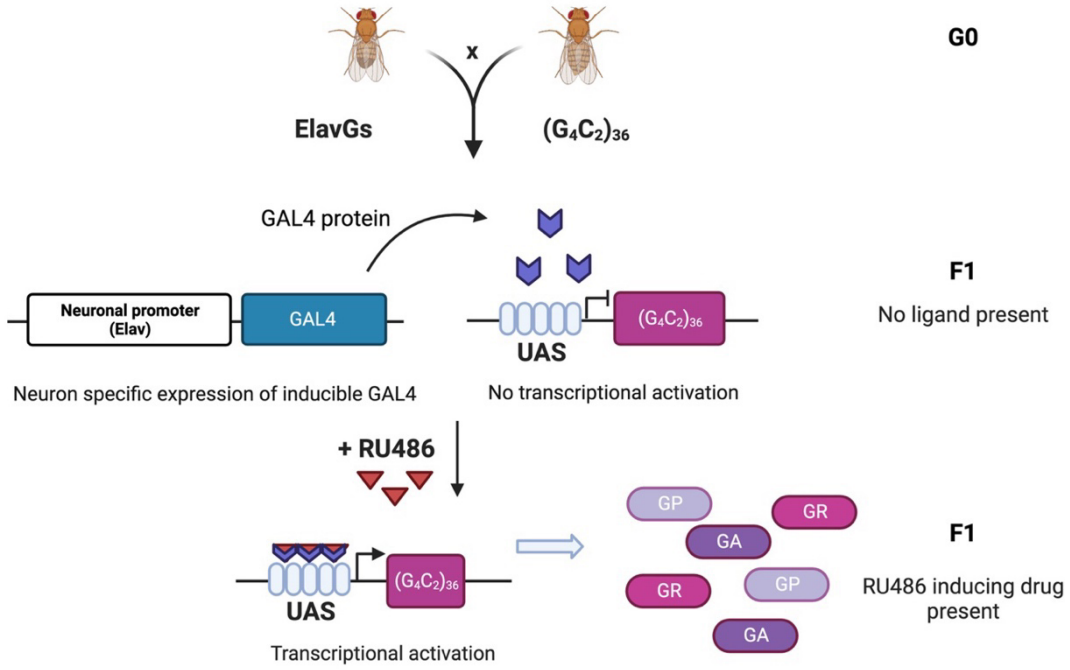

Figure 1.9. RU486-inducible gene switch system.
Figure adapted from (Osterwalder *et al.*, 2001) and produced using BioRender.

1.3.1 *Drosophila* as an animal model for genetic screens

Expansive collections of *Drosophila* lines are available to the community to overexpress, knockdown or knockout genes of interest, facilitating large scale genetic screens (Perkins *et al.*, 2015; Bischof *et al.*, 2013; Dietzl *et al.*, 2007; Bellen *et al.*, 2004). High-throughput, unbiased screens for genetic modifiers of DPR toxicity in *Drosophila* have already yielded important insights into disease mechanisms, with confirmation in patient iPSC-neuronal models (Yuva-Aydemir

et al., 2019; Lopez-Gonzalez *et al.*, 2019; Freibaum *et al.*, 2015). However, the genetic screens published so far using *C9orf72 Drosophila* models have relied upon overexpression of toxic constructs to investigate developmental phenotypes (Yuva-Aydemir, Almeida and Gao, 2018). Genetic screens utilising adult neuronal expression models have the potential to reveal novel pathways mediating toxicity and uncover new therapeutic targets and may prove a powerful approach upon confirmation of hits in patient iPSC neurons and mouse models.

1.4 iPSC neuronal models of C9ALS/FTD

Since 2007, when it was first demonstrated that induced pluripotent stem cells can be generated from adult human fibroblasts, researchers have recognised the potential of differentiated patient-derived iPSCs to propel the study of human disease *in-vitro* (Takahashi et al., 2007). This advance has enabled neurodegenerative disease researchers to study the earliest stages of cellular dysfunction in patient iPSC-derived neurons, astrocytes and glia, as opposed to studying end stage disease in post-mortem patient brain tissue (Penney, Ralvenius and Tsai, 2020).

CRISPR/Cas9 genome editing has been used to introduce disease-causing mutations into iPSC lines from healthy donors, and to correct mutations in iPSCs from patients (Penney, Ralvenius and Tsai, 2020). This has enabled researchers to directly compare isogenic lines, generated from a single individual, with an otherwise identical genetic background, except for the presence or absence of the disease-causing mutation (Ramos *et al.*, 2021; Selvaraj, Livesey and Chandran, 2017). Many iPSC lines are now available to the community, generated from sporadic or *C9orf72* ALS, FTD and ALS/FTD patients, and the neurons derived from these cells produce RNA foci and DPRs, with some models having *C9orf72* haploinsufficiency (Baxi *et al.*, 2022; Selvaraj *et al.*, 2018; Dafinca *et al.*, 2016; Almeida *et al.*, 2013; Donnelly *et al.*, 2013; Sareen *et al.*, 2013). More recent studies have used iPSC co-culture models and iPSC-cortical organoid models to investigate the interactions of neurons and glia, enabling the study of

cell extrinsic contributions to neurodegeneration in *C9orf72* ALS/FTD (Vahsen *et al.*, 2022; Szebényi *et al.*, 2021).

1.5 Transcription factor involvement in C9ALS/FTD

Given the extensive transcriptional deregulation observed in C9ALS/FTD, it is plausible that transcription factor activity is altered in these diseases. Transcription factors act in the nucleus where they bind to specific motifs upstream of target genes to influence their transcription (Latchman, 1997). Indeed, poly(PR) has been demonstrated to alter chromatin accessibility, and stabilise the transcription factor p53, activating its target genes, resulting in neuronal cell death (Maor-Nof *et al.*, 2021). Also, the localisation of transcription factors has been found to be altered in neurodegenerative diseases possibly due to impaired nucleocytoplasmic transport, which is also implicated in *C9orf72* ALS/FTD (Freibaum *et al.*, 2015; Chu *et al.*, 2007). Furthermore, when considering genetic modifiers of toxicity for complex diseases like ALS and FTD, single gene manipulations may not be sufficient to meaningfully modify toxicity. Rather, manipulating the activity of transcriptional coactivators and transcription factors may be a more promising approach to simultaneously modify transcriptional networks and cellular pathways. This has recently been demonstrated with *PGC1*α overexpression to ameliorate mitochondrial dysfunction and restore axonal homeostasis in *C9orf72* iPSC-motor neurons (Mehta *et al.*, 2021).

1.6 Lipids and ALS/FTD

The brain has the second highest lipid content of all tissues in the body, after adipose tissue, constituting 50% dry weight of the brain and therefore lipid dysregulation could have widespread devastating consequences for neuronal health (Figure 1.10) (Hornemann, 2021; Chung *et al.*, 2013). Lipids are a large heterogenous group of biomolecules with essential energetic, structural, and signalling roles (Tracey *et al.*, 2018) (Figure 1.11). The importance of lipids to

eukaryotic cellular function is underscored by the fact that 5% of all genes are devoted to lipid synthesis (van Meer, Voelker and Feigenson, 2008).

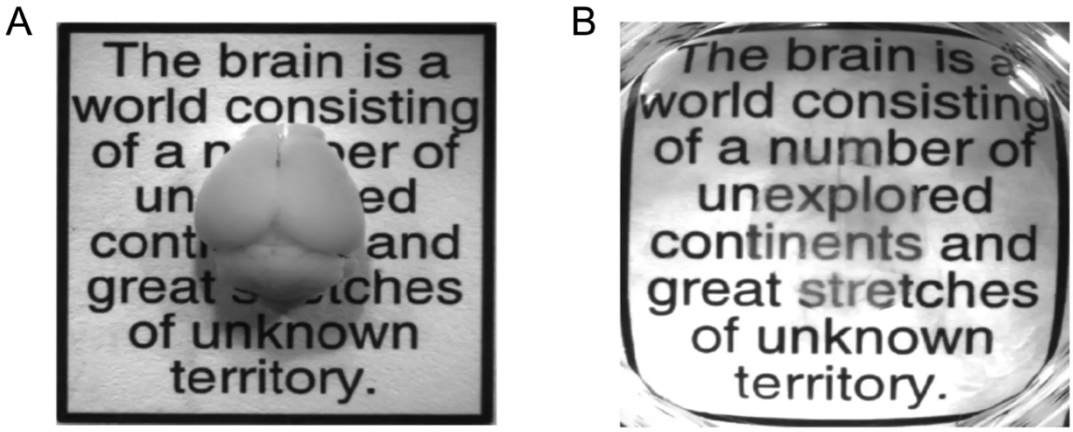

Figure 1.10. Lipids are a substantial structural component of the brain.
A. Mouse brain before CLARITY treatment to remove all lipids. B. Mouse brain 48-hour after CLARITY treatment, which removes all lipids but maintains remaining structure with a nanoporous hydrogel. Figure adapted from (Chung *et al.*, 2013).

Fatty acids (FAs), serve as the building blocks of most complex lipid classes, including glycerophospholipids, triglycerides (TGs), diacylglycerols (DGs), sphingolipids, ceramides, and cholesterol esters. Diversity between these lipid classes is conferred by head group composition, attachment to aliphatic chains, and conjugation to fatty acids (Fahy *et al.*, 2009; Holthuis and Menon, 2014). The presence or absence of double bonds in the acyl chain of fatty acids determines its saturation profile - saturated fatty acids have zero double bonds in their acyl chain, monounsaturated fatty acids contain one, whereas polyunsaturated fatty acids (PUFAs) contain at least two double bonds. The length of the fatty acid acyl chain, the number and position of double bonds, as well as head group composition influences the physicochemical properties of complex lipids and therefore can influence physiological functions of lipids (Holthuis and Menon, 2014; de Kroon, Rijken and De Smet, 2013).

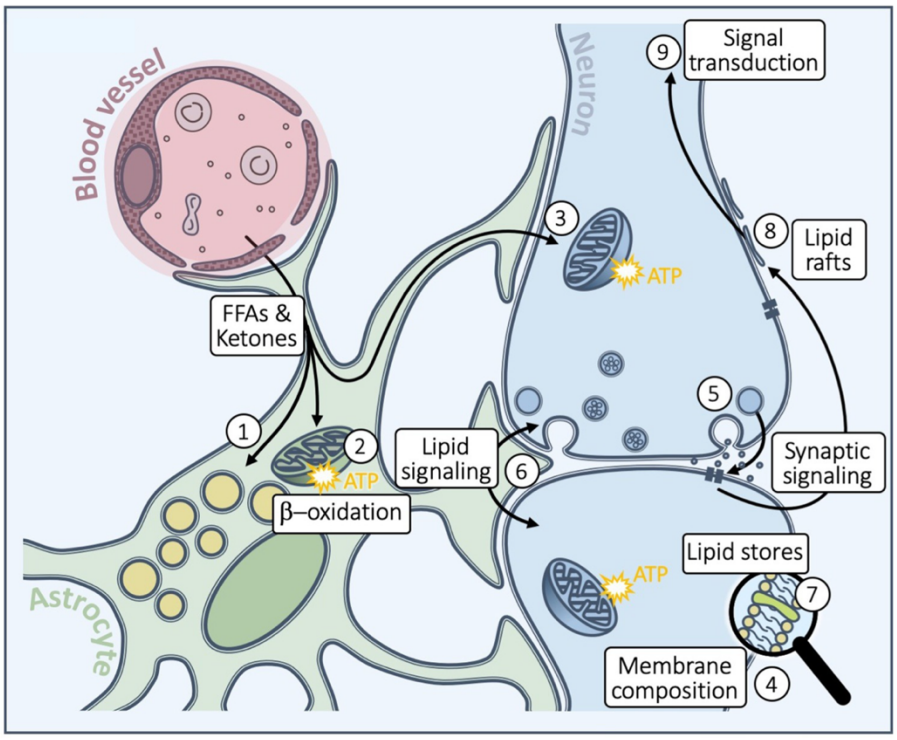

Figure 1.11. The functional roles of lipids in the brain.
(1) Astrocytes take up free fatty acids and ketones from systemic circulation which are then stored as lipid droplets or undergo β-oxidation in mitochondria (2). (3) Astrocytes shuttle lipid-derived metabolites to neurons, as a fuel source. (4) Lipids are a major structural component of cellular membranes in the CNS. The composition of phospholipid membranes, and in particular the fatty acids attached to these phospholipids can influence signalling, particularly synaptic transmission between neurons (5), and between neurons and astrocytes (6). Neuronal membranes also store various lipids (7). (8) Neuronal lipid rafts composed of sphingolipids, phospholipids and cholesterol also play important roles in signal transduction (9). Figure adapted from (Tracey *et al.*, 2021).

Over the past decade, several studies have investigated dysregulated lipid metabolism in ALS and FTD (Tracey *et al.*, 2021; Tracey *et al.*, 2018; Schmitt *et al.*, 2014). There are conflicting reports in the literature whether an increased body mass index or hyperlipidaemia is a protective factor in ALS (Kostic Dedic *et al.*, 2012; Paganoni *et al.*, 2011; Dupuis *et al.*, 2008). Dysregulation of triglyceride metabolism has been linked to ALS, with decreased triglyceride levels associated with faster disease progression (Sol *et al.*, 2021) and shortened survival (Dorst *et al.*, 2011). Hypermetabolism with elevated resting energy expenditure is seen in approximately 60% of ALS patients and negatively predicts survival (Fayemendy *et al.*, 2021; Desport *et al.*, 2005; Desport *et al.*, 2001). The LIPCAL-

ALS study reported high fat diets have survival benefit for a subgroup of fast-progressing ALS patients (NCT02306590) (Ludolph *et al.*, 2020). High total cholesterol levels have been causally associated with ALS risk (van Rheenen *et al.*, 2021). Analyses of UK Biobank data reported reduced levels of total cholesterol and low-density lipoprotein cholesterol in blood up to 7 years prior to symptom onset in ALS cases, which then stabilises or rises (Thompson *et al.*, 2023). Furthermore, elevated blood high density lipoprotein and apolipoprotein A were associated with a decreased risk of ALS (Thompson, Talbot and Turner, 2022). Similarly, the Apolipoprotein-related MOrtality RISk study reported a higher incidence of ALS among those with increased blood low-density lipoprotein cholesterol, apolipoprotein B, apolipoprotein B/apolipoprotein A ratio or low density lipoprotein cholesterol/high density lipoprotein cholesterol ratio in the years before symptom onset (Mariosa *et al.*, 2017). Therefore, premorbid metabolic changes are found years prior to diagnoses, with biomarker potential and may play a role in ALS pathogenesis.

PUFAs have also been linked to ALS pathogenesis. As previously mentioned, esterified PUFAs influence the physicochemical properties of membrane lipids, including membrane fluidity. Additionally, PUFAs can be de-esterified from phospholipids to act as both pro- and anti-inflammatory signalling molecules (Harayama and Shimizu, 2020; Bazinet and Layé, 2014). Multiple epidemiological studies have demonstrated that increased dietary consumption of PUFAs, particularly omega-3 (ω3) PUFAs, is associated with decreased risk of disease (Veldink *et al.*, 2007; Fitzgerald *et al.*, 2014). Higher levels of the PUFA alpha-linolenic acid have been associated with a longer survival and slower functional decline after disease onset (Bjornevik *et al.*, 2023). The PUFAs docosahexaenoic acid (DHA; 22:6 ω3), and arachidonic acid (AA; 20:4 ω6) are particularly enriched in the brain and both have been linked to disease pathogenesis (Bazinet and Layé, 2014). Dysregulated AA metabolism has been reported across *SOD1, C9orf72, TDP-43* and sporadic ALS spinal motor neurons. AA can be processed by 5-lipoxgenase (5-LOX) to produce pro-inflammatory leukotrienes. 5-LOX inhibition increased cell viability of *SOD1* and *C9orf72* motor neurons and partially ameliorated neurodegenerative phenotypes

in a *Drosophila* and *SOD1*$_{G93A}$ mouse model (Lee *et al.*, 2021). Furthermore, the levels of PUFA-derived mediators are found to be altered in the CSF of patients with FTD, with *C9orf72* carriers having higher levels of the DHA-derived specialised pro-resolving mediators maresins and resolvins, as well as higher levels of AA-derived leukotrienes (Sogorb-Esteve *et al.*, 2021).

Despite the accumulating evidence implicating altered lipid metabolism, particularly involving PUFAs in C9ALS/FTD, it is yet to be determined if PUFA-containing lipids are altered in ALS/FTD neurons and whether this contributes directly to neuronal loss.

1.7 Thesis aims

Significant progress has been made in understanding the mechanisms of toxicity associated with the *C9orf72* mutation. However, the key downstream effector pathways mediating neuronal loss are still unclear. Combining unbiased omics approaches with large scale genetic screens in *Drosophila* models of C9ALS/FTD can reveal novel protective pathways for further validation in patient cells and mammalian models, thus enabling the development of much needed therapies for these devastating diseases.

Therefore, the overarching aims of this thesis were to reveal novel insights into the pathogenesis of GGGGCC repeat expansion in *Drosophila* models of *C9orf72* ALS/FTD, and to identify protective genes and pathways for further investigation.

1. Specifically, in Chapter 3 I investigated the mechanisms underlying the protective effects of the Odd-skipped transcription factors *odd* and *bowl*, which had previously been identified as suppressors of the reduced survival phenotype of $(G_4C_2)_{36}$ flies in a large genetic overexpression screen. Utilising transcriptomics and bioinformatic approaches, I aimed to identify and validate downstream Odd-skipped target genes and pathways mediating rescue effects.

2. In Chapter 4, I aimed to characterise *Trpγ* overexpression as a suppressor of toxicity in C9ALS/FTD *Drosophila* using lifespans, activity, and sleep analyses, combined with MSD immunoassays to measure DPR levels.

3. Lastly, in Chapter 5, the role of lipid metabolism was investigated in $(G_4C_2)_{36}$ toxicity in *Drosophila* models using transcriptomic and lipidomic approaches, as well as genetic and pharmacological manipulation, with further validation performed in iPSC neuronal models and patient post-mortem brains.

Chapter 2: Methods

2.1 *Drosophila* food recipes

2.1.1 SYA medium

Per 1 L final volume: 15 g of agar was dissolved in 700 mL of distilled H_2O, and heated until boiling. To this, 100 g of brewer's yeast (MP Biomedical) and 50 g of sugar were added. 170 mL of distilled water was added and the mixture allowed to cool. When temperature reached below 60°C, 30 mL per litre nipagin (10% in ethanol) and 3 mL propionic acid were added. Food was dispensed directly, or for RU486 experiments food was supplemented with 200 µM RU486 (mifepristone) dissolved in ethanol, or an equal volume of ethanol and mixed well before dispensing. Media was stored at 4°C until use and used within a month of cooking.

2.1.2 Grape plates

Per 1 L: 25 g of agar was dissolved in 500 mL of distilled water and brought to the boil. To this, 300 mL of red grape juice (Young's definitive) was added. 50 mL distilled water was added to cool the mixture. Once the mixture was cooled below 60°C, 21 mL of 10% nipigin stock was added. Media was stored at 4°C until use.

2.1.3 Fatty acid supplementation to *Drosophila* food

Fatty acids were added to SYA food, along with 200 µM RU486 (Sigma), while it was still liquid but had cooled to 50°C. The food was mixed thoroughly with an electric handheld blender, before dispensing into individual vials. Fatty acids used were palmitic acid (W283215, Merck), stearic acid (10002390, Fisher Scientific), oleic acid (W281506, Merck), linoleic acid (436305, Merck Millipore) and alpha-linolenic acid (L2376, Merck).

2.2 *Drosophila* stocks and maintenance

2.2.1 *Drosophila* maintenance

Drosophila stocks were maintained on SYA food at 25°C in a 12-hour light/dark cycle with 60% constant humidity. For RU486 induced experiments, food was supplemented with 200 μM RU486 (mifepristone) from a 500X stock dissolved in ethanol or an equal volume of ethanol.

2.2.2 *Drosophila* stocks

The elavGS stock was derived from the original elavGS 301.2 line (Osterwalder *et al.*, 2001), and generously provided by Hervé Tricoire (CNRS, France) (Latouche *et al.*, 2007). The daGS stock was generously provided by Véronique Monnier (Tricoire *et al.*, 2009). UAS-FASN1 and UAS-FASN2 lines were a gift from Jacques Montagne (Université Paris-Sud) (Garrido *et al.*, 2015). The UAS-Trpγ-AB and UAS-Trpγ-D lines were generously provided by Orkun Akin (UCLA) (Bajar *et al.*, 2022). The UAS-mCD8::GFP line was a kind gift from Liqun Luo (Lee and Luo, 1999). The w1118 line (BDSC:3605), GMR-Gal4 (BDSC:9146), UAS-Trpγ RNAi (BDSC:53313), UAS-Arc1 RNAi (BDSC:25954), UAS-hec RNAi (BDSC:29623), UAS-Ect3 RNAi (BDSC:41655), CG9394 RNAi (BDSC:64586), Trpγ[1] (BDSC:64311) were obtained from the Bloomington *Drosophila* Stock Centre. The UAS-bowl (FlyORF:F000444) and UAS-odd (FlyORF:F000020) lines were obtained from the FlyORF collection (Bischof *et al.*, 2013). The 'empty' FlyORF line was generated by injecting a pUAST plasmid in a w-;M{3xP3-RFP.attP}ZH-86Fb stock and selecting w+ flies (Xu *et al.*, 2023). The UAS-Desat1 (DGRC:118679) and UAS-fat-2 (DGRC:118682) lines were obtained from the KYOTO *Drosophila* Stock Centre (Suito *et al.*, 2020). The UAS-$(G_4C_2)_{36}$ and UAS-$(GR)_{36}$ stocks have been previously described (Mizielinska *et al.*, 2014). All stocks were backcrossed to the w1118 strain for six generations before using for experiments. Genotypes of all stocks used are described in Table 2.1.

Table 2.1. Genotypes of *Drosophila* stocks used throughout

Stock	Genotype
w1118	w[1118]
v-w+	w v^1
elavGS	w[1118];P{elavGSGAL4}
da-GS	w[1118];P{da-GSGAL4.T}
GMR-Gal4	w[1118];P{GMR-GAL4.w[-]}2
UAS-$(G_4C_2)_{36}$	w[1118];P{UAS-GGGGCC.36}attP40
UAS-$(GR)_{36}$	w[1118];P{UAS-poly-GR.PO-36}attP40
UAS-bowl	M{UAS-bowl.ORF.3xHA.GW}ZH-86Fb
UAS-odd	M{UAS-odd.ORF.3xHA.GW}ZH-86Fb
UAS-Trpγ RNAi	P(Perkins *et al.*)attP2
UAS-Arc1 RNAi	v[1];P{y[+t7.7]v[+t1.8]=TRiP.JF01974}attP2
UAS-hec RNAi	P(Perkins *et al.*)attP2
UAS-Ect3 RNAi	P(Perkins *et al.*)attP2
CG9394 RNAi	P(Perkins *et al.*)attP40
UAS-FASN1	w[1118]; P{UAS-FASN1.G}
UAS-FASN2	w[1118]; P{UAS-FASN2.G}
UAS-Desat1	w[1118]; P{w[+mC]=UAS-Desat1.S}16
UAS-fat-2	w[1118]; P{w[+mC]=UAS-Cefat-2.S}3
UAS-Trpγ-AB	w[1118]; P{UAS-Trpγ.AB}attP1
UAS-Trpγ-D	w[1118]; P{UAS-Trpγ.D}attP1
Trpγ[1]	w[1118]; TI{TI}Trpγ1
UAS-mCD8::GFP	w[1118]; P{UAS-mCD8::GFP}

2.3 Generation of fly lines

2.3.1 Generation of OSR1 and OSR2 transgenic flies

Human OSR1 transcript variant 1 and OSR2 transcript variant 1 cDNA were purchased from Origene: OSR1: CAT#RC206666, OSR2: CAT#RC204502. Constructs were cloned into pUAST attB (Figure 2.1). Transgenic fly lines were generated by phiC31-integrase-mediated, site-directed insertion into the attp2

locus (Markstein *et al.*, 2008). The phiC31 integrase was removed by crossing transgenic males to w1118 females for two successive generations. Integration into the attp2 landing site was verified by PCR using primers SOL179 (ACTGAAATCTGCCAAGAAGTA), a primer specific for the pUAST attB vector, and a reverse primer in the OSR1 sequence (CAGATGTCACAGGTGTAGGGCCG) or OSR2 sequence (CGTTTTGGAGGGCAACCTTCC).

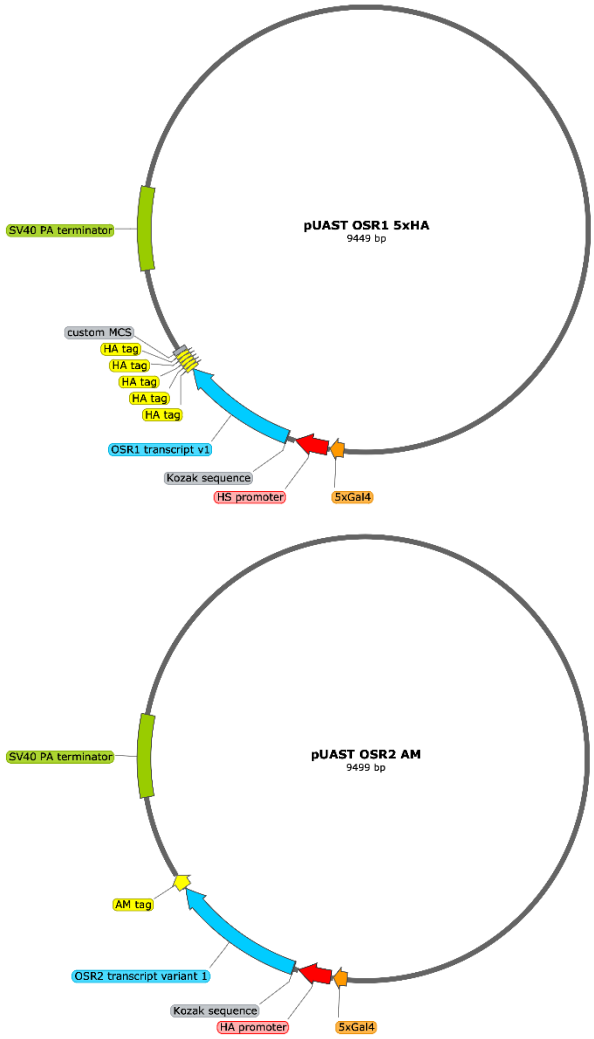

Figure 2.1 Plasmid maps for UAS-OSR1 and UAS-OSR2.

2.3.2 Generation of Fad2 flies

The pUAST-Fad2 vector (UFO08718) was purchased from *Drosophila* Genomics Resource Center (DGRC Stock 1642876;

https://dgrc.bio.indiana.edu//stock/1642876; RRID:DGRC_1642876) (Figure 2.2). UAS-Fad2 flies were generated using the phiC31-integrase-mediated, site-directed insertion into the attp2 locus (Markstein *et al.*, 2008). The phiC31 integrase was removed by crossing transgenic males to w1118 females for two successive generations. Integration into the attp2 landing site was verified by PCR using primers SOL179 (ACTGAAATCTGCCAAGAAGTA), a primer specific for the pUAST attB vector and a reverse primer in the Fad2 sequence (GTGGTCTTCCGATTGCTTAGC).

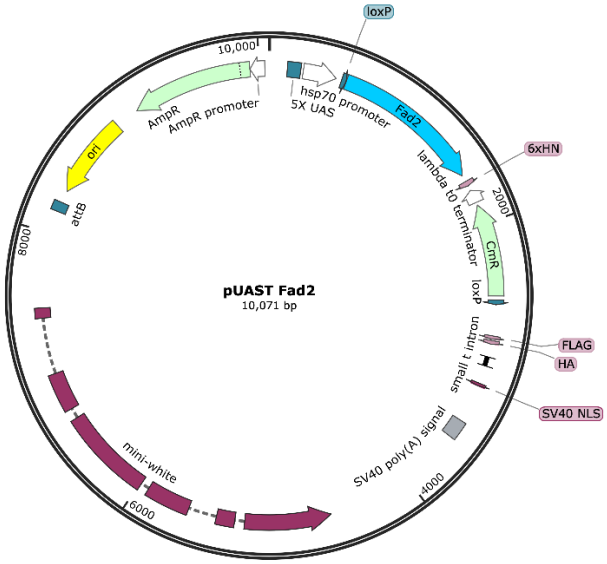

Figure 2.2. Plasmid map for UAS-Fad2.

2.4 *Drosophila* behavioural and lifespan assays

2.4.1 Lifespan assays

Flies were reared at a standard density in 200 mL bottles on SYA medium at 25°C. the parental generation was allowed to lay for 24 hr on grape-agar plates supplemented with yeast paste (Saf-Levure). Eggs were washed briefly in 1X PBS (pH 7.4) before being dispensed into bottles using a pipette at a standard density (20 µL of eggs in PBS, approximately 300 eggs). Two days post-eclosion flies were allocated to experimental vials at a density of 15 flies per vial (total of 150 flies per condition) containing SYA medium with or without 200 µM RU486. Deaths were scored, and flies tipped onto fresh food three times a week. All

lifespans were performed at 25°C, on mated females unless otherwise stated. Data are presented as survival curves and comparison between groups was performed using a log-rank test.

2.4.2 Activity and sleep analysis

Two-day-old mated female flies (N=32) developed and eclosed under 12 hr:12 hr light:dark cycle conditions (12L:12D) were fed with food containing either 200 μM RU486 or ethanol vehicle. After transferring into tubes, locomotor activity and sleep behaviour were recorded in 12L:12D using the *Drosophila* Activity Monitor (DAM, TriKinetics Inc, MA) system within the experimental incubator (Percival), set at 25°C and 65% humidity. Fly activity is measured by infra-red beam crosses in the DAM tube. After 24 hours of acclimatisation, data were acquired from a 24 hr period (beginning at the onset of lights-on). A custom Microsoft Excel workbook (Chen *et al.*, 2019) was used to calculate total activity counts per fly in the day and night periods, and to calculate sleep (continuous periods of fly inactivity lasting 5 min or longer). Flies with more than 12 hr of continuous inactivity at the end of the experiment were excluded as potentially dead.

2.4.3 Assessment of *Drosophila* feeding

Two-day-old mated female flies were transferred to SYA food containing 200 μM RU486 or ethanol vehicle control with PUFAs, at a density of 5 per vial on the evening before the assay. Vials were coded and placed in a randomised order in rows on viewing racks at 25°C overnight. A feeding event was scored when a fly had its proboscis extended and touching the food surface while performing a bobbing motion. At the end of the assay, the vial labels were decoded, and the feeding data expressed as a proportion by experimental group (sum of scored feeding events divided by total number of feeding opportunities, where total number of feeding opportunities=number of flies in vial×number of vials in the group×number of observations) (Wong *et al.*, 2009). For statistical analyses, comparisons between experimental groups were made on the totals of feeding events by all flies within a vial, to avoid pseudoreplication.

2.4.4 Cold stress recovery assay

Two days post-eclosion flies were allocated to experimental vials at a density of 15 flies per vial containing SYA medium with or without 200 μM RU486. Three vials were used per condition. After seven days, *Drosophila* were exposed to 4°C for 18 hours. Afterwards the vials were kept at room temperature for one hour. The number of flies exhibiting a full recovery (walking), partial recovery (partial paralysis) or death were recorded and expressed as a percentage of total per vial.

2.5 *Drosophila* eye phenotyping

Females carrying UAS-FlyORF, UAS-bowl or UAS-odd constructs were crossed to the male GMR-GAL4 or GMR-GAL4; UAS-$(G_4C_2)_{36}$ driver lines. The progeny was allowed to develop and eclose at 25°C. Adult female eyes were photographed two days after emergence, using a digital camera mounted to the eyepiece of a dissecting microscope. All images were obtained under the same magnification with eye area calculated from each image using ImageJ (Schneider, Rasband and Eliceiri, 2012).

2.6 SCope database images

Images from the SCope database (Davie *et al.*, 2018) (https://scope.aertslab.org/) were obtained using the following settings: *Drosophila*, Brain, Aerts_Fly_AdultBrain_Filtered_57k, Log transform ‘on’, CPM normalize ‘on’, Expression-based plotting ‘on’, and default values for all other settings.

2.7 Multiple sequence alignment

Multiple protein sequence alignments were performed using Clustal Omega https://www.ebi.ac.uk/Tools/msa/clustalo/. *Drosophila* odd (UniProt ID P23803), bowl (UniProt ID Q9VQU9), mouse Osr1 (UniProt ID Q9WVG7), Osr2a (UniProt ID Q91ZD1), and human OSR1 (UniProt ID Q8TAX0), OSR2A (UniProt ID Q8N2R0) were compared.

2.8 RNA extraction

Adult female flies were induced on SYA medium containing 200 µM RU486 or ethanol vehicle control, and subsequently snap frozen. 15 heads were placed in cold 2 mL screw cap tubes (Sarstedt) containing 425-600 µm acid-washed glass beads (Merck). 1 mL of cold TRIzol reagent (GIBCO) was added to each tube and samples were ribolysed at maximum speed for 30 seconds. Chloroform (200 µL) was added to each tube before vortexing for 15 seconds. Samples were then centrifuged at full speed for 5 minutes, and the upper colourless phase was collected to a new tube. Samples were incubated with isopropanol (500 µL) for 15 minutes at room temperature, followed by a 15 minute centrifugation at 4°C. The RNA pellet was washed three times with 70% ethanol before resuspending in 40 µL nuclease-free H_2O (Ambion).

2.9 cDNA synthesis and qRT-PCR

Total RNA was extracted from 15 heads per sample as above. Approximately 1 µg of RNA per sample (10.6 µL) was incubated with 2 µL TURBO DNase (Thermo Fisher Scientific), in 1.4 µL TURBO DNase buffer (Thermo Fisher Scientific) at 37°C for 15 minutes. Following this, the reaction was inhibited with addition of 2 µl EDTA to a final concentration of 3.4 mM, followed by incubation at 75°C for 5 minutes. 2 µL 0.5 µg/ µL oligo dT and 2 µL dNTP mix (10 mM stock made from individual 100 mM dNTP stocks, Invitrogen) were added to each sample followed by a 5 minute incubation at 65°C, after which, samples were placed on ice. To each reaction, the following was added: 8 µL 5X first-strand buffer, 8 µL 25 mM

$MgCl_2$, 4 µL 0.1 M DTT, 2 µL RNaseOut RNase inhibitor (40 units/µl), 1 µl SuperScript II reverse transcriptase (Invitrogen) was added. All reagents part of the Thermo Fisher Superscript II kit. Samples were incubated at 42°C for 50 minutes, then heat inactivated at 70°C for 15 minutes. Quantitative PCR was performed using the QuantStudio 6 Flex Real-Time PCR System (Applied Biosystems) using SYBR® Green master mix (Applied Biosystems). Values were obtained using the relative standard curve method, cDNA was diluted 1/10 and compared to a relative standard curve of pooled cDNA from all tested samples (standard curve ranged from 1/1 dilution of pooled cDNA to 1/256, diluting serially in half), nuclease-free H_2O alone was used as a blank sample. Relative mRNA levels were normalised to alpha-tubulin and then expressed as a fold change compared to controls. Primers used are shown in the table below.

Table 2.2. Primer sequences

Primer name	Sequence
bowl_for:	CTGAGGGATCACAGGTATATTC
bowl_rev:	GGATCTTGTGGACAGCCAAGG
odd_for:	TCCTCTTCAGCAAAGTCTTCTTC
odd_rev:	ATGTCTTCGGCCTCA
OSR1_for:	CGACGTGACCAAGCTGTCTCC
OSR1_rev:	CAGATGTCACAGGTGTAGGGCCG
OSR2_for:	GACTTTGCCAATTTGGCGGTG
OSR2_rev:	CGTTTTGGAGGGCAACCTTCC
Tub84B_for:	TGGGCCCGTCTGGACCACAA
Tub84B_rev:	TCGCCGTCACCGGAGTCCAT
AcCoAS_for:	GAGCCACTTCAGTGATTTTCG
AcCoAS_rev:	ACTTCATGAGGGCACGAATC
FASN1_for:	GCTTGCTCCAGTTCTCTGTA
FASN1_rev:	GTATCCATTGCCAGACTCAT
Desat1_for:	CCGGAGTGCTCTTCGAGTG
Desat1_rev:	CAGCCAGATGGAGGTAACCG
Trpγ_for	AAAACGTCACCTTTCACAGCG
Trpγ_rev	GCGACTGAACGCACTCATCA

Trpγ-D_for	CCCACACAACTACACGAATA
Trpγ-D_rev	CAACATATTGTTGCTGCTCC

2.10 *Drosophila* RNA sequencing

For sequencing total RNA was extracted as above (2.8). RNA was depleted of ribosomal RNA and libraries were generated at the Max Planck Genome Centre Cologne (Germany) for RNA-sequencing experiment 1 or UCL Genomics for RNA-sequencing experiment 2. Experiments were performed in quadruplicate. RNA sequencing experiment 1 was performed with an Illumina Hi-Seq2500, 35 million single-end reads/sample and 100 bp read length. Raw sequence reads were quality-trimmed using Trim-Galore! (v2.0.14) against the Dm6 reference genome. Multi-mapped reads were filtered using SAMtools (Li *et al.*, 2009). Differential expression analysis was performed with DESeq2 (Love, Huber and Anders, 2014) controlling for false discovery rate using the Benjamini-Hochberg method. RNA sequencing experiment 2 was performed with an Illumina NextSeq2000 and 16 million paired-end reads/sample and 100 bp read length at UCL Genomics. Raw sequence reads were aligned to the Dm6 reference genome. DESeq2 (default parameters) was used to perform differential expression analysis. The “runTest” function from topGO package (v2.53.0, Alexa and Rahnenführer, 2009) was used to perform GO enrichment analysis on differentially expressed genes (|log2FoldChange| > 0.58). The “weight01” algorithm and “fisher” statistic were used when running topGO. The "GenTable" function was used to generate a table with the top biological process GO terms. Plots with top GO terms were plotted using ggplot2 (v3.4.2). We generated a heatmap for top GO terms showing the percentage of significantly differentially expressed genes among all genes of a GO term expressed in a dataset using the pheatmap function from pheatmap package (v1.0.12, https://CRAN.R-project.org/package=pheatmap). Volcano plots of differentially expressed genes were plotted using VolcaNoseR (https://huygens.science.uva.nl/VolcaNoseR/) for Figure 3.17 and Figure 4.3. Volcano plots of differentially expressed genes were plotted using ggVolcanoR (https://ggvolcanor.erc.monash.edu/) for Figure 5.1.

2.11 Re-analyses of RNA sequencing datasets

2.11.1 Odd-skipped target gene expression in rat primary neurons overexpressing OSR1 or OSR2

RNA-sequencing was performed on rat primary cortical neurons overexpressing either *OSR1* or *OSR2*. Primary rat cortical neurons were transduced with *OSR1* or *OSR2* lentivirus 6 days after plating, and RNA was collected 6 days later (DIV 12). RNA libraries were prepared for sequencing with KAPA mRNA HyperPrep kit. RNA-sequencing (Next Seq 2000) was carried out at a depth of 20 million reads by UCL Genomics. Differential expression analyses was carried out by UCL Genomics. Raw sequence reads were aligned to the rn6 reference genome. DESeq2 (default parameters) was used to perform differential expression analysis. Differentially expressed genes were plotted using VolcaNoseR. Gridlines were set to -Log10(p-value) = 1.3 on the y-axis, equivalent to adjusted p-value <0.05 and Log2(Fold change) = 0.5 on the x-axis.

2.11.2 *TRPC4* and *TRPC5* expression in *C9orf72* iPSC motor neurons

Published Fragments Per Kilobase of transcript per Million mapped reads (FPKM) values for *TRPC4* and *TRPC5* were plotted from transcriptomic datasets of *C9orf72* iPSC motor neurons versus controls at day in vitro 21 (DIV 21) (Sommer *et al.*, 2022; Mehta *et al.*, 2021; Selvaraj *et al.*, 2018).

2.11.3 *TRPC1*, *TRPC4* and *TRPC5* expression in *C9orf72* ALS frontal cortex excitatory neurons

Differentially expressed genes from a published single cell RNA sequencing dataset of *C9orf72* ALS post-mortem frontal cortex excitatory neurons (Li *et al.*, 2023) were plotted using VolcaNoseR. Gridlines were set to -Log10(p-value) = 1.3 on the y-axis, equivalent to adjusted p-value <0.05 and Log2(Fold change) = 0.3 on the x-axis.

2.11.4 Fatty acid synthesis and desaturation gene expression in ALS post-mortem cervical spinal cord

Differentially expressed genes from a published bulk RNA sequencing dataset of ALS post-mortem cervical spinal cord of 149 patients with ALS (101 sporadic, 39 *C9orf72*, 4 SOD1, 2 FUS, 2 ANG, 1 OPTN) and 40 non-neurological disease controls from the New York Genome Center ALS Consortium published in (Humphrey *et al.*, 2023) were plotted using ggVolcanoR. Gridlines were set to -Log10(p-value) = 1.3 on the y-axis, equivalent to adjusted p-value <0.05 and Log2(Fold change) = 0.2 on the x-axis.

2.12 *Drosophila* head protein preparation

Flies were set up as described for lifespan assays at a standard density, and allowed to mate for 48 hours, before being split onto control food or food supplemented with RU486 for 7 days. Following this, flies were snap frozen in liquid nitrogen. Heads were removed, and 10 heads per sample were homogenised in 100 µL 2% SDS buffer (Cat No. 428018, Merck) containing 1X RIPA buffer (Cat No. R0278, Sigma-Aldrich) and complete mini EDTA-free protease inhibitor cocktail (Cat No. 11836170001, Roche) at room temperature for about 30 seconds until the heads were no longer intact. Samples were then heated at 95°C for 10 minutes. After centrifugation at 14,000 rpm for 20 minutes at room temperature, the supernatants were collected in the new tubes. The protein concentration was determined using Pierce BCA Protein Assay Kit (Cat No. 23325, ThermoFisher) according to the manufacturer's manual. Samples were diluted to 1 mg/mL with homogenisation buffer.

2.13 Immunoblotting

To each sample, Pierce™ LDS Sample Buffer (4X) (Cat No. 84788, ThermoFisher) with 100 mM DTT was added, and samples vortexed, and briefly

centrifuged before being boiled at 95°C for 10 minutes. 10 µL of sample was loaded per well in a 15 well 4-12% Novex Bis-Tris gel (Invitrogen). Protein was transferred to a PVDF (Millipore) membrane using the Trans-Blot Turbo transfer system (BioRad). Membrane was blocked for 1 hour at room temperature in 5% milk (Sigma) in TBS-Tween-20 (0.1%) before incubating with primary antibodies diluted in 0.1% TBST at 4°C overnight. Primary antibodies used were anti-GP 1:3000 (custom generated by Adrian Isaacs lab), anti-actin 1:10000 (Abcam, ab1801), anti-GFP 1:10000 (Merck, 11814460001). Secondaries used were anti-rabbit and anti-mouse (Abcam ab6789 and ab6721) at 1:10000 dilutions for 1 hour at room temperature. Bands were visualized with Luminata Crescendo (Millipore) and imaged with ImageQuant LAS4000 (GE Healthcare Life Sciences). Quantification was carried out with ImageQuant software or ImageJ.

2.14 i3Neuron protein preparation

i3Neuron replicates for DPR MSDs were collected alongside those used for lipidomic analyses from the same neuronal inductions. One well of a 6-well plate was used per replicate for MSD. At DIV 21, neurons were lifted with PBS, centrifuged and pelleted at 1500 x g for 5-10 minutes, snap frozen on dry ice, and stored at -80°C until use. For protein preparation, cell pellets were resuspended in 200 µL 2% SDS buffer (Cat No. 428018, Merck) containing 1X RIPA buffer (Cat No. R0278, Sigma-Aldrich) and cOmplete mini EDTA-free protease inhibitor cocktail (Cat No. 11836170001, Roche) and sonicated 2 x 10 seconds at 30 A at 4°C. Sonicated samples were centrifuged at 17,000g for 20min at 16°C, after which supernatants were collected and used in MSD assays.

2.15 DPR MSD immunoassays

Meso Scale Discovery (MSD) immunoassay was performed in singleplex using 96-well SECTOR plates (MSD, Rockville, Maryland) to quantify poly(GR), poly(GP) and poly(GA) expression levels. The assays were performed as previously described (Simone et al, 2018). Plates were coated with unlabelled

capture antibody, anti-poly(GR) (GR660, 2 µg/mL, custom-made from Eurogentec), anti-poly(GP) (GP658, 2 µg/mL, custom-made from Eurogentec) or anti-poly(GA) (clone 5E9, AB_2728663; 1 µg/mL, Merck Millipore). After blocking, samples were loaded at 22.5 µg of protein per well. Biotinylated detector antibodies anti-poly(GR) (GR660, 1 µg/mL), anti-poly(GP) (GP658, 1 µg/mL) and anti-poly(GA) ((GA5F2, 1 µg/mL) kindly provided by Prof. Dr Edbauer), were used, followed by sulfo-tagged streptavidin (Meso Scale Discovery, R32AD). Plates were read with the MSD reading buffer (Meso Scale Discovery, R92TC) using the MSD Sector Imager 2400. Signals correspond to intensity of emitted light upon electrochemical stimulation of the assay plate. Prior to analysis, the average reading from a calibrator containing no peptide was subtracted from each reading. A four-parameter logistic regression curve was fit to the values obtained from a standard curve using GraphPad Prism, and concentrations were interpolated.

2.16 Triglyceride (TG) content quantification

For triglyceride content quantification, ten fly heads were homogenized in 0.05% Tween20. 6 biological replicates were used per condition. TG content was quantified using the Triglyceride Infinity Reagent (ThermoScientific) using Glycerol standards (Sigma). Protein content was determined using the Pierce BCA protein assay kit (Cat No. 23325, ThermoFisher). Student's t test (Excel) was used to assess statistical difference between two conditions.

2.17 LC-MS/MS lipidomics of *Drosophila* heads

LC-MS/MS lipidomics was performed by Dr Bebiana da Costa Sousa and Dr Andrea Lopez, Babraham Institute, as previously described (Sousa *et al.*, 2023). 20 mg of *Drosophila* head tissue (approximately 200 heads) was subjected to Folch extraction for analysis of phospholipids, neutral lipids and free fatty acids analysis. 20 mg of *Drosophila* head tissue was subjected to Folch-butanol extraction for the analysis of each of lysolipids, phosphatidylinositol phosphate and sphingolipids. After extraction and before analysis, the lipid mixtures were

resuspended in either 50 µL of chloroform:methanol (1:1) for the lipid species extracted using the Folch method or acidified methanol for those extracted using the Folch-butanol method. A mixture of 2-propanol:ethyl acetate (570 µL, 8:2 v/v) was added to 20 mg of *Drosophila* head tissue spiked with 10 µL of internal standard for quantitation of ceramide molecular species. Isolated lipids were analysed by LC–MS/MS using an Orbitrap Elite mass spectrometer (Thermo Fisher Scientific) with both positive and negative electrospray ionization. Lysolipid and ceramide species were detected using a QTRAP 6500 mass spectrometer. Lipid species were normalized to synthetic standards to quantify their absolute abundance.

2.18 $(G_4C_2)_{92}$ or $(G_4C_2)_2$ lentiviral construct subcloning

pCDH-EF1-MCS-IRES-copGFP lentiviral plasmid (System Biosciences) was used as the backbone to create $(G_4C_2)_{92}$ and $(G_4C_2)_2$ lentiviral constructs. This subcloning was undertaken in a two-step process. First, we synthesized a DNA fragment consisting of a custom multiple cloning site (MCS) sandwiched in between 300 bp each of upstream and downstream sequence from *C9orf72* intron 1 and then inserted it into the internal MCS of pCDH-EF1-MCS-IRES-copGFP with InFusion cloning (Takara Bio) in between XbaI and NotI restriction sites. This interim construct, termed "pCDH-EF1-C9up-MCS-C9down-IRES-copGFP" was verified with diagnostic restriction digests and Sanger sequencing across the insert. Then, to create the $(G_4C_2)_{92}$ construct, a 92-repeat sequence was isolated from a previously verified in-house construct with NheI and NotI restriction digests and subcloned into the MCS of pCDH-EF1-C9up-MCS-C9down-IRES-copGFP with overnight ligation at 4°C (T4 ligase, NEB). To maintain repeat stability, bacterial clones were grown at room temperature, in 0.5 mg/mL ampicillin in low-salt LB broth (Sigma). A repeat-stable clone was selected and subsequently maxi-prepped (Qiagen) for use in lentiviral production. Thus, the final construct consisted of 92 repeats immediately surrounded on either side by 300 bp of endogenous *C9orf72* intronic sequence to facilitate RAN translation and upstream of an IRES-copGFP sequence for fluorescent visualization of transduction efficiency. To create the $(G_4C_2)_2$ control lentiviral constructs, two

complementary short oligos were synthesized containing 2 G_4C_2 repeats and NheI and NotI restriction site overhangs. Oligos were resuspended in annealing buffer (NEB buffer 2.1), heated to 95°C, and allowed to cool slowly to room temperature to anneal. Annealed oligos were used directly in ligation reactions into pCDH-EF1-C9up-MCS-C9down-IRES-copGFP with the same protocol as used for the 92-repeat construct.

2.19 Lentiviral production

HEK293T cells were grown at 37°C and 5% CO_2 in T175 flasks. At ~70% confluency, cells were transfected with either $(G_4C_2)_{92}$ and $(G_4C_2)_2$ lentiviral transfer plasmids along with PAX (Addgene #12260) and VSV-G (Addgene #12259) lentiviral packaging plasmids with Lipofectamine 3000 Transfection Reagent (Invitrogen) with manufacturer protocol. 48 hours later, media was collected, centrifuged at 500 x g for 10 minutes at 4°C to remove cell debris, after which Lenti-X Concentrator (Takara Bio) was added at a 1:3 ratio. After a minimum incubation of 24 hours at 4°C, lentiviral mix was centrifuged at 1500 x g at 4°C for 45 minutes and resulting concentrated lentivirus was resuspended in sterile PBS, aliquoted, and stored at -80°C until use.

2.20 i3Neuron differentiation

iPSC donor information is provided in Table 2.3. i3 iPSCs were generated via expression of a piggyBac-integrated doxycycline-inducible Neurogenin 2 (Ngn2) transcription factor. This allows for rapid differentiation into cortical neurons (i3Neurons) using a method previously described (Fernandopulle *et al.*, 2018). Briefly, i3 iPSCs were grown to 70-80% confluency. On DIV 0 of neuronal induction, cells were washed with PBS and lifted with Accutase (Gibco). Cells were plated at 375,000 cells/well of a 6-well plate onto Geltrex-coated plates. Cells were maintained in DMEM-F12 (Gibco) containing 1x N2 (Thermo Fisher Scientific), 1x Glutamax (Gibco), 1x HEPES (Gibco), 1x Non-essential amino acids (Gibco), doxycycline (2 µg/mL) and 10 µM Y-27632 (DIV 0 only; Tocris). Media was changed every day for 3 days. On DIV 3, neural progenitor cells were

dissociated with accutase and replated onto poly-L-ornithine (Merck) or polyethyleneimine and laminin-coated plates in neuronal maintenance media: Neurobasal (Gibco), supplemented with 1x B27 (Gibco), 10 ng/mL BDNF (PeproTech), 10 ng/mL NT-3 (PeproTech) and 1 µg/mL laminin. Neurons were plated at 600,000 cells/well of a 6-well plate. From DIV 3 to DIV 21, cells were maintained in neuronal maintenance media, with ⅓ media changes once weekly.

2.21 Lentiviral transduction and ASO treatment of i3 Neurons

Lentiviral transduction to overexpress $(G_4C_2)_{92}$ or $(G_4C_2)_2$ constructs and was done 1 hour after DIV 3 replating. Likewise, antisense oligonucleotide (ASO) treatments to target the *C9orf72* sense strand or a non-targeting control were also begun on DIV 3 and supplemented in media changes thereafter. In brief, 1 hour after replating, ASOs were transiently transfected using Lipofectamine Stem (Invitrogen STEM00015) at 5 µM final concentration according to manufacturer's protocol. 1 day after ASO treatment, a full media change was done to remove remaining Lipofectamine Stem and replaced with neuronal maintenance media containing 5 µM ASO. From DIV 3 to DIV 21, cells were maintained in neuronal maintenance media, with ⅓ media changes once weekly. ASOs were previously published in (Lagier-Tourenne *et al.*, 2013), and have fully modified phosphorothioate backbones. C9 sense-targeting ASO (ISIS ID: 577061) hybridizes to sequence within intron 1, upstream of the hexanucleotide expansion, and thereby exclusively targets expansion-containing RNAs (Lagier-Tourenne *et al.*, 2013). Non-targeting ASO (CTRL ASO, ISIS ID: 141923), has no targets in the human genome and was used as a transfection control.

ASO sequences are as follows, with the 5 base pairs on either end modified to 2' O-Methyl RNA to enhance stability and reduce toxicity:

C9 sense-targeting: mUmAmCmAmGGCTGCGGTTGmUmUmUmCmC
Non-targeting: mCmCmUmUmCCCTGAAGGTTmCmCmUmCmC

2.22 Targeted lipidomics of i3Neurons and post-mortem brain samples

2.22.1 Sample collection

At DIV 21, i3Neurons were pelleted and stored at −80°C until analysis. Brains were donated to the Queen Square Brain Bank (QSBB) (UCL Queen Square Institute of Neurology) with full, informed consent. Clinical and demographic data for all brains used in this study were stored electronically in compliance with the 1998 data protection act and are summarised in Table 2.4. Ethical approval for the study was obtained from the NHS research ethics committee (NEC) and in accordance with the human tissue authority's (HTA's) code of practice and standards under license number 12198. All cases underwent a pathological diagnosis for FTLD according to current consensus criteria (Mackenzie *et al.*, 2011; Cairns *et al.*, 2007). The cohort included pathologically diagnosed cases of FTLD without *C9orf72* expansion (N=32), FTLD with *C9orf72* expansion (N=15) and neurologically normal controls (N=13). Frontal cortex grey matter was dissected from each brain and stored at − 80°C until analysis.

2.22.2 Targeted lipidomic measurements

Comprehensive targeted lipidomics was accomplished using a flow-injection assay based on lipid class separation by differential mobility spectroscopy and selective multiple reaction monitoring (MRM) per lipid species (Lipidyzer platform; SCIEX, Framingham, USA). A very detailed description of lipid extraction, software and the quantitative nature of the approach can be found elsewhere (Ghorasaini *et al.*, 2021; Su *et al.*, 2021; Ghorasaini *et al.*, 2022). In short, after the addition of >60 deuterated internal standards, lipids were extracted using methyl tert-butyl ether. Organic extracts were combined and subsequently dried under a gentle stream of nitrogen and reconstituted in running buffer. Lipids were then analyzed using flow-injection in MRM mode employing a Shimadzu Nexera series HPLC and a Sciex QTrap 5500 mass spectrometer. For the internal calibration, deuterated IS lipids for each lipid class were used within the lipidomics workflow manager. Each lipid species was corrected by the closest deuterated IS

within its lipid class and afterwards the obtained area ratio was multiplied by the concentration of the IS and further corrected for the volume and weight of the sample.

2.22.3 Analyses of targeted lipidomic datasets

2.22.3.1 Filtering and normalizations

Raw amounts of individual lipid species were obtained from the Lipidyzer platform as above and then imported into the Simple Omics Data Analysis (SODA) platform (v0.6.5) for filtering and normalization. Datasets were first filtered for low-abundance and undetected lipid species. To pass filtering, a lipid species must be detected in at least 80% of all samples in the analysis as well as 60% of samples in any given group and must also be at least 2-fold more abundant than the average of the blanks. After filtering, missing sample values were imputed as the median of other samples in their group; this step was found to be necessary for subsequent normalizations, as missing values skew proportional datasets. Next, filtered and imputed datasets were normalized by lipid class. Thus, these processing steps result in proportional lipidomic measurements, relative to the total amount of lipid within each class.

2.22.3.2 Fold-changes in lipid species in i3Neurons

For these analyses, “biological replicates” were considered as different i3Neuron lines and “technical replicates” were individual cell pellets from those lines that were grown, collected, and analysed separately. Technical replicates were obtained across a minimum of two neuronal inductions (three for most conditions). To attain fold-changes for i3Neurons, each technical replicate was filtered and normalised individually. Fold-changes were then calculated for each lipid species as the average amount across technical replicates in an induction over the average in its internal control condition.

Table 2.3. iPSC donor information for lines used for lipidomic analyses

iPSC Line Name	Sex (M/F)	Clinical diagnoses	Number of G_4C_2 repeats	Source of iPSCs
Becker S6 (BS6) *C9orf72* line 1	F	ALS/FTD	~750	Siddharthan Chandran lab, Edinburgh
2H9 (Isogenic control of BS6)	F	N/A	~2 Repeat expansion removed by CRISPR-Cas9	Siddharthan Chandran lab, Edinburgh
D08 *C9orf72* line 2	M	N/A	KOLF2.1J with ~ 200 repeats knocked-in	iNDI project (Pantazis *et al.*, 2022; Ramos *et al.*, 2021)
F05 *C9orf72* line 3	M	N/A	KOLF2.1J with ~ 200 repeats knocked-in	iNDI project (Pantazis *et al.*, 2022; Ramos *et al.*, 2021)
KOLF2.1J	M	N/A	Parental line	iNDI project (Pantazis *et al.*, 2022; Ramos *et al.*, 2021)

Table 2.4. Clinical and demographic data for all brains used in lipidomic analyses

QSBB number	Age at onset	Age at death	Sex (M/F)	Pathological diagnoses	Mutations
P16/14	66	71	M	FTLD-TDPA	*C9orf72*
P23/15	59	65	M	FTLD-TDPA	*C9orf72*
P17/17	64	73	M	FTLD-TDPA	*C9orf72*
P76/05	66	74	F	FTLD-TDPA	*C9orf72*
P15/12	56	67	F	FTLD-TDPA	*C9orf72*
P65/08	54	60	M	FTLD-TDPA	*C9orf72*
P16/09	62	68	M	FTLD-TDPA	*C9orf72*
P54/10	43	45	M	FTLD-TDPA	*C9orf72* homozygous
P70/10	53	63	M	FTLD-TDPA	*C9orf72*
P56/13	57	62	F	FTLD-TDPA	*C9orf72*
P24/15	58	66	F	FTLD-TDPA	*C9orf72*
P99/17	52	58	M	FTLD-TDPA	*C9orf72*
P57/19	52	68	M	FTLD-TDPB	*C9orf72*

P69/19	65	72	F	FTLD-TDPB	*C9orf72*
P53/04	75	79	F	FTLD-TDPA	N/A
P41/05	83	87	F	FTLD-TDPA	N/A
P56/07	47	53	M	FTLD-TDPA	N/A
P65/10	57	62	M	FTLD-TDPA	N/A
P75/15	66	72	M	FTLD-TDPA	N/A
P8/16	51	61	M	FTLD-TDPA	N/A
P59/17	57	60	M	FTLD-TDP A & MND-TDP43	N/A
P6/19	61	65	F	FTLD-TDPA	N/A
P40/04	58	66.8	F	FTLD-TDPA	GRN C31fs/*C9orf72*
P89/05	62	68	F	FTLD-TDPA	GRN Q130fs
P40/09	53	61	M	FTLD-TDPA	GRN C31fs
P17/13	57	63	F	FTLD-TDPA	GRN C31fs
P17/14	49	55	M	FTLD-TDPA	GRN C31fs
P60/15	59	70	M	FTLD-TDPA	GRN R493X
P46/16	57	71	M	FTLD-TDPA	GRN R493X
P76/19	58	70	M	FTLD-TDPA	GRN R493X
P42/20	57	72	F	FTLD-TDPA	GRN splice site variant
P63/05	58	73	F	FTLD-TDPC	N/A
P67/06	59	73	F	FTLD-TDPC	N/A
P11/07	64	78	M	FTLD-TDPC	N/A
P28/07	64	74	M	FTLD-TDPC	N/A
P89/08	50	65	M	FTLD-TDPC	N/A
P51/09	61	66	M	FTLD-TDPC	N/A
P7/15	44	67	M	FTLD-TDPC	N/A
P45/15	77	80	F	FTLD-TDPC	N/A
P70/15	58	72	F	FTLD-TDPC	N/A
P27/17	73	83	M	FTLD-TDPC	N/A
P37/17	53	71	M	FTLD-TDPC	N/A
P1/18	57	72	M	FTLD-TDPC	N/A
P37/18	70	79	M	FTLD-TDPC	N/A
P76/18	56	65	F	FTLD-TDPC	N/A
P40/19	61	75	F	FTLD-TDPC	N/A
P42/21	60	69	F	FTLD-TDPC	N/A
P78/06		68	F	Control	N/A
P29/17		71	F	Control	N/A
P26/11		73	F	Path Ageing	N/A
P47/11		79	F	Control	N/A
P21/00		70	F	Control	N/A
P45/04		78	F	Control	N/A
P21/17		76	M	Control	N/A

P87/17		79	M	Control	N/A
P10/20		64	M	Control	N/A
P15/10		69	M	Control	N/A
P10/20		64	M	Control	N/A
P85/19		73	M	Control	N/A
P14/20		73	M	Control	N/A

2.23 Glutamate-induced excitotoxicity assays in iPSC-derived motor neurons

2.23.1 Subcloning for BFP, *fat-1* and *fat-2* overexpression constructs

mTagBFP (Addgene #89685*), fat-1* (Genscript), and *fat-2* (Genscript) cDNAs were amplified with PCR and subcloned into the pHR-hSyn-EGFP vector (Addgene #114215) along with a T2A-NLS-mApple minigene for fluorescent visualization. In brief, EGFP was removed with BamHI and NotI (NEB) and BFP/*fat-1*/*fat-2* and T2A-NLS-mApple fragments were inserted with InFusion cloning (Takara Bio), as per manufacturer's protocol. Resulting plasmids were restriction digest and Sanger sequencing verified prior to being maxi-prepped (Qiagen) for subsequent use in excitotoxicity assays.

2.23.2 Glutamate excitotoxicity assay

These experiments were performed by collaborator Dr Alyssa Coyne (Johns Hopkins University School of Medicine). Non-neurological control and *C9orf72* iPSCs were obtained from the Answer ALS repository at Cedars Sinai (see Table 2.5 for demographics) and maintained in mTeSR Plus medium at 37°C with 5% CO_2. iPSNs were differentiated according to the diMNs protocol (Baxi *et al.*, 2022; Coyne *et al.*, 2021; Coyne *et al.*, 2020) and maintained at 37°C with 5% CO_2. iPSCs and iPSNs routinely tested negative for mycoplasma. On day 12 of differentiation, iPSNs were dissociated with Trypsin. 5 x 10^6 iPSNs were nucleofected with 4 µg plasmid DNA in suspension as previously described (Coyne *et al.*, 2021; Coyne *et al.*, 2020). Following nucleofection, 100 µL of cell suspension was plated in each well (total of 6 wells per cuvette) of a glass bottom

or plastic 24 well plate for PI and Alamar blue toxicity and viability experiments respectively. Media was exchanged daily for a total of 20 days to facilitate the removal of iPSNs that failed to recover post-nucleofection. On the day of the experiment (day 32 of differentiation), iPSN media was replaced with artificial CSF (ACSF) solution containing 10 μM glutamate. For those iPSNs undergoing Alamar Blue viability assays (plastic dishes), Alamar blue reagent was additionally added to each well according to manufacturer protocol at this time. Following incubation, iPSNs for PI cell death assays were incubated with PI and NucBlue live ready probes for 30 minutes and subjected to confocal imaging as previously described (Coyne *et al.*, 2020). The number of PI spots and nuclei were automatically counted in FIJI. Alamar Blue cell viability plates were processed according to manufacturer protocol. As a positive control, 10% Triton X-100 was added to respective wells 1 hour prior to processing.

Table 2.5. iPSC donor information for lines used in glutamate-excitotoxicity assay

iPSC Line Name	Age at Time of Collection	Sex (M/F)	Clinical diagnosis	Source
CS0201	56	F	Non-neurologic control	Cedars-Sinai
CS0002	51	M	Non-neurologic control	Cedars-Sinai
CS0206	72	F	Non-neurologic control	Cedars-Sinai
CS9XH7	53	M	Non-neurologic control	Cedars-Sinai

CS8PAA	58	F	Non-neurologic control	Cedars-Sinai
CS1ATZ	60	M	Non-neurologic control	Cedars-Sinai
CS0NKC	52	F	*C9orf72*	Cedars-Sinai
CS0LPK	67	M	*C9orf72*	Cedars-Sinai
CS0BUU	63	F	*C9orf72*	Cedars-Sinai
CS7VCZ	64	M	*C9orf72*	Cedars-Sinai
CS6ZLD	Unknown	F	*C9orf72*	Cedars-Sinai
CS8KT3	60	M	*C9orf72*	Cedars-Sinai

2.24 List of Software used

Adobe Illustrator 2023 (Adobe), BioRender Scientific Image and Illustration Software (https://www.biorender.com/), ImageQuant™ TL v10.2 analysis software (Cytiva), GraphPad Prism v10.0.2 (171) (GraphPad software inc.), ImageJ v1.53 (National Institute of Health), Fiji v2.1.4, MSD discovery workbench v4.0 (Meso scale Discovery), SnapGene Viewer v6.0.3 (Snapgene), Simple Omics Data Analysis (SODA) software package v0.7, Clustal Omega (EMBL-EBI) (https://www.ebi.ac.uk/Tools/msa/clustalo/), VolcaNoseR (https://huygens.science.uva.nl/VolcaNoseR/), ggVolcanoR (https://ggvolcanor.erc.monash.edu/), DRSC Integrative ortholog Prediction Tool DIOPT Version 9.0, http://bioinformatics.sdstate.edu/go/), Simple Omics Data Analysis (SODA) platform (v0.6.5).

2.25 Statistical Analysis

Statistical analyses were performed with Prism 10 (GraphPad Software). Normality of data was tested using the D'Agostino-Pearson omnibus normality test. When data were normally distributed, a Student's t-test, one-way ANOVA,

or two-way ANOVA was performed followed by Tukey, Šídák's or Dunnett's multiple comparisons test as appropriate. The statistical test used for each experiment is indicated in the figure legends. For all data figures, the N values can be found in the figure legends and correspond to the number of biological repeats used in the analysis, n values correspond to the number of technical repeats used in the analysis. Results were presented as mean ± standard deviation (S.D.) unless stated otherwise. Statistical differences were considered significant at $p<0.05$. Lifespans were compared by log-rank tests, performed in Microsoft Excel (template described in (Piper and Partridge, 2016)).

Chapter 3: The Odd-skipped family of C_2H_2 transcription factors as modifiers of *C9orf72* toxicity

3.1 Introduction

Our understanding of the mechanisms by which the *C9orf72* mutation causes toxicity has greatly advanced since 2011, however, the key downstream effector pathways mediating neuronal loss are still unclear. Genetic modifier screens in disease models of C9ALS/FTD can help reveal the important downstream pathways leading to neurodegeneration as well as uncover novel protective genes and pathways, thus enabling the development of much needed therapies for these devastating diseases. Here, we used a *Drosophila* model of *C9orf72* toxicity that inducibly expresses RNA from 36 GGGGCC repeats in adult neurons. This construct undergoes RAN translation to generate DPRs, resulting in a reduced lifespan compared to uninduced controls (Mizielinska *et al.*, 2014). Utilising this robust lifespan phenotype, an unbiased overexpression screen for genetic modifiers of *C9orf72*-associated repeat toxicity was previously performed in the lab (Niccoli *et al*., in preparation). Over 2000 single gene overexpression lines from the FlyORF collection were screened for their effect on survival of C9 flies. *Odd skipped (odd*) and *brother of odd with entrails limited (bowl),* both of which belong to the Odd-skipped family of C_2H_2 zinc-finger transcription factors, were two of the 17 suppressors of shortened lifespan (Figure 3.1). In this chapter, the role of the Odd-skipped family in suppressing *C9orf72* toxicity was further investigated.

Odd was first discovered in *Drosophila* in a genetic screen for mutants that alter segmental patterning of larvae. *Odd* mutant embryos have defects in the odd-numbered segments of the cuticle, hence its name and classification as a pair-rule gene (Nüsslein-Volhard and Wieschaus, 1980). The Odd-skipped family has four members in *Drosophila*: *odd, bowl, drumstick (drm)* and *sister of odd and bowl (sob)* (Hart, Wang and Coulter, 1996). They play important roles during

development, with Odd-skipped genes shown to function downstream of Notch to promote leg segmentation (Hao *et al.*, 2003; de Celis Ibeas and Bray, 2003). Furthermore, *bowl* and *drm* are required for patterning of the foregut and hindgut, where the first zinc finger of Drm physically interacts with Lin, another transcriptional regulator, to relieve repression of Bowl (Johansen *et al.*, 2003; Green *et al.*, 2002; Iwaki *et al.*, 2001). This relief of repression role has also been described in patterning of the embryonic epidermis and in the developing wing (Nusinow, Greenberg and Hatini, 2008; Hatini *et al.*, 2005). Regarding neuronal functions, the Odd-skipped genes are required to activate hedgehog expression, triggering retinogenesis in *Drosophila* (Bras-Pereira, Bessa and Casares, 2006). Moreover, loss-of function, mis- and over-expression of *odd* affects neurite branching and arborisation (Lynn *et al.*, 2020). In the adult *Drosophila* brain, *odd* is expressed in a subset of 'odd' neurons, the majority of which are cholinergic. These odd neurons project dendrites into the mushroom body calyx and axons into the optic lobe (Slater *et al.*, 2015; Levy and Larsen, 2013).

Like the *Drosophila* Odd-skipped genes, *OSR1* and *OSR2* also play important roles during development of various tissues and organs including heart, kidneys, gonads, bone and palate (Kawai *et al.*, 2007; Tena *et al.*, 2007; Wang *et al.*, 2005; Lan *et al.*, 2004). *OSR1* and *OSR2* are functionally redundant in mouse development, with *OSR1* gene substitution capable of compensating or rescuing developmental defects of *OSR2* mutants (Gao *et al.*, 2011; Gao *et al.*, 2009). Additionally, *OSR1* functions as a tumour suppressor, since its downregulation promotes while its overexpression prevents cell proliferation in multiple cancer cell lines (Wang *et al.*, 2020; Wang *et al.*, 2018; Chen *et al.*, 2018; Zhang *et al.*, 2017; Otani *et al.*, 2014).

The Odd-skipped family are C_2H_2 zinc finger proteins, with the C_2H_2 (C-X2-C-X12-H-X3-H) zinc finger motif conferring DNA-binding ability (Coulter *et al.*, 1990). The proteins vary in their number of zinc finger motifs, with Odd containing four, Bowl and Sob containing five, and Drm containing two (Green *et al.*, 2002; Hart, Wang and Coulter, 1996; Coulter *et al.*, 1990). This protein family is evolutionarily conserved, with two mammalian homologs, OSR1 and OSR2 (Lan *et al.*, 2001; So and Danielian, 1999). OSR1 contains three zinc-finger motifs

while OSR2 contains either three (OSR2B) or five (OSR2A), due to alternative splicing leading to two distinct isoforms (Kawai *et al.*, 2005; Katoh, 2002; So and Danielian, 1999). *Drosophila* and mammalian Odd-skipped transcription factors bind similar, specific DNA sequence motifs, GCTACTGTA and GCTGCTCT, respectively, to influence target gene expression (Noyes *et al.*, 2008; Kawai *et al.*, 2007; Meng, Brodsky and Wolfe, 2005).

The aims of the work described in this Chapter were:

1. To characterise the Odd-skipped family of transcription factors as modifiers of C9 toxicity.
2. To identify potential downstream mediators of the beneficial effects on survival.

Transgenic flies expressing *Odd skipped-related 1* (*OSR1*) or *Odd skipped-related 2* (*OSR2*) were generated, to assess the functional conservation of the rescue that has been seen with *odd* and *bowl* in the original *Drosophila* screen. Both human *OSR1* and *OSR2*, like *Drosophila bowl* and *odd*, were able to extend survival of C9 *Drosophila.* To identify shared genes and pathways altered by overexpressing these related transcription factors in the context of C9 repeats, RNA-sequencing was performed. Gene ontology enrichment analysis did not identify common pathways altered across all Odd-skipped gene rescues. Therefore, prioritisation for target follow up was given to individual genes commonly altered across Odd-skipped conditions and/or containing a conserved Odd-skipped binding motif. Shortlisted genes of interest were assessed for their effect on C9 survival and proved to have either no effect or small effects on survival. Therefore, a combination of genes, rather than single genes, are likely to be driving the rescues observed by the Odd-skipped family.

3.2 Results

3.2.1 *Bowl* and *odd* are suppressors of *C9orf72* repeat toxicity in *Drosophila*

An overexpression screen for genetic modifiers of *C9orf72* repeat toxicity previously performed in the lab identified two of four *Drosophila* Odd-skipped family members as suppressors of the reduced lifespan of C9 flies (Niccoli *et al*., in preparation). Over 2000 single gene overexpression lines from the FlyORF collection were assessed. *Odd* and *bowl* were two of the 17 suppressors identified (Figure 3.1).

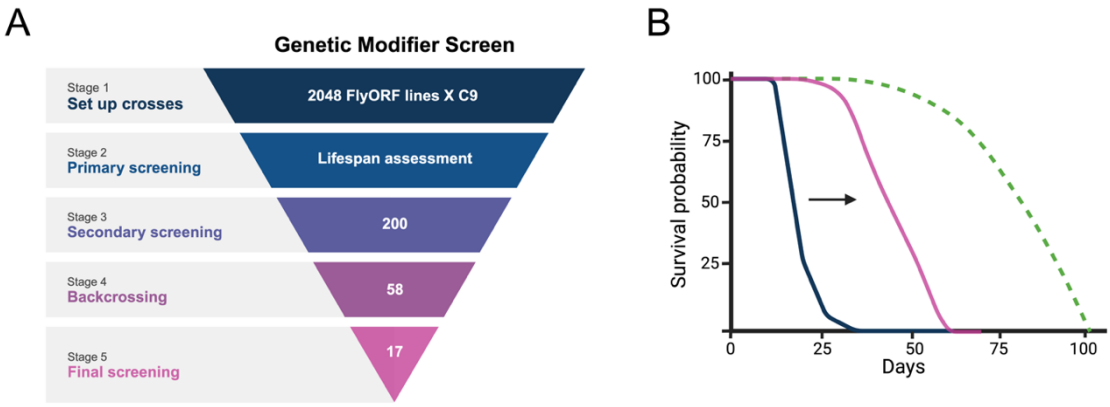

Figure 3.1. Genetic overexpression screen identifies bowl and odd as suppressors of C9 toxicity.
A. Genetic modifier screen design**.** 2048 FlyORF overexpression lines were crossed to $(G_4C_2)_{36}$; elavGS flies and progeny lifespans were assessed. 200 lines were identified as modifiers of survival, and re-screened. The 58 lines that showed replicate rescue were backcrossed to the w1118 strain. After backcrossing, 17 FlyORF lines were identified as strong modifiers of toxicity, two of which, *odd-skipped* and *bowl*, belong to the Odd-skipped family of transcription factors. B. Survival curve indicating C9 lifespan (navy line), C9 lifespan extension by genetic suppressor (pink line) and C9 uninduced control lifespan (green broken line). Figure produced with BioRender.

3.2.2 *Bowl* and *odd* are expressed in neurons

The overexpression screen for genetic modifiers of *C9orf72*-associated toxicity utilised the pan-neuronal driver elavGS, to express both $(G_4C_2)_{36}$ repeats and the candidate rescue genes. To assess whether *odd* and *bowl* are normally

expressed in neurons, we utilised a published single cell RNA-sequencing dataset from adult *Drosophila* brains (Davie *et al.*, 2018). Both *bowl* and *odd* were found to co-localise with *elav*-expressing (neuronal) cell populations rather than *repo*-expressing (glial) cell populations (Figure 3.2). *Bowl* and *odd* are lowly expressed in the *Drosophila* brain and expressed in a subset of neuronal cells. Therefore, the pan-neuronal overexpression of *odd* and *bowl* is largely ectopic.

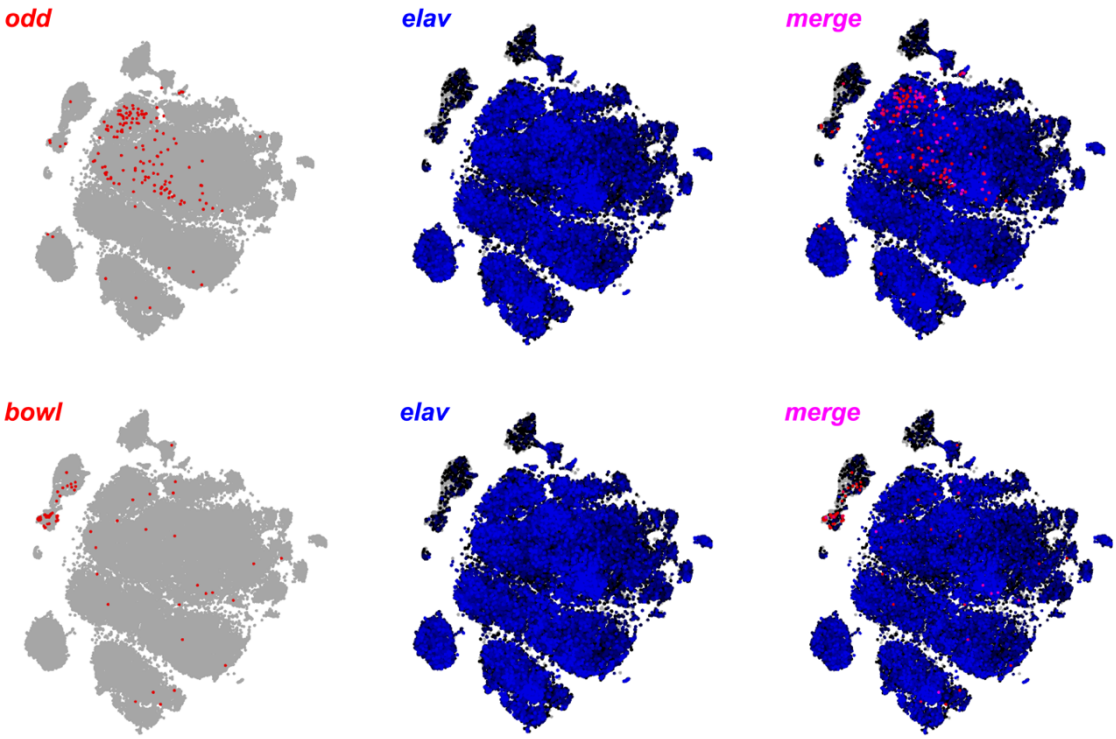

Figure 3.2. *Bowl* and *odd* are expressed in adult *Drosophila* brain, and mostly localise to elav-expressing (neuronal) cell populations.
Images from SCope database (Davie *et al.*, 2018).

3.2.3 Odd-skipped rescues are specific to C9 toxicity

To determine whether the survival rescues were attributable to a general improvement in organismal health, or a more specific rescue of C9 toxicity, *bowl* and *odd* were overexpressed in the neurons of wildtype flies. Survival was compared to the uninduced sibling control for each condition. Lifespan of wildtype flies was significantly reduced by both *bowl* and *odd* overexpression, suggesting that there was rescue of a disease-specific pathology (Figure 3.3). Median survival of flies expressing the empty FlyORF vector was 79 days compared to

76.5 days for uninduced sibling controls, with no significant difference in survival between induced and uninduced flies (p=0.106). Median survival of flies expressing *bowl* was 65 days compared to 72 days for uninduced sibling controls, with a significant reduction in survival between *bowl* induced and *bowl* uninduced flies (p=0.0002). Median survival of flies expressing *odd* was 67.5 days compared to 76.5 days for uninduced sibling controls, with a significant reduction in survival between *odd* induced and *odd* uninduced flies ($p=9x10^{-5}$).

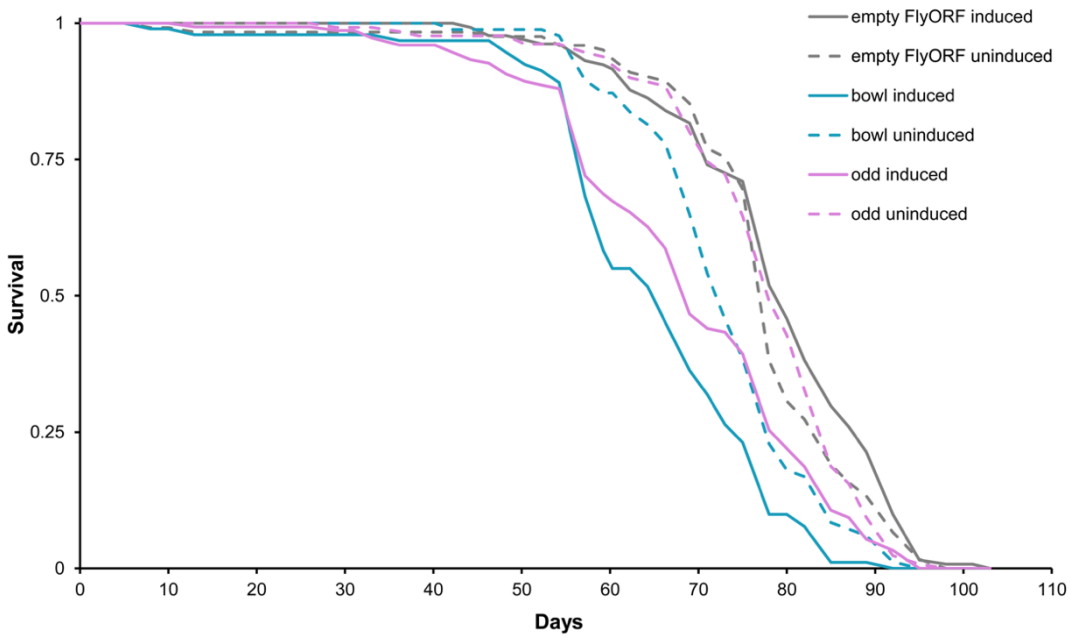

Figure 3.3. Lifespan of wild-type flies expressing *bowl* or *odd* in neurons. Lifespan was significantly reduced in flies expressing *bowl* (p=0.0002, log-rank test) and *odd* ($p=9x10^{-5}$, log-rank test), versus their respective uninduced sibling controls. Empty FlyORF vector expression had no effect on survival (p=0.106, log-rank test). N=86-150 flies per condition. Genotypes: *elavGS/UAS-empty FlyORF; elavGS/UAS-bowl; elavGS/UAS-odd*.

3.2.4 Human orthologs of *bowl* and *odd*, *OSR1* and *OSR2* also rescue C9 toxicity

To assess whether Odd-skipped rescues might be conserved, percent identity matrices and multiple sequence alignments of the amino acid sequences of these transcription factors were performed. *Drosophila* Odd (UniProt ID P23803), Bowl (UniProt ID Q9VQU9), mouse Osr1 (UniProt ID Q9WVG7), Osr2a (UniProt ID Q91ZD1), and human OSR1 (UniProt ID Q8TAX0), OSR2A (UniProt ID Q8N2R0)

amino acid sequences were aligned using Clustal Omega. The amino acid sequences of these proteins are very similar (Table 1 and Figure 3.4), especially in the zinc finger regions (Figure 3.4).

Table 3.1. Percent identity matrix of Odd-skipped protein sequences

	odd	bowl	mOSR1	hOSR1	mOSR2	hOSR2
odd	100.00	44.31	42.86	42.86	44.58	45.00
bowl	44.31	100.00	42.21	41.80	51.19	51.19
mOSR1	42.86	42.21	100.00	97.74	67.95	68.34
hOSR1	42.86	41.80	97.74	100.00	67.18	67.57
mOSR2	44.58	51.19	67.95	67.18	100.00	98.08
hOSR2	45.00	51.19	68.34	67.57	98.08	100.00

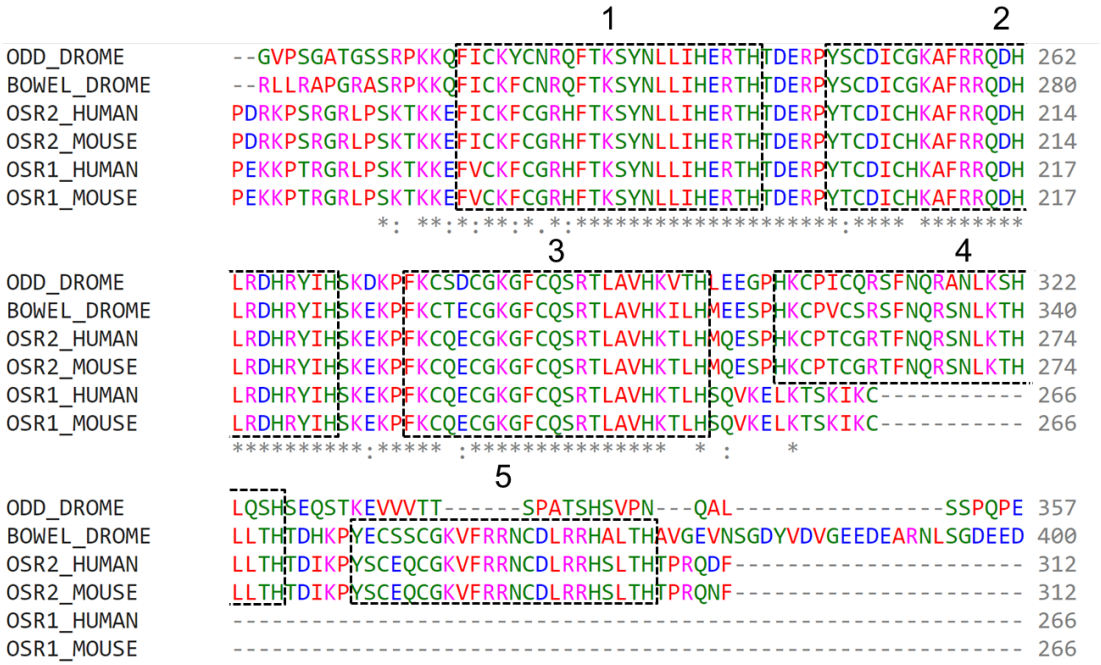

Figure 3.4. Amino acid conservation between Odd, Bowl and mammalian OSR1 and OSR2.
Multiple sequence alignment of Odd, Bowl, OSR1 and OSR2 shows considerable amino acid conservation, particularly among the zinc finger regions (dotted line boxes). Bowl and OSR2 contain 5 zinc finger nucleases (ZFNs), Odd contains 4 ZFNs, OSR1 contains 3 ZFNs. Amino acid multiple sequence alignments were generated with Clustal Omega.

Given the high degree of amino acid conservation between *Drosophila* Odd and Bowl and mammalian OSR1 and OSR2A, particularly in the zinc finger regions (Figure 3.4), which are important for DNA binding ability, transgenic flies expressing human *OSR1* or *OSR2A* were generated. Dr Alex Cammack, a postdoctoral fellow in the Isaacs lab, performed the cloning. Constructs were inserted into the attP2 locus (3rd chromosome). These lines were backcrossed for six generations to the w1118 strain. Stocks containing UAS-$(G_4C_2)_{36}$ on the second chromosome and one of either UAS-*bowl*, UAS-*odd*, UAS-*OSR1* or UAS-*OSR2* on the third chromosome were generated. These flies were then crossed to the pan-neuronal RU486-inducible elavGS driver line for experiments, unless otherwise stated. To confirm transgene expression, qPCR was performed on heads from female progeny crossed to the elavGS driver, 48 hours after induction with RU486. Overexpression of all transgenes was achieved when induced with RU486 compared to respective uninduced controls (Figure 3.5).

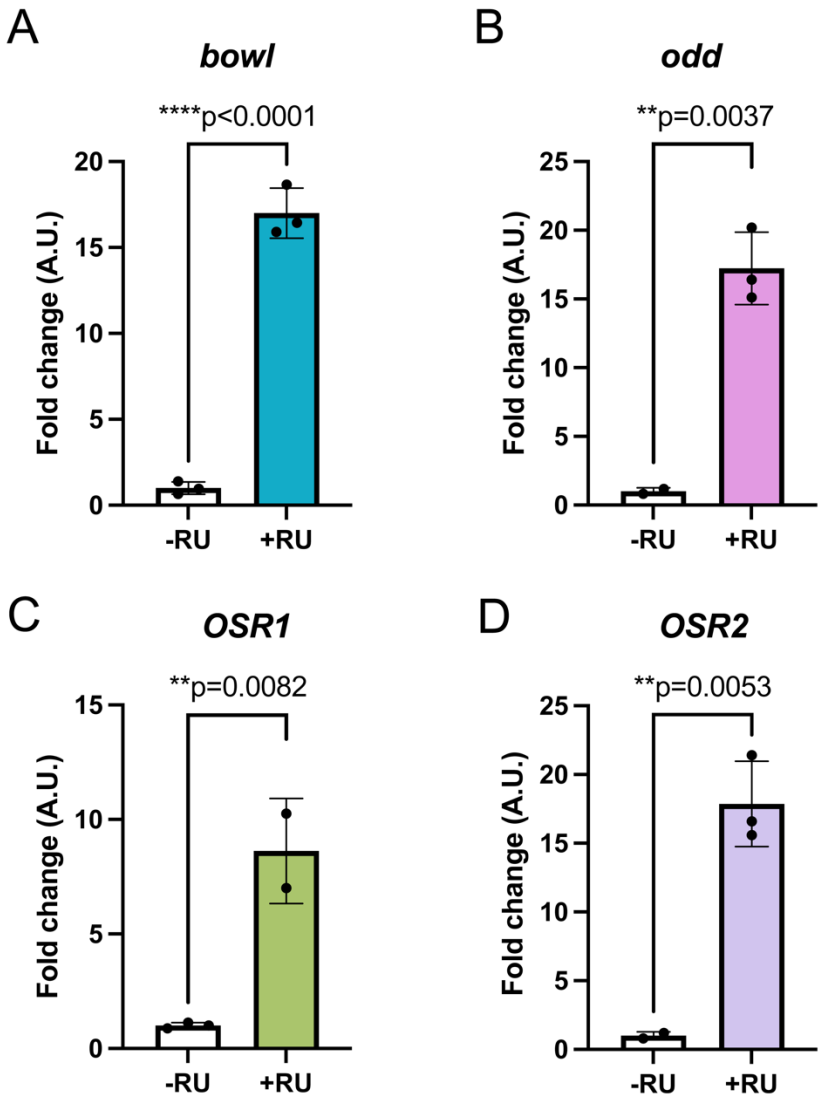

Figure 3.5. Confirmation of transgene overexpression.
A. *Bowl* mRNA levels measured by qPCR, relative to tubulin in C9 expressing flies (+RU) and uninduced controls (-RU). B. *Odd* mRNA levels measured by qPCR, relative to tubulin in C9 expressing flies (+RU) and uninduced controls (-RU). C. *OSR1* mRNA levels measured by qPCR, relative to tubulin in C9 expressing flies (+RU) and uninduced controls (-RU). B. *OSR2* mRNA levels measured by qPCR, relative to tubulin in C9 expressing flies (+RU) and uninduced controls (-RU). **p<0.01, ****p<0.0001 by unpaired t-test. N=2-3 biological replicates, containing 15 fly heads per replicate. Genotypes: *UAS-$(G_4C_2)_{36}$, elavGS; UAS-$(G_4C_2)_{36}$, elavGS/UAS-bowl; UAS-$(G_4C_2)_{36}$, elavGS/UAS-odd; UAS-$(G_4C_2)_{36}$, elavGS/UAS-OSR1; UAS-$(G_4C_2)_{36}$, elavGS/UAS-OSR2.*

To assess whether human *OSR1* or *OSR2* expression could also reduce C9 toxicity in *Drosophila*, survival experiments were performed in parallel with *odd* and *bowl*, with a shared control expressing only $(G_4C_2)_{36}$. Human *OSR1* and *OSR2* significantly extended survival of C9 *Drosophila,* as did *odd* and *bowl*

(Figure 3.6). However, the extent of survival benefit varied between the Odd-skipped family genes, despite similar levels of overexpression (Figure 3.5). Percentage increases in median survival compared to $(G_4C_2)_{36}$; elavGS alone (median 12 days), were 95% (*bowl*, median 23.5 days), 541% (*odd*, median 77 days), 75% (*OSR1*, median 21 days), 316% (*OSR2*, median 50 days) (Figure 3.6).

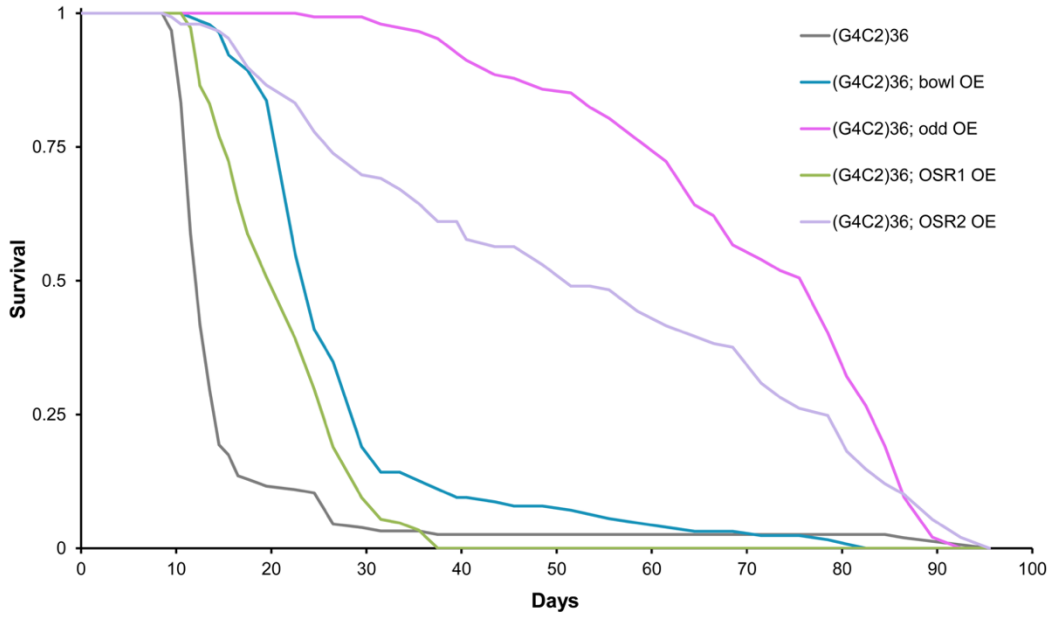

Figure 3.6. Lifespan of $(G_4C_2)_{36}$ expressing flies with and without Odd-skipped gene co-expression.
Lifespan of $(G_4C_2)_{36}$ flies was significantly extended by co-expression of *bowl* ($p=2.3\times10^{-24}$), *odd* ($p=4.6\times10^{-51}$), *OSR1* ($p=2\times10^{-14}$), and *OSR2* ($p=1.5\times10^{-39}$), all log-rank test. N=150 flies per condition. Genotypes: *UAS-$(G_4C_2)_{36}$, elavGS; UAS-$(G_4C_2)_{36}$, elavGS/UAS-bowl; UAS-$(G_4C_2)_{36}$, elavGS/UAS-odd; UAS-$(G_4C_2)_{36}$, elavGS/UAS-OSR1; UAS-$(G_4C_2)_{36}$, elavGS/UAS-OSR2*.

3.2.5 Odd-skipped genes have divergent effects on DPRs - odd and OSR2 reduce DPR levels, while bowl and OSR1 do not

To determine whether the substantial differences in the magnitude of survival extension might be explained by varying effects on DPR levels, western blots for poly(GP) and MSD immunoassays for poly(GR) were performed. *Odd*, but not *bowl*, overexpression led to a decrease in poly(GP) as measured by western blot (Figure 3.7 A and E), potentially explaining the greater rescue by *odd* compared

to *bowl* overexpression. Similarly, *OSR2*, but not *OSR1* led to a reduction in poly(GP) (Figure 3.7 B and F), again consistent with the relative magnitude of their rescues of lifespan. Instead of the expected size band, a fainter low molecular weight band was detected in both the *odd* and *OSR2* conditions, but not in the *bowl* or *OSR1* conditions (Figure 3.7 C-E). Furthermore, *odd* but not *bowl* also reduced levels of poly(GR) as quantified by MSD immunoassay (Figure 3.7 G). Similarly, *OSR2* but not *OSR1* decreased levels of poly(GR), albeit non-significantly (Figure 3.7 H). Therefore, differences in the magnitude of survival extension correlated with differential effects on DPR levels – *odd* and *OSR2* overexpression produced greater survival extensions than *bowl* or *OSR1*, and *odd* and *OSR2* decreased DPR levels, whereas *bowl* and *OSR1* did not.

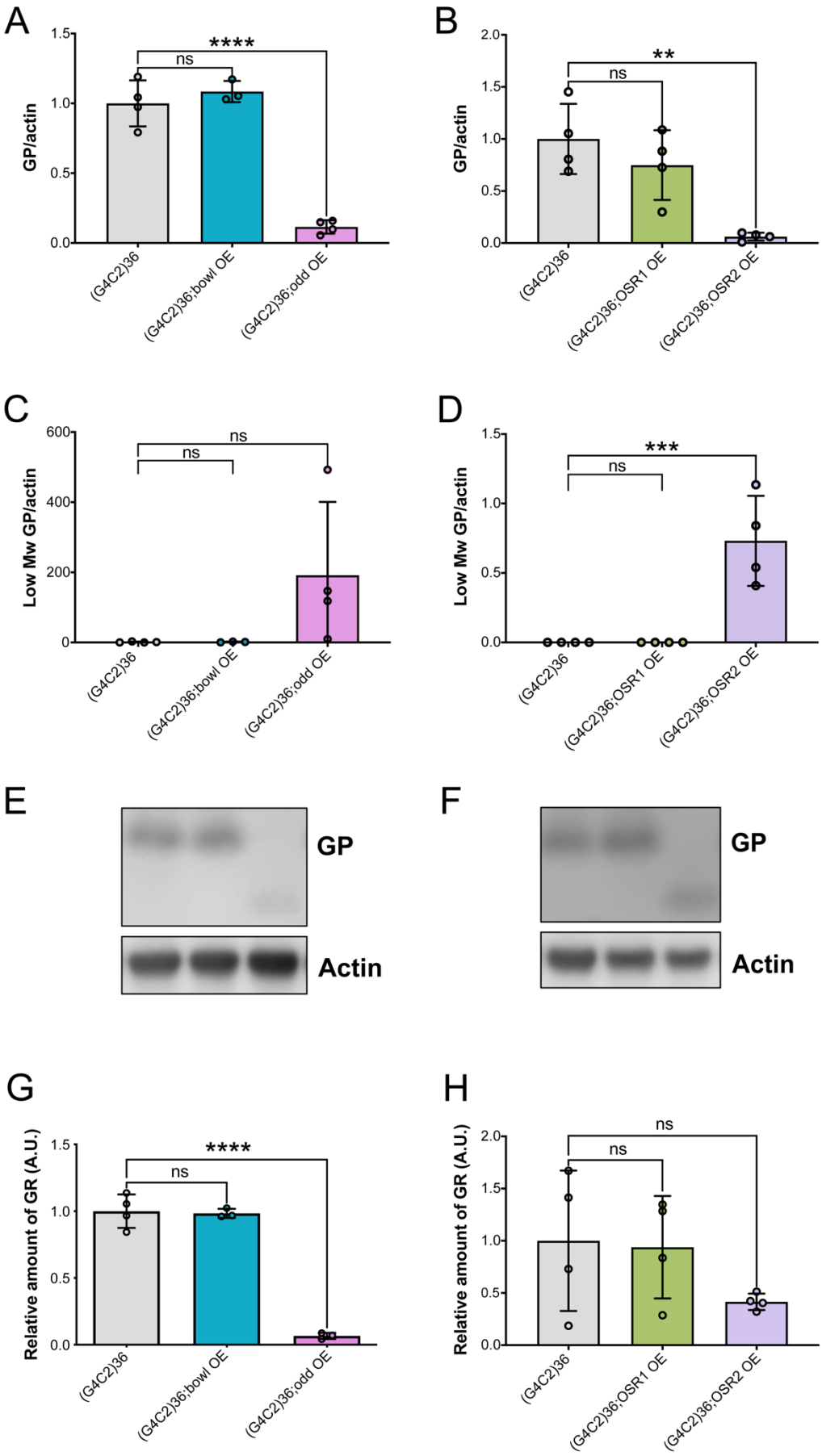
A
GP/actin
1.5
1.0
0.5
0.0
****
ns
(G4C2)36
(G4C2)36;bowl OE
(G4C2)36;odd OE
B
GP/actin
2.0
1.5
1.0
0.5
0.0
**
ns
(G4C2)36
(G4C2)36;OSR1 OE
(G4C2)36;OSR2 OE
C
Low Mw GP/actin
600
400
200
0
ns
ns
(G4C2)36
(G4C2)36;bowl OE
(G4C2)36;odd OE
D
Low Mw GP/actin
1.5
1.0
0.5
0.0
***
ns
(G4C2)36
(G4C2)36;OSR1 OE
(G4C2)36;OSR2 OE
E
GP
Actin
F
GP
Actin
G
Relative amount of GR (A.U.)
1.5
1.0
0.5
0.0
****
ns
(G4C2)36
(G4C2)36;bowl OE
(G4C2)36;odd OE
H
Relative amount of GR (A.U.)
2.0
1.5
1.0
0.5
0.0
ns
ns
(G4C2)36
(G4C2)36;OSR1 OE
(G4C2)36;OSR2 OE

Figure 3.7. Odd-skipped family genes have different effects on DPR levels. A. GP levels in C9 fly heads with or without *bowl* or *odd* co-expression. N=3-4 biological replicates, containing 10 fly heads per replicate. One way ANOVA with Tukey's multiple comparison test. B. GP levels in C9 fly heads with or without *OSR1* or *OSR2* co-expression. N=4 biological replicates, containing 10 fly heads per replicate. One way ANOVA with Tukey's multiple comparison test. C. Low molecular weight GP quantification in C9 fly heads with or without *bowl* or *odd* co-expression. N=3-4 biological replicates, containing 10 fly heads per replicate. One way ANOVA with Tukey's multiple comparison test. D. Low molecular weight GP quantification in C9 fly heads with or without *OSR1* or *OSR2* co-expression. N=4 biological replicates, containing 10 fly heads per replicate. One way ANOVA with Tukey's multiple comparison test. E. Western blot for GP levels in C9 fly heads with or without *bowl* or *odd* co-expression, as quantified in A and C. F. Western blot for GP levels in C9 fly heads with or without *OSR1* or *OSR2* co-expression, as quantified in B and D. G. GR levels in C9 fly heads with or without *bowl* or *odd* co-expression. N=4 biological replicates, containing 10 fly heads per replicate. One way ANOVA with Tukey's multiple comparison test. H. GR levels in C9 fly heads with or without *OSR1* or *OSR2* co-expression. N=4 biological replicates, containing 10 fly heads per replicate. One way ANOVA with Tukey's multiple comparison test. Data is presented as mean ± S.D. **p<0.01, ***p<0.001, ****p<0.0001. *Genotypes: UAS-*$(G_4C_2)_{36}$*, elavGS; UAS-*$(G_4C_2)_{36}$*, elavGS/UAS-bowl; UAS-*$(G_4C_2)_{36}$*, elavGS/UAS-odd; UAS-*$(G_4C_2)_{36}$*, elavGS/UAS-OSR1; UAS-*$(G_4C_2)_{36}$*, elavGS/UAS-OSR2*.

3.2.6 General translation efficiency is not affected by *odd* or *bowl*

A reduction in DPRs could be due to an indirect effect on the inducible expression system, causing a general decrease in translation efficiency. To determine if this was the case, the levels of GFP driven by the elavGS RU486 inducible driver, were measured, with or without *bowl* or *odd* co-expression. GFP levels were unchanged by *bowl* or *odd* co-expression, confirming that general translation efficiency was not altered by the Odd-skipped family (Figure 3.8).

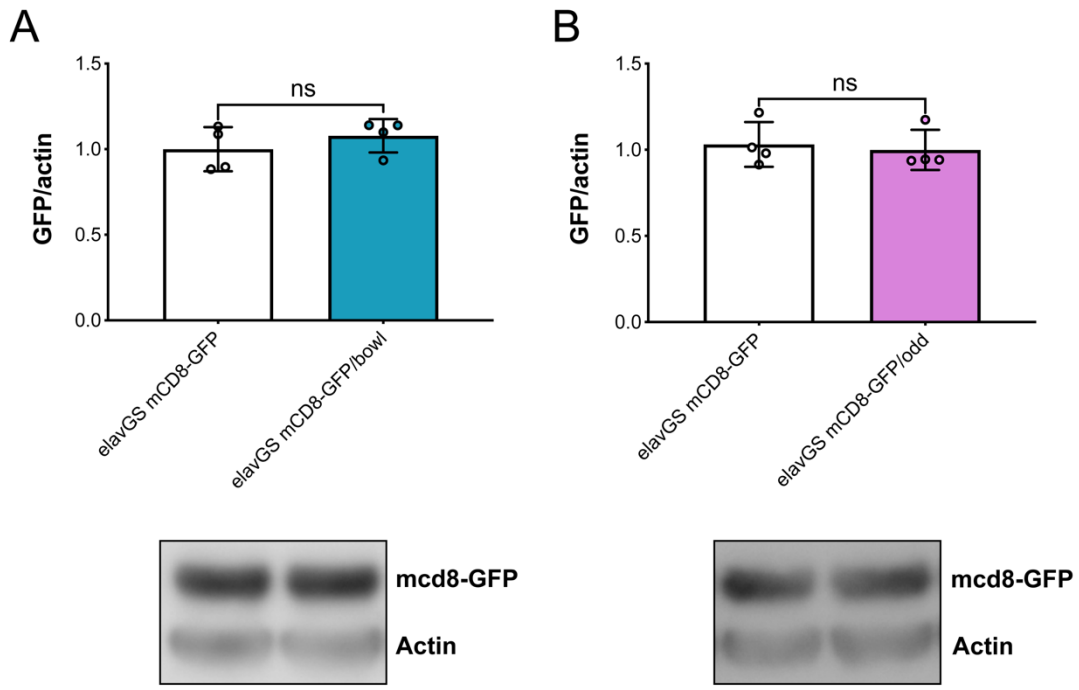

Figure 3.8. General translation efficiency is not affected by expression of *odd* or *bowl*.
A. mCD8-GFP levels in fly heads over-expressing mCD8-GFP and the FlyORF empty vector or *bowl* after 7 days of induction, p=0.3705 by unpaired t-test. B. mCD8-GFP levels in fly heads over-expressing mCD8-GFP and the FlyORF empty vector or *odd* after 7 days of induction, p=0.7284 by unpaired t-test. N=4 biological replicates, each containing 10 heads. Data is presented as mean ± S.D. Genotypes: *UAS-mCD8GFP, elavGS/UAS-bowl, UAS-mCD8GFP, elavGS/UAS-odd.*

3.2.7 Odd-skipped family can extend survival of $(GR)_{36}$ flies

A reduction in DPR levels could be due to specific effects on RAN translation of DPRs or due to enhanced degradation of DPRs. To distinguish between these possibilities, *odd* and *bowl* were crossed to flies expressing a recodonised construct, that allows AUG-initiated expression of poly(GR) alone without an underlying GGGGCC repeat sequence capable of undergoing RAN translation. Both *odd* and *bowl* extended survival of flies expressing ATG-driven $(GR)_{36}$, with percentage increases in median survival compared to (GR)36; elavGS alone (median 15 days), of 6.6% (*bowl*, median 16 days) and 13% (*odd*, median 17 days) (Figure 3.9). However, the magnitude of the extensions was much less than those observed when *odd* and *bowl* were overexpressed in $(G_4C_2)_{36}$ pure repeat

flies capable of undergoing RAN translation from the underlying GGGGCC repetitive sequence. Therefore, rescue by *odd* and *OSR2* may be in part due to effects on RAN translation, while non-RAN translation effects, that have a more modest suppression of toxicity, may account for the shared survival benefits by *odd*, *bowl*, *OSR1* and *OSR2*. This would provide an explanation as to why there is only modest rescue of survival in the UAS-$(GR)_{36}$ flies.

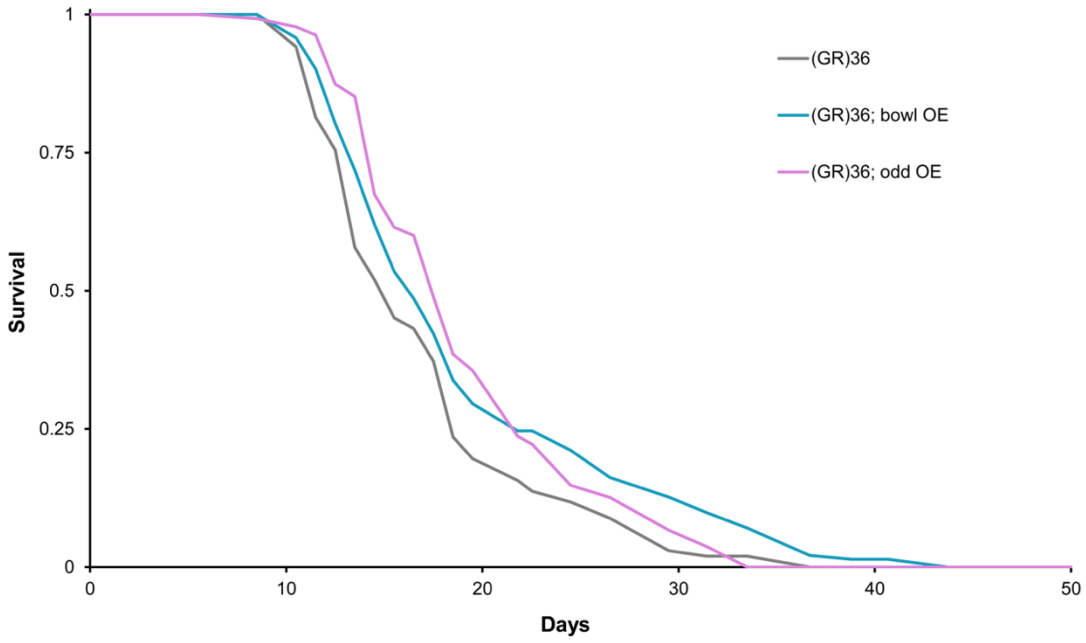

Figure 3.9. Lifespan of $(GR)_{36}$ expressing flies with and without *odd* or *bowl* co-expression.
Lifespan of $(GR)_{36}$ flies was significantly extended by co-expression of *bowl* (p=0.015) or *odd* (p=0.012), both log-rank test. N=102-142 flies per condition. *Genotypes: UAS-$(GR)_{36}$, elavGS; UAS-$(GR)_{36}$, elavGS/UAS-bowl; UAS-$(GR)_{36}$, elavGS/UAS-odd*.

3.2.8 Odd-skipped rescues of C9 toxicity are limited to post-mitotic neurons

Expression of poly(GR) in the developing eye using the GMR-Gal4 driver leads to mild degeneration and a reduction in eye size (Mizielinska *et al.*, 2014). Therefore, to assess whether *odd* and *bowl* could also rescue this alternative model of $(GR)_{36}$ toxicity, UAS-*bowl* and UAS-*odd* flies were crossed to flies expressing $(GR)_{36}$ using the GMR-Gal4 driver. As previously reported, a rough eye phenotype, and reduction of eye area was exhibited in flies expressing $(GR)_{36}$

(Figure 3.10). Both *odd* and *bowl* overexpression in the absence of $(GR)_{36}$ expression led to a reduction in eye size (Figure 3.10). *Bowl* but not *odd* overexpression also exacerbated poly(GR) toxicity, as quantified by a reduction in eye area compared to $(GR)_{36}$ expression alone (Figure 3.10). This result indicates that Odd-skipped rescues are limited to post-mitotic neurons as their overexpression in developing eyes exacerbated rather than rescued toxicity.

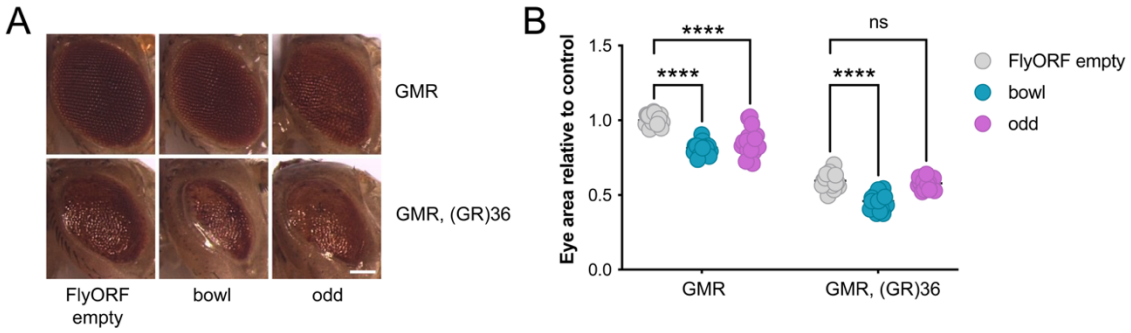

Figure 3.10. Odd-skipped expression in the developing eye exacerbates poly(GR) toxicity.
A. Stereomicroscopy images of representative 2-day-old adult *Drosophila* eyes expressing bowl or odd using the GMR-Gal4 driver (top panel) or co-expressing both (GR)36 and *bowl* or *odd* constructs (bottom panel). Scale bar = 0.1mm. B. Overexpression of bowl or odd in a wildtype background with GMR driver decreased eye area (****p<0.0001, N=20 individual fly eyes per condition). Overexpression of *bowl* decreased eye area of $(GR)_{36}$ flies (****p<0.0001), while *odd* had no significant effect on eye area of $(GR)_{36}$ flies (p=0.48) (N=20 individual fly eyes per condition). Two-way ANOVA followed by Tukey's multiple comparison test was used. A significant interaction effect between Odd-skipped genotype and expression of the repeats was found (p<0.0001). Data is presented as mean ± S.D. *Genotypes: GMR-Gal4; GMR-Gal4, UAS-bowl; GMR-Gal4, UAS-odd; GMR-Gal4, UAS-$(GR)_{36}$; GMR-Gal4, UAS-$(GR)_{36}$, UAS-bowl; GMR-Gal4, UAS-$(GR)_{36}$, UAS-odd.*

3.2.9 Odd-skipped family ameliorate motor impairments in C9 flies

To assess whether overexpressing Odd-skipped family members could rescue a distinct neuronal phenotype in $(G_4C_2)_{36}$ flies, motor activity was recorded using a *Drosophila* activity monitor system. As previously reported, expression of $(G_4C_2)_{36}$ in adult neurons led to a reduction in motor activity (Figure 3.11) (Atilano *et al.*, 2021). This phenotype was abolished by overexpression of *bowl* or *odd* (Figure 3.11).

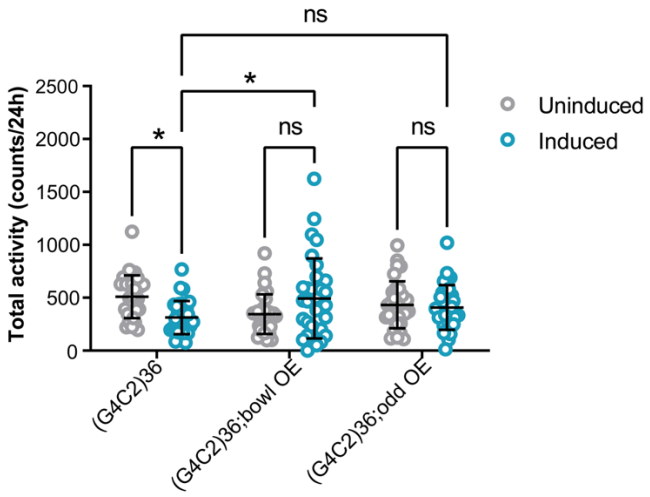

Figure 3.11. Neuronal overexpression of odd or bowl improves motor activity of $(G_4C_2)_{36}$ flies.
Total activity of flies expressing $(G_4C_2)_{36}$ in neurons was significantly reduced compared with uninduced control flies (*p= 0.0129). $(G_4C_2)_{36}$ flies co-expressing *bowl* showed increased activity (*p=0.0307) compared with flies expressing $(G_4C_2)_{36}$ alone, and no significant difference in activity compared to their uninduced sibling controls (p=0.1289). $(G_4C_2)_{36}$ flies co-expressing *odd* showed no significant difference in activity compared with flies expressing $(G_4C_2)_{36}$ alone (p=0.3245) and no significant difference in activity compared to their uninduced sibling controls (p=0.9983). There was a significant interaction effect of genotype x RU486 induction (p=0.0003). Two-way ANOVA followed by Tukey's multiple comparison test was used for statistical analyses. Data are presented as mean ± S.D. N=32 per genotype. Genotypes: *UAS-$(G_4C_2)_{36}$, elavGS; UAS-$(G_4C_2)_{36}$, elavGS/UAS-bowl; UAS-$(G_4C_2)_{36}$, elavGS/UAS-odd.*

3.2.10 Odd-skipped rescues of C9 toxicity are not limited to neurons

To determine whether Odd-skipped rescue of C9 toxicity is limited to adult neurons, C9 repeats were expressed throughout the whole body of *Drosophila*, using a daughterless Gal4-gene switch driver (daGS). Overexpression of *odd* or *bowl* extended survival of flies expressing $(G_4C_2)_{36}$ repeats in all tissues (Figure 3.12). Percentage increases in median survival compared to $(G_4C_2)_{36}$; daGS alone (median 24.5 days), were 141% (*bowl*, median 59 days) and 114% (*odd*, median 52.5 days). This finding demonstrates that *odd* and *bowl* rescues are not limited to neurons and/ or most of the toxicity associated with this model is driven by the neuronal contribution, which *bowl* and *odd* are also rescuing with daGS

expression. The magnitude of rescue provided neuronal expression of *odd* and *bowl*, using the elavGS driver (Figure 3.6), was greater than that provided by whole body expression using the daGS driver, suggesting that the rescue effect is greatest in neurons.

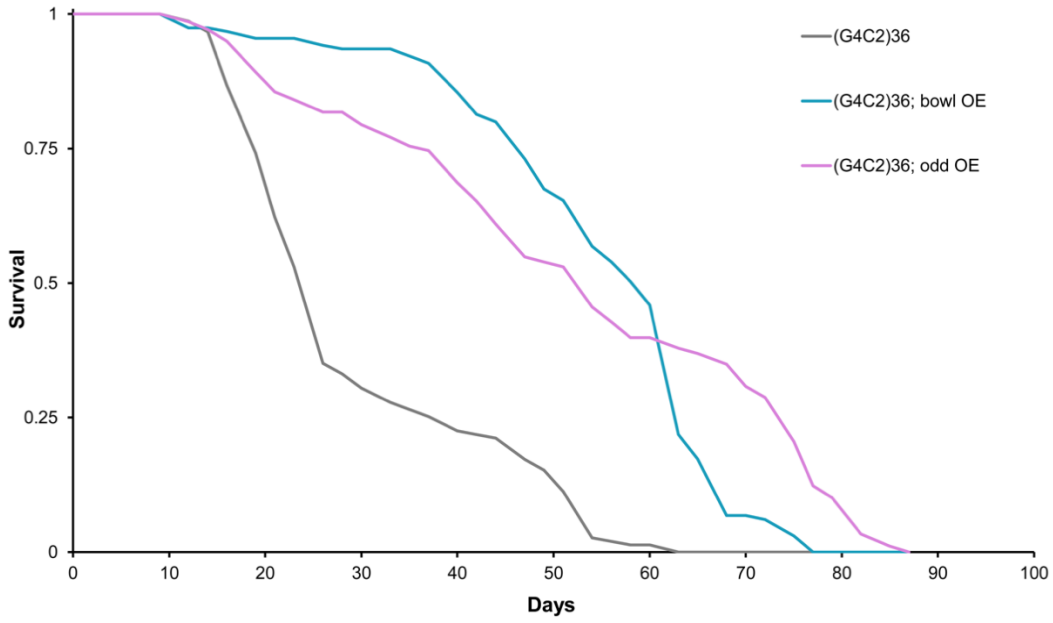

Figure 3.12. Lifespan of flies expressing $(G_4C_2)_{36}$ in all tissues with and without *odd* or *bowl* co-expression.
Lifespan of $(G_4C_2)_{36}$ flies was significantly extended by co-expression of *bowl* ($p=2.8x10^{-34}$) or *odd* ($p=8.1x10^{-20}$), both log-rank test. N=139-155 flies per condition. Genotypes: *UAS-$(G_4C_2)_{36}$, daGS; UAS-$(G_4C_2)_{36}$, daGS/UAS-bowl; UAS-$(G_4C_2)_{36}$, daGS/UAS-odd.*

3.2.11 RNA-sequencing identifies Odd-skipped targets

The second aim of this study was to identify potential downstream targets of the Odd-skipped family of transcription factors that may be mediating the beneficial effects on survival. Since Odd, Bowl, OSR1 and OSR2 are highly conserved within the zinc finger regions, it is likely that they bind similar target DNA sequences and produce similar transcriptional profiles. The Odd and Bowl lines used here were C-terminally tagged with 3xHA. Therefore, a chromatin immunoprecipitation experiment was conducted using a HA antibody to experimentally identify direct targets of both Odd and Bowl. However, sequencing results revealed that the experiment was unsuccessful, as the pull downs had

very little DNA compared to the inputs and no significant peaks were detected (data not included). Inaccessibility of the HA tags or technical failure may have been factors in this unsuccessful experiment. As an alternative approach, RNA-sequencing was performed to identify shared genes and pathways that were altered by Odd-skipped family genes in the context of C9 repeats. RNA was isolated from heads of C9 flies with or without co-expression of *odd, bowl, OSR1* or *OSR2*, after 5 days of induction with RU486. Four biological replicates, each consisting of 15 heads, were used per condition. RNA library preparation, sequencing and DESeq2 analysis was carried out by UCL Genomics core facility. RNA libraries were prepared for sequencing with KAPA mRNA HyperPrep kit. RNA-sequencing (Next Seq 2000) was carried out on these samples at a depth of 16 million reads. Principal component analysis revealed that biological replicates clustered together, indicating that biological variability is the main source of variance in the data. One potential outlier was identified in the C9 OSR1 condition (Figure 3.13).

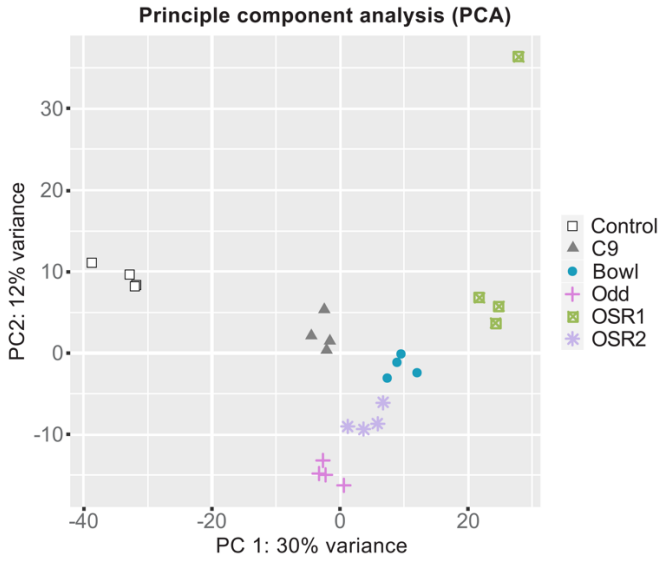

Figure 3.13. Principal component analysis plot of biological groups.
Most replicates within biological conditions cluster together. One potential outlier is identified for C9 OSR1 condition. Genotypes: *UAS-$(G_4C_2)_{36}$, elavGS; UAS-$(G_4C_2)_{36}$, elavGS/UAS-bowl; UAS-$(G_4C_2)_{36}$, elavGS/UAS-odd; UAS-$(G_4C_2)_{36}$, elavGS/UAS-OSR1; UAS-$(G_4C_2)_{36}$, elavGS/UAS-OSR2.*

Gene ontology (GO) biological enrichment analysis was performed on all C9 Odd-skipped conditions versus C9. GO analysis was performed by Dr Alla Mikheenko,

a postdoctoral bioinformatician in the Isaacs lab. GO enrichment terms for both upregulated and downregulated genes were distinct for each set of comparisons (Figure 3.14). The four Odd-skipped transcription factors appear to affect expression of genes involved in different high-level pathways, with no shared pathways between all four conditions. However, there were some overlaps in pathway enrichments between the conditions - cellular modified amino acid metabolic process was enriched among downregulated genes in both Bowl and Odd conditions; mating behaviour was enriched among upregulated genes in Odd, OSR1 and OSR2 conditions; multicellular organism development enriched among upregulated genes in both Odd and OSR2 conditions; double strand break repair was enriched among downregulated genes in Odd and OSR2 conditions but enriched among upregulated genes in the OSR1 condition; lipid metabolic process was enriched among downregulated genes in OSR1 and OSR2 conditions.

A

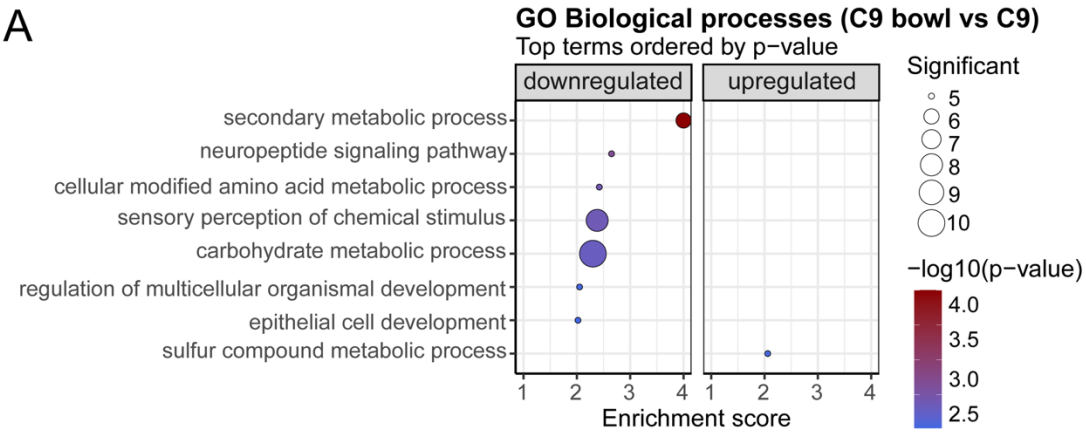
GO Biological processes (C9 bowl vs C9)
Top terms ordered by p−value
downregulated
upregulated
secondary metabolic process
neuropeptide signaling pathway
cellular modified amino acid metabolic process
sensory perception of chemical stimulus
carbohydrate metabolic process
regulation of multicellular organismal development
epithelial cell development
sulfur compound metabolic process
1 2 3 4
Enrichment score
Significant
5
6
7
8
9
10
−log10(p−value)
4.0
3.5
3.0
2.5

B

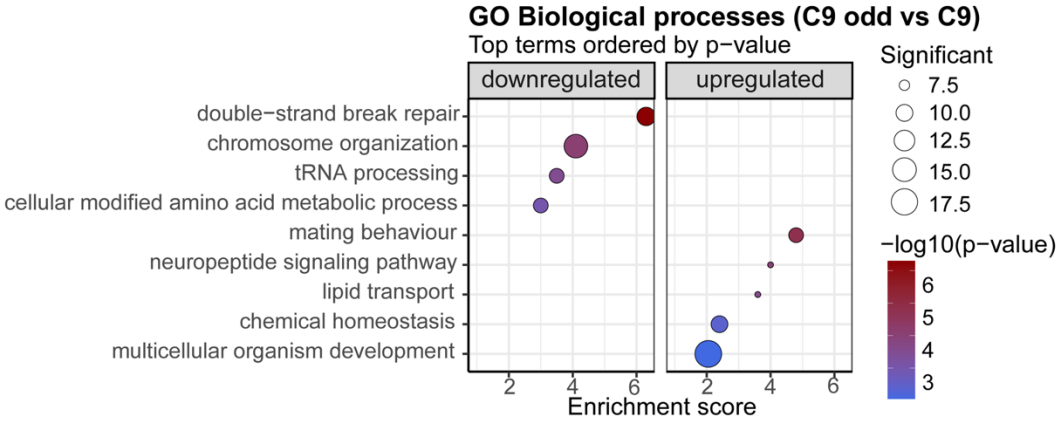
GO Biological processes (C9 odd vs C9)
Top terms ordered by p−value
downregulated
upregulated
double−strand break repair
chromosome organization
tRNA processing
cellular modified amino acid metabolic process
mating behaviour
neuropeptide signaling pathway
lipid transport
chemical homeostasis
multicellular organism development
2 4 6
Enrichment score
Significant
7.5
10.0
12.5
15.0
17.5
−log10(p−value)
6
5
4
3

C

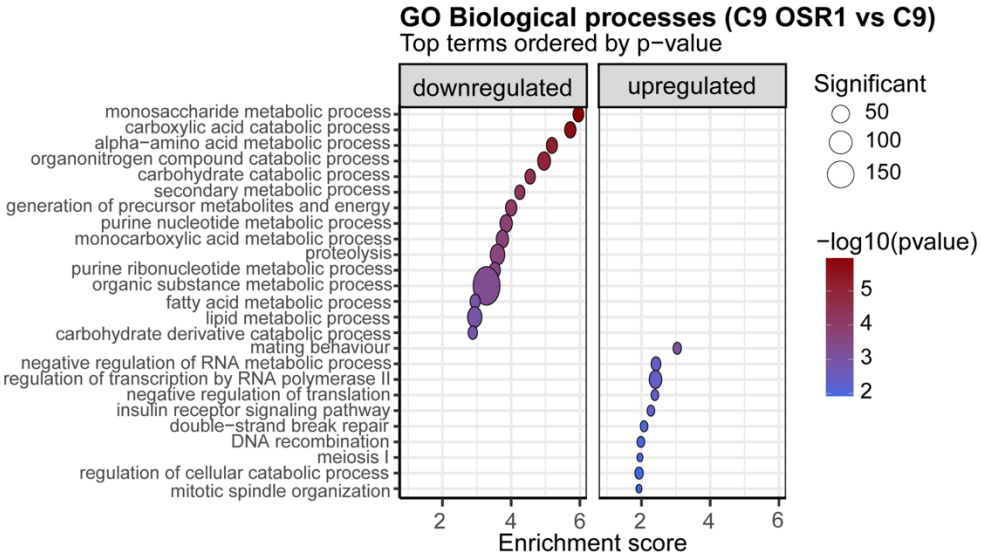
GO Biological processes (C9 OSR1 vs C9)
Top terms ordered by p−value
downregulated
upregulated
monosaccharide metabolic process
carboxylic acid catabolic process
alpha−amino acid metabolic process
organonitrogen compound catabolic process
carbohydrate catabolic process
secondary metabolic process
generation of precursor metabolites and energy
purine nucleotide metabolic process
monocarboxylic acid metabolic process
proteolysis
purine ribonucleotide metabolic process
organic substance metabolic process
fatty acid metabolic process
lipid metabolic process
carbohydrate derivative catabolic process
mating behaviour
negative regulation of RNA metabolic process
regulation of transcription by RNA polymerase II
negative regulation of translation
insulin receptor signaling pathway
double−strand break repair
DNA recombination
meiosis I
regulation of cellular catabolic process
mitotic spindle organization
2 4 6
Enrichment score
Significant
50
100
150
−log10(pvalue)
5
4
3
2

D

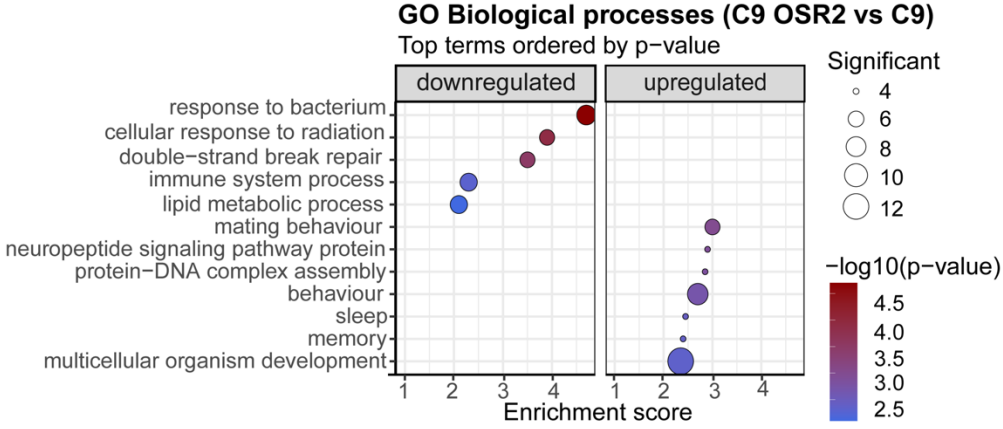
GO Biological processes (C9 OSR2 vs C9)
Top terms ordered by p−value
downregulated
upregulated
response to bacterium
cellular response to radiation
double−strand break repair
immune system process
lipid metabolic process
mating behaviour
neuropeptide signaling pathway protein
protein−DNA complex assembly
behaviour
sleep
memory
multicellular organism development
1 2 3 4
Enrichment score
Significant
4
6
8
10
12
−log10(p−value)
4.5
4.0
3.5
3.0
2.5

Figure 3.14. Gene ontology biological process enrichment plots of differentially expressed genes in C9 Odd-skipped conditions versus C9. Circle colour indicates negative log-transformed, adjusted p-values for Fisher's exact enrichment test. X axis indicates log2-fold change as enrichment. Size of circles represents significance. A. GO plot of differentially expressed genes in C9 bowl versus C9 fly heads, after 5 days. B. GO plot of differentially expressed genes in C9 odd versus C9 fly heads. C. GO plot of differentially expressed genes in C9 OSR1 versus C9 fly heads. D. GO plot of differentially expressed genes in C9 OSR2 versus C9 fly heads. Genotypes: *UAS-$(G_4C_2)_{36}$, elavGS; UAS-$(G_4C_2)_{36}$, elavGS/UAS-bowl; UAS-$(G_4C_2)_{36}$, elavGS/UAS-odd; UAS-$(G_4C_2)_{36}$, elavGS/UAS-OSR1; UAS-$(G_4C_2)_{36}$, elavGS/UAS-OSR2.*

Common individual genes or groups of genes belonging to disparate biological pathways may instead be mediating Odd skipped rescues. To increase the probability of direct Odd-skipped target identification, an analysis was performed by Dr Alla Mikheenko to identify differentially expressed genes containing the highly conserved Odd-skipped binding motif (GCTACTG) (Noyes *et al.*, 2008). 465 differentially expressed genes, including both upregulated and downregulated genes across all comparisons contained an Odd-skipped binding motif. The top differentially expressed genes, based on fold change, containing an Odd-skipped binding motif are presented as a heatmap (Figure 3.15). The C9 Odd versus C9 and C9 OSR2 versus C9 comparisons clustered together, as did C9 Bowl versus C9 and C9 OSR1 versus C9 (Figure 3.15). This is interesting given that both *odd* and *OSR2* reduced DPR levels, whereas *bowl* and *OSR2* did not (Figure 3.7).

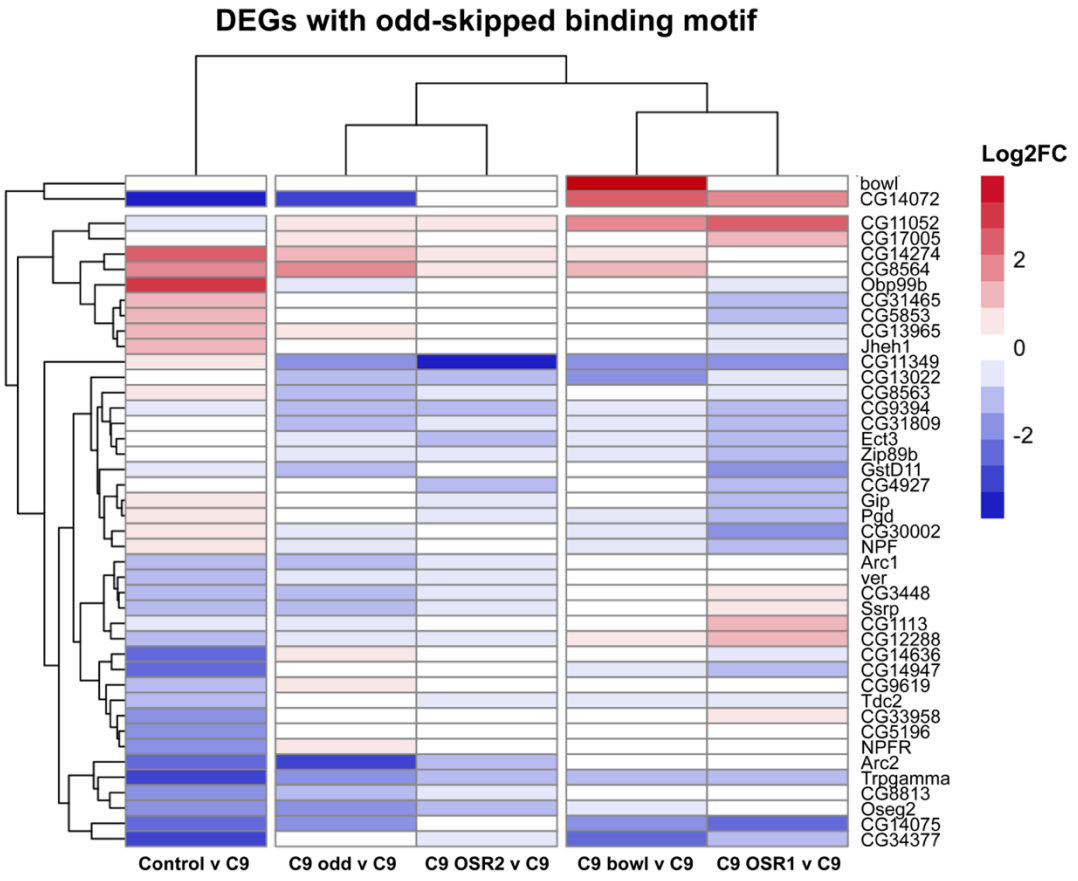

Figure 3.15. Heatmap of top differentially expressed genes by fold change containing a highly conserved Odd-skipped binding motif.
Genotypes: *UAS-$(G_4C_2)_{36}$, elavGS; UAS-$(G_4C_2)_{36}$, elavGS/UAS-bowl; UAS$(G_4C_2)_{36}$, elavGS/UAS-odd; UAS-$(G_4C_2)_{36}$, elavGS/UAS-OSR1; UAS-$(G_4C_2)_{36}$, elavGS/UAS-OSR2.*

Prioritisation for target follow-up was given to individual genes commonly altered across two or more Odd-skipped conditions, which contained a conserved Odd-skipped binding motif and which had mammalian orthologs. Using these criteria, *hec*, *Trpγ, Arc1, Ect3, CG9394* and *Odc2* were selected for follow up. The raw count data for each of these targets is graphed below (Figure 3.16).

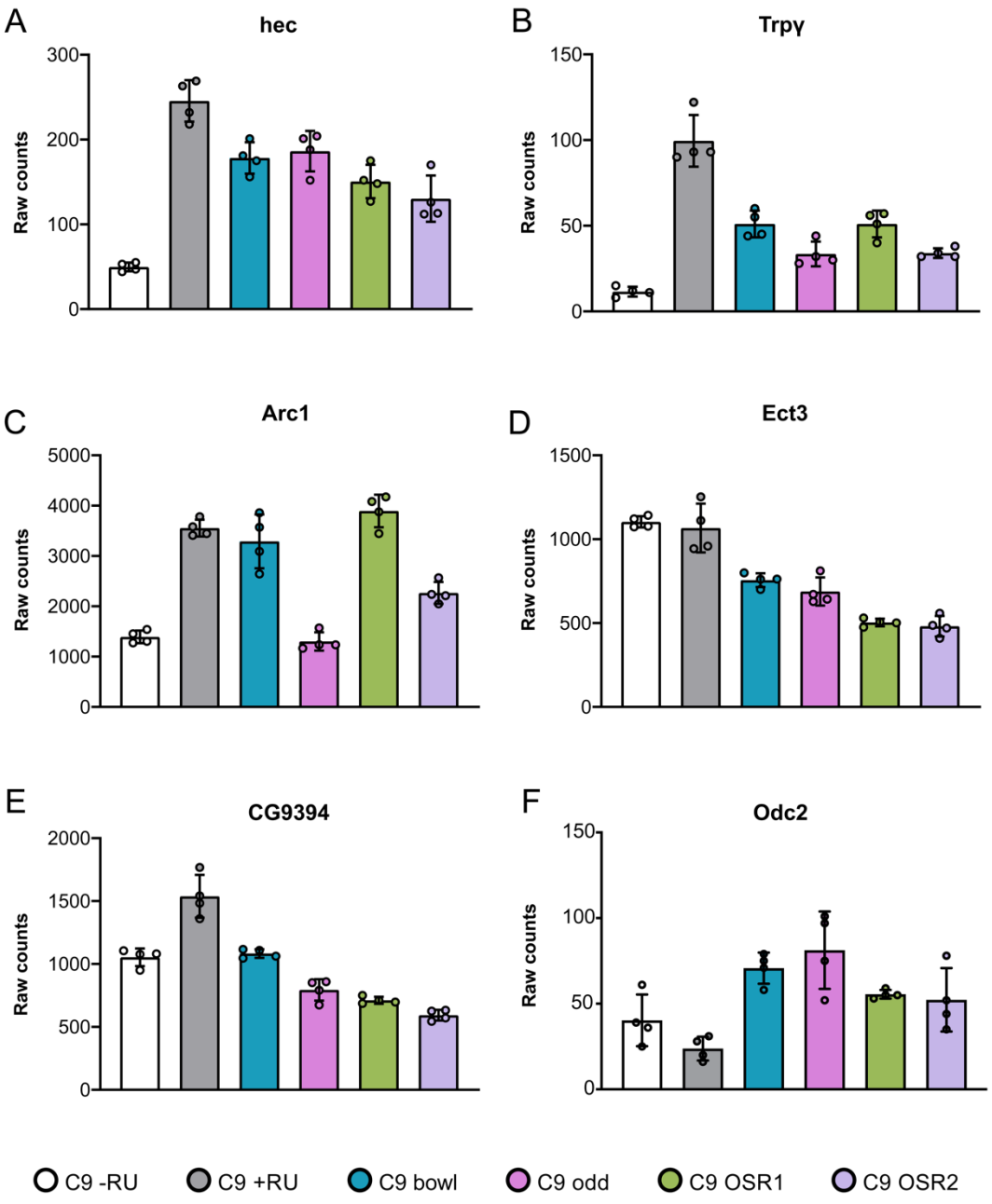

Figure 3.16. RNA-sequencing count data for putative Odd-skipped target genes.

A. Raw count data for hector (hec). B. Raw count data for *Trpγ*. C. Raw count data for *Arc1*. D. Raw count data for *Ect3*. E. Raw count data for *CG9394*. F. Raw count data for *Odc2*. Raw counts were used for direct comparisons. Genotypes: *UAS-$(G_4C_2)_{36}$, elavGS; UAS-$(G_4C_2)_{36}$, elavGS/UAS-bowl; UAS-$(G_4C_2)_{36}$, elavGS/UAS-odd; UAS$(G_4C_2)_{36}$, elavGS/UAS-OSR1; UAS-$(G_4C_2)_{36}$, elavGS/UAS-OSR2.*

To visualise the results of differential expression analysis, volcano plots were produced for C9 versus control and all C9 Odd-skipped conditions versus C9

comparisons. The six genes selected for follow-up are highlighted in the volcano plots (Figure 3.17). Overexpression of *bowl* and *odd* was also confirmed for this RNA-sequencing experiment, with *bowl* and *odd* each being the most significantly upregulated genes in C9 bowl versus C9 (Figure 3.17 B) and C9 odd versus C9 (Figure 3.17 C) respectively. *Trpγ, Ect3, CG9394* and *Arc1* are classified among the top differentially expressed genes containing an Odd-skipped binding motif, by fold change (Figure 3.13). The expression of *hec, Trpγ* and *CG9394* is increased by C9 and decreased by all Odd-skipped genes (Figure 3.16 and Figure 3.17). *Ect3* expression is unchanged by C9 but decreased by all Odd-skipped genes. *Arc1* expression is increased by C9 and decreased by both *odd* and *OSR2* overexpression. *Odc2* expression is decreased by C9 and increased by all Odd-skipped genes (Figure 3.16 and Figure 3.17).

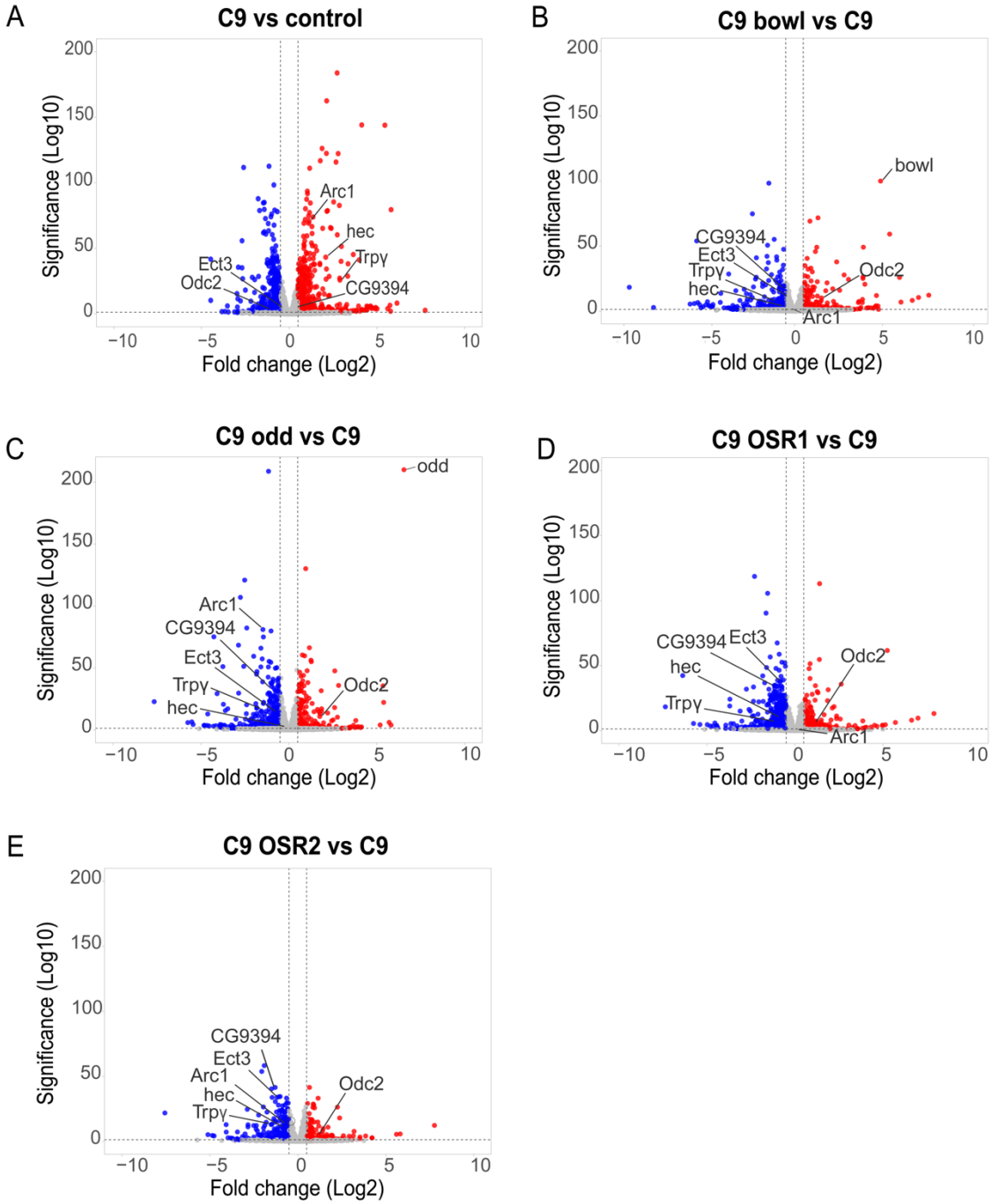

Figure 3.17. Volcano plots of fly transcriptomic data with shortlisted Odd-skipped target genes highlighted.

A. Volcano plot of differentially expressed genes in induced $(G_4C_2)_{36}$ (C9) versus uninduced (control) fly heads, after 5 days. B. Volcano plot of differentially expressed genes in C9 bowl versus C9 fly heads. C. Volcano plot of differentially expressed genes in C9 odd versus C9 fly heads. D. Volcano plot of differentially expressed genes in C9 OSR1 versus C9 fly heads. E. Volcano plot of differentially expressed genes in C9 OSR2 versus C9 fly heads. Dotted lines denote significance and fold change thresholds (-log10pvalue: 1.3, log2FC: 0.5). Graphs were produced with VolcaNoseR. Genotypes: *UAS-$(G_4C_2)_{36}$, elavGS; UAS-*

$(G_4C_2)_{36}$, elavGS/UAS-bowl; UAS$(G_4C_2)_{36}$, elavGS/UAS-odd; UAS-$(G_4C_2)_{36}$, elavGS/UAS-OSR1; UAS-$(G_4C_2)_{36}$, elavGS/UAS-OSR2.

3.2.12 Analysis of Odd-skipped targets in mammalian neurons

To assess whether the Odd-skipped targets identified were also differentially regulated in a non-disease neuronal and mammalian context, RNA-sequencing was performed on rat primary cortical neurons overexpressing either *OSR1* or *OSR2*. *OSR1* and *OSR2* were the most significantly upregulated genes when either one was overexpressed confirming successful transduction efficiency (Figure 3.18 A and B, respectively). *Calcrl*, the rat ortholog of *hec*, was downregulated by OSR1 (FC 0.387, padj $1.2x10^{-19}$) and OSR2 (FC 0.271, padj $5.43x10^{-30}$). *Trpγ* ortholog *Trpc4* was downregulated by both OSR1 (FC 0.723, padj 0.0003) and OSR2 (FC 0.752, padj 0.001). A second *Trpγ* ortholog, *Trpc5* was also downregulated by OSR1 (FC 0.779, paj $3.37x10^{-5}$) and OSR2 (FC 0.615, paj 0.002). *Arc1* ortholog *Arc* was not significantly changed by either OSR1 or OSR2. *Ect3* orthologous gene *Glb1l* was significantly upregulated by OSR2 (FC 1.276, padj 0.0.12), but not OSR1. *Gpcpd1* is the closest homolog of *CG9394*. *Gpcpd1* expression was not altered by either OSR1 (FC 1.121 padj 0.155) or OSR2 (FC 1.005, padj 0.973). *Odc1*, the rat ortholog of *Odc2* was not significantly altered by OSR1 (FC 0.962, padj 0.548) or OSR2 (FC 0.961, padj 0.456). A second orthologous gene to *Odc2*, *Azin1*, was also unchanged by either OSR1 (FC 1.028, padj 0.609) or OSR2 (FC 0.941, padj 0.067). This experiment validates three of the shortlisted Odd-skipped targets, *hec* (*Calcrl*), *Trpγ* (*Trpc4* and *Trpc5*) and *Arc1* (*Arc*), as conserved targets downregulated by Odd-skipped family transcription factors, so these were prioritised for follow-up (Figure 3.18). A disadvantage of this approach is that many of the differentially expressed genes identified by RNA-seq are likely to be indirect, rather than reflecting direct targets of these Odd-skipped transcription factors.

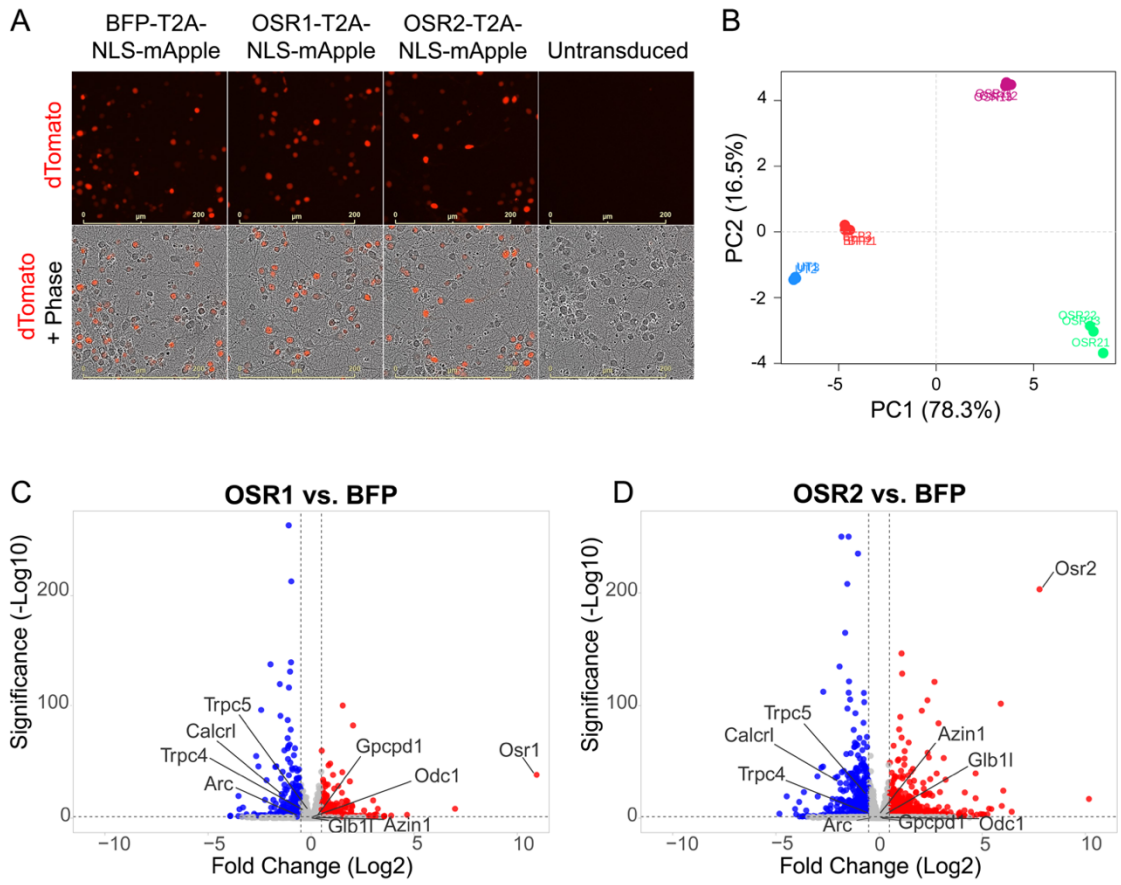

Figure 3.18. RNA-sequencing of rat primary cortical neurons overexpressing OSR1 or OSR2.
A. Incucyte images at DIV 12, confirming expression of mApple tagged OSR1 and OSR2. B. PCA plot of transcriptomic data shows clear separation of biological groups. C. Volcano plot of rat primary cortical neurons overexpressing *OSR1*. D. Volcano plot of rat primary cortical neurons overexpressing *OSR2*. Gridlines were set to -Log10(p-value) = 1.3 on the y-axis, equivalent to adjusted p-value <0.05 and Log2(Fold change) = 0.5 on the x-axis. Graphs were produced with VolcaNoseR.

3.2.13 Testing short-listed genes for effects on C9 *Drosophila* survival

To determine whether any of the shortlisted target genes could rescue C9 toxicity, the directionality of their regulation by Odd-skipped genes would need to be replicated. Therefore, TriP RNAi lines were obtained from BDSC for *hec, Trpγ, Arc1, Ect3* and *CG9394*. Overexpression lines were not available for *Odc2*; therefore, this gene was dropped from further analysis. RNAi lines were backcrossed for at least three generations into a standard v-w1118 stock before being assessed for effects on C9 survival (Figure 3.19). Knockdown of *hec*

significantly reduced C9 survival, decreasing median survival by 25%, from 19.5 days to 14.5 days (p=0.0002) (Figure 3.19 A). *Trpγ* RNAi produced a significant extension in the lower portion of the curve that increased mean survival by one day, from 17 to 18 days. However, knocking down *Trpγ* had no effect on median survival (Figure 3.19 C). Knocking down *Arc1* significantly extended C9 survival, increasing median survival by 22% from 11.5 days to 14 days. Neither *Ect3* nor *CG9394* RNAi significantly altered C9 survival.

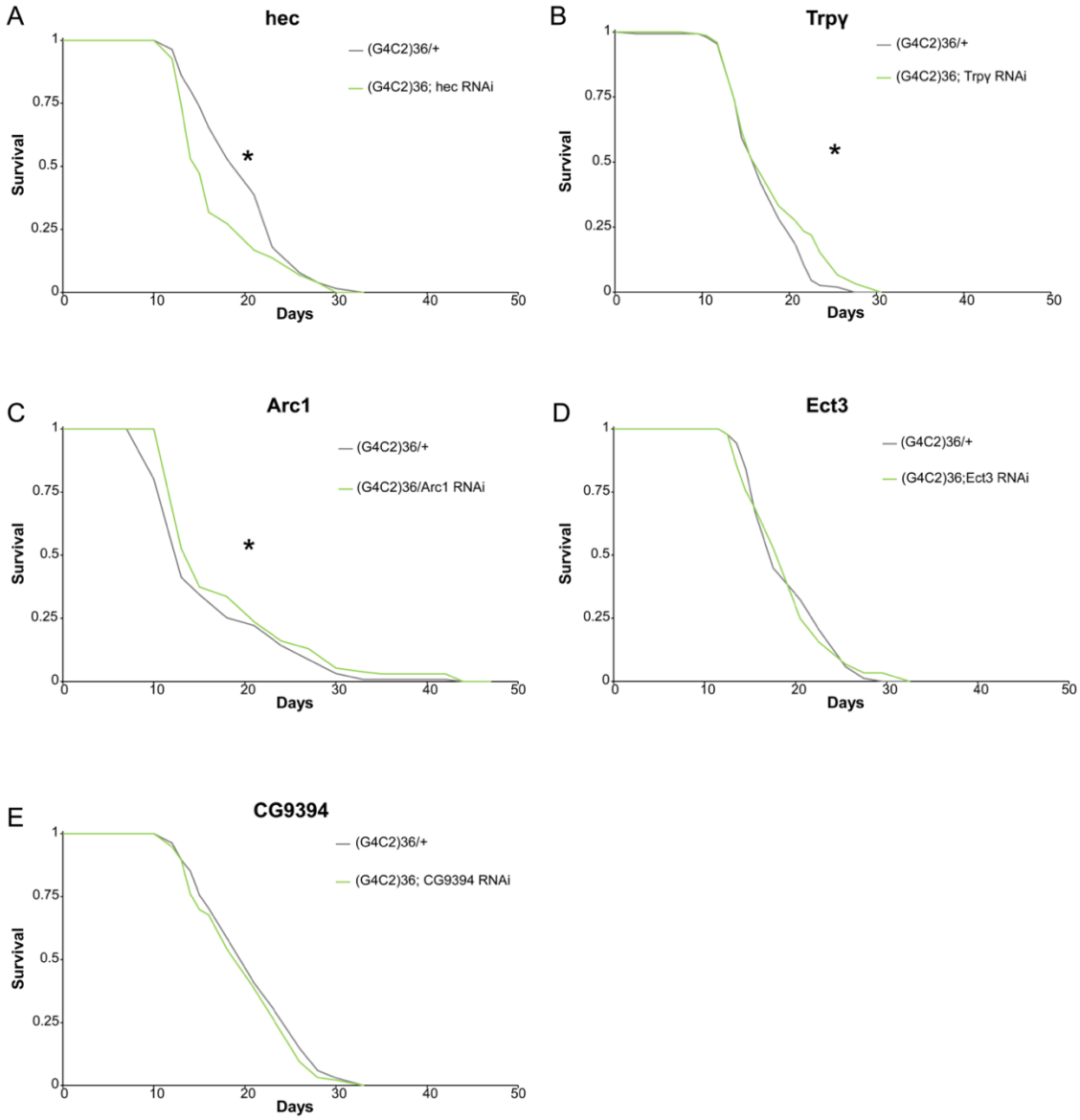

Figure 3.19. Survival curves for predicted Odd-skipped target genes.
hec RNAi shortens C9 fly survival (p=0.0002, log-rank test). B. *Trpγ* RNAi extends mean survival, without affecting median survival (p=0.006, log-rank test). C. *Arc1* RNAi extends C9 survival (p=0.02, log-rank test). D. *Ect3* RNAi has no effect on C9 fly survival (p=0.999, log-rank test). E. *CG9394* RNAi has no effect on C9

survival p=0.298. N=90-140 flies per condition. Genotypes: *UAS-$(G_4C_2)_{36}$, elavGS; UAS-$(G_4C_2)_{36}$, elavGS/UAS-hec RNAi; UAS-$(G_4C_2)_{36}$, elavGS/UAS-Trpγ RNAi; UAS-$(G_4C_2)_{36}$, elavGS/UAS-Arc1 RNAi; UAS-$(G_4C_2)_{36}$, elavGS/UAS-Ect3 RNAi, UAS-$(G_4C_2)_{36}$, elavGS/UAS-CG9394 RNAi*.

Therefore, *Trpγ and Arc1* could partially rescue C9 toxicity, modestly increasing C9 survival when the directionality of their regulation by Odd-skipped genes was replicated, using RNAi lines. However, the small effects of perturbing individual Odd-skipped target genes cannot explain the magnitude of survival extensions seen with the Odd-skipped family on $(G_4C_2)_{36}$ fly survival. This finding suggests that the individual gene targets tested have at most, minor effects and that rather, rescue is attributable to other specific genes that were not tested, or combinatorial effects of gene targets such that Odd-skipped family overexpression rescues through regulation of multiple genes.

3.3 Discussion

3.3.1 Summary of findings

In this chapter, a characterisation of the Odd-skipped family of transcription factors as modifiers of C9 toxicity was performed to identify downstream targets mediating rescue. Novel *Drosophila* lines expressing human *OSR1* and *OSR2* were generated. *OSR1* and *OSR2*, like *Drosophila bowl* and *odd*, were able to extend survival of C9 *Drosophila.* The extent of survival benefit varied between the Odd-skipped family genes tested. The differences in the magnitude of survival extension correlated with differential effects on DPR levels – *odd* and *OSR2* overexpression produced greater survival extensions than *bowl* or *OSR1*, and *odd* and *OSR2* decreased DPR levels, whereas *bowl* and *OSR1* did not. Overexpression of *bowl* and *odd* also extended survival of UAS-$(GR)_{36}$ flies, albeit modestly in comparison to their effect on survival of $(G_4C_2)_{36}$ flies.

To identify shared genes and pathways altered by overexpressing these related transcription factors in the context of C9 repeats, RNA-sequencing was performed at a pre-degeneration timepoint on C9 flies with or without co-

expression of *odd*, *bowl*, *OSR1* or *OSR2*. Odd-skipped transcription factors have been described to act as both transcriptional activators and transcriptional repressors, dependent on the cellular context, therefore we did not limit our study to only upregulated or downregulated genes, but instead looked for genes commonly upregulated or downregulated across the Odd-skipped conditions (Dréan *et al.*, 1998; Tena *et al.*, 2007). Gene ontology enrichment analysis did not identify pathways that are commonly altered across all Odd-skipped conditions. Therefore, prioritisation for target follow up was given to individual genes commonly altered across Odd-skipped conditions and containing a conserved Odd-skipped binding motif. Shortlisted genes of interest were assessed for their effect on C9 *Drosophila* survival, with either no effect or small effects on survival. Therefore, individual genes are unlikely to be driving the rescues observed by the Odd-skipped family.

3.3.2 Odd-skipped rescue is specific to C9 toxicity in adult neurons

Expression of $(G_4C_2)_{36}$ in adult *Drosophila* neurons greatly reduces lifespan, mostly due to the production of arginine-rich DPRs (Mizielinska *et al.*, 2014). Co-expressing *odd* or *bowl* in neurons of these C9 flies significantly extends survival, as does co-expression of human *OSR1* and *OSR2*. *Odd* and *bowl* also extend survival of flies expressing ATG driven $(GR)_{36}$, albeit to a lesser extent. This lifespan extension by Odd-skipped family transcription factors is due to a rescue of C9 specific toxicity, as *odd* or *bowl* overexpression in neurons of wildtype flies led to a significant reduction in lifespan. In adults, transcription factors can preserve cellular function in response to environmental insults by temporarily adjusting gene expression (Webb and Brunet, 2014). The transient nature of this responsiveness is essential to maintain cellular homeostasis, and this is achieved by tight regulation of transcription factor levels and activities (Latchman, 1997). Therefore, continuously overexpressing a transcription factor in the absence of disease can create cellular disequilibrium, leading to negative consequences for organismal health.

Here, expression of *odd* or *bowl* in developing eye neurons using a GMR-Gal4 driver, led to a reduced eye area in both the absence and presence of poly(GR). Furthermore, in contrast to our data showing increased expression of *odd* and *bowl* in adult neurons is beneficial, knocking down *odd* in developing *Drosophila* wings has previously been found to suppress poly(GR) toxicity (Lopez-Gonzalez *et al.*, 2019). During development, transcription factors are crucial determinants of cellular and tissue identity (Leyva-Díaz and Hobert, 2019). The Odd-skipped family are known to have important roles during development, including in the developing wing (Del Signore, Hayashi and Hatini, 2012) and retina (Bras-Pereira, Bessa and Casares, 2006), therefore, genetic manipulation in either direction during developmental stages might be expected to have consequences on morphological phenotypes. The original screen carried out by our lab that identified *odd* and *bowl* as suppressors of C9 toxicity, restricted expression of both the C9 repeats and *odd* and *bowl* to adult post-mitotic neurons, thereby avoiding developmental expression.

3.3.3 Odd-skipped transcription factors have varying effects on DPR levels

Here, Odd-skipped transcription factors were found to have different effects on DPR levels. As well as decreasing DPRs, *odd* and *OSR2* produced a low molecular weight poly(GP) band on western blot. This low molecular weight band may be due to effects on RAN translation, with alternative start codon usage leading to a shorter poly(GP) product, or due to proteolytic cleavage of poly(GP) in the *odd* and *OSR2* conditions. The fact that this low molecular weight poly(GP) product is present only in the conditions with the greatest survival extensions may be indicative of an additional mechanism at play for *odd* and *OSR2*. *Odd* and *OSR2* also decreased levels of poly(GR), while *bowl* and *OSR1* had no effect on poly(GR) levels in UAS-$(G_4C_2)_{36}$ flies. Both *odd* and *bowl* extended survival of UAS-$(GR)_{36}$ flies. It will be important to determine whether *odd* reduces poly(GR) levels in UAS-$(GR)_{36}$ flies, which do not undergo RAN translation, in order to better address the mechanism by which *odd* reduces DPRs. The reduction in DPR levels was not due to decreased general translation efficiency as levels of an mCD8-GFP protein, also driven by the elavGS driver was not affected by *odd*

or *bowl* expression. We have not ruled out the possibility that expression of *odd* and *OSR2* have a direct effect on the transcription of the G_4C_2 transgene, with resulting impacts on DPR levels. Future work should determine the G_4C_2 transcript repeat levels by RNA dot blot analysis to determine whether G_4C_2 transcription is altered by *odd* and *OSR2*, as another potential mechanism by which *odd* and *OSR2* reduce DPR levels. Alternatively, increased clearance of DPRs in *odd* and *OSR2* conditions could be responsible for reduced DPR levels, however, protein degradation pathways were not enriched among differentially expressed genes in either *odd* or *OSR2* conditions.

The similar effects of Odd and OSR2 on DPR levels cannot be attributed to sequence similarity of Odd and OSR2 or number of zinc finger domains, as Bowl and OSR2 are more similar than Odd and OSR2 in both respects (see Figure 3.4). Divergent effects among these Odd-skipped proteins may be independent of their shared sequence specific DNA binding and transcription factor activity. Transcription factors, and particularly C_2H_2 transcription factors, are known to physically interact with other transcription factors and proteins, thereby diversifying their functions and downstream effects (Brayer and Segal, 2008). Bowl but not Odd has been experimentally shown to physically interact with FOXO, TP53 and Relish (*Drosophila* NF-κB), which likely confers distinct functions (Shokri *et al.*, 2019). There is clearly more than one mechanism of rescue attributable to the Odd-skipped family, and further research into these other mechanisms of C9 rescue by Odd-skipped family members are warranted.

3.2.4 Limitations of this work

Here we focused on shared, conserved differentially expressed genes, between Odd, Bowl, OSR1 and OSR2, that contained an Odd-skipped binding motif for target follow-up, regardless of effects on DPR levels. However, if Odd and OSR2 are providing much of their rescue by affecting RAN translation, this would mean that shared genes for all four Odd-skipped transcription factors will be relevant to pathways not impacting RAN translation. Grouping the conserved genes into two groups, those shared by Odd/OSR2 and those shared by Bowl/OSR1 may

provide important insights into genes affecting RAN translation and genes providing rescue independent of effects on DPRs. Additionally, transcription factors will affect expression of both direct target genes and indirect target genes, both of which may be responsible for the rescue effects. We may have missed important shared indirect target genes with our approach, which focussed on genes with an Odd-skipped binding motif.

A limitation of this work is the utilisation of RNA-sequencing data combined with motif searching to infer putative transcriptional targets of the Odd-skipped family in a *C9orf72* disease context. It is difficult to separate causality from correlation or consequence when comparing differentially expressed genes between disease versus control and disease versus rescue interventions. However, to increase the probability of identifying direct Odd-skipped targets in disease contexts, an early timepoint was chosen for RNA-sequencing, four different Odd-skipped genes were included, and bioinformatic searching for Odd-skipped motifs in promoter regions of differentially expressed genes was conducted. Further, RNA-sequencing was performed in rat primary cortical neurons overexpressing *OSR1* or *OSR2* in the absence of disease. Putative targets shortlisted for functional follow-up in *Drosophila* were compared against this dataset to validate target specificity. Transcription factors bind to DNA in a sequence specific manner leading to activation or repression of target gene transcription. However, this binding depends on accessibility of target DNA. Assay for Transposase-Accessible Chromatin with next generation sequencing (ATAC-seq) can decipher chromatin accessibility by utilising a hyperactive Tn5 transposase to insert sequencing adapters into open chromatin regions. Chromatin accessibility has recently been shown to be altered by expressing poly(PR), and therefore chromatin accessibility may be altered in *C9orf72* disease contexts (Maor-Nof *et al.*, 2021). Combining ATAC-seq with ChIP-seq and RNA-seq approaches, in the context of *C9orf72* hexanucleotide repeat toxicity would be a powerful approach to determine direct targets of Odd-skipped transcription factors in this disease context.

A further limitation of this work is the use of whole *Drosophila* heads for RNA-sequencing and other molecular experiments. *Drosophila* heads constitute head

fat body and cuticle, as well as eyes and brain. The presence of these other tissues may mask small effects occurring only in neurons, or they can reflect systemic changes. Additionally, the use of bulk RNA sequencing provides a global overview of transcriptional changes occurring across the population of cells but precludes analysis of individual cells that are either resistant or vulnerable to the disease. Therefore, it would be highly informative to perform single cell RNA sequencing on *Drosophila* brains of control flies compared to flies neuronally expressing $(G_4C_2)_{36}$ with and without co-expression of Odd-skipped transcription factors.

Additionally, since both the Odd-skipped genes and $(G_4C_2)_{36}$ are driven by the same Gal4-GS driver, it is possible that binding to the Odd-skipped transgene promoter is titrating out the driver protein, leading to a drop in $(G_4C_2)_{36}$ expression and therefore, a phenotypic rescue. To account for any dilution effects, it would be beneficial to include, in the C9 control line, a second irrelevant transgene such as UAS-GFP when performing experiments involving co-expression of $(G_4C_2)_{36}$ with a potential modifier, to ensure that rescues observed are not due to titration effects on the GAL4/UAS system. Previously, flies carrying an empty vector inserted in the same location as the UAS-odd and UAS-bowl FlyORF construct was found to have no effect on lifespan of C9 expressing flies, confirming that the rescue is due to Odd-skipped genes and not to a non-specific dilution of the driver. Nevertheless, it would have been beneficial to include this condition, or similar, in all experiments.

By using an inducible elav Gal4-GeneSwitch driver, we avoid expression of the toxic DPRs throughout development, allowing us to study the impact of DPRs on adult neurons. This is useful from the point of view that ALS and FTD are adult-onset neurodegenerative diseases. However, the *C9orf72* expansion mutation is present throughout embryonic stages in patients, and therefore by avoiding developmental expression of DPRs, we are not able to investigate the potential synergistic contributions or independent effects of developmental expression of DPRs in our *Drosophila* model of ALS/FTD. There is now evidence that the *C9orf72* expansion mutation can alter neurodevelopment, impairing neural stem cell proliferation and decreasing cortical and thalamic size, mediated by poly(AP)

binding to the ribosomal maturation factor LRRC47, and lowering protein synthesis (Hendricks *et al.*, 2023). Therefore, developmental expression of DPRs can influence neuronal health, and contribute to later neurodegeneration, and as such, the study of DPRs during developmental stages is also important.

3.2.5 Conclusions

Odd-skipped transcription factors were identified as strong suppressors of C9 toxicity in *Drosophila*. The extent of survival benefit varied between the Odd-skipped family genes tested, *odd* and *OSR2* overexpression produced greater survival extensions than *bowl* or *OSR1*, and this difference in the magnitude of survival extension was attributable to *odd* and *OSR2* decreasing DPR levels, whereas *bowl* and *OSR1* did not. Evidently, the Odd-skipped family of transcription factors rescue C9 toxicity in multiple ways and further research into these other mechanisms of C9 rescue by Odd-skipped family members are warranted.

Chapter 4 - Transient receptor potential gamma is a modifier of *C9orf72*-repeat toxicity

4.1 Introduction

Transient receptor potential (TRP) channels are conserved, receptor-operated, non-selective, calcium permeable, cation channels that were first discovered in *Drosophila* (Montell and Rubin, 1989). A subgroup of this family are the canonical TRP (TRPC) channels. Transient receptor potential cation channel γ (Trpγ) is one of three TRPC members in the *Drosophila* genome, which also includes transient receptor potential (trp) and transient-receptor-potential-like (trpl). Trpγ is orthologous to human TRPC4 and TRPC5. In mammals, TRPC proteins can be divided into three groups: TRPC1/C4/C5, TRPC3/C6/C7 and TRPC2. The proteins within these groups can assemble into homo or heterotetramers, which affects the physiological properties of these ion channels (Strübing et al., 2001; Hofmann et al., 2002). TRPC1 is a negative regulator of TRPC4 and TRPC5 channels (Kim et al., 2019). Similar to mammals, Trpγ can form homo or heteromers, with Trpγ homodimers constitutively active, while heterodimerisation with TRPL forms a regulated cation channel (Xu et al., 2000).

Riluzole was the first approved drug to delay progression of ALS (Amyotrophic Lateral Sclerosis/Riluzole Study *et al.*, 1996). Riluzole affects the activity of several ion channels, leading to reduced neuronal firing through inhibition of Na+ channels, and enhancement of calcium dependent potassium currents (Bellingham, 2011). Additionally, riluzole is a direct activator of TRPC5 channels at physiologically relevant concentrations (Richter, Schaefer and Hill, 2014). Riluzole binds within the voltage sensor-like domain of human TRPC5, acting synergistically with calcium ions (Yang, Wei and Chen, 2022). TRPC5 is involved in regulation of neurite outgrowth, axon formation and synaptic plasticity in the hippocampus (Schwarz *et al.*, 2019; Davare *et al.*, 2009; Greka *et al.*, 2003), and dendrite morphogenesis in the cerebellum (Puram *et al.*, 2011). Additionally,

TRPC4 is necessary for neurite outgrowth of dorsal root ganglia following nerve injury (Wu et al., 2008). In flies, Trpγ coordinates brain-wide developmental activity and synaptogenesis (Bajar *et al.*, 2022), is involved in nutrient sensing behaviour (Dhakal *et al.*, 2022) and plays a role in fine motor control via Ca^{2+} influx in adults (Akitake *et al.*, 2015). The role of TRPC channels in *C9orf72* ALS/FTD has not previously been investigated.

Here, we show that *Trpγ* is upregulated at an early timepoint in *Drosophila* expressing expanded G_4C_2 repeats. Furthermore, the mammalian orthologs *TRPC4* and *TRPC5*, are upregulated in multiple patient-derived iPS motor neuron transcriptomic datasets. *TRPC4* expression levels are decreased in end-stage C9ALS post-mortem cortical excitatory neurons. Overexpression of *Trpγ* improved neurodegenerative phenotypes in our *C9orf72* fly model, and the mechanism by which *Trpγ* reduces toxicity in flies is partially due to a reduction in levels of poly(GR). Early upregulation of *Trpγ* and *TRPC4/5* is likely a protective response which for some reason this fails in end stage disease, which may contribute to neurodegeneration. Overall, our data suggest that modulation of *Trpγ/TRPC4* expression or activity in neurons could be an effective therapeutic approach against *C9orf72* ALS/FTD.

4.2 Results

4.2.1 *Trpγ* is upregulated in C9 *Drosophila* heads

Trpγ is normally expressed by less than 2% of neurons in the developing *Drosophila* brain (Bajar *et al.*, 2022). We examined the endogenous expression of *Trpγ* in the adult *Drosophila* brain using a published single-cell RNA-sequencing dataset (Davie *et al.*, 2018). Indeed, *Trpγ* messenger RNA co-localised with cells expressing the canonical neuronal marker *elav*, and not the glial marker, *repo* (Figure 4.1).

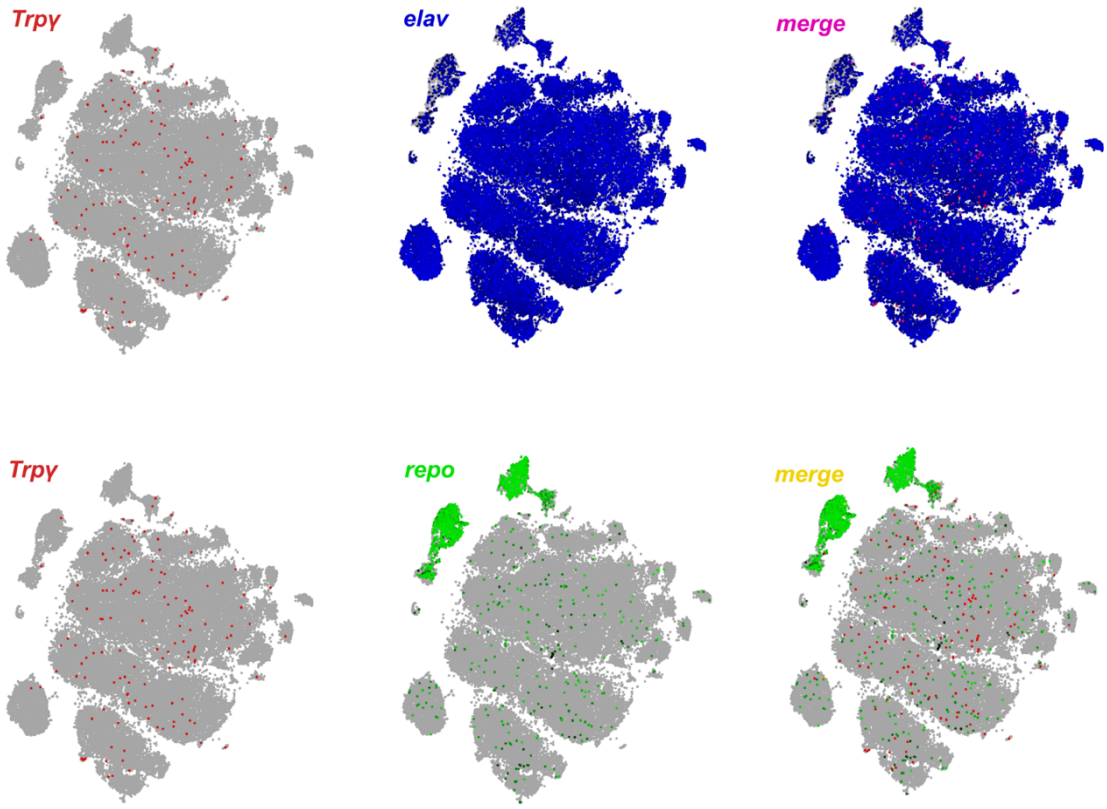

Figure 4.1. *Trpγ* co-localises with neuronal cells in the *Drosophila* brain. Images from the SCope database (Davie *et al.*, 2018) show mRNA expression of *Trpγ* largely in *elav*-expressing (neuronal) cell populations and not *repo*-expressing (glial) cell populations in the *Drosophila* brain.

Given the importance of *Trpγ* in normal synaptic development, we wanted to restrict our study of the role of *Trpγ* in *C9orf72* neurodegeneration to post-mitotic adult neurons (Bajar *et al.*, 2022). Therefore, we utilised our RU486-inducible C9 fly model, which expresses $(G_4C_2)_{36}$ repeats under the control of the pan-neuronal elav Gal4-GS driver (Mizielinska *et al.*, 2014; Osterwalder *et al.*, 2001). This system allows us to spatiotemporally restrict transgene expression to adult neurons, bypassing confounding effects of developmental expression. We analysed two independent transcriptomic datasets produced in the lab, in which $(G_4C_2)_{36}$ was inducibly expressed in adult neurons for five days. *Trpγ* was significantly upregulated in fly heads expressing $(G_4C_2)_{36}$ compared to uninduced controls at this relatively early timepoint in both datasets (Figure 4.3 A and B). *Trpγ* produces three transcript variants, *Trpγ-A* which is 4232 nucleotides, *Trpγ-B* which is 4189 nucleotides, and *Trpγ-D* which is 5274 nucleotides in length (Figure 4.2).

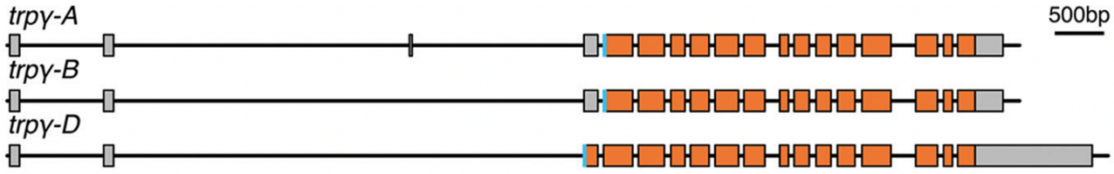

Figure 4.2. Trpy has three transcript variants.
Trpγ-A, *Trpγ*-B and *Trpγ-D* isoforms are shown. Exons (orange rectangles), untranslated regions (grey rectangles), and introns (black lines between exons or untranslated regions). *Trpγ-D* has an extra exon at the N-terminus compared to *Trpγ-A* and *Trpγ-B.* Scale bar = 500 base pairs.

We performed qPCR on induced versus uninduced $(G_4C_2)_{36}$ fly heads after 5 days using a set of primers designed to target all *Trpγ* transcript variants, and found that *Trpγ* was upregulated in $(G_4C_2)_{36}$ expressing flies, albeit non-significantly (Figure 4.3 C). To assess whether there was a particular transcript variant that was driving the upregulation detected by RNA-sequencing, we designed primers targeting the N-terminal exonic region unique to *Trpγ-D.* We found that *Trpγ-D* expression is increased approximately 7-fold in $(G_4C_2)_{36}$ fly heads after 5 days of RU486 induction (Figure 4.3 D).

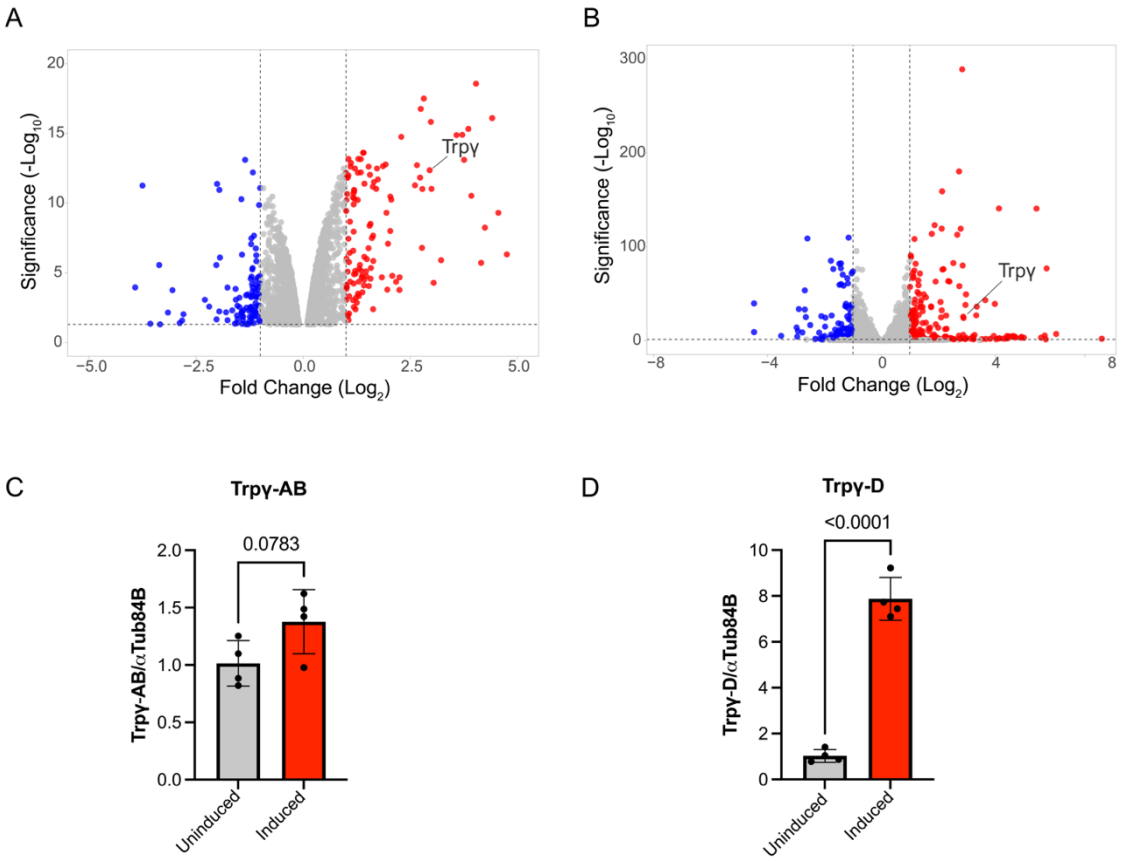

Figure 4.3. *Trpγ* is upregulated at early timepoints in $(G_4C_2)_{36}$ *Drosophila* heads.
A. Volcano plot of differentially expressed genes in RNA-sequencing experiment 1 on fly heads inducibly expressing $(G_4C_2)_{36}$ for 5 days, versus uninduced controls. N=4 biological replicates containing 15 heads per replicate. B. Volcano plot of differentially expressed genes in RNA-sequencing experiment 2 on fly heads inducibly expressing $(G_4C_2)_{36}$ for 5 days, versus uninduced controls. N=4 biological replicates containing 15 heads per replicate. For both A and B, gridlines are set to $-Log_{10}$(p-value) = 1.3 on the y-axis, equivalent to adjusted p-value <0.05 and Log_2(Fold change) = 1 on the x-axis. Differentially expressed genes were plotted using VolcaNoseR. C. *Trpγ-AB* isoform is non-significantly increased in induced $(G_4C_2)_{36}$ flies after 5 days as determined by qPCR (p=0.0783, Student's unpaired t-test). N=4 biological replicates containing 15 heads per replicate. D. *Trpγ-D* isoform is significantly increased in induced $(G_4C_2)_{36}$ flies after 5 days as determined by qPCR (p<0.0001, Student's unpaired t-test). N=4 biological replicates containing 15 heads per replicate. qPCR data are presented as mean ± S.D. Genotype: *UAS-$(G_4C_2)_{36}$, elavGS*.

4.2.2 Human homologs *TRPC4* and *TRPC5* are dysregulated in patient iPSC neurons and post-mortem brains

Trpγ is most homologous to human *TRPC4* with 47% identity (64% similarity), and *TRPC5* with 44% identity (61% similarity). We analysed three publicly available transcriptomic datasets of *C9orf72* ALS/FTD patient iPSC-motor neurons, to check whether *TRPC4* or *TRPC5* expression was altered in a model closer to human disease. *TRPC4* was found to be upregulated in *C9orf72* iPSC-motor neurons at day in vitro 21 in two transcriptomic datasets analysed (Mehta *et al.*, 2021; Selvaraj *et al.*, 2018) (Figure 4.3 A and B). *TRPC4* was found to be downregulated, while *TRPC5* was upregulated in *C9orf72* iPSC-motor neurons in a third dataset at the same timepoint (Sommer *et al.*, 2022) (Figure 4.4 C and D).

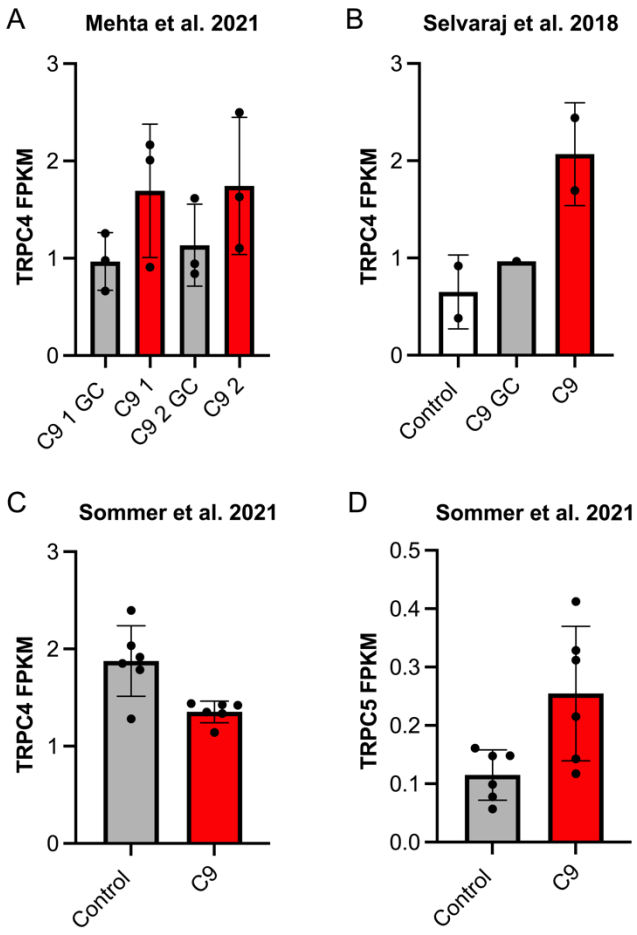

Figure 4.4. *TRPC4* and *TRPC5* are dysregulated in C9ALS/FTD motor neurons.
A. *TRPC4* is upregulated in two patient *C9orf72* iPSC-motor neuron lines versus their gene corrected controls at DIV 21 (Mehta *et al.*, 2021). B. *TRPC4* is upregulated in a patient *C9orf72* iPSC-motor neuron line versus its gene corrected control and a healthy control line at DIV 21 (Selvaraj *et al.*, 2018). C. *TRPC4* is downregulated in *C9orf72* iPSC motor neurons at DIV 21 (Sommer *et al.*, 2022). D. *TRPC5* is upregulated in *C9orf72* iPSC motor neurons at DIV 21 (Sommer *et al.*, 2022). Data plotted from published Fragments Per Kilobase of transcript per Million mapped reads (FPKM) values.

TRPC channel expression is also dysregulated in a single cell transcriptomic dataset generated from post-mortem ALS patient brains, with *TRPC4* downregulated while *TRPC1* is upregulated in cortical excitatory neurons (Figure 4.5) (Li *et al.*, 2023).

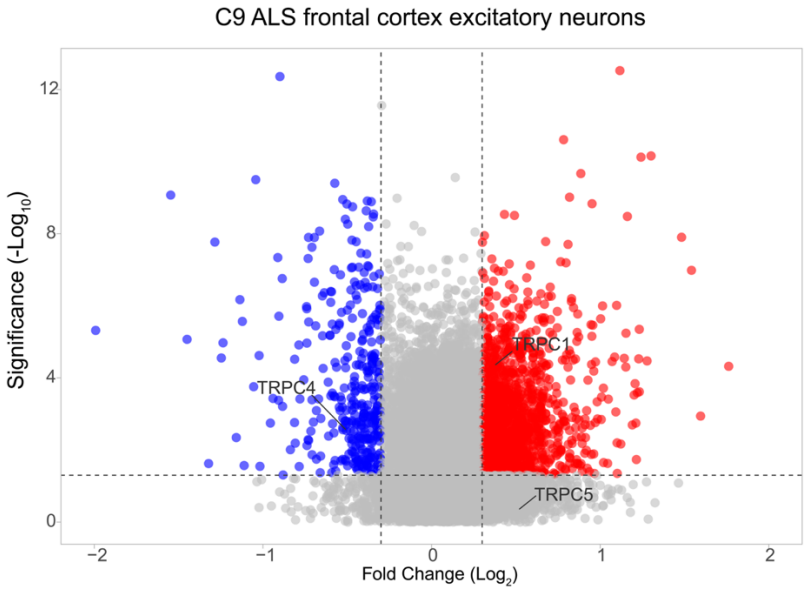

Figure 4.5. *TRPC4* is downregulated in post-mortem frontal cortex excitatory neurons.
Volcano plot showing differentially expressed genes in *C9orf72* ALS post-mortem frontal cortex excitatory neurons. *TRPC4* is downregulated while *TRPC1* is upregulated (Li *et al.*, 2023). Gridlines are set to -Log_{10}(p-value) = 1.3 on the y-axis, equivalent to adjusted p-value <0.05 and Log_2(Fold change) = 0.3 on the x-axis. Volcano plot produced using published differentially expressed genes (Li *et al.*, 2023) and plotted using VolcaNoseR.

4.2.3 *Trpγ* extends C9 *Drosophila* survival

The *Trpγ* gene produces three isoforms - *Trpγ-A, Trpγ-B* and *Trpγ-D*. *Trpγ-A* and *Trpγ-B* have identical amino acid sequences, however, *Trpγ-D* has an extra 60-amino-acids at its N-terminus, with additional functions described for this isoform during development (Bajar *et al.*, 2022). To test whether the shared *Trpγ* sequence influences C9 fly survival, or whether there may be isoform specificity to the role of *Trpγ* in C9 neurodegeneration, we obtained flies expressing either *Trpγ-A* and *Trpγ-B* (*Trpγ-AB*) or *Trpγ-D* as a generous gift from Dr Orkun Akin (UCLA). Neuronal overexpression of either *Trpγ-AB* or *Trpγ-D* markedly increased C9 survival. *Trpγ-AB* increased median survival by 177%, from 11 to 30.5 days. *Trpγ-D* increased median survival by 156%, from 11.5 to 29.5 days. This result indicates that elevated *Trpγ* expression in C9 flies is a compensatory protective response (Figure 4.6 A and B). Given the similar survival extensions

observed for both *Trpγ-AB* and *Trpγ-D*, it can be concluded that the rescue is due to the shared amino acid sequence of all isoforms.

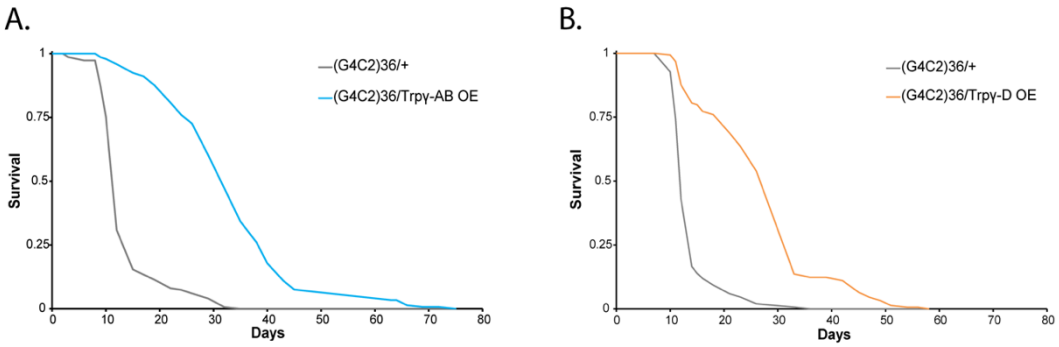

Figure 4.6. *Trpγ* overexpression in neurons of C9 flies extends survival.
A. Neuronal overexpression of *Trpγ-AB* extends C9 survival ($p=1.94x10^{-48}$, log-rank test), N=150 flies per condition. B. Neuronal overexpression of *Trpγ-D* extends C9 survival ($p=3.9x10^{-39}$, log-rank test), N=150 flies per condition. Genotypes: *UAS-$(G_4C_2)_{36}$, elavGS; UAS-$(G_4C_2)_{36}$, elavGS/ UAS-Trpγ-AB, UAS-$(G_4C_2)_{36}$, elavGS/ UAS-Trpγ-D.*

While RNAi-mediated knockdown of *Trpγ* in neurons had no effect on median survival of C9 flies (Figure 3.19 B), a *Trpγ* mutant allele, Trpγ[1], significantly reduced median survival by 22%, from 11 to 8.5 days (Figure 4.7). Why *Trpγ* overexpression in neurons greatly extends survival while neuronal knockdown by RNAi has limited effects may be because less that 2000 neurons in the *Drosophila* brain normally express *Trpγ*. Therefore, knocking down *Trpγ* in so few neurons, while toxic C9 repeats are expressed in all neurons, may not be sufficient to see any effect on survival. However, ectopically overexpressing *Trpγ* in all neurons which are also expressing C9 repeats, is sufficient to reduce toxicity and extend survival (Figure 4.6 A and B). As well as being expressed by neurons, *Trpγ* is also highly expressed in *Drosophila* muscle, proprioceptive organs and scolopale cells and has been shown to be necessary for coordination and fine motor control (Akitake *et al.*, 2015). The different effects observed when using *Trpγ* RNAi and a *Trpγ* mutant may be because the RNAi line will specifically knockdown *Trpγ* in neurons, under control of the elavGS driver, while the mutant will lead to reduced expression in all tissues expressing *Trpγ*.

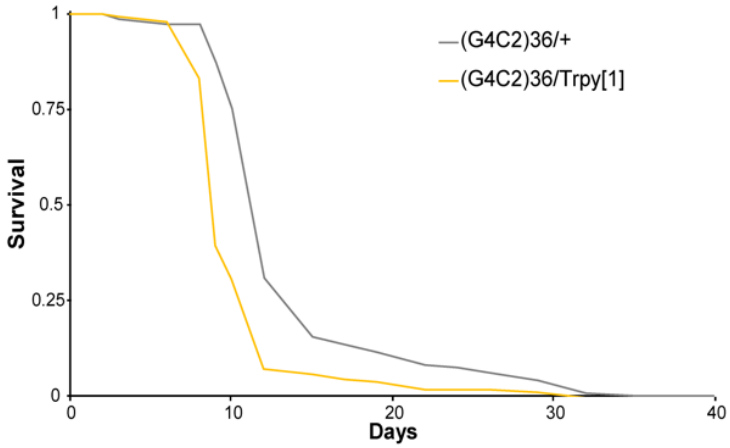

Figure 4.7. *Trpγ* mutant allele decreases median survival.
Trpγ[1] significantly decreases C9 survival ($p=4.8x10^{-13}$, log-rank test). N=150 flies per condition. Genotypes: *UAS-$(G_4C_2)_{36}$, elavGS; UAS-$(G_4C_2)_{36}$, elavGS/Trpγ[1].*

4.2.4 *Trpγ* rescue is specific to C9 toxicity

To assess whether the survival extension by *Trpγ* overexpression was attributable to a specific rescue of C9 toxicity or a more general improvement of health, *Trpγ* was overexpressed in the neurons of wild type flies. Feeding RU486 to the driver alone condition led to a lifespan extension, with median survival increasing from 85.5 to 91.5 days (Figure 4.8 A). However, overexpression of *Trpγ-AB* decreased median survival by 18%, from 91.5 days in uninduced controls versus 74.5 days in induced flies (Figure 4.8 B). Similarly, *Trpγ-D* overexpression also led to a reduction in survival, with medians decreasing by 9.5%, from 94.5 to 85.5 days (Figure 4.8 C). Lifespan was significantly decreased by overexpression of both *Trpγ* isoforms in wild-type neurons, suggesting that the rescues observed are specific to C9 toxicity (Fig. 4.8 B, C).

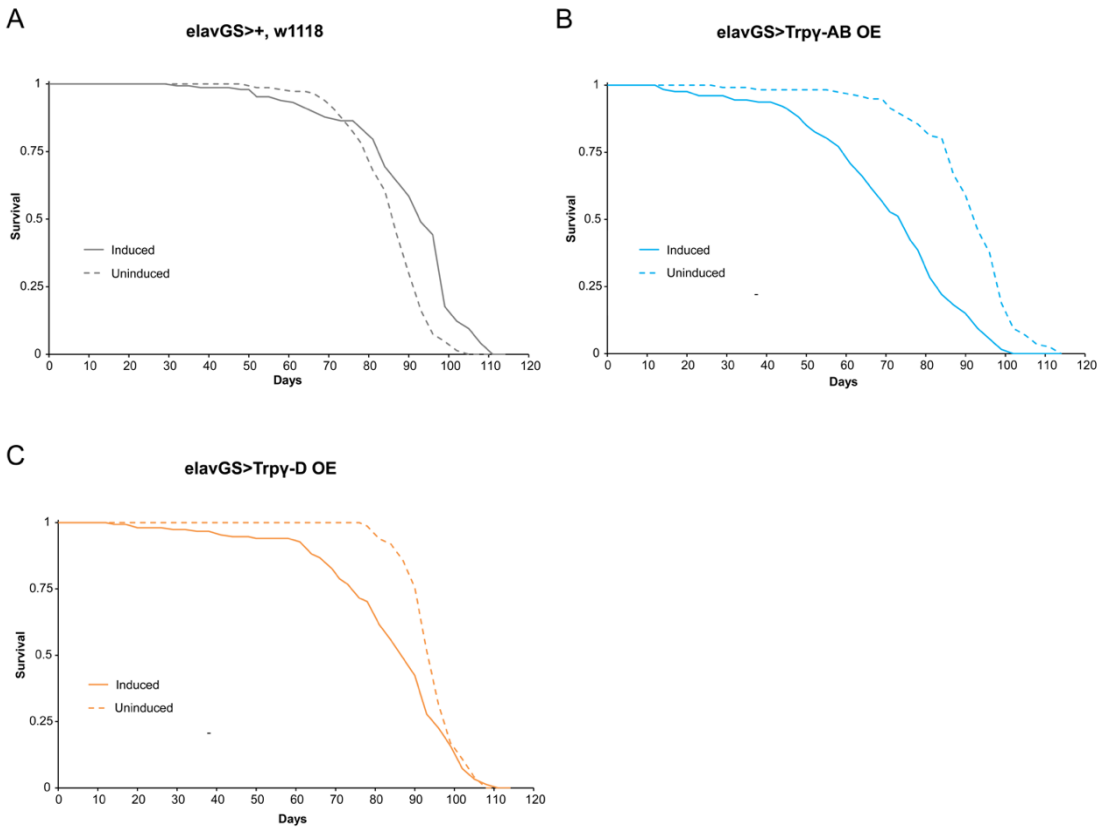

Figure 4.8. *Trpγ* overexpression in wildtype neurons decreases lifespan. RU486 led to a lifespan extension in the driver alone condition ($p=5.26x10^{-10}$, log-rank test). N=150 flies per condition. B. *Trpγ-AB* overexpression in neurons of wildtype flies decreased survival ($p=8.43\ x10^{-20}$, log-rank test). N=120-130 flies per condition. C. *Trpγ-D* overexpression in neurons of wildtype flies decreased survival (p=0.0001, log-rank test). N=150 flies per condition. Genotypes: *elavGS; elavGS/UAS-Trpγ-AB; elavGS/UAS-Trpγ-D.*

To assess whether a reduction in expression of *Trpγ* has any effect on wildtype lifespan, we first knocked down *Trpγ* in neurons using an RNAi line. Feeding RU486 to the driver alone condition had no effect on median survival compared to uninduced controls (90.5 days) (Figure 4.9 A). Knocking down *Trpγ* expression in neurons of wildtype flies had no effect on median survival compared to its matched uninduced control (90.5 days) but did cause some early mortality (Figure 4.9 B). Feeding RU486 to the driver alone condition run in parallel to *Trpγ[1]* increased median survival from 87.5 days to 93.5 days (Figure 4.9 C). Loss of one copy of *Trpγ* using a mutant allele led to a reduction in median survival from 84.5 to 78.5 days (Figure 4.9 D).

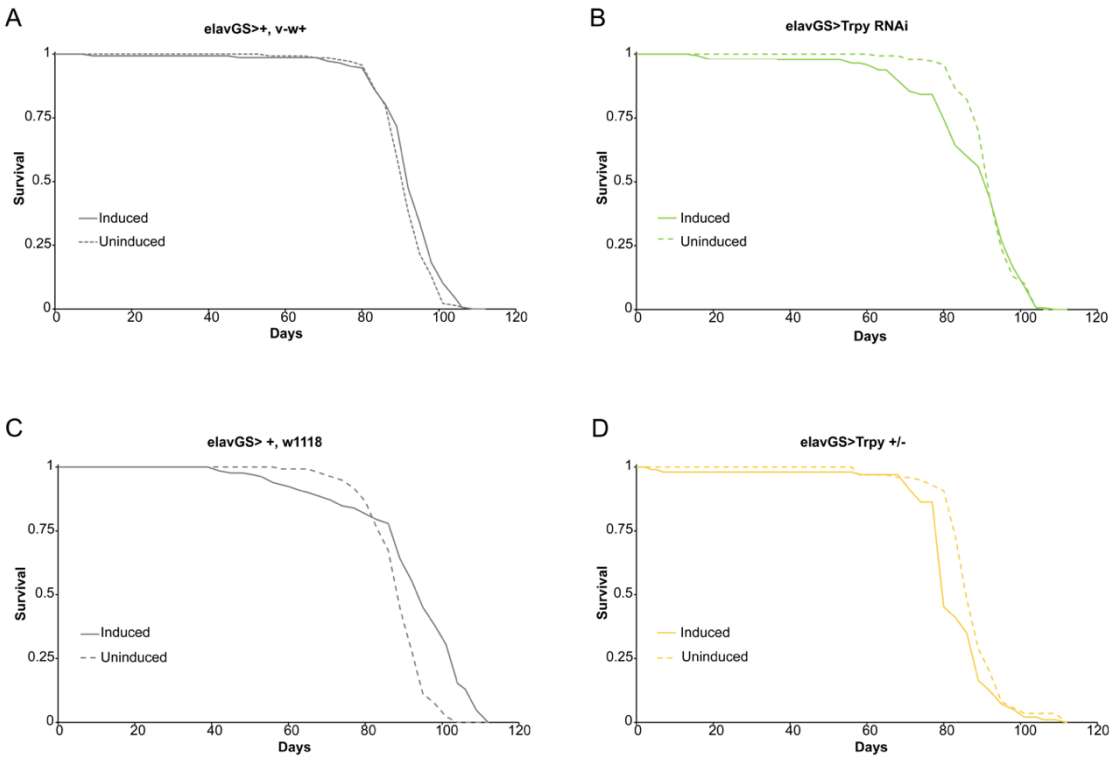

Figure 4.9. *Trpγ* knockdown in wildtype neurons has no effect on lifespan, while *Trpγ* mutant allele significantly decreases wildtype lifespan.
A. Driver alone control lifespan run in parallel to B. There is a slight extension in lifespan between RU486 induced and uninduced flies (p=0.02, log-rank test). Uninduced N=130-140 flies per condition. B. *Trpγ RNAi* in neurons of wildtype flies had no effect on lifespan (p=0.302, log-rank test). N=150 flies per condition. C. Driver alone control lifespan run in parallel to D. There is a significant extension in lifespan between RU486 induced and uninduced flies ($p=9.4x10^{-10}$, log-rank test). N=130-135 flies per condition. D. Loss of one copy of *Trpγ* in wildtype flies reduces lifespan (p=0.003, log-rank test). N=100 flies per condition. Genotypes: *elavGS; elavGS/UAS-Trpγ RNAi; Trpγ[1]/+, elavGS;.*

4.3.5. *Trpγ* rescues early hyperactivity phenotype in C9 flies

C9 flies display an early hyperactivity phenotype, with increased locomotor activity around day 4 (Xu *et al.*, 2023). This early hyperactivity then progresses to reduced activity prior to organismal death (Atilano *et al.*, 2021). To assess whether neuronal overexpression of *Trpγ* could rescue this additional neurodegenerative phenotype of early hyperactivity, motor activity and sleep were recorded using a *Drosophila* activity monitor system. For this and subsequent experiments, we focussed on *Trpγ-AB* (from hereafter referred to as

Trpγ). Like previously reported, neuronal expression of $(G_4C_2)_{36}$ for four days led to a significant increase in total activity over a 24-hour period. This hyperactivity phenotype was rescued by co-overexpression of *Trpγ*, bringing activity back down to control levels (Figure 4.10).

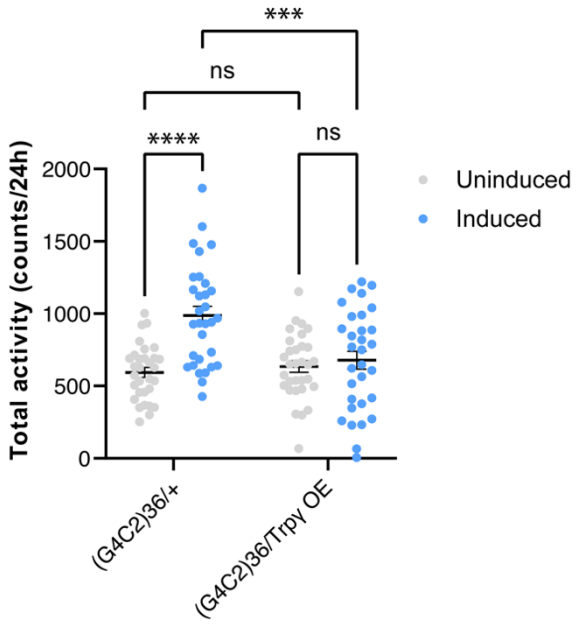

Figure 4.10. Trpγ rescues early hyperactivity phenotype in C9 flies.
Total activity of flies expressing $(G_4C_2)_{36}$ in neurons was significantly increased compared with matching uninduced controls (****p<0.0001). Co-expression of *Trpγ* with $(G_4C_2)_{36}$ prevented this hyperactivity phenotype compared with matching uninduced flies (ns, p=0.9331). Flies co-expressing *Trpγ* with $(G_4C_2)_{36}$ displayed reduced activity compared to $(G_4C_2)_{36}$ alone (***p=0.0003). There was a significant interaction effect of genotype x RU486 induction (p=0.001). Two-way ANOVA followed by Tukey's multiple comparisons test. Data are presented as mean ± S.D. N=31 flies per condition. Genotypes: *UAS-$(G_4C_2)_{36}$, elavGS; UAS-$(G_4C_2)_{36}$, elavGS/UAS-Trpγ-AB.*

Activity and sleep patterns over a 24-hour period were further assessed. The first 12 hours of this period are defined as day with lights on, the subsequent 12 hours are defined as night with lights off. Activity and sleep traces indicate that C9 flies have increased activity and decreased sleep over the day and night periods, ameliorated by *Trpγ* overexpression (Figure 4.11 A and B).

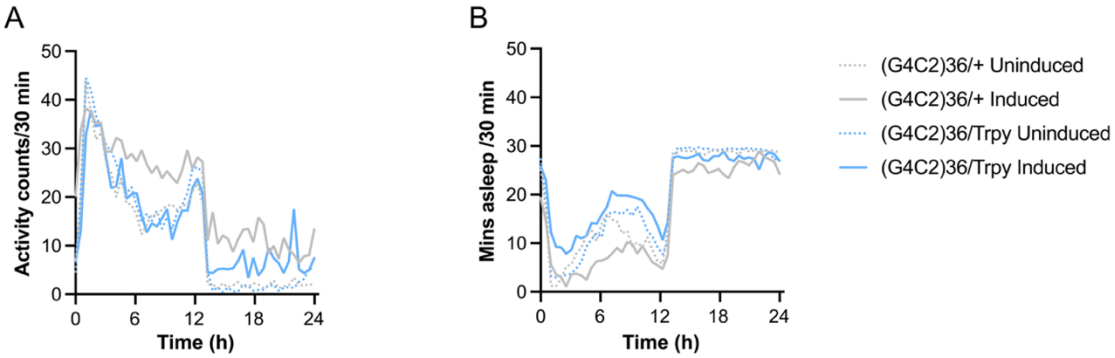

Figure 4.11. Activity and sleep traces for $(G_4C_2)_{36}$ flies with or without co-expression of *Trpγ* in neurons.

A. Induced $(G_4C_2)_{36}$ flies have increased day and night activity versus uninduced controls. Co-expression of *Trpγ* with $(G_4C_2)_{36}$ normalizes activity traces to that of uninduced controls. N=31 flies per condition. B. Induced $(G_4C_2)_{36}$ flies have reduced day and night sleep versus uninduced controls. Co-expression of *Trpγ* with $(G_4C_2)_{36}$ normalises sleep trace to one more closely resembling uninduced controls. N=31 flies per condition. Genotypes: *UAS-$(G_4C_2)_{36}$, elavGS; UAS-$(G_4C_2)_{36}$, elavGS/ UAS-Trpγ-AB.*

We next quantified day and night activity and sleep, separately (Figure 4.12). Like our results for total activity, we found that neuronal expression of $(G_4C_2)_{36}$ led to a significant increase in both day and night activity (Figure 4.12 A and B, respectively). This hyperactivity phenotype was rescued by co-overexpression of *Trpγ*, bringing activity back down to uninduced control levels during the day (Figure 4.12 A) and night periods (Figure 4.12 B). We next measured sleep, defined as continuous bouts of five or more minutes of inactivity. Given the increase in activity observed during day and night periods for C9 flies, a corresponding decrease in sleep would be expected. We found that night sleep (Figure 4.12 D) but not day sleep (Figure 4.12 C) was significantly decreased in C9 flies, while *Trpγ* significantly increased day and night sleep compared to flies expressing $(G_4C_2)_{36}$ alone (Figure 4.12 C and D, respectively). Sleep fragmentation was also assessed by quantifying the number of sleep bouts. C9 flies had a significant increase in night but not day sleep bouts, which was ameliorated by *Trpγ* (Figure 4.12 E and F).

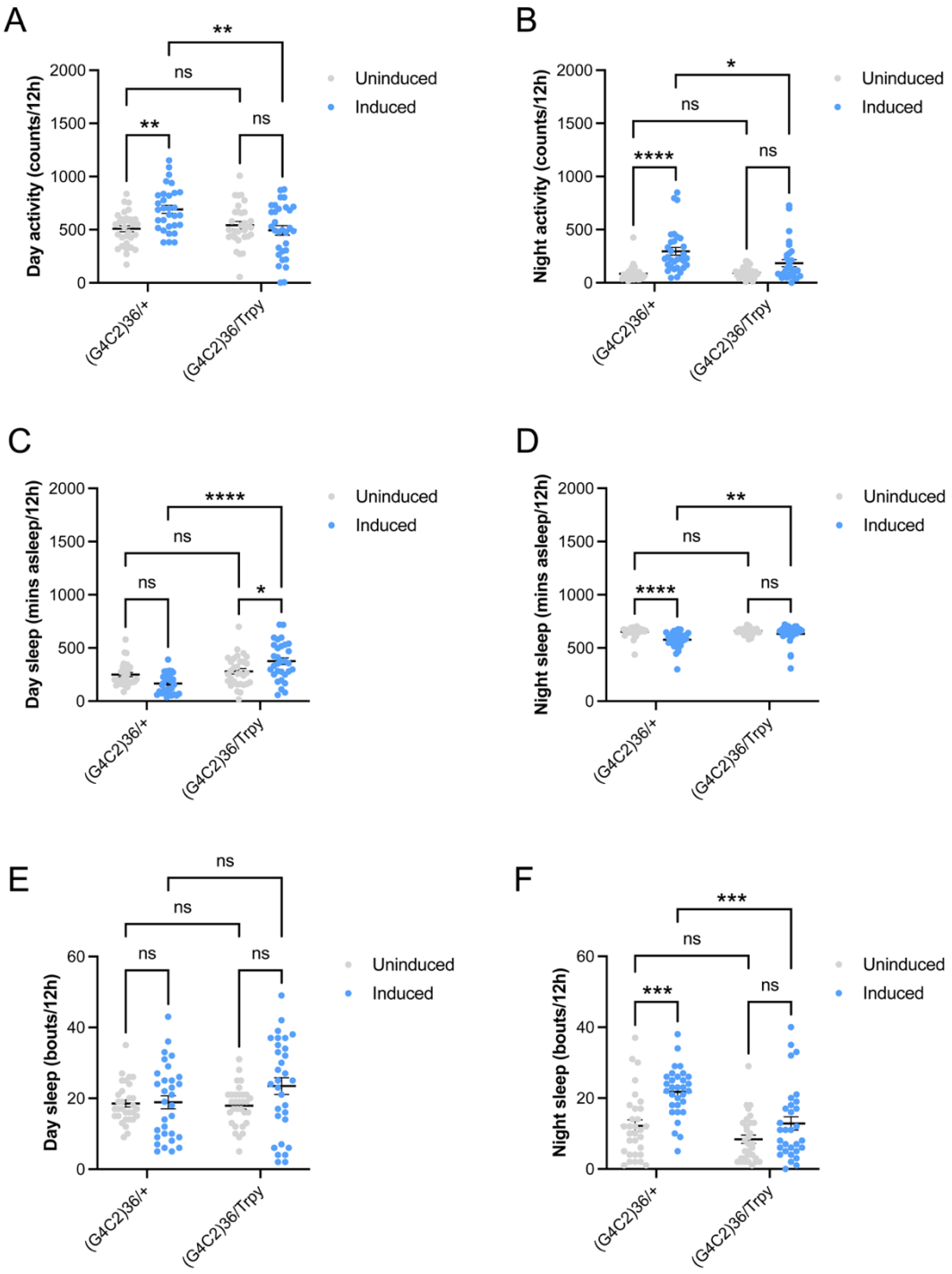

Figure 4.12. *Trpγ* overexpression ameliorates early hyperactivity phenotype in C9 flies.

A and B. $(G_4C_2)_{36}$ flies have increased day (**p=0.0036) and night activity (****p<0.0001) compared to uninduced controls. *Trpγ* co-expression with $(G_4C_2)_{36}$ significantly reduces day activity (**p=0.0014) and night activity (*p=0.0158) compared to $(G_4C_2)_{36}$ flies alone. C and D. $(G_4C_2)_{36}$ flies have reduced night sleep (****p<0.0001) but not day sleep (ns, p=0.078) compared to uninduced controls. *Trpγ* co-expression with $(G_4C_2)_{36}$ significantly increases day sleep (****p<0.0001) and night sleep (**p=0.0075) compared to $(G_4C_2)_{36}$ flies alone. E and F. $(G_4C_2)_{36}$

flies have increased night sleep bouts (***p=0.0001) but not day sleep bouts (ns, p=0.9988), compared to uninduced controls. *Trpγ* co-expression with $(G_4C_2)_{36}$ significantly reduces night sleep bouts (***p=0.0004) compared to $(G_4C_2)_{36}$ flies alone. Two-way ANOVA followed by Tukey's multiple comparisons test used for all comparisons. Data are presented as mean ± S.D. N=31 flies per condition. Genotypes: *UAS-$(G_4C_2)_{36}$, elavGS; UAS-$(G_4C_2)_{36}$, elavGS/UAS-Trpγ-AB.*

4.2.6 *Trpγ* rescue is due to a reduction in poly(GR) levels

Accumulation of poly(GR) is the main driver of toxicity in C9 pure repeat flies, therefore poly(GR) levels were measured by MSD immunoassay. *Trpγ* significantly reduced levels of poly(GR), suggesting that rescue is via a reduction in toxic DPRs (Figure 4.13).

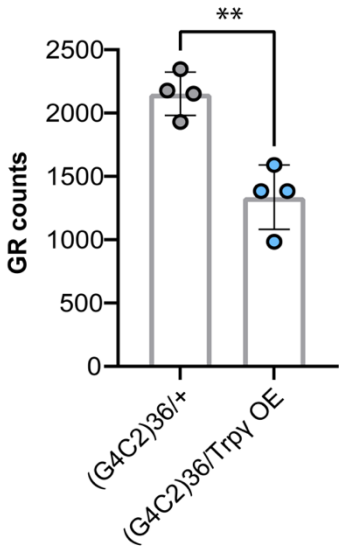

Figure 4.13. Neuronal overexpression of Trpγ reduces poly(GR) levels.
GR levels in C9 fly heads with or without *Trpγ* co-expression, as determined by poly(GR) MSD-immunoassay (**p=0.0018, Student's unpaired t-test). Data is presented as mean ± S.D. N=4 biological replicates, containing 15 fly heads per replicate. Genotypes: *UAS-$(G_4C_2)_{36}$, elavGS; UAS-$(G_4C_2)_{36}$, elavGS/UAS-Trpγ-AB.*

This decrease in poly(GR) was not due to indirect effects on the inducible protein expression system, as levels of an mCD8-GFP protein, also driven by the elav-Gal4GS driver was not affected by *Trpγ* expression (Figure 4.14).

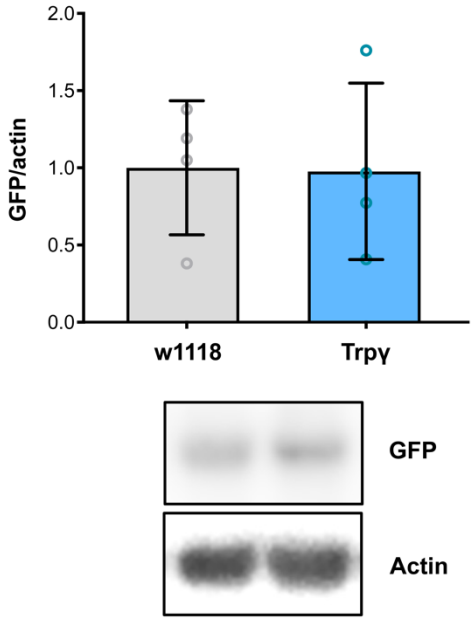

Figure 4.14. Neuronal overexpression of Trpγ does not affect the inducible protein expression system.
There was no significant difference (p=0.951) in GFP levels with *Trpγ* expression (Student's unpaired t-test). Data is presented as mean ± S.D. N=4 biological replicates, containing 15 fly heads per replicate. Genotypes: *UAS-mCD8-GFP/elavGS; UAS-mCD8-GFP/elavGS, UAS-Trpγ-AB.*

4.3 Discussion

4.3.1. Summary of findings

In this Chapter, *Trpγ* and its homologs *TRPC4* and *TRPC5*, were found to be transcriptionally dysregulated in C9 *Drosophila* heads, patient-derived iPSC-neurons, and post-mortem brains. Neuronal overexpression of *Trpγ* ameliorated survival and motor activity phenotypes in C9 *Drosophila*, by reducing poly(GR) levels, suggesting that upregulation of *Trpγ* is a protective response.

4.3.2. Isoform-specific upregulation

The Trpγ-D isoform was found to be specifically upregulated in $(G_4C_2)_{36}$ flies after 5 days of induction with RU486, as determined by qPCR (Figure 4.3). This

isoform-specific upregulation may be due to a longer C-terminal untranslated region present in the D isoform of Trpγ compared to the A and B isoforms (Figure 4.2). The 3'untranslated region (3'UTR) is involved in post-transcriptional regulation, with longer 3'UTRs shown to increase transcript stability but reduce efficiency of translation (Kuersten and Goodwin, 2003; Mayr, 2019). Transcripts with longer 3'UTRs are more often found in the brain than in other tissues (Hilgers *et al.*, 2011; Miura *et al.*, 2013), and are specifically enriched among transcripts encoding transporters and ion channels, permitting an additional layer of post-transcriptional regulation through microRNA binding (Wehrspaun, Ponting and Marques, 2014).

4.3.3. *Trpγ* as a modifier of DPR toxicity

Here, we report that *Trpγ* expression in neurons can reduce toxicity in C9 *Drosophila* by reducing the levels of toxic poly(GR). *TRPC4* has previously been shown to promote autophagy in vascular endothelial cells, through the Ca^{2+}-CaMKKβ-AMPK pathway (Zhang *et al.*, 2015b). A block in late-stage autophagy has been previously reported in *C9orf72* fly models (Xu *et al.*, 2023; Cunningham *et al.*, 2020). Therefore, further experiments investigating Trpγ channel activity, and effects on autophagy would be informative to understand how exactly *Trpγ* reduces poly(GR) levels.

Given the modest reduction in poly(GR) levels by overexpression of *Trpγ* in neurons of C9 *Drosophila*, *Trpγ* may provide protection by additional means. Indeed, TRPC4 and TRPC5 are known to play important roles in neurite outgrowth (Wu *et al.*, 2008; Greka *et al.*, 2003). Therefore, it would be interesting to look at whether *Trpγ* rescue is in part due to effects on neurite outgrowth.

Whether the effect of *Trpγ* overexpression on sleep/wake activity is specific to a C9 disease context, or is an additive effect, has not been investigated here. It will be beneficial in future experiments to test the effect of *Trpγ* overexpression in neurons of otherwise wildtype flies to assess whether this can also affect activity

of flies, particularly given that *Trpγ* mutants have impaired fine motor activity (Akitake et al., 2015).

The polyunsaturated fatty acids linoleic acid and linolenic acid have been shown to activate all three *Drosophila* TRPC ion channels (Riehle *et al.*, 2018; Jörs *et al.*, 2006; Chyb, Raghu and Hardie, 1999). Linoleic and linolenic acid supplementation can increase survival of C9 flies (Chapter 5), which may be in part due to activation of Trpγ.

4.3.4. Potential involvement of TRPC channels in ALS

Here, we report that *TRPC4* and *TRPC5* mRNA expression is dysregulated in C9ALS/FTD iPS motor neurons and post-mortem brains. Riluzole, one of the few approved drugs for treating ALS, is a potent agonist of TRPC5 channels, yet the involvement of TRPC channels in this neurodegenerative disease has not yet been studied (Yang, Wei and Chen, 2022; Zhu *et al.*, 2019; Richter, Schaefer and Hill, 2014; Miller, Mitchell and Moore, 2012). *TRPC4* and *TRPC5*, are upregulated in patient-derived iPS motor neuron transcriptomic datasets, which is likely to represent an early disease stage, whereas *TRPC4* expression levels are decreased in end-stage *C9orf72* ALS post-mortem cortical excitatory neurons. Given that neuronal overexpression of *Trpγ* rescues multiple neurodegenerative phenotypes associated with expression of expanded G_4C_2 repeats, early upregulation of *Trpγ and TRPC4/5* is likely a protective response which fails in end stage disease, and this reduction in Trpc4 expression may contribute to neurodegeneration. Therefore, further studies investigating whether overexpression of *TRPC4* or *TRPC5* can reduce *C9orf72* toxicity in mammalian models are needed.

4.3.5. Conclusions

Trpγ has been identified as a genetic modifier of *C9orf72* toxicity in *Drosophila*, extending survival and ameliorating motor impairments by decreasing poly(GR) levels. Given that the homologs of *Trpγ, TRPC4* and *TRPC5* are transcriptionally

dysregulated in *C9orf72* patient iPSC neurons and post-mortem brains, and that riluzole can activate TRPC5 channels, further experiments investigating the potential of *TRPC4* or *TRPC5* to modify *C9orf72* toxicity in mammalian models is warranted.

Chapter 5 - Neuronal polyunsaturated fatty acids are protective in *C9orf72* ALS/FTD

5.1 Introduction

Lipids are a diverse class of biomolecules that play a variety of important roles in cells, serving as structural components of membranes, acting as bioactive intercellular signaling molecules, and providing a key energy source through fatty acid oxidation (van Meer, Voelker and Feigenson, 2008). Fatty acids (FAs), serve as the building blocks of most complex lipid classes, including glycerophospholipids, triacylglycerols (TGs), diacylglycerols (DGs), sphingolipids, ceramides, and cholesterol esters. Diversity between these lipid classes is conferred by head group composition, attachment to aliphatic chains, and conjugation to fatty acids (Holthuis and Menon, 2014; Fahy *et al.*, 2009). The presence or absence of double bonds in the acyl chain of fatty acids determines its saturation profile - saturated fatty acids have no double bonds in their acyl chain, monounsaturated fatty acids contain one, whereas polyunsaturated fatty acids (PUFAs) contain at least two double bonds. The length of the fatty acid acyl chain, the number and position of double bonds, as well as head group composition influences the physicochemical properties of complex lipids and therefore can influence physiological functions of lipids (Holthuis and Menon, 2014; de Kroon, Rijken and De Smet, 2013) .

Lipids constitute greater than 50% of the human brain in dry weight, yet the contribution of lipids to neurodegenerative diseases has been understudied until recent years, when compared to other classes of biomolecules such as RNA or proteins (Piomelli, Astarita and Rapaka, 2007). This is largely due to technical difficulties in the detection of lipids, however a revolution in lipidomic technologies is now providing the opportunity to investigate the role of lipids in maintaining neuronal health, and to reveal whether lipid dysregulation may contribute to neurodegenerative diseases (Hornburg *et al.*, 2023; Murphy, 2018; Schmelzer *et al.*, 2007; Wenk, 2005; van Meer, 2005).

Recent work has begun to link dysregulated lipid homeostasis to neurodegenerative diseases, including ALS/FTD. Several studies have shown altered levels of lipid species in ALS/FTD patient post-mortem tissue (Hanrieder and Ewing, 2014), cerebrospinal fluid (Sol *et al.*, 2021; Blasco *et al.*, 2017), and blood (Area-Gomez *et al.*, 2021; FernÁndez-Eulate *et al.*, 2020; Dorst *et al.*, 2011), as well as ALS rodent models (Chaves-Filho *et al.*, 2019). Dysregulation of TG metabolism has been linked to ALS, with decreased TG levels associated with faster disease progression (Sol *et al.*, 2021) and shorter survival (Dorst *et al.*, 2011). PUFAs have also been linked to ALS pathogenesis, as multiple epidemiological studies have demonstrated that increased dietary consumption of PUFAs, particularly omega-3 (ω3) PUFAs, is associated with decreased risk of disease (Fitzgerald *et al.*, 2014; Veldink *et al.*, 2007). Higher levels of the PUFA α-linolenic acid (C18:3, ω3) have been associated with a longer survival and slower functional decline after disease onset in ALS patients (Bjornevik *et al.*, 2023). The PUFAs docosahexaenoic acid (DHA; 22:6, ω3), and arachidonic acid (AA; 20:4 ω6) are particularly enriched in the brain and both have been linked to disease pathogenesis, with DHA and its mediators involved in anti-inflammatory signaling, while AA and its mediators are generally pro-inflammatory (Bazinet and Layé, 2014).

Despite the accumulating evidence implicating altered lipid metabolism, particularly involving PUFAs in ALS/FTD, it is yet to be determined if PUFA-containing lipids are altered in ALS/FTD neurons and whether this contributes directly to neuronal loss. Therefore, the aim of this study was to characterize potential lipid alterations in ALS/FTD neurons and possible involvement in mediating neuronal toxicity.

Here, we performed RNA sequencing on C9 *Drosophila* heads at an early timepoint to identify early dysregulated pathways associated with GGGGCC repeat expansion. This C9 *Drosophila* model expresses 36 GGGGCC repeats upon feeding with the drug RU486, which is done post-eclosion to avoid developmental expression. Using the elavGS driver, we restricted expression of these toxic repeats to neurons. RNA sequencing was performed after five days induction with RU486, a time prior to overt neurodegeneration. Fatty acid and

lipid metabolism pathways were enriched among downregulated genes, with multiple genes encoding enzymes in the canonical fatty acid synthesis and desaturation pathway downregulated. Remarkably, this transcriptomic downregulation of fatty acid synthesis and desaturation was conserved in human ALS post-mortem spinal cord. Lipidomic assays in C9ALS/FTD iPSC-neurons revealed a loss of highly unsaturated phospholipid species. Similar reductions in highly unsaturated phospholipids was found upon lipidomic analyses of frontotemporal lobar degeneration (FTLD) post-mortem brain tissue, particularly in the frontal cortex. Finally, promoting neuronal lipid unsaturation by desaturase overexpression was sufficient to extend survival in C9 flies and protect against excitotoxicity in C9 iPSC-derived motor neurons. In summary, we have identified alterations in neuronal lipid metabolism, particularly involving phospholipid saturation, conserved across disease models and species implicating this as a novel pathway in the pathogenesis of C9ALS/FTD. These results suggest that modulating neuronal lipid metabolism is a potent approach for ameliorating C9-associated neurodegeneration.

5.2 Results

5.2.1 Transcriptomics of C9 *Drosophila* heads identifies lipid metabolism as an early dysregulated pathway

To identify early dysregulated pathways related to DPR toxicity, RNA sequencing was performed at an early timepoint of 5 days in a *Drosophila* model of C9ALS/FTD, which expresses 36 GGGGCC repeats exclusively in adult neurons (Mizielinska *et al.*, 2014). Gene ontology enrichment analysis was performed on significantly differentially expressed genes between RU486 induced and uninduced fly heads. Microtubule based movement, G protein-coupled receptor signalling pathway and detection of stimulus were the only three pathways enriched among upregulated genes (Figure 5.1 B). Multiple pathways related to metabolism, and specifically fatty acid and lipid metabolism, were enriched among significantly downregulated genes. These included carboxylic acid catabolic and biosynthetic processes, cellular lipid catabolic process, fatty acid

metabolic process, lipid modification as well as processes related to immune response (Figure 5.1 B). Genes encoding enzymes in the fatty acid synthesis and desaturation pathway were downregulated in C9 *Drosophila* heads including acetyl Coenzyme A synthase (*AcCoAS*), fatty acid synthase 1 (*FASN1*), fatty acid synthase 2 (*FASN2*) and desaturase 1 (*Desat1*) (Figure 1C, D). Quantitative PCR confirmed downregulation of a selection of these genes (*AcCoAS, FASN1 and Desat1*) encoding enzymes acting at various stages of fatty acid synthesis and desaturation (Figure 1 D and E).

RNA library preparation, sequencing and DESeq2 analysis was carried out by UCL Genomics core facility. GO analysis was performed by Dr Alla Mikeenko.

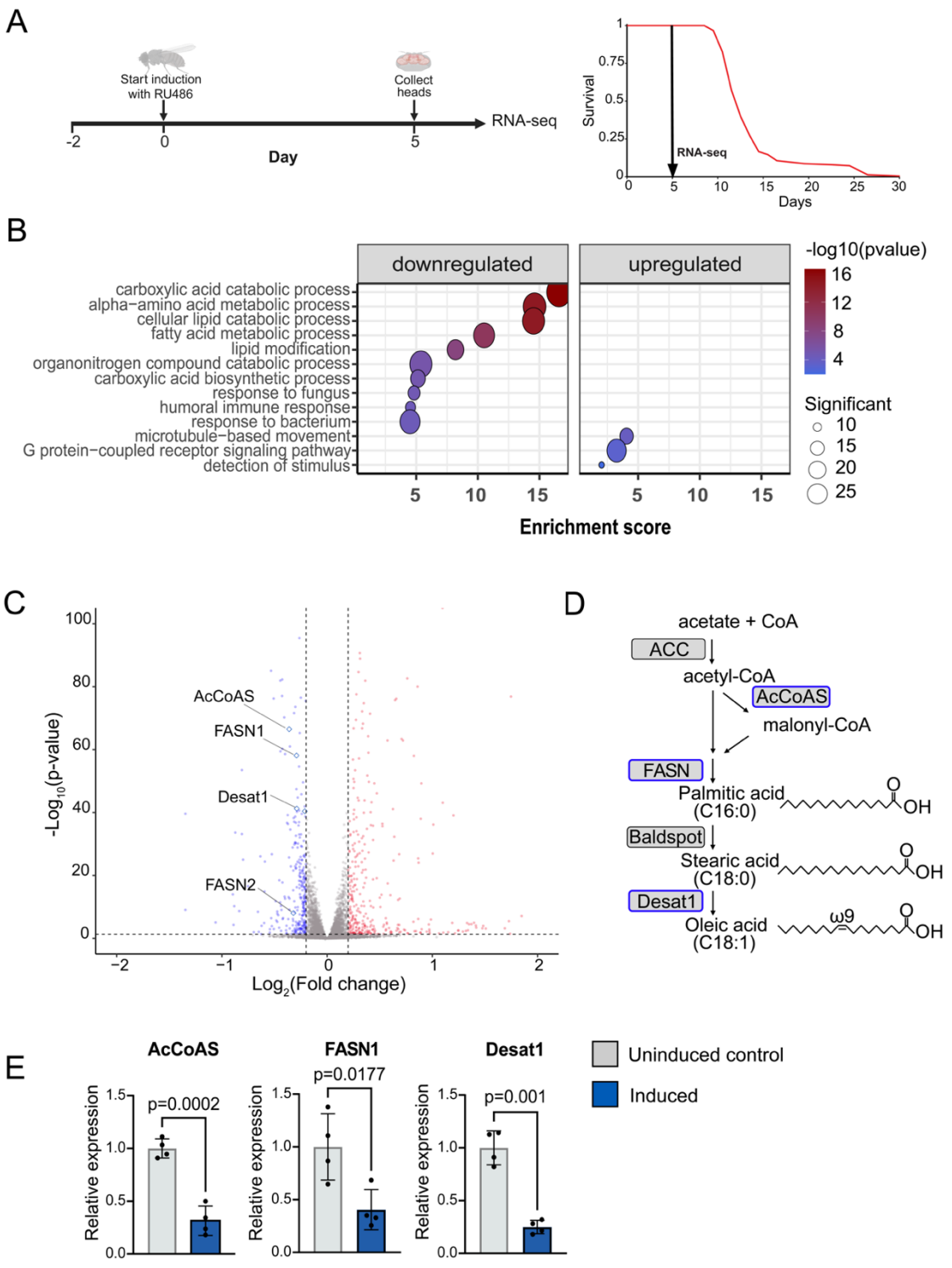

Figure 5.1. Lipid metabolism is an early dysregulated pathway in $(G_4C_2)_{36}$ *Drosophila*.

A. RNA sequencing experimental design. B. Gene Ontology (GO) biological process enrichment analyses showing lipid metabolism terms significantly enriched among downregulated genes in C9 flies. C. Volcano plot highlighting *AcCoAS, FASN1, FASN2* and *Desat1* as significantly downregulated in $(G_4C_2)_{36}$ flies. D. Simplified canonical lipid synthesis and desaturation pathway highlighting

genes that are downregulated in C9 flies (in blue). E. Confirmation of reduction in *AcCoAS, FASN1* and *Desat1* in C9 fly heads by qPCR, normalised to *αTub84B* (*p<0.05, ***p<0.001). N=4 biological replicates (15 fly heads per replicate). Genotype: *UAS-(G_4C_2)$_{36}$, elavGS*.

5.2.2 Conserved transcriptomic dysregulation of lipid metabolism in ALS patient post-mortem spinal cord and brain

We analysed a recently published RNA sequencing dataset from ALS post-mortem cervical spinal cord. This dataset consisted of 149 ALS patients in total, of which 39 had a *C9orf72* mutation and 40 non-neurological disease controls from the New York Genome Center ALS Consortium (Humphrey *et al.*, 2023)**.** Multiple orthologous genes in the fatty acid synthesis and desaturation pathway were downregulated in ALS post-mortem cervical spinal cord. These included *ACACA* (orthologous to *Drosophila ACC*), *ACSS2* (orthologous to *Drosophila AcCoAS*), *FASN* (orthologous to *Drosophila FASN1* and *FASN2*), *ELOVL1*, *ELOVL2* and *ELOVL6* (orthologous to *Drosophila Baldspot*) and *SCD* (orthologous to *Drosophila Desat1*) (Figure 5.2).

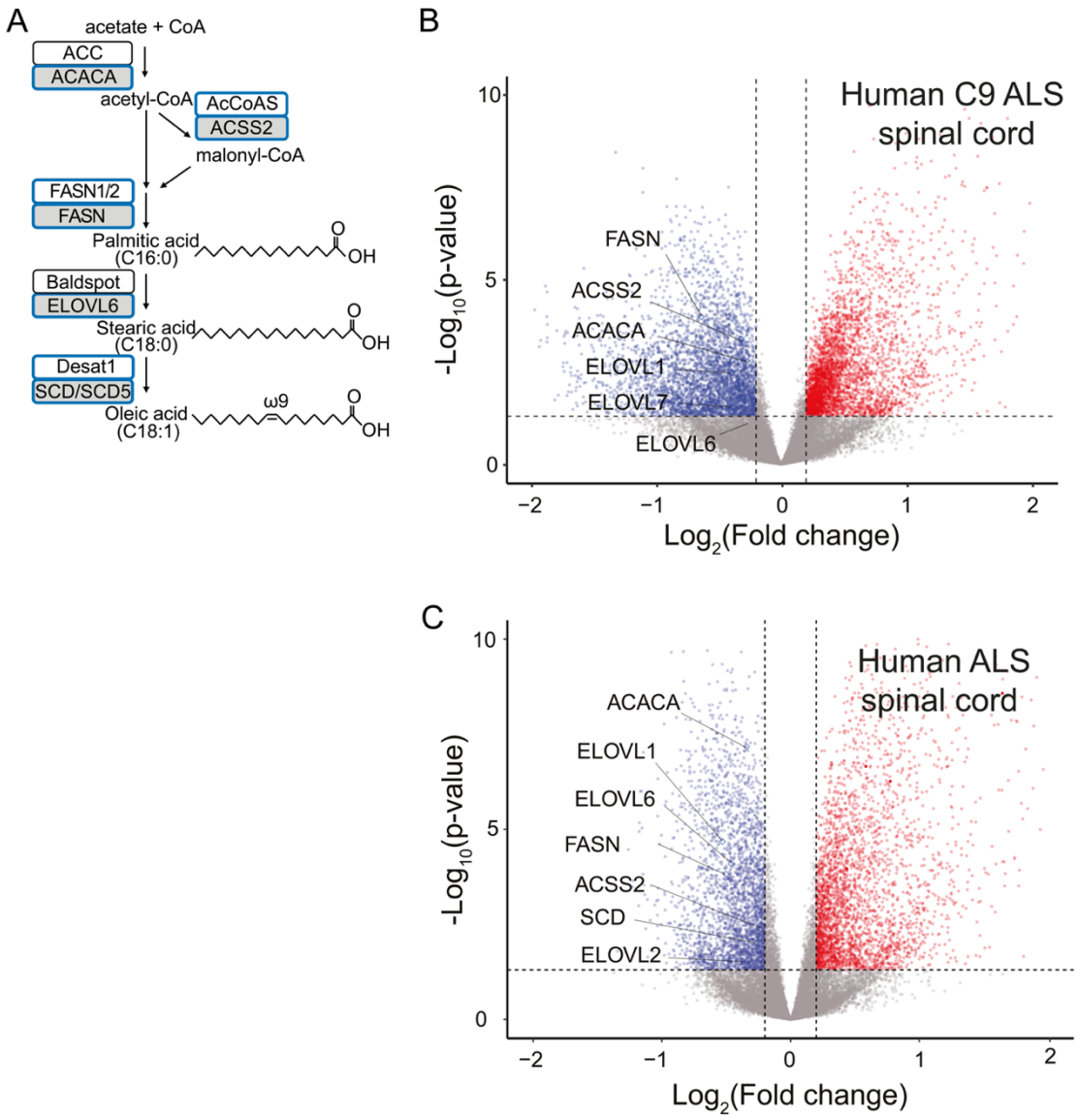

Figure 5.2. Fatty acid synthesis and desaturation pathway genes are downregulated in C9ALS patient post-mortem cervical spinal cord.
A. Simplified canonical fatty acid synthesis and desaturation pathway highlighting genes that are decreased in human ALS patient cervical spinal cord. Human genes are in grey, with *Drosophila* orthologs in white. Blue border indicates significant downregulation in either the C9 *Drosophila* RNA-seq dataset, or the ALS post-mortem cervical spinal cord RNA-seq dataset B. Volcano plot of RNA-seq data from cervical spinal cord of 39 patients with *C9orf72* ALS and 40 non-neurological disease controls from the New York Genome Center ALS Consortium (Humphrey *et al.*, 2023), highlighting downregulated canonical fatty acid synthesis and desaturation pathway genes. C. Volcano plot of RNA-seq data from cervical spinal cord of 149 patients with ALS and 40 non-neurological disease controls from the New York Genome Center ALS Consortium (Humphrey

et al., 2023), highlighting downregulated canonical fatty acid synthesis and desaturation pathway genes.

5.2.3 Lipidomics of C9 fly heads reveals class disturbances in complex lipids

To assess lipid alterations related to this transcriptional deregulation, we performed quantitative shotgun lipidomics on C9 fly heads. Dr Bebiana Da Costa Sousa and Dr Andrea Lopez (Babraham Institute, Cambridge) performed the LC-MS/MS lipidomics. TGs were globally decreased in C9 *Drosophila* heads versus uninduced controls (Figure 5.3 B, Figure 5.4 A and B). Significant lipid class alterations were observed, with TGs and O-TGs decreased, while galactosylceramide (Gal-Cer) and glucosylceramide (Glc-Cer) were increased in C9 *Drosophila* heads versus controls (Figure 5.4 A). An independent colorimetric assay was used to quantify TGs, which confirmed that TGs are decreased in C9 *Drosophila* heads (Figure 5.4 B). *Drosophila* heads contain the head fat body, which is rich in lipids, particularly TGs. Therefore, the presence of this tissue may mask neuronal lipid alterations. Additionally, it would have been beneficial to include a control for RU486 feeding alone, as it is possible that RU486 could itself lead to lipidomic changes in flies.

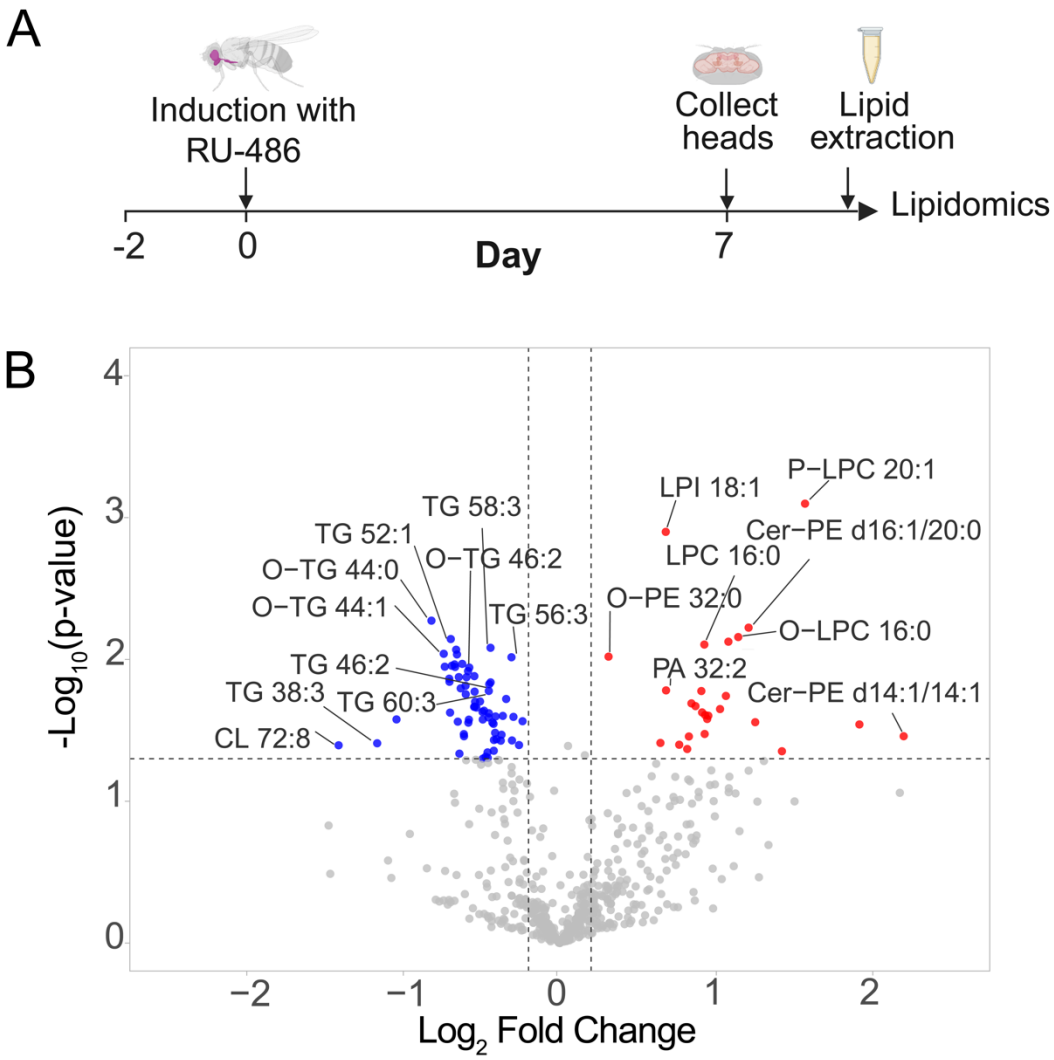

Figure 5.3. Lipidomics of C9 flies reveals class disturbances.
A. Experimental design for fly lipidomic experiment. Flies were induced with RU486 at 2 days post-eclosion, and induced for 7 days before collecting heads for lipidomic analysis. B. Volcano plot highlighting significantly downregulated or upregulated lipid species in $(G_4C_2)_{36}$ induced versus uninduced fly heads. Gridlines are set to -Log10(adjusted p-value) = 1.3 on the y-axis, equivalent to adjusted p-value <0.05 and Log2(Fold change) = 1 on the x-axis. N=4 biological replicates per condition. Volcano plot of differentially expressed lipid species were plotted using VolcaNoseR. Genotype: *UAS-$(G_4C_2)_{36}$, elavGS.*

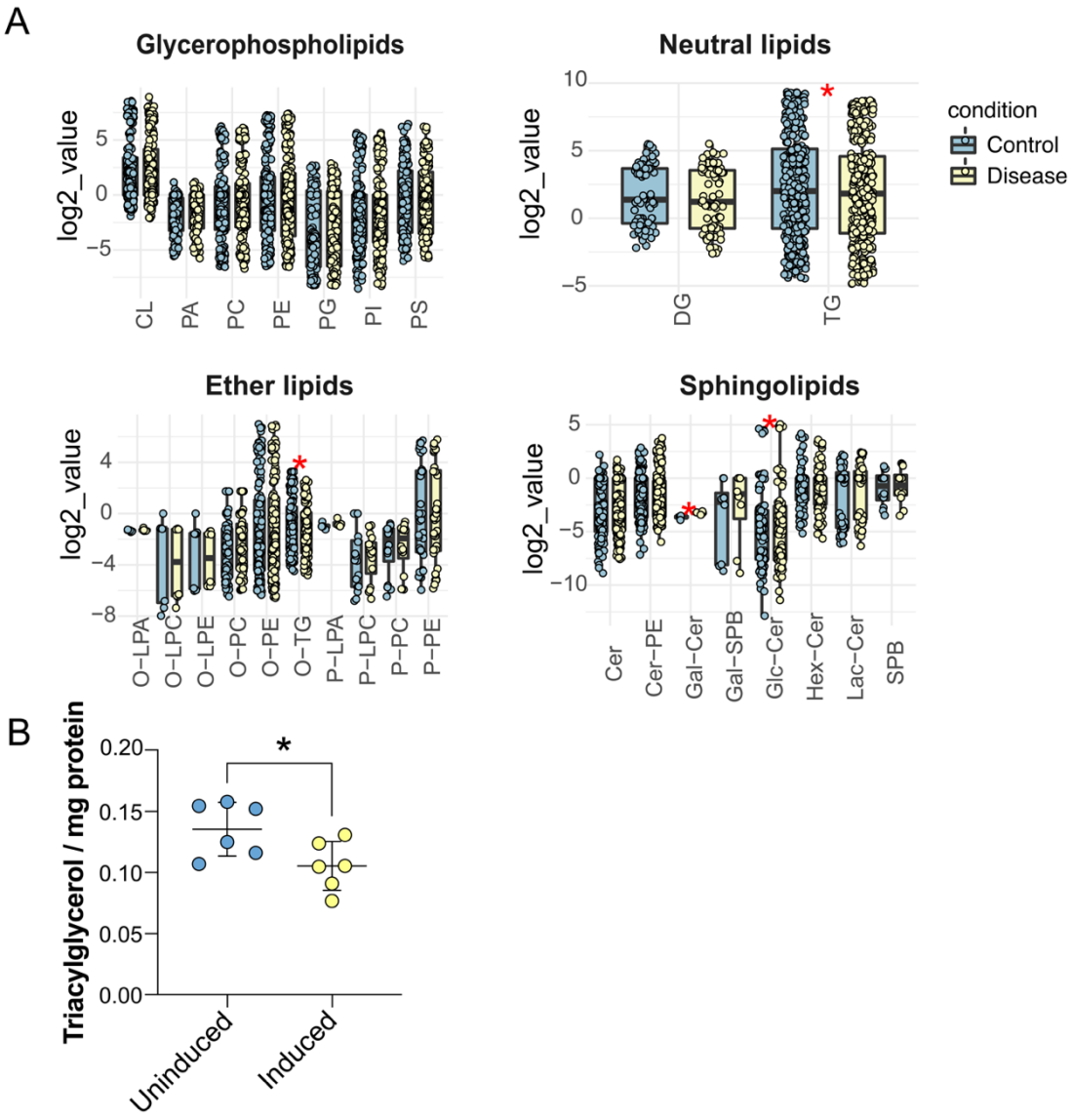

Figure 5.4. Lipidomics of C9 flies reveals class disturbances.
A. Triacylglycerol (TG) and alkyl-triacylglycerol (O-TG) were decreased in induced flies, while the sphingolipids alpha-galactosyl ceramide (Gal-Cer) and glucosylceramide (Glc-Cer) were significantly increased in induced versus uninduced flies. B. Confirmation of TGs as decreased in C9 *Drosophila* induced versus uninduced fly heads, using a colorimetric assay. Student's unpaired t-test, p=0.032. Genotype: *UAS-(G_4C_2)$_{36}$, elavGS.*

5.2.4 Dysregulated fatty acid synthesis and desaturation directly contributes to neurotoxicity *in vivo* in a *Drosophila* model of *C9orf72* repeat expansion

To test whether dysregulated lipid metabolism directly contributes to neurotoxicity, we asked whether overexpression of fatty acid synthase or desaturase genes, which encode enzymes that produce long chain fatty acids and PUFAs, could prevent C9-associated neurodegeneration. Indeed, neuronal overexpression of fatty acid synthases *FASN1* or *FASN2* was sufficient to extend the survival of C9 flies (Figure 5.5 A and B). Both *FASN1* and *FASN2* extended median survival from 13.5 days to 20 days, an increase of 48%. Overexpressing the fatty acid desaturase *Desat1* in neurons of $(G_4C_2)_{36}$ flies significantly extended survival, increasing median survival from 15 days to 25 days, an increase of 67% (Figure 5.5 C). Furthermore, neuronal expression of *C. elegans fat-2*, that encodes a Δ12 fatty acid desaturase which produces the essential PUFAs linoleic acid and α-linolenic acid from monounsaturated fatty acids (Suito *et al.*, 2020), was sufficient to extend survival of C9 flies, providing the largest genetic rescue, extending median survival by 83%, from 15 days to 27.5 days (Figure 5.5 D). Furthermore, supplementing fly food with the essential polyunsaturated fatty acids linoleic acid (C18:2) or α-linolenic acid (C18:3) each extended median survival of C9 flies by 12.5% (Figure 5.6 A and B, respectively). This data shows that enhancing FA desaturation in neurons is a potent method of protecting against C9 repeat toxicity.

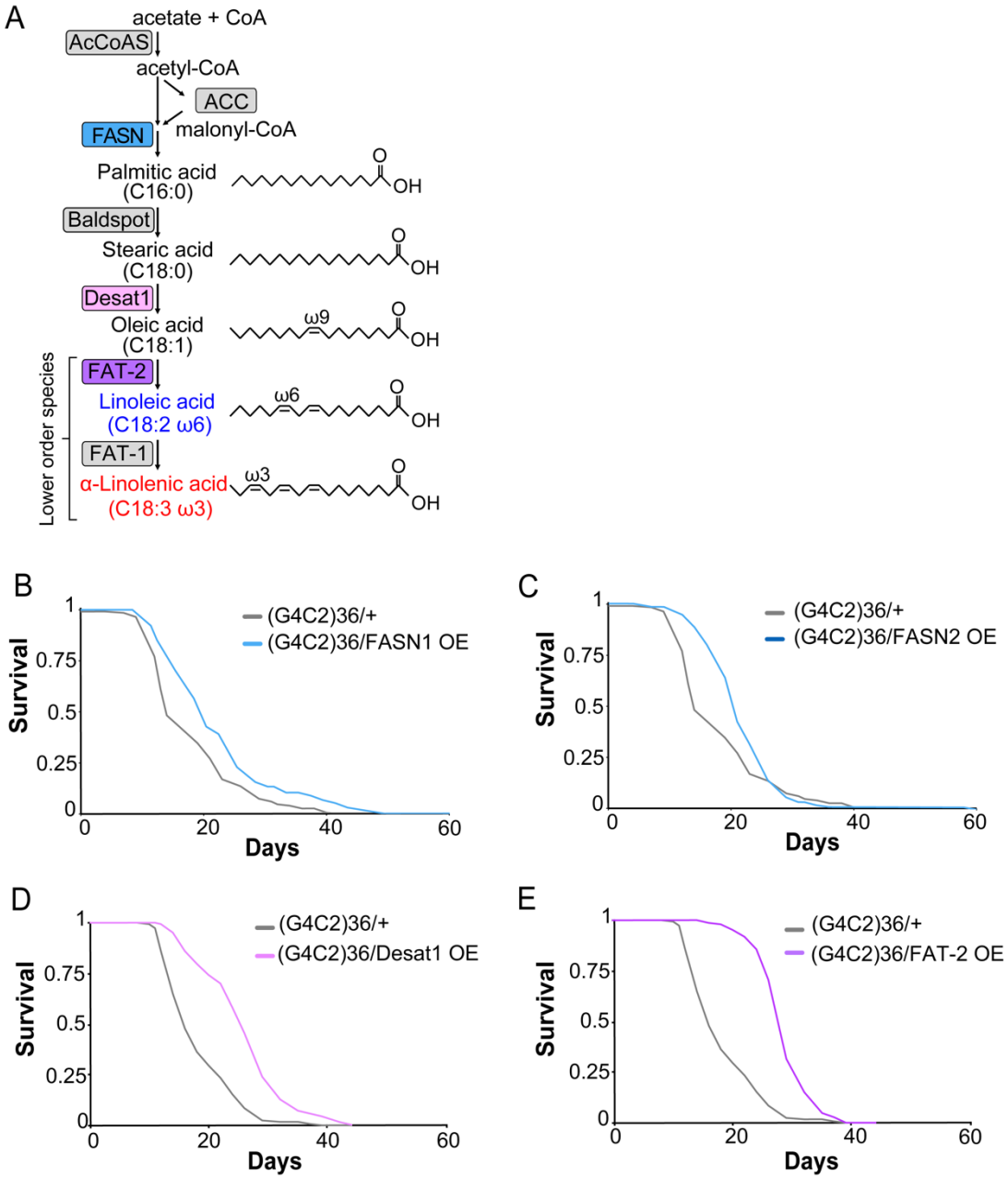

Figure 5.5. Genetic manipulation of fatty acid synthesis and desaturation is sufficient to extend survival of C9 flies.

A. Simplified lipid synthesis and desaturation pathway, including *C. elegans* FAT-1 and FAT-2. B. Neuronal overexpression of *FASN1* extends survival of C9 flies ($p=1.157x10^{-5}$). C. Neuronal overexpression of *FASN2* extends survival of C9 flies ($p=0.003$). D. Neuronal overexpression of *Desat1* extends survival of C9 flies ($p=5.839x10^{-20}$). E. Neuronal overexpression of *fat-2* extends survival of C9 flies ($p=5.119x10^{-38}$). Log-rank test was used for all comparisons. Genotypes: *UAS-$(G_4C_2)_{36}$, elavGS; UAS-$(G_4C_2)_{36}$/UAS-FASN1, elavGS; UAS-$(G_4C_2)_{36}$ /UAS-FASN2, elavGS; UAS-$(G_4C_2)_{36}$, elavGS/UAS-Desat1; UAS-$(G_4C_2)_{36}$, elavGS/UAS-fat-2.*

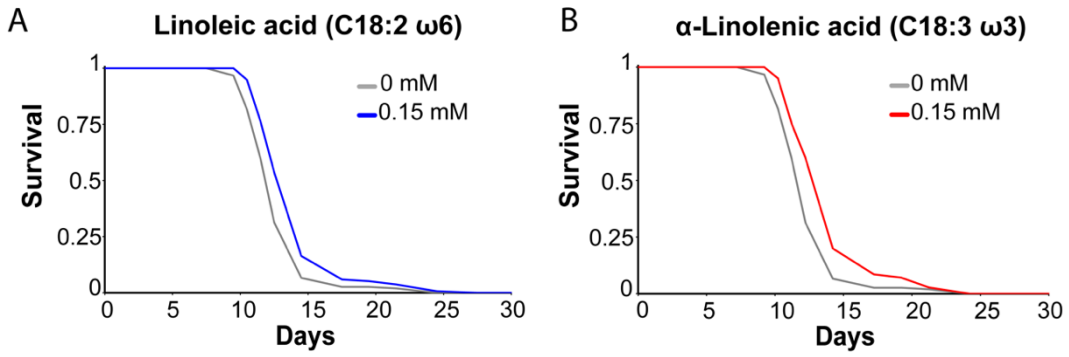

Figure 5.6. Pharmacological manipulation of fatty acid desaturation is sufficient to extend survival of C9 flies.
A. Supplementation of linoleic acid (0.15 mM) extends survival of C9 flies ($p=5.697x10^{-5}$). B. Supplementation of α-linolenic acid (0.15 mM) extends survival of C9 flies ($p=2.951x10^{-6}$). Log-rank test was used for all comparisons. Genotypes: *UAS-$(G_4C_2)_{36}$, elavGS.*

Genetic rescues were not due to an effect on DPR levels as poly(GP) levels in $(G_4C_2)_{36}$ fly heads were unchanged by overexpression of either *FASN1* or *FASN2* (Figure 5.7 A) or overexpression of *Desat1* or *fat-2* (Figure 5.7 B). Therefore, enhancing fatty acid synthesis and desaturation is neuroprotective, downstream of DPRs, making neurons more resistant to DPR toxicity.

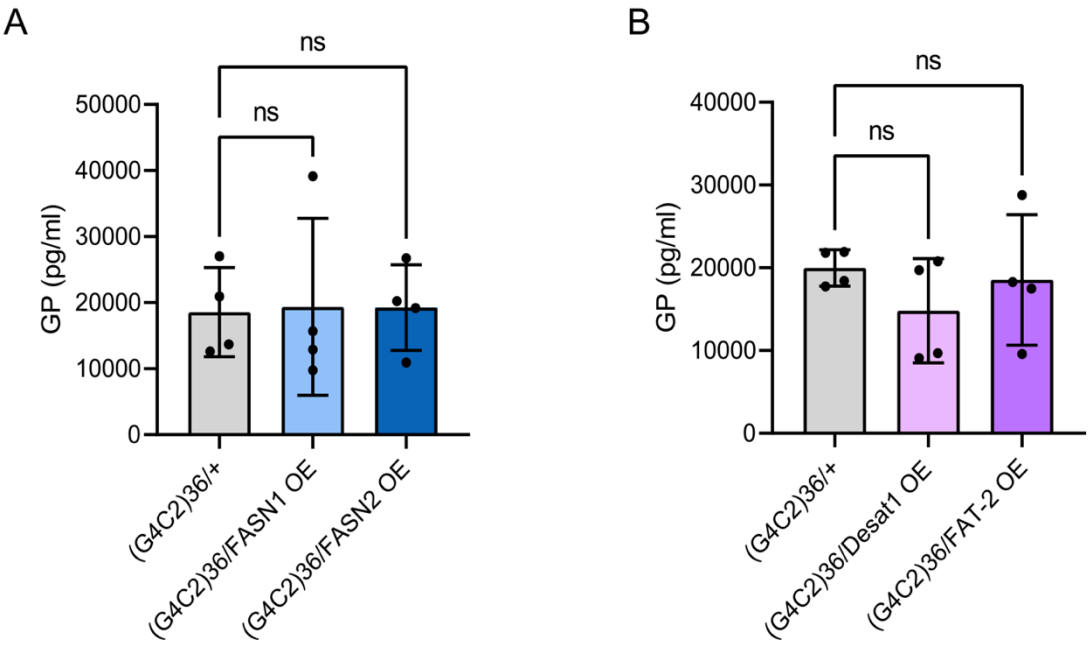

Figure 5.7. Overexpression of fatty acid synthases or desaturases does not alter poly(GP) levels.
A. Co-expression of *FASN1* or *FASN2* does not alter GP levels in $(G_4C_2)_{36}$ fly heads. B. Co-expression of *Desat1* or *fat-2* does not significantly alter GP levels in $(G_4C_2)_{36}$ fly heads. One-way ANOVA, followed by Tukey's post-hoc test. Data presented as mean ± S.D. Genotypes: *UAS-$(G_4C_2)_{36}$, elavGS; UAS-$(G_4C_2)_{36}$/UAS-FASN1, elavGS; UAS$(G_4C_2)_{36}$/UAS-FASN2, elavGS; UAS-$(G_4C_2)_{36}$, elavGS/UAS-Desat1; UAS-$(G_4C_2)_{36}$, elavGS/UAS-fat-2.*

Genetic rescues were specific to disease as overexpressing fatty acid synthases or desaturases in neurons of healthy control flies either had no effect on survival, or increased survival to a smaller magnitude than that seen in the context of *C9orf72* repeats (Figure 5.8). Neuronal expression of *FASN1* in wildtype flies significantly increased lifespan, increasing median survival by 13% from 68 days to 77 days (Figure 5.8 B). Neuronal overexpression of *FASN2* did not significantly alter lifespan of wildtype flies (Figure 5.8 C). Neuronal overexpression of *Desat1* in wildtype flies significantly increased lifespan, increasing median survival by 12%, from 81.5 days to 91 days. (Figure 5.8 E). Neuronal overexpression of *fat-2* did not significantly affect lifespan of wildtype flies (Figure 5.8 F).

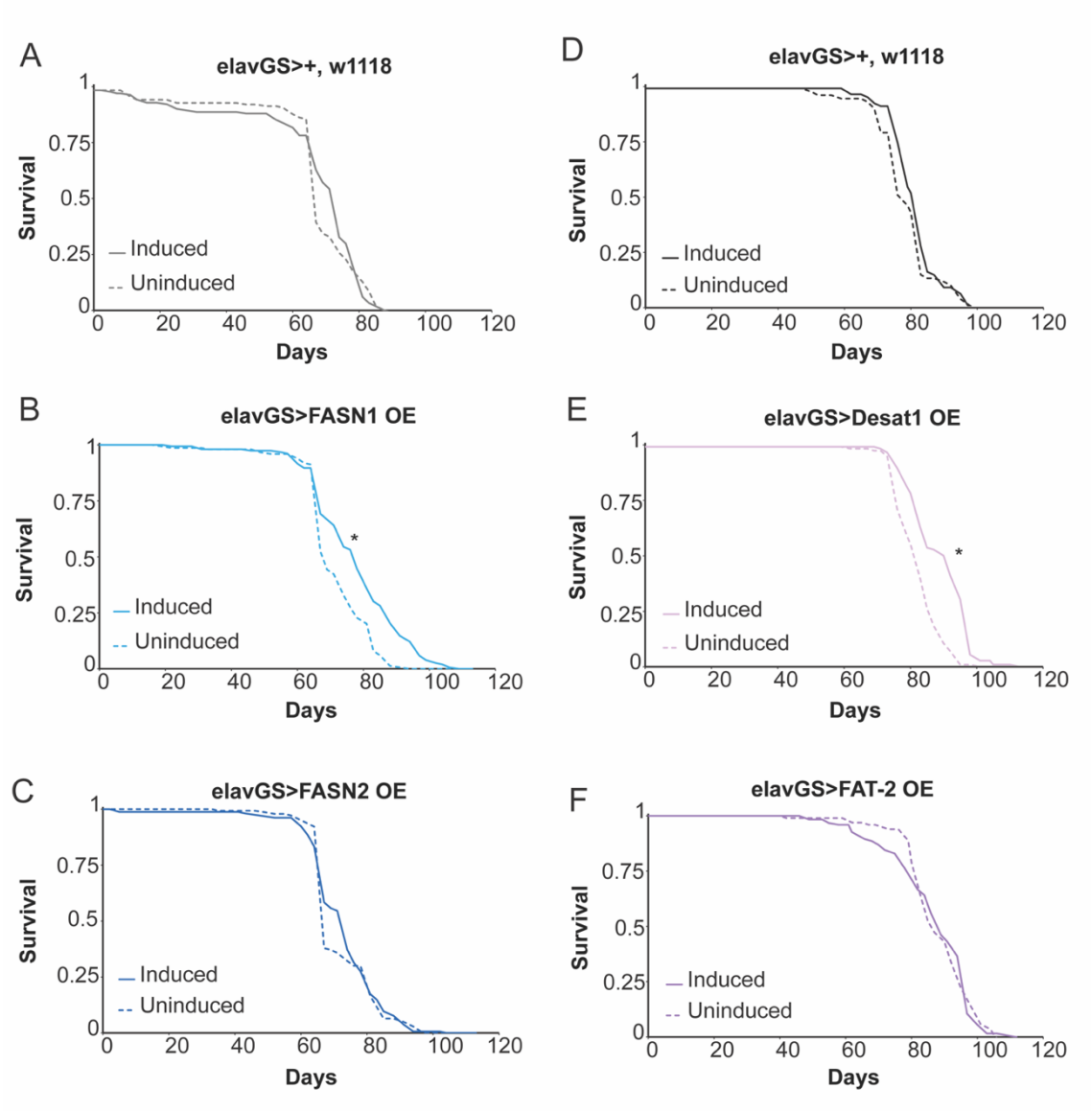

Figure 5.8. Lifespans of wildtype flies overexpressing fatty acid synthases or desaturases.

A. Driver alone control lifespan run in parallel to B and C. There is no difference in lifespan between RU486 induced and uninduced flies (p=0.408). B. *FASN1* overexpression in neurons of wildtype flies extends lifespan ($p=3.386x10^{-8}$). C. *FASN2* overexpression in neurons of wildtype flies has no effect on lifespan (p=0.866). D. Driver alone control lifespan run in parallel to E and F. There is no difference in lifespan between RU486 induced and uninduced flies (p=0.197). E. *Desat1* overexpression in neurons of wildtype flies extends lifespan ($p=1.567x10^{-10}$). F. Overexpression of *fat-2* in neurons of wildtype flies has no effect on lifespan (p=0.589). N=150 flies per condition. Log-rank test used for all comparisons. Genotypes: *elavGS; elavGS/UAS-FASN1; elavGS/UAS-FASN2; elavGS/UAS-Desat1; elavGS/UAS-fat-2.*

5.2.5 Feeding polyunsaturated but not saturated or monounsaturated fatty acids extends C9 *Drosophila* survival

To determine whether the saturation profile of supplemented long chain fatty acids has any effect on *C9orf72* repeat toxicity, a direct comparison between saturated, monounsaturated, and polyunsaturated fatty acids was performed. The saturated fatty acids palmitic acid (C16:0) and stearic acid (C18:0), and the monounsaturated fatty acid oleic acid (C18:1) were selected. The essential polyunsaturated fatty acids linoleic acid (C18:2) and α-linolenic acid (C18:3) which were previously shown to increase survival of C9 flies (Figure 5.6) were also included. *Drosophila* lack C20 and C22 PUFAs, therefore these were not tested (Shen *et al.*, 2010). Fatty acids were supplemented in *Drosophila* food at three different concentrations, selected based on previous literature (Mori *et al.*, 2019; Randall *et al.*, 2015; Shen *et al.*, 2010). Experiments were performed in parallel with one shared control (0 mM) (Figure 5.9). Supplementation of saturated or monounsaturated fatty acids either had no significant effect on survival of C9 flies or significantly decreased survival, in the case of stearic acid (C18:0), at the 15 mM concentration ($p=0.008$) (Figure 5.8 B-D). Only supplementation of the PUFAs linoleic acid (C18:2) and α-linolenic acid (C18:3) increased C9 *Drosophila* survival at the concentrations tested. Linoleic acid supplemented at 0.15 mM ($p=0.036$) and 1.5 mM ($p=0.002$), and α-linolenic acid, supplemented at 0.15 mM ($p=0.049$) extended survival of C9 *Drosophila*. These results show that supplementation of PUFAs, rather than saturated or monounsaturated fatty acids, are protective in C9 *Drosophila*.

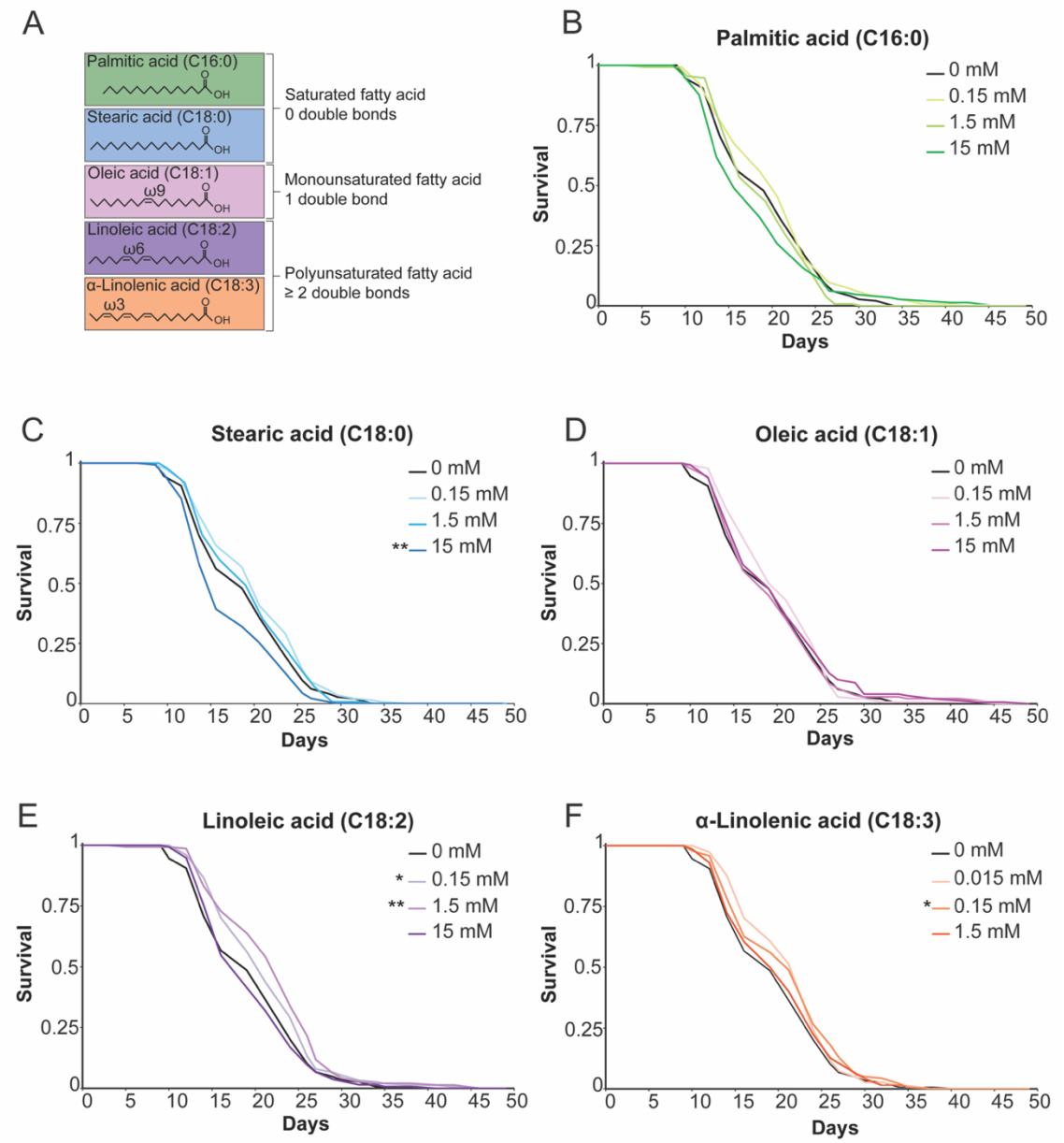

Figure 5.9. Lifespans of C9 flies fed saturated, monounsaturated, and polyunsaturated long chain fatty acids.

A. Structure and saturation of selected fatty acids. B. Palmitic acid had no significant effect on survival of C9 flies at any of the concentrations tested (0.15 mM, p=0.052, 1.5 mM p=0.182, 15 mM p=0.473). C. Stearic acid had no significant effect at 0.15 mM (p=0.079) or 1.5 mM (p=0.992), but significantly decreased survival at 15 mM (p=0.008). D. Oleic acid had no significant effect on survival at any of the concentrations tested (0.15 mM, p=0.285, 1.5 mM p=0.782, 15 mM p=0.186). E. Linoleic acid significantly increased survival of C9 flies at 0.15 mM (p=0.036) and 1.5 mM (p=0.002) concentrations, but not 15 mM (p=0.663). F. Supplementation of α-linolenic acid significantly increased survival of C9 flies at 0.15 mM (p=0.049), but not at 0.015 mM (p=0.055) or 1.5 mM (p=0.216). N=135-150 flies per condition. All log-rank test. Genotype: *UAS-$(G_4C_2)_{36}$, elavGS.*

The extensions in survival observed by PUFA supplementation were specific to disease, as supplementing wildtype flies with linoleic acid or α-linolenic acid, either decreased or had no effect on wildtype survival. All flies were fed RU486 at 200 μM to match conditions in which rescue was observed for $(G_4C_2)_{36}$ flies. Linoleic acid supplementation had no effect on wildtype lifespan at 0.15 mM and significantly shortened wildtype lifespan at the 1.5 mM, decreasing median survival by 8%, from 92.5 days to 85 days (Figure 5.10 A). Similarly, α-linolenic acid supplementation had no significant effect on lifespan at 0.015 mM, but significantly shortened lifespan of wildtype flies at 0.15 mM, decreasing median survival by 6%, from 92.5 to 87 days (Figure 5.10 B).

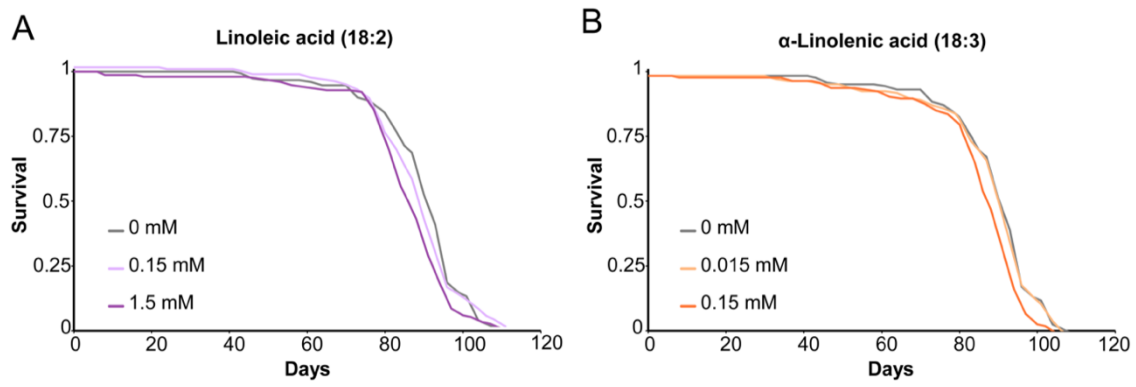

Figure 5.10. Lifespans of wildtype flies fed linoleic or α-linolenic acid.
A. Linoleic acid supplementation had no effect on wildtype lifespan at 0.15 mM (p=0.162) and significantly shortened wildtype lifespan at the 1.5 mM ($p=4.352x10^{-5}$) concentration. B. α-linolenic acid supplementation had no effect on wildtype lifespan at 0.015 mM (p=0.599), and significantly shortened wildtype lifespan at the 0.05 mM concentration ($p=6.22x10^{-6}$). N=150 flies per condition. All log-rank test. Genotype: *elavGS.*

The RU486 inducible elavGS driver requires flies to consume RU486 in the food. One possible explanation for the small lifespan extensions with PUFA supplementation is reduced feeding behaviour, and therefore less induction of the $(G_4C_2)_{36}$ transgene. To exclude this possibility, feeding behaviour was assessed with the proboscis extension assay. Proboscis extension response was

not significantly altered 24 hours after exposure to RU486, or linoleic or α-linolenic acid, in wildtype flies (Figure 5.11 A) or $(G_4C_2)_{36}$ flies (Figure 5.11 B). Therefore, the lifespan extensions observed in C9 *Drosophila* with linoleic acid or α-linolenic supplementation are due to a protective effect, and not due to alterations in feeding behaviour.

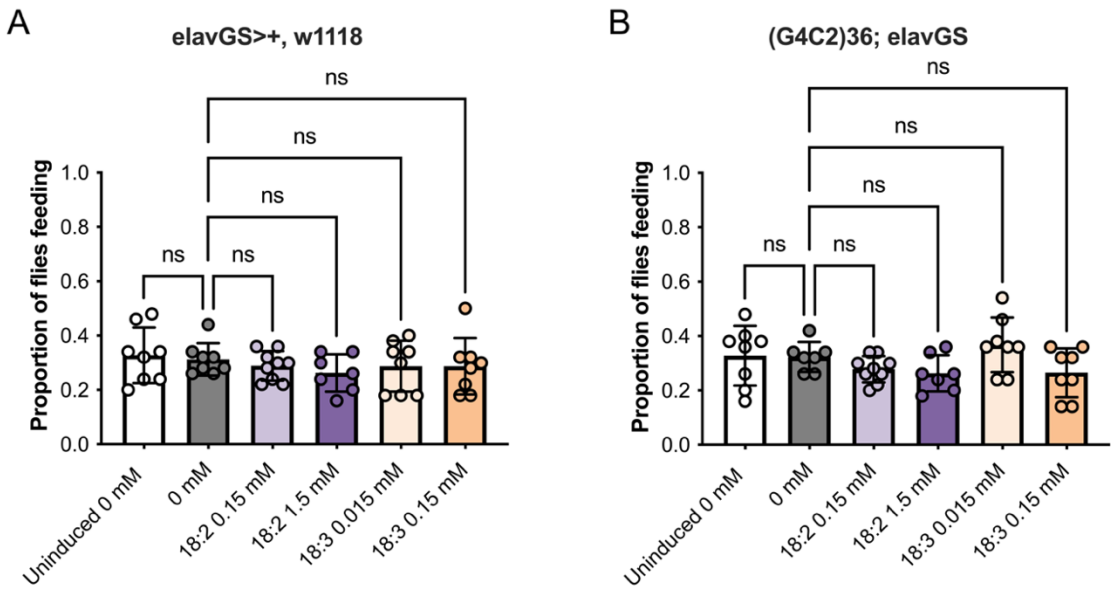

Figure 5.11. Food supplementation with linoleic or α-linolenic acid does not alter proboscis extension response of wildtype or C9 flies.
A. Food supplementation with linoleic or α-linolenic acid does not alter proboscis extension response of wildtype flies. B. Food supplementation with linoleic or α-linolenic acid does not alter proboscis extension response of C9 flies. Flies were placed onto new food 24 hours before assay was performed, at a density of five flies per vial, N=7-9 biological replicates. All groups were induced with RU486 except for the uninduced conditions. Two-way ANOVA with Tukey's multiple comparison test was used to calculate statistical significance. Data presented as mean ± S.D. Genotypes: *elavGS; UAS-$(G_4C_2)_{36}$, elavGS*.

5.2.6 Neuronal expression of a *Drosophila* desaturase gene, that synthesises di-unsaturated long chain fatty acids also extends survival of C9 flies

Drosophila, like mammals, in general cannot synthesise essential PUFAs. However, Fad2 is a female-specific transmembrane desaturase enzyme in *Drosophila* that synthesises cuticular long chain di-unsaturated fatty acids, that

act as sex pheromones (Shirangi *et al.*, 2009; Chertemps *et al.*, 2006). To assess whether ectopic expression of this endogenous desaturase in neurons could also modify *C9orf72* repeat toxicity, *UAS-Fad2* flies were generated. After backcrossing for six generations, *UAS-Fad2* was ectopically expressed in adult neurons using the elavGS driver. Overexpression of *Fad2* in neurons of $(G_4C_2)_{36}$ flies was sufficient to extend survival, increasing median survival by 21%, from 11 to 14 days (Figure 5.12). This demonstrates that multiple approaches increasing fatty acid desaturation can extend C9 *Drosophila* survival.

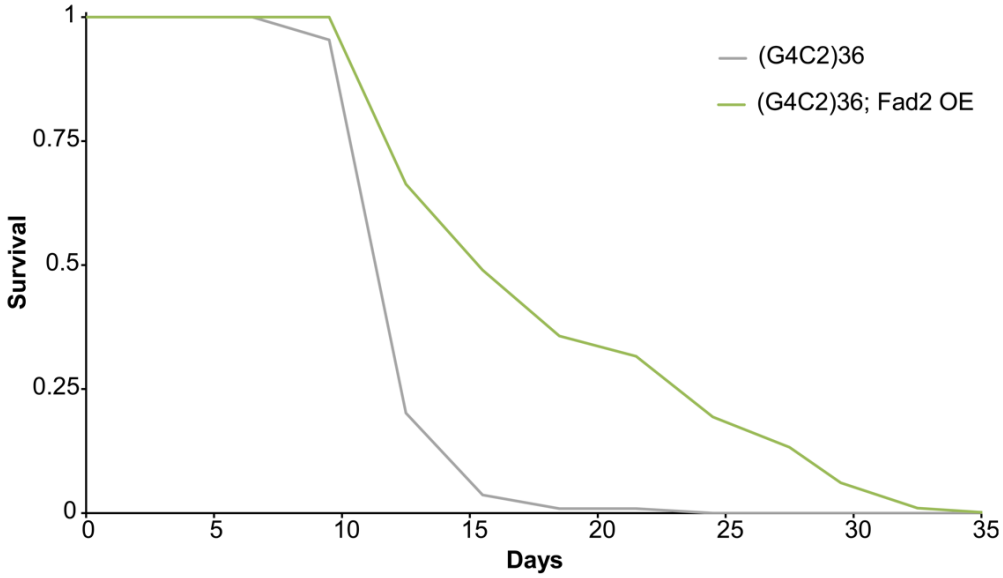

Figure 5.12. Neuronal overexpression of *Fad2* extends survival of C9 flies. Survival curve of $(G_4C_2)_{36}$ expressing flies, with or without co-expression of *Fad2* ($p=3.367x10^{-17}$, by log-rank test). N=100-110 flies per condition. Genotypes: *UAS-$(G_4C_2)_{36}$, elavGS; UAS-$(G_4C_2)_{36}$, elavGS/UAS-Fad2.*

5.2.7 Desaturase overexpression in $(G_4C_2)_{36}$ neurons ameliorates cold-stress sensitivity

Lipid unsaturation is known to influence the biophysical properties of cellular membranes, particularly the packing of membrane phospholipids with resulting effects on membrane fluidity (Levental *et al.*, 2020; Rawicz *et al.*, 2000). Since temperature can impact membrane fluidity, poikilothermic *Drosophila* must acclimate to temperature fluctuations for survival (Brankatschk *et al.*, 2018;

Slotsbo *et al.*, 2016). *Drosophila* have been shown to undergo homeoviscous adaptation, switching feeding preference from yeast to plants, thereby increasing incorporation of plant-derived PUFAs into lipid bilayers in response to cold exposure (Brankatschk *et al.*, 2018). Therefore, *Drosophila* that have dysregulated expression of desaturases, and unsaturated fatty acids might be expected to have a heightened sensitivity to cold stress, while desaturase overexpression may compensate for this phenotype. To test this hypothesis, *Drosophila* were exposed to 4°C for 18 hours, which causes a cold-induced paralysis (Moraru *et al.*, 2017). Recovery was scored after one hour at room temperature. Whereas all uninduced control flies were alive and walking after this period, 42% of flies expressing $(G_4C_2)_{36}$ were dead, and 54% were partially paralysed, with only 2% alive and walking. Overexpressing either *Desat1* or *fat-2* in neurons prevented death after cold exposure in $(G_4C_2)_{36}$ flies. *Desat1* neuronal overexpression in $(G_4C_2)_{36}$ flies led to 24% partial paralysis, and 76% full recovery. Neuronal overexpression of *fat-2* in $(G_4C_2)_{36}$ flies led to 18% partial paralysis, and 82% full recovery (Figure 5.13).

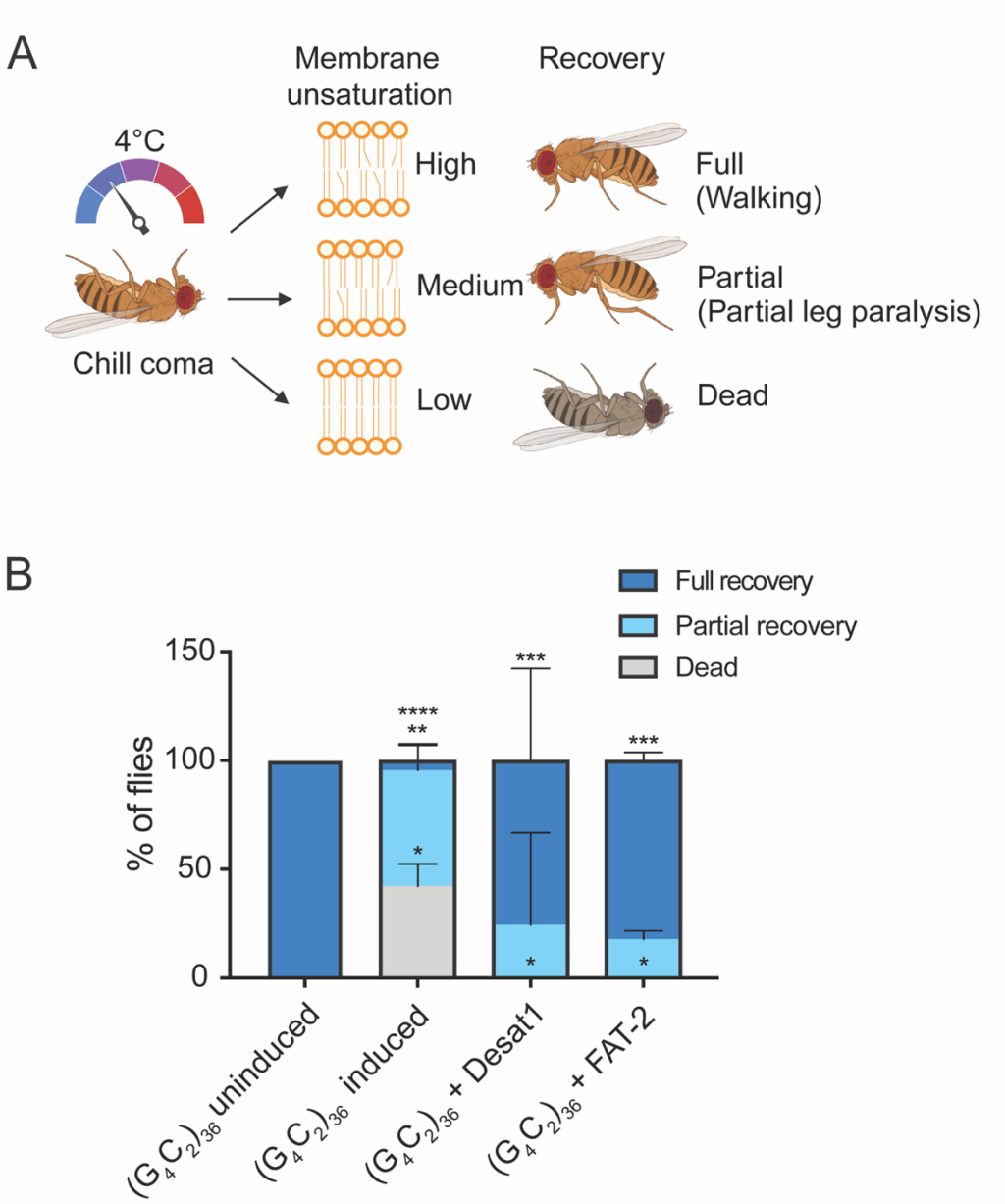

Figure 5.13. Desat1 and FAT-2 ameliorate cold-stress sensitivity of C9 flies.

A. Schematic diagram of cold stress assay. Flies were exposed to 4°C, which induces a chill coma or cold-induced paralysis response. Membrane unsaturation influences tolerance to cold-stress, with higher membrane unsaturation providing greater tolerance to cold stress. After 18 hours, flies were moved to room temperature for 1 hour, and recovery was assessed. B. $(G_4C_2)_{36}$ flies are sensitive to cold stress, with significantly increased death ($p=0.047$), increased partial paralysis ($p=0.007$), and decreased recovery evident as walking ($p<0.0001$) compared to uninduced controls. Overexpression of *Desat1* in $(G_4C_2)_{36}$ flies significantly increased the proportion of flies experiencing a full recovery compared to $(G_4C_2)_{36}$ alone ($p=0.0003$), and significantly reduced death post-exposure compared to $(G_4C_2)_{36}$ alone ($p=0.047$). Overexpression of *fat-2* in $(G_4C_2)_{36}$ flies significantly increased the proportion of flies experiencing a full

recovery (p<0.0001) and significantly reduced death post-exposure compared to $(G_4C_2)_{36}$ alone (p=0.047). *p<0.05, **p<0.01, ***p<0.001, ****p<0.0001. N=3 biological replicates, containing 15 flies per replicate vial. Two-way ANOVA followed by Tukey's post-hoc test. Data presented as mean ± S.D. Genotypes: *UAS-$(G_4C_2)_{36}$, elavGS; UAS-$(G_4C_2)_{36}$, elavGS/UAS-Desat1; UAS-$(G_4C_2)_{36}$, elavGS/UAS-fat-2.*

For the following results in this chapter, relating to lipidomics, Dr Alex Cammack, a postdoctoral fellow in the Isaacs lab performed the cell culture with Ashling Giblin. Dr Cammack designed the $(G_4C_2)_{92}$ and $(G_4C_2)_2$ lentiviral constructs and performed analyses of lipidomic data. Dr Mireia Carcole performed the MSD immunoassays. Professor Tammaryn Lashley, director of research at the Queen Square Brain Bank UCL, processed and provided post-mortem brain tissue used for lipidomics. Niek Blomberg, a research technician in the lab of our collaborator, Dr Martin Giera (Leiden, Netherlands) performed lipidomics on all neuronal and brain samples.

5.2.8 Lipid unsaturation is altered in *C9orf72* iPSC-neuronal models

To determine whether lipid alterations were conserved in mammalian models of *C9orf72* ALS/FTD, targeted lipidomics was performed on *C9orf72* patient iPSC-cortical neurons using the Lipidyzer platform (Figure 5.14 A). Specific changes in phospholipid species were identified, characterised by a shift from unsaturated to saturated lipids, with a striking decrease of phospholipids containing highly unsaturated fatty acids, with four or more double bonds (Figure 5.14 F). To assess whether lipid alterations could be recapitulated by introducing G_4C_2 repeats into healthy neurons, control i3 cortical neurons were transduced with $(G_4C_2)_{92}$ or $(G_4C_2)_2$ lentivirus and unbiased shotgun lipidomic analyses was performed at DIV 21. $(G_4C_2)_{92}$ transduction in i3 neurons showed similar findings to the *C9orf72* patient neurons, with specific reduction of phospholipids containing the highly unsaturated PUFAs (Figure 5.14 F). DPR production in cells transduced with the $(G_4C_2)_{92}$ lentivirus was confirmed by poly(GA) MSD immunoassay (Figure 5.14 D). After establishing a clear lipid signature in C9 models of decreased PUFA-containing phospholipids, we wondered whether this signature could be prevented by antisense oligonucleotide (ASO) treatment

targeting the GGGGCC expanded repeat sequence. To this end, C9 patient cortical neurons were treated with a *C9orf72* sense ASO from DIV 3 until DIV 21, at which timepoint lipidomics was performed. ASO treatment significantly reduced DPRs, confirming it was effective at reducing *C9orf72* repeat RNA levels (Figure 5.14 E). The ASO prevented much of the perturbed lipid signature observed in *C9orf72* patient neurons, demonstrating that the lipid signature observed across *C9orf72* models is caused the presence of expanded repeats (Figure 5.14 F). Details and sequences of ASOs used are provided in Chapter 2 Methods, section 2.21.

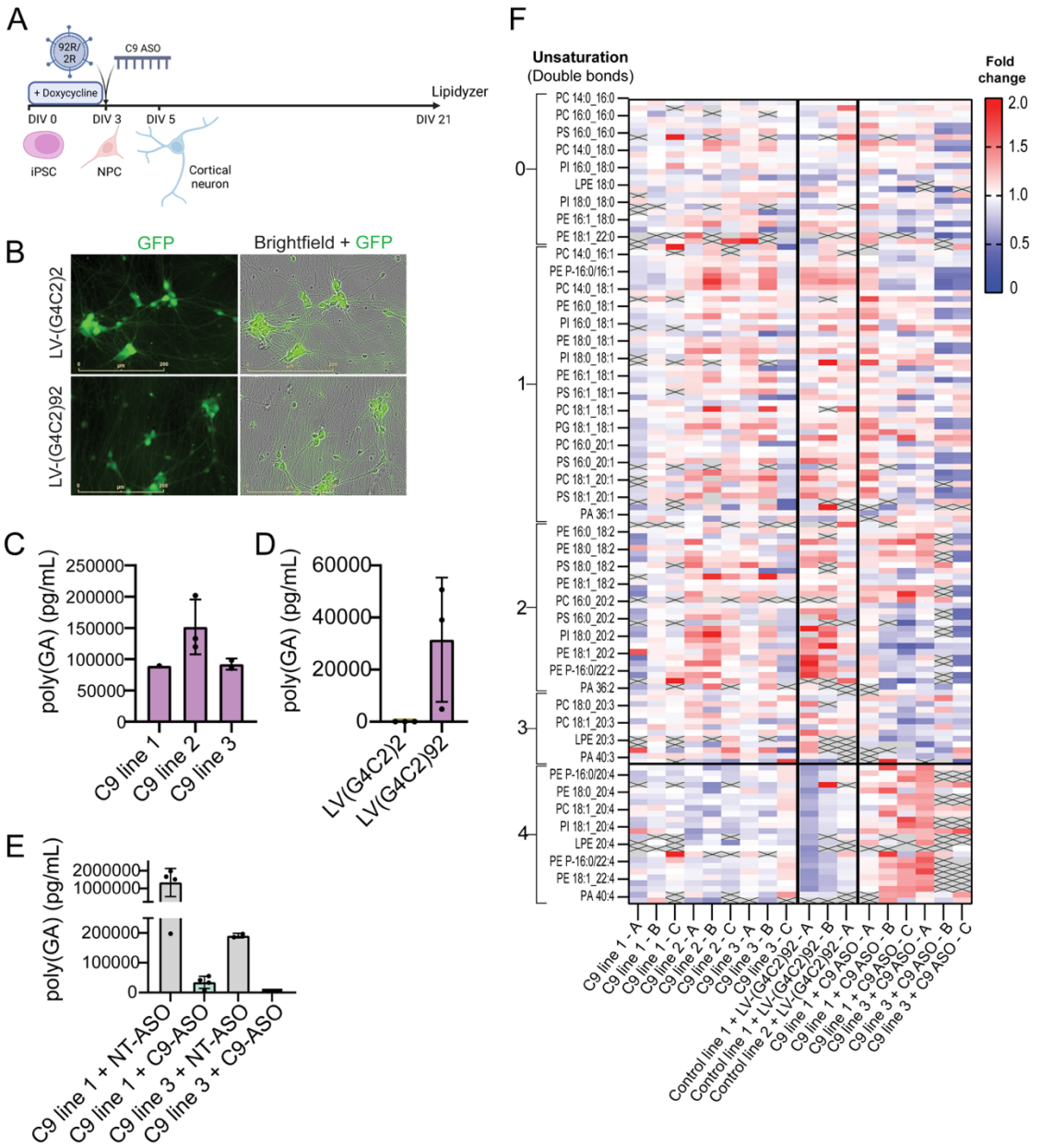

Figure 5.14. The presence of *C9orf72* hexanucleotide repeats causes a shift from unsaturated to saturated lipids.

A. *C9orf72* iPSC-derived neuron lines (or isogenic controls) were induced with i3 NGN2 protocol and grown to DIV 21 for lipidomic analyses. To confirm C9-specificity of lipid changes, control lines were transduced with novel $(G_4C_2)_{92}$ repeat lentivirus (or $(G_4C_2)_2$ control), and repeats were knocked down with a *C9orf72* sense-targeted antisense oligonucleotide (ASO; or a non-targeting (NT) control) in the *C9orf72* lines. B. Representative images of 2H9 isogenic control neurons transduced with $(G_4C_2)_{92}$ or $(G_4C_2)_2$ lentivirus co-expressing GFP. C. Confirmation of GA dipeptide production in *C9orf72* lines determined by MSD immunoassay at DIV 21. D. Confirmation of GA dipeptide production in control neurons transduced with $(G_4C_2)_{92}$ determined by MSD immunoassay at DIV 21. E. Confirmation of *C9orf72* knockdown, by GA MSD immunoassay in *C9orf72* neurons treated with a *C9orf72* sense-targeted antisense oligonucleotide (ASO) at DIV 21. F. Heatmap displaying all detected phospholipids as fold-change over control in each experiment and line. Highly unsaturated phospholipid species (≥4 double bonds) are reduced in *C9orf72* and LV-$(G_4C_2)_{92}$ lines but increased in *C9orf72* lines treated with the C9-ASO, indicating that these lipid changes are specific to the presence of *C9orf72* repeats. N=3 biological replicates (individual iPSC lines) and n=2-3 technical replicates.

5.2.9 Lipid unsaturation is altered in FTD patient post-mortem frontal cortex

Given the conserved lipid signature observed across multiple models of *C9orf72* ALS/FTD at relatively early timepoints, we next asked whether this signature persists throughout the disease course in patients. To address this question, lipidomics was performed on post-mortem frontal cortex brain tissue from 47 individuals with a pathological diagnosis of FTLD, 15 of which had a *C9orf72* mutation, and 13 age-matched, non-neurological controls. Similar to the lipid changes observed in pure neuronal culture models of *C9orf72* ALS/FTD, a decrease in phospholipids containing highly unsaturated PUFAs was observed in *C9orf72* FTLD frontal cortex compared to non-neurological controls (Figure 5.15 D). In contrast to our results in *C9orf72* neuronal monocultures, a decrease in phospholipids containing the PUFA linoleic acid (C18:2), was found in *C9orf72* FTLD frontal cortex. Additionally, while the highly unsaturated PUFA arachidonic acid (C20:4) was decreased in *C9orf72* neuronal models, we found an increase in AA-containing phospholipids in *C9orf72* FTLD brains versus non-neurological controls. These differences between iPSC neuronal models and patient post-mortem brains are likely due to different disease stages, and complex tissue

versus neuronal monoculture. Despite these differences in complexity and disease stage, the largely conserved loss of PUFA containing phospholipids is quite remarkable.

A strikingly similar lipidomic profile was observed between FTLD-all and FTLD-C9 groups versus non-neurological controls, with a specific loss of phospholipids containing highly unsaturated PUFA species (Figure 5.15 D). This indicates that phospholipid PUFA dysregulation is not only found in *C9orf72* mutation carriers but can also be found in non-*C9orf72* FTLD frontal cortex, suggesting a shared disease mechanism implicating PUFA metabolism (Figure 5.15 D).

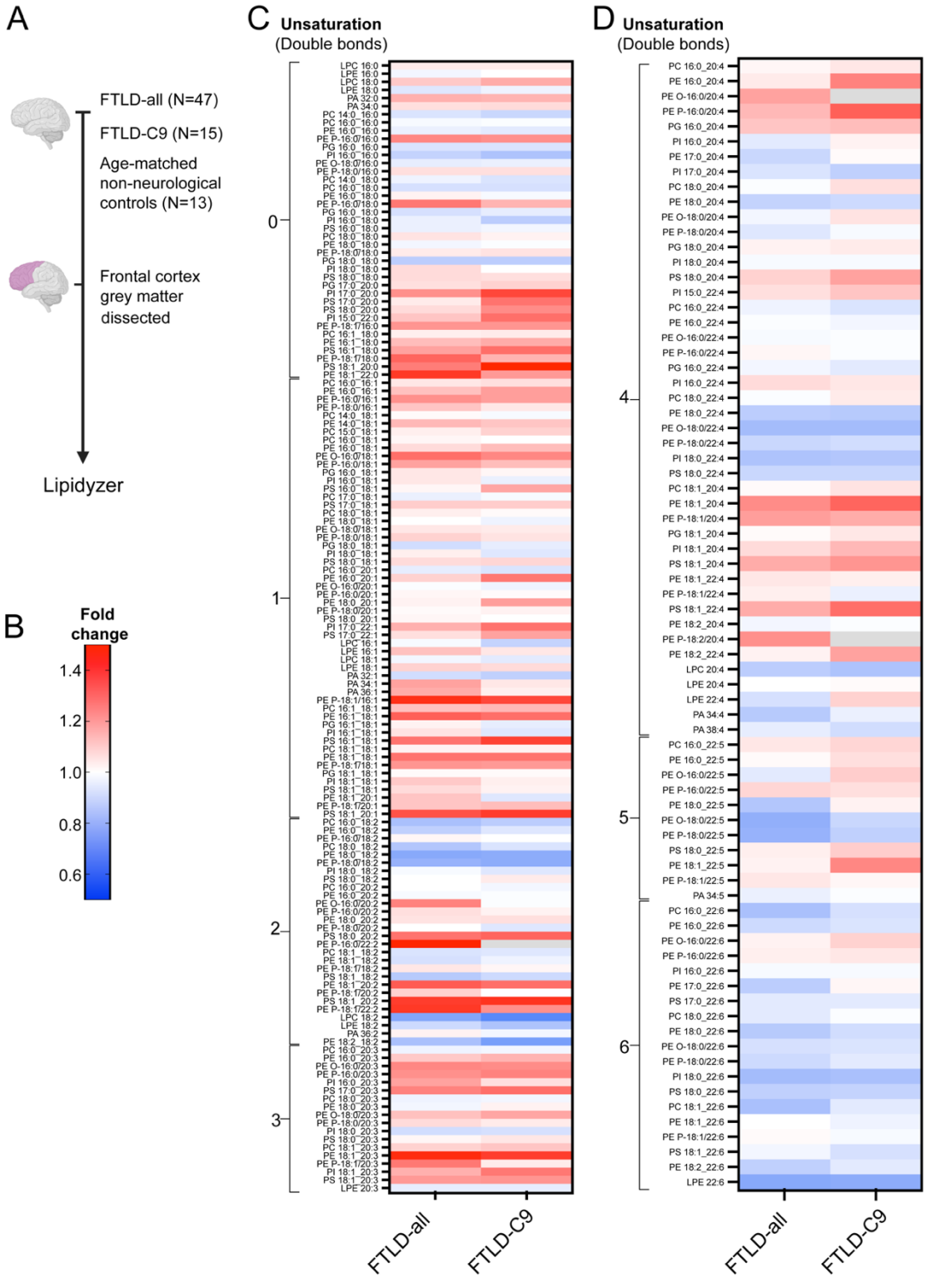

Figure 5.15. Specific polyunsaturated fatty acids are decreased in FTLD post-mortem frontal cortex grey matter compared to age matched controls.

A. Schematic of post-mortem brain lipidomics. Post-mortem brains with a pathological diagnosis of FTLD (N=47), including *C9orf72* mutation carriers (N=15) and age-matched non-neurological controls (N=13) were included. The

frontal cortex grey matter was used for Lipidyzer lipidomic analyses. B. Heatmap key for fold changes relative to age matched controls, relevant to C and D. C. Heatmap depicting fold changes in phospholipids containing 0-3 double bonds in FTLD-all and FTLD-C9 compared to age-matched controls. D. Heatmap depicting fold changes in phospholipids containing four or more double bonds between FTLD-all and FTLD-C9 compared to age-matched controls.

Dr Alyssa Coyne, a collaborator at John Hopkins University, Maryland, performed the following experiment.

5.2.10. FAT-1 or FAT-2 desaturase expression was sufficient to rescue glutamate stressor toxicity in *C9orf72* patient spinal motor neurons

Finally, to test whether this conserved dysregulation of PUFA metabolism directly contributes to neurotoxicity, we asked whether overexpression of desaturase genes, which boost PUFA levels, could prevent C9-associated neurodegeneration. Indeed, *fat-1* and *fat-2* overexpression was sufficient to rescue glutamate toxicity in *C9orf72* iPSC-derived motor neurons, decreasing the proportion of propidium iodide staining compared to *C9orf72* motor neurons transfected with BFP (Figure 5.16 B). Similarly, *fat-1* and *fat-2* desaturase overexpression increased cell viability of *C9orf72* iPSC-derived motor neurons after glutamate exposure, measured by Alamar Blue (Figure 5.16 C).

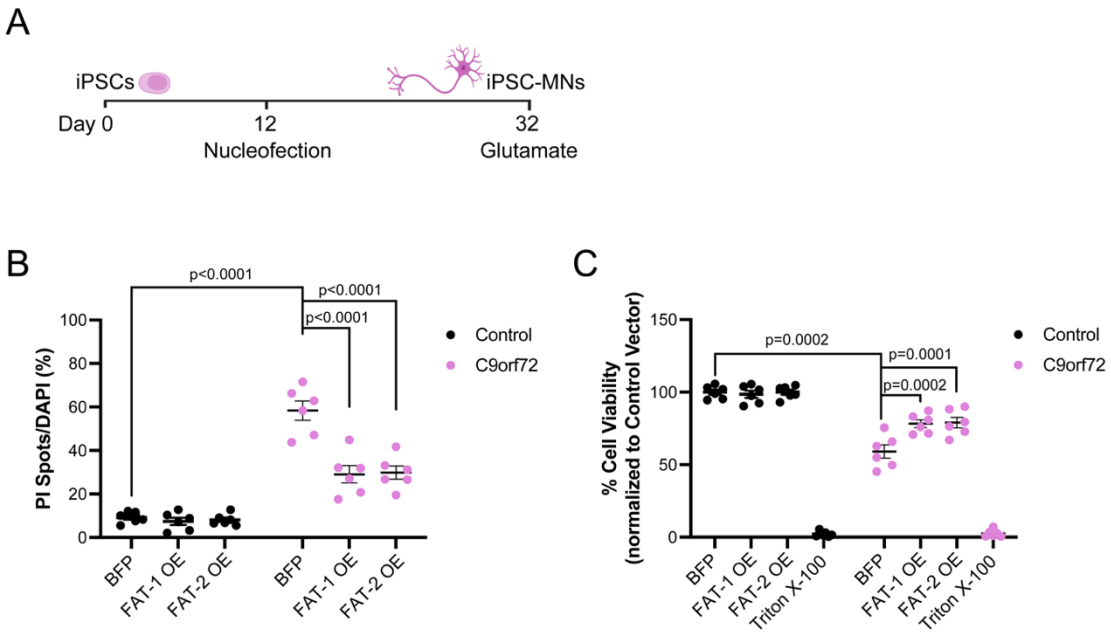

Figure 5.16. FAT-1 and FAT-2 rescue glutamate stressor induced toxicity in vitro in *C9orf72* patient spinal motor neurons.
A. Experimental design schematic, with timepoints for nucleofection of BFP/*fat-1*/*fat-2* constructs indicated. At DIV 32, motor neurons were exposed to glutamate stress (10 μM for 4 hours), after which propidium iodide (PI) and Alamar blue staining was performed. B. Quantification of the ratio of PI positive spots to DAPI positive nuclei (quantification of cell death) following 4-hour exposure to 10 μM glutamate. N=6 control and 6 *C9orf72* iPSC lines. Data points represent average percent cell death across 10 images per well. Two-way ANOVA with Tukey's multiple comparison test was used to calculate statistical significance. Data presented as mean ± S.D. C. Percent cell viability as measured by Alamar Blue following 4-hour exposure to 10 μM glutamate. N=6 control and 6 *C9orf72* iPSC lines. Data points represent average percent viability from 3 replicate wells for each condition. Two-way ANOVA with Tukey's multiple comparison test was used to calculate statistical significance. Data presented as mean ± S.D.

5.3 Discussion

5.3.1 Summary of findings

In this work, lipid metabolism was found to be dysregulated across multiple models of ALS/FTD, from transgenic *C9orf72 Drosophila* to *C9orf72* patient iPSC-neurons and *C9orf72* repeat-transduced neurons, to ALS patient post-mortem spinal cord and FTLD post-mortem brain. Transcriptional dysregulation of canonical fatty acid synthesis and desaturation genes was identified at an early

timepoint in *Drosophila* heads neuronally expressing $(G_4C_2)_{36}$. Transcriptional dysregulation of canonical fatty acid synthesis and desaturation genes was conserved and found to persist to end stage disease in ALS patient post-mortem spinal cords. Quantitative lipidomic assays in *C9orf72* iPSC-derived cortical neurons and FTLD post-mortem brains identified a loss of highly unsaturated phospholipids, which was recapitulated by transduction of control iPSC neurons with 92 GGGGCC repeats, and prevented by treatment with a *C9orf72* GGGGCC ASO, demonstrating a *C9orf72* specific lipid disease signature. PUFA supplementation prolonged survival of *C9orf72 Drosophila*, while upregulation of lipid desaturation was sufficient to significantly extend *C9orf72 Drosophila* survival and rescue glutamate-induced excitotoxicity in *C9orf72* patient iPSC-derived motor neurons. Overall, the results presented here suggest that dysregulated PUFA metabolism is a direct contributor to neuronal toxicity in *C9orf72* ALS/FTD, while modulating neuronal PUFA metabolism is a promising approach for ameliorating *C9orf72*-associated neurodegeneration.

5.3.2 Limitations and strengths of this study

Linoleic acid (LA, C18:2) and α-linolenic acid (ALA, C18:3) supplementation prolonged survival of *C9orf72 Drosophila* here, however, the magnitude of survival extension was much less than that seen when desaturases were neuronally expressed. To reach the brain, PUFAs need to pass the gut barrier, as well as the brain barrier, and therefore the absolute quantities that reach neurons is not known. This delivery issue likely explains the differences in survival benefits observed between genetic overexpression of desaturases versus pharmacological supplementation of their products. It is also possible that dietary LA and ALA are mediating their survival benefits in *C9orf72 Drosophila* through systemic actions.

The initial findings linking dysregulated lipid metabolism were made in C9 *Drosophila* heads. *Drosophila* heads contain the head fat body, and therefore alterations in lipid metabolism need to be interpreted with this caveat in mind. Given that large quantities of material were required for the lipidomic analyses, it

was not practically feasible in this work to perform lipidomics on dissected *Drosophila* brains. However, future experiments measuring the mRNA levels of *AcCoAS*, *FASN* and *Desat1* in dissected *Drosophila* brains would be informative to remove contamination of head fat body from the results.

Here we found that transcriptomic downregulation of genes involved in fatty acid synthesis and desaturation first observed in our C9 *Drosophila* model, was conserved in human ALS post-mortem spinal cord. However, we have not directly assessed whether this transcriptional deregulation of lipid metabolism is driven by neurons, or other cell types. However, a recently published single nucleus RNA sequencing dataset from C9ALS post-mortem frontal cortex excitatory neurons reported enrichment of lipid metabolism pathways among downregulated genes, including ‘regulation of lipid metabolic process’, 'lipid modification' and 'inositol lipid-mediated signalling’ (Li *et al.*, 2023). This suggests that neurons play a role in the transcriptomic downregulation of lipid metabolism we have reported here.

A strength of this study was the ability to investigate the impact of *C9orf72* lipid dysregulation specifically in neurons, by using an inducible neuronal driver in *Drosophila* and employing pure neuronal cultures from patient iPSCs for lipidomic analyses. In future studies, it will be important to characterise *C9orf72*-induced lipid dysregulation not only in monocultures, but also in co-cultures of neurons with microglia, astrocytes and oligodendrocytes to more closely model the complexities of this human disease. Additionally, with the advent of single cell lipidomic technologies, it will be highly informative to study cellular resistance and vulnerability in ALS/FTD with regards to lipids (Capolupo, 2023).

5.3.3 Epidemiological evidence for PUFA involvement in ALS/FTD

Previous epidemiological studies have suggested a protective role for dietary polyunsaturated fatty acids in individuals with ALS (Fitzgerald *et al.*, 2014; Veldink *et al.*, 2007; Okamoto *et al.*, 2007). A recent study of plasma fatty acids from 449 ALS patients enrolled in the EMPOWER trial revealed that higher levels of plasma

ALA at baseline are associated with a prolonged survival and slower functional decline. Furthermore, increased plasma levels of LA as well as the omega-3 fatty acid, eicosapentaenoic acid (EPA, C20:5) were associated with a reduced risk of death during follow-up in that study (Bjornevik *et al.*, 2023).

5.3.4 Why are specific PUFAs depleted?

Here, we report that phospholipids containing AA (C20:4) and adrenic acid (AdA) (C22:4) are specifically depleted in *C9orf72* iPSC-neurons. Phospholipids containing AdA and DHA (C22:6) were also depleted in FTLD post-mortem frontal cortex, while phospholipids containing AA were increased. Why AA is decreased in *C9orf72* cortical neurons but increased in post-mortem frontal cortex is possibly due to differences in disease stage as well as neuronal culture versus complex tissue. LA and ALA are essential PUFAs that must be obtained from the diet, and serve as precursors for both arachidonic acid (AA) and docosahexaenoic acid (DHA) (Bazinet and Layé, 2014). Therefore, it is possible that dietary intake of these precursors is not sufficient or is reduced in patients, or that the transport of PUFAs to the brain is impaired. Alternatively, altered esterification (attachment of PUFAs to phospholipids) or processing of PUFAs in ALS/FTD neurons and brains might be responsible for the decreased PUFA containing phospholipids reported here. Once PUFAs enter the brain from the plasma via fatty acid transporters, lipoprotein receptors or passive diffusion they are activated by long-chain fatty acid CoA synthases (ACSL), producing fatty acyl-CoAs, which can then be attached to membrane phospholipids (Watkins, 1997). AA and DHA are esterified at the sn-2 position of membrane phospholipids, and their removal or de-esterification is carried out by phospholipase A2 (PLA2), which can be triggered by activation of PLA2 coupled receptors (Vial and Piomelli, 1995; Axelrod, 1990; Felder *et al.*, 1990; Dumuis *et al.*, 1988). These released PUFAs can be converted into signalling molecules by cyclooxygenase (COX), lipoxygenases (LOX) and cytochrome P450 enzymes, producing bioactive mediators. Arachidonic acid derivatives are mostly pro-inflammatory eicosanoids including prostaglandins and leukotrienes, while EPA (C20:5) and DHA (C22:6) derivatives are mostly pro-resolving or anti-inflammatory mediators that include resolvins,

protectins and maresins (Serhan, 2014; Orr *et al.*, 2013; Bosetti, 2007). Arachidonic acid pathway activation has previously been reported in ALS motor neurons, while inhibiting the production of AA-derived eicosanoids through 5-LOX inhibition has been shown to rescue eye toxicity in a *C9orf72 Drosophila* model (Lee *et al.*, 2021). It would be interesting to assess the spatiotemporal levels of AA and DHA mediators, as well as the activity of PLA2 and FADS1 and FADS2 enzymes in future work, as decreases in the levels of esterified AA and DHA may be due to increased expression or activity of PLA2 enzymes, or decreased synthesis by FADS1 and FADS2.

5.3.5 Membrane dynamics

The role of unsaturated lipids in modulating membrane fluidity has been well described (Ruiz *et al.*, 2023; Levental *et al.*, 2020; Ruiz *et al.*, 2019a). Our study explored membrane fluidity in a behavioural paradigm testing the ability to recover from chill coma in *Drosophila.* Flies neuronally expressing $(G_4C_2)_{36}$ had a sensitivity to cold stress which was ameliorated by overexpression of either *Desat1* or *fat-2*, suggesting that the enzymes encoded by these genes are fluidising membranes. Future studies of membrane fluidity in *C9orf72* iPSC neurons using Laurdan dye imaging or fluorescence recovery after photobleaching are warranted to further explore this phenotype. Additionally, DHA has been shown to increase the stability of lipid rafts by increasing disorder of non-raft domains (Levental *et al.*, 2016). Lipid rafts functionally partition the plasma membrane and are important platforms facilitating protein interactions, signalling and trafficking (Lingwood and Simons, 2010). Altered protein composition of lipid rafts has been reported in *SOD1* mouse spinal cords (Zhai et al., 2009). Therefore, it is worth studying the stability and composition of lipid rafts in *C9orf72* models, given that the levels of PUFAs, including DHA were affected. Furthermore, the biophysical properties of the lipid bilayer can directly regulate the structure, opening probability and activity of integral membrane proteins, including ion channels (Levental and Lyman, 2023). Therefore, alterations in plasma membrane phospholipid composition, and dynamics can be hypothesised

to be an upstream player with wide-ranging downstream consequences in the context of *C9orf72* ALS/FTD disease.

Adiponectin Receptor 2 (ADIPOR2) has recently been described as a conserved master regulator of membrane fluidity, essential for maintaining fatty acid desaturase expression and unsaturated FA levels in membrane phospholipids (Ruiz *et al.*, 2023; Ruiz *et al.*, 2021; Ruiz *et al.*, 2019b; Bodhicharla *et al.*, 2018; Devkota *et al.*, 2017). This regulation occurs via ADIPOR2 intrinsic ceramidase activity in response to membrane rigidification, producing sphingosine from ceramides which can be phosphorylated to produce the signalling molecule sphingosine-1-phosphate that is proposed to then activate the lipid transcription factor sterol regulatory element-binding protein 1 (SREBP1) and separately, peroxisome proliferator-activated receptor gamma (PPARγ), with resulting upregulation of lipid synthesis and desaturation genes, in particular upregulation of *SCD* which then increases membrane unsaturation (Ruiz *et al.*, 2022; Vasiliauskaité-Brooks *et al.*, 2017). Interestingly, in the lipidomics performed on C9 fly heads, the sphingolipids glucosylceramide and galactosylceramide were significantly increased (Figure 5.3). Additionally, *ADIPOR2* was downregulated in post-mortem C9ALS and ALS cervical spinal cord, as was the *Drosophila* ortholog of *ADIPOR2*, *AdipoR* in C9 fly heads, using the RNA-sequencing datasets previously analysed in this chapter (Table 5.1). Therefore, *AdipoR*/*ADIPOR2* downregulation may result in decreased protein levels of AdipoR/ADIPOR2, thereby reduced activation of SREBP-1 and PPARγ via sphingosine-1-phosphate. Future work investigating AdipoR/ADIPOR2 protein levels and activity might help explain the widespread transcriptomic changes to lipid synthesis and desaturation genes, as well as the loss of unsaturated membrane phospholipids reported here.

Table 5.1. *ADIPOR2*/*AdipoR* transcript levels in C9 fly heads and ALS cervical spinal cord

Gene	Dataset	Fold change	Adjusted p-value
ADIPOR2	ALS vs control	0.805	3.92E-04
ADIPOR2	C9ALS vs control	0.861	0.061
AdipoR	C9 vs control	0.863	4.00E-41

5.3.6 DHA is important for neuronal survival via PI3K/AKT

Phosphatidylinositol 3-kinase/Akt signalling is a major pro-survival pathway in cells. DHA has been shown to mediate membrane translocation and phosphorylation of Akt by increasing phosphatidylserine levels, with resulting effects on neuronal survival (Eady *et al.*, 2012; Akbar *et al.*, 2005). Activation of the PI3K/AKT pathway has already been shown to be neuroprotective in poly(GR) repeat *Drosophila*, in part by decreasing GR levels (Atilano *et al.*, 2021). Interestingly, in ALS post-mortem excitatory cortical neurons, many genes involved in activating the PI3K/AKT pathway are downregulated (Li *et al.*, 2023), which is possibly in part due to reduced DHA containing phospholipids.

5.3.7 Synaptic functions

PUFAs are enriched at synapses where they have been shown to influence the localisation of synaptic proteins and regulate synaptic vesicle recycling (Ben Gedalya *et al.*, 2009; Marza *et al.*, 2007). A recent study described altered presynaptic protein expression in ALS post-mortem spinal cords (Aly *et al.*, 2023). Additionally, impaired pre-synaptic vesicle dynamics have been reported in *C9orf72* cortical neurons (Perkins *et al.*, 2021), while defective synaptic vesicle recycling has been described in *C9orf72 Drosophila* L3 larvae (Coyne *et al.*, 2017). Therefore, desaturase overexpression may be mediating its rescue by ameliorating presynaptic deficits through upregulation of PUFAs. We are actively testing this hypothesis in the lab.

Additionally, the AA derivatives anandamide and 2-arachidonylglycerol are the major endocannabinoids present in the brain and are also important regulators of synaptic function. Anandamide is produced from AA through the action of N-acyl phosphatidylethanolamine phospholipase D, while 2-arachidonylglycerol is produced by diacylglycerol lipase. Endocannabinoids are retrograde messengers which are released from the post-synaptic terminal in an activity-dependent manner and bind to presynaptic cannabinoid receptor type 1 (CB1), to suppress

further neurotransmitter release. This retrograde signalling of endocannabinoids modulates synaptic plasticity as well as long term depression at excitatory and inhibitory synapses (Castillo *et al.*, 2012; Lafourcade *et al.*, 2007). AA and DHA can regulate endocannabinoid levels in the brain, while ω3 PUFAs have been shown to modulate CB1 signalling activity (Larrieu *et al.*, 2012; Lafourcade *et al.*, 2011; Piscitelli *et al.*, 2011; Berger *et al.*, 2001). Given the decreased levels of AA and DHA in our models, it would be interesting to look at whether endocannabinoid levels and signalling is altered in *C9orf72* ALS/FTD.

5.3.8 Conclusions

In summary, this work identified C9-induced alterations in neuronal lipid metabolism, particularly neuronal PUFA metabolism, conserved across disease models and species, implicating this as a novel pathway in the pathogenesis of *C9orf72* ALS/FTD. Promoting neuronal lipid unsaturation by desaturase overexpression was sufficient to extend survival in C9 flies and protect against excitotoxicity in C9 iPSC-derived motor neurons. Therefore, modulating neuronal PUFA metabolism can ameliorate C9-associated neurodegeneration. Additionally, our results suggest that dysregulated lipid and PUFA metabolism may be a converging pathway among *C9orf72* and non-*C9orf72* ALS and FTD, expanding the potential utility of our findings.

Chapter 6 General Discussion

6.1 Final summary

The aims of this thesis were to reveal novel insights into the pathogenesis of GGGGCC repeat expansion to identify protective genes and pathways for further investigation. Specifically, I investigated *odd* and *bowl*, *Trpγ* and lipid metabolism as modifiers of $(G_4C_2)_{36}$ toxicity in *Drosophila* models of *C9orf72* ALS/FTD, with further validation performed in iPSC neuronal models.

The mechanism by which the Odd-skipped family reduces toxicity in C9 *Drosophila* was investigated in this work (Chapter 3). Both *odd* and *bowl* were confirmed to extend C9 *Drosophila* survival when overexpressed in neurons of disease model flies, but to reduce it when expressed in neurons of wildtype flies, suggesting that rescue was specific to disease. To assess whether Odd-skipped rescue of toxicity was conserved, novel transgenic lines expressing human *OSR1* and *OSR2* were generated. Both *OSR1* and *OSR2* extended C9 *Drosophila* survival when overexpressed in neurons. The magnitudes of survival extensions observed with each of the four genes varied greatly. *Odd* and *OSR2* extended survival to a much larger extent than *bowl* or *OSR1*. This correlated with a decrease of DPR levels with *odd* and *OSR2* overexpression, whereas *bowl* and *OSR1* overexpression had no effect on DPR levels.

RNA sequencing was carried out on C9 fly heads overexpressing *odd, bowl, OSR1* or *OSR2* versus C9 alone, to identify target genes or groups of genes mediating the shared rescue effect. Priority was given to potential targets with an Odd-skipped transcription factor binding motif, that were commonly altered across two or more Odd-skipped conditions, had mammalian orthologs whose directionality was conserved by overexpressing *Osr1* or *Osr2* in rat primary neurons, and for which RNAi or overexpression lines were publicly available. Based on these criteria, *Trpγ, hec, Arc1, Ect3 and CG9394* were selected for follow up. Odd-skipped led to a reduction in the levels of each of these genes therefore RNAi was used. However, small or no effect on survival was seen upon

perturbing individual Odd-skipped target genes, suggesting that Odd-skipped rescues are more likely attributable to combinatorial effects of multiple gene targets. There is evidently more than one mechanism of rescue attributable to the Odd-skipped family, given that *odd* and *OSR2* decrease DPR levels, while *bowl* and *OSR1* do not. Further research into these other mechanisms of C9 rescue by Odd-skipped family members are warranted.

The role of *Trpγ* in modulating C9 toxicity in *Drosophila* was further investigated in this work given that riluzole, an approved drug for ALS, is a direct activator of orthologous TRPC5 channels (Richter, Schaefer and Hill, 2014) (Chapter 4). *Trpγ* is upregulated in C9 *Drosophila* at an early timepoint. Additionally, human orthologs *TRPC4* and *TRPC5*, are upregulated in patient-derived iPS motor neurons, which are likely to represent an early disease stage. At end-stage disease, *TRPC4* is downregulated in post-mortem frontal cortex excitatory neurons (Li *et al.*, 2023). *Trpγ* extended C9 survival and rescued early motor and sleep phenotypes when overexpressed in neurons, and this reduction in toxicity was mediated by a decrease in toxic poly(GR) levels, by an unknown mechanism. Therefore, early upregulation of *Trpγ*/*TRPC4/TRPC5* is likely a protective response that fails in end stage disease, which may contribute to neurodegeneration.

Lastly, RNA sequencing in flies expressing G_4C_2 repeats specifically in adult neurons revealed a significant downregulation of fatty acid and lipid metabolism genes. This signature was conserved in human post-mortem ALS spinal cord (Chapter 5). To further investigate lipid alterations in ALS/FTD neurons, we performed lipidomics on C9ALS/FTD iPSC-neurons and found widespread changes in phospholipid species, characterised by a shift from unsaturated to saturated lipids, with a pronounced loss of polyunsaturated fatty acids (PUFAs). This signature was recapitulated by overexpressing $(G_4C_2)_{92}$ and prevented by treating with a *C9orf72* sense targeting ASO. Lipidomics on post-mortem frontal cortex grey matter from 46 individuals with a pathological diagnosis of FTLD and 12 aged, non-neurological controls, also revealed a decrease in PUFA containing phospholipids. Finally, to test whether this dysregulation in lipid metabolism directly contributes to neurotoxicity, we asked whether overexpression of

desaturation genes could prevent C9-associated neurodegeneration. Indeed, desaturase overexpression was sufficient to rescue toxicity in iPSC-derived motor neurons and improve cold sensitivity and extend survival in a C9 *Drosophila* model when expressed in neurons. G_4C_2 repeat expansion was found to alter neuronal lipid metabolism, particularly among PUFA-containing phospholipids, and this dysregulation was conserved across disease models and species. These results implicate neuronal PUFA metabolism in C9ALS/FTD pathogenesis and suggest that modulating neuronal PUFA metabolism is a potent approach for ameliorating C9-associated neurodegeneration.

6.2 Transcription factors in ALS/FTD

Here, the Odd-skipped family of transcription factors were found to suppress *C9orf72* repeat associated toxicity in *Drosophila* when ectopically expressed in all neurons. Transcription factor dysregulation has already been implicated in the pathogenesis of several neurodegenerative diseases, with disease-linked single nucleotide polymorphisms (SNPs) enriched in regulatory regions, particularly in enhancers (Nott *et al.*, 2019; Nativio *et al.*, 2018; Coetzee *et al.*, 2016; Soldner *et al.*, 2016; Hnisz *et al.*, 2013). Transcription factors bind to specific motifs consisting of 6-12 nucleotides, located in promoter or enhancer regions to alter expression of their set of target genes (Chen and Pugh, 2021). The activity of particular sets of transcription factors are major determinants of cellular identity (Leyva-Díaz and Hobert, 2019). Therefore, SNPs in transcription factor binding motifs could alter the likelihood of transcription factor binding, with consequences for cellular homeostasis. Epigenetic dysregulation has recently been described in C9ALS/FTD (Li *et al.*, 2023; Zhang *et al.*, 2019). Disease associated alterations in H3K27 acetylation at promoters and distal regulatory elements have recently been reported in post-mortem brains from C9ALS patients, with resulting impacts on chromatin accessibility and gene expression (Li *et al.*, 2023). Poly(PR) has been shown to localise to regions of heterochromatin, that is condensed transcriptionally silent chromatin, in poly(PR) mice and in C9ALS/FTD post-mortem brains and alter histone H3 methylation, with resulting increases in the expression of repetitive elements and accumulation of double stranded RNA

(Zhang *et al.*, 2019). Additionally, poly(PR) alters chromatin accessibility in rat primary cortical neurons, with resulting activation of p53 (Maor-Nof *et al.*, 2021). Disease-mediated SNPs in enhancer regions as well as alterations in chromatin accessibility can influence the ability of transcription factors to bind their specific DNA sequence motifs, with resulting effects on transcriptional programs. Epigenetic alterations and transcription factor dysregulation may be an important pathogenic mechanism in C9ALS/FTD that should be further explored, particularly in the interpretation of transcriptomic data.

6.3 Evidence of Odd-skipped transcription factor involvement from other *Drosophila* models of C9ALS/FTD

Odd has previously been identified as a genetic modifier of poly(GR) toxicity in a deficiency screen performed using vestigial-Gal4 (Vg-Gal4) to drive expression of poly(GR) in the developing wing. Partial loss of function of *odd* suppressed $(GR)_{80}$ induced loss of non-neuronal cells in the *Drosophila* wing (Lopez-Gonzalez *et al.*, 2019). This finding contrasts with ours, where overexpression of Odd-skipped genes rescued C9-related toxicity, and extended survival. In our *Drosophila* model of C9ALS/FTD, in which Odd-skipped overexpression was found to suppress toxicity, we restricted expression to post-mitotic, adult neurons, allowing us to avoid any confounding developmental effects. When *odd* and *bowl* were overexpressed in a developmental context, using the GMR-Gal4 to drive expression in developing photoreceptor neurons, we saw a reduction in eye area, in both the presence and absence of poly(GR) expression. Lopez-Gonzalez *et al*. do not report whether knock down of *odd* in the absence of poly(GR) disrupts wing development, however, our results indicate that manipulation of Odd-skipped expression during development disrupts cell and tissue morphogenesis independent of an effect on DPR related toxicity. $(GR)_{80}$ expression in the developing wing was previously reported to suppress Notch signalling, while expression of Notch could prevent the toxic cell loss phenotype (Yang *et al.*, 2015). Notch signalling is a critical determinant of cellular and tissue morphogenesis (Diaz-Benjumea and Cohen, 1995), and the Odd-skipped family act downstream of Notch signalling during development to determine the

patterning and morphogenesis of multiple tissues (Laddada, Jagla and Soler, 2019; Greenberg and Hatini, 2009; de Celis Ibeas and Bray, 2003; Hao *et al.*, 2003). Given that Notch and Odd-skipped genes play critical roles during development, their genetic manipulation during developmental stages might be expected to have very different effects to their manipulation in adult tissues. There are now multiple published genetic screens in *Drosophila* models of C9ALS/FTD, mostly performed using developmental expression (Lopez-Gonzalez *et al.*, 2019; Goodman *et al.*, 2019a; Goodman *et al.*, 2019b; Boeynaems *et al.*, 2016; Zhang *et al.*, 2015a; Freibaum *et al.*, 2015). The results of such screens have been informative; however, screens of this nature need to be sufficiently controlled to be interpreted appropriately, particularly when using visual readouts of toxicity. Furthermore, given that ALS and FTD are adult-onset diseases, hits from such developmental expression screens should be confirmed in adult, neuronal expression models.

6.4 TRPC channel involvement in neuronal health and neurodegeneration

Here we found that *TRPC4 and TRPC5* genes are dysregulated at the transcriptional level in C9ALS/FTD patient cells and post-mortem brains, while the *Drosophila* TRPC channel, *Trpγ*, is upregulated in $(G_4C_2)_{36}$ flies. Neuronal overexpression of *Trpγ* ameliorated multiple neurodegenerative phenotypes in this fly model of C9ALS/FTD, however, neuronal overexpression of *Trpγ* in wildtype flies reduced survival. The TRPC channels are calcium permeable, non-selective cation channels that have been reported to promote neuronal survival (Huang *et al.*, 2011) as well as contribute to neurodegeneration by excitotoxicity (Hong *et al.*, 2020; Jeon *et al.*, 2021). Transient elevations in intracellular calcium can promote neuronal survival via activity-dependent and neurotrophic signalling pathways (Ghosh, Carnahan and Greenberg, 1994), however sustained elevations in intracellular calcium can lead to excitotoxicity (Sattler and Tymianski, 2000). TRPC1 has been shown to mediate glutamate-induced hippocampal cell death (Narayanan *et al.*, 2008). TRPC3 and TRPC6 are necessary for BDNF-induced CREB phosphorylation and neuronal survival in

cerebellar granule neurons (Jia *et al.*, 2007). *TRPC3* is highly expressed in cerebellar Purkinje cells and is required for synaptic transmission and motor co-ordination, with loss-of function leading to an ataxia-like phenotype (Hartmann *et al.*, 2008). Gain of function mutations in *TRPC3,* causing altered phosphorylation and sustained channel opening also lead to motor and coordination impairments in mice, modelling cerebellar ataxia, with altered dendritic development and eventual loss of Purkinje cells (Becker *et al.*, 2009). TRPC4 has been reported to play a role in neurite extension in post-mitotic neurons (Weick, Austin Johnson and Zhang, 2009), while TRPC5 has been described to regulate neurite length and growth cone morphology (Greka *et al.*, 2003), as well as promote neuronal axon formation (Davare *et al.*, 2009).

Dendritic mushroom spines of the hippocampus are import for memory formation, and their loss is reported in Alzheimer's disease (AD) patients and mouse models of neurodegeneration (Knobloch and Mansuy, 2008). *TRPC6* overexpression promotes the formation of dendritic spines and excitatory synapses, and improves spatial learning and memory (Zhou *et al.*, 2008). TRPC6 and Orai2 form a STIM2-regulated store operated Ca^{2+} channel complex in hippocampal mushroom spines. Pharmacological activation of TRPC6 can stimulate STIM2-SOC pathway and rescue hippocampal mushroom spine loss in presenilin and APP knock-in mouse models of AD (Zhang *et al.*, 2016a) and ameliorates long-term potentiation deficits in 5xFAD mice (Popugaeva *et al.*, 2019). *TRPC6* loss of function mutations have been implicated in autism spectrum disorder (Griesi-Oliveira *et al.*, 2015), while mutations in *Trpγ* cause autism-like behavioural deficits in *Drosophila* including hyperactivity, anxiety-like behaviour, social interaction impairments and deficits in sleep, learning and memory, which could be ameliorated by a TRPC6 agonist drug (Palacios-Muñoz *et al.*, 2022). Despite the involvement of TRPC channels in maintaining neuronal development, health and disease, their involvement in ALS and FTD has not yet been studied. Our results describing *Trpγ* as a genetic modifier of $(G_4C_2)_{36}$ toxicity in *Drosophila* along with dysregulated expression of *TRPC4* and *TRPC5* in patient motor neurons as well as post-mortem brain tissue, combined with the fact that riluzole can bind and activate TRPC5 channels, warrants further investigation into the role of TRPC channels in the pathogenesis of C9ALS/FTD.

6.5 Lipid dysregulation in neurodegenerative diseases

6.5.1 C9ORF72 is a regulator of lipid metabolism

C9ORF72 was recently reported to promote the lysosomal degradation of coactivator-associated arginine methyltransferase 1 (CARM1), an epigenetic activator of autophagy and lipid synthesis under conditions of nutrient stress (Liu *et al.*, 2018). Homozygous knockout of *C9orf72* in cells enhanced autophagic digestion of lipids, increased protein levels of lipid synthetic enzymes as well as increased free fatty acids, under conditions of starvation stress, through loss of CARM1 degradation (Liu *et al.*, 2018). These authors confirmed their findings in two patient iPSC motor neuron lines and demonstrated increased CARM1 protein levels in three *C9orf72* ALS/FTD patient spinal cords (Liu *et al.*, 2018). While homozygous knockout of *C9orf72* is not representative of the haploinsufficiency seen in *C9orf72* patients, it suggests that loss of C9ORF2 function can contribute to lipid metabolic defects, particularly under starvation stress. The authors of that study did not perform lipidomic analyses or transcriptomic analyses on *C9orf72* patient cells or post-mortem tissue and therefore we cannot directly compare our findings to that of Liu et al. Our results are most likely driven by *C9orf72* gain of function mechanisms as *Drosophila* lack a *C9orf72* ortholog. However, it is apparent that both *C9orf72* gain of function and loss of function mechanisms can contribute to lipid metabolic defects. Further work exploring the relative roles of haploinsufficiency, RNA foci and DPRs on lipid metabolism defects in *C9orf72* ALS/FTD is needed.

6.5.2 Hypermetabolism and dyslipidaemia in neurodegenerative diseases

Hypermetabolism with increased resting energy expenditure is well described in ALS patients and mouse models, and is associated with a worse disease prognosis (He *et al.*, 2022; Jésus *et al.*, 2018; Steyn *et al.*, 2018; Bouteloup *et al.*, 2009; Dupuis *et al.*, 2004). The is also some evidence of increased resting energy expenditure in FTD patients (Ahmed *et al.*, 2017). Hypermetabolism has also

been described in Huntington's disease, a dominantly inherited neurodegenerative disorder cause by polyglutamine repeat expansion in the huntingtin gene (Mochel *et al.*, 2007; Pratley *et al.*, 2000). There is also some evidence to suggest that hypermetabolism may play a role in Alzheimer's disease (Demetrius, Eckert and Grimm, 2021; Knight *et al.*, 2012). The hypermetabolism seen in these neurodegenerative diseases likely reflects shared pathogenic mechanisms related to mitochondrial dysfunction and loss of metabolic homeostasis.

Dyslipidaemia has been implicated in ALS risk, with elevated levels of triglycerides and cholesterol correlating with a prolonged survival (Sol *et al.*, 2021; Dorst *et al.*, 2011; Dupuis *et al.*, 2008). However, higher cholesterol levels have also been causally linked to ALS (van Rheenen *et al.*, 2021). Furthermore, a high fat diet prolonged survival in fast-progressing ALS patients in the LIPCAL-ALS clinical trial (NCT02306590) (Ludolph et al., 2020). A recently published prospective cohort study including over 18,000 participants from the ASPREE trial (NCT01038583) and 68,200 UK Biobank participants aged 65 or older, reported a decreased risk of dementia with increased plasma triglyceride levels (Zhou *et al.*, 2023). Obesity in midlife increases risk of dementia in later life (Kivipelto *et al.*, 2005), whereas late-life obesity is protective against dementia (Fitzpatrick *et al.*, 2009), highlighting the need to interpret studies of this nature with age and disease stage in mind. Interestingly, the TARDBP gene has been shown to play a role in lipid metabolic homeostasis, with deletion of *TDP-43* in mice found to promote rapid loss of body fat, with increased lipid oxidation through downregulation of the obesity-related gene *Tbc1d1* (Chiang *et al.*, 2010). TDP-43 pathology is found in multiple neurodegenerative diseases and therefore may be an important factor to consider when studying shared metabolic disturbances.

6.5.3 PUFA dysregulation in neurodegenerative diseases

Increased dietary intake of PUFAs, particularly omega-3 (ω3) PUFAs, is associated with decreased risk of ALS (Fitzgerald *et al.*, 2014; Veldink *et al.*,

2007). An analysis of PUFA levels in 449 participants of the EMPOWER clinical trial (NCT01281189) found that elevated plasma levels of the omega-3 PUFA alpha-linolenic acid were associated with a longer survival and slower functional decline after ALS onset, while increased plasma levels of omega-6 PUFA linoleic acid and omega-3 PUFA eicosapentaenoic acid were associated with a reduced risk of death during the follow up period in this study (Bjornevik *et al.*, 2023). Higher dietary intake of PUFAs is associated with a decreased risk of Parkinson's disease (PD) (Qu *et al.*, 2019), while increased intake of the omega-3 PUFA DHA has been associated with a reduced risk of Alzheimer's disease (Zhang *et al.*, 2016b). However, a systematic review of omega-3 PUFA supplementation or enriched diets in randomised control trials of Alzheimer's disease (AD), vascular dementia, dementia with Lewy bodies, Parkinson's disease dementia or FTD found no evidence of improved cognitive function or quality of life after 6 months (Burckhardt *et al.*, 2016).

While a high fat diet has been shown to worsen behavioural and neuropathological phenotypes in the *APP/PS1* mouse models of Alzheimer's disease (Bracko et al., 2020), omega-3 fatty acid supplementation shows beneficial effects on pathology and cognition in AD rodent models (Hooijmans *et al.*, 2012). Genetic manipulation of endogenous omega-3 PUFA levels in mice through expression of *C. elegans*-derived *fat-1* has been shown to enhance hippocampal neurogenesis and neuritogenesis, with enhanced spatial learning performance versus wildtype mice (He *et al.*, 2009; Kang *et al.*, 2004). FAT-1 has been shown to ameliorate disease-related phenotypes in AD mouse models. *APP* mice crossed to transgenic *fat-1* mice show improved cognition, behaviour and neuropathology (Wu *et al.*, 2016), while *Tau P301S* mice have improved learning and memory, and increased survival when crossed to transgenic *fat-1* mice (Fang *et al.*, 2019). In this thesis, *fat-2* expressed in neurons of C9 *Drosophila* could improve survival, while *fat-1* and *fat-2* partially rescued motor neurons from glutamate excitotoxicity stress. It will be very interesting to cross *fat-1* and *fat-2* transgenic mice to mouse models of *C9orf72* ALS/FTD to assess whether endogenous expression is sufficient to rescue disease-related phenotypes in mice.

Fatty acid desaturase 2 (FADS2), an enzyme involved in DHA synthesis, was reported to be increased at the protein level in spinal cord from sporadic ALS patients (Cacabelos *et al.*, 2016), despite DHA being decreased in these same samples (Ilieva *et al.*, 2007). Contrastingly, that paper reported increased levels of DHA in frontal cortex brain tissue of the same ALS patients (Ilieva *et al.*, 2007). Desaturase upregulation reported in that study may be a compensatory response, however measuring activity rather than protein levels would be more informative. That study also suggested that there are regional differences in PUFA dysregulation. Further studies are needed to address the temporal and regional dynamics of PUFA dysregulation in ALS, as well as uncover the underlying mechanisms.

Dysregulated arachidonic acid (AA) metabolism has been reported across *SOD1, C9orf72, TDP-43* and sporadic ALS spinal motor neurons, with inhibition of 5-LOX, an enzyme that processes AA into inflammatory eicosanoids, improving cell survival of *SOD1* and *C9orf72* motor neurons and partially rescuing neurodegenerative phenotypes in a *Drosophila* and $SOD1_{G93A}$ mouse model (Lee et al., 2021). The levels of PUFA-derived mediators have also been reported to be altered in the CSF of patients with frontotemporal dementia. In a pilot study of lipid mediators in FTD CSF, *C9orf72* mutation carriers had higher levels of the DHA-derived, specialised pro-resolving mediators maresins and resolvins compared to controls. Among pro-inflammatory eicosanoids, AA-derived leukotrienes were increased in *MAPT*, *C9orf72* and *GRN* FTD groups, while AA-derived thromboxane was higher in CSF from *MAPT* and *GRN* groups but not *C9orf72* (Sogorb-Esteve et al., 2021). We did not measure lipid mediators in this thesis however, it would be very interesting to assess their levels, given that PUFA levels were altered.

6.6 Potential ways in which *C9orf72* repeat expansion leads to global lipid dysregulation

Here, we have described a new pathway implicated in C9ALS/FTD. We show a dysregulated phospholipid saturation signature caused by the presence of

expanded *C9orf72* repeats in iPSC neurons, post-mortem brain and spinal cord and a *Drosophila* model. These lipid changes must be occurring due to the presence of repeat RNA or DPRs, or both, as flies do not have a *C9orf72* ortholog. In our *Drosophila* model, toxicity is mainly driven by poly(GR) (Mizielinska *et al.*, 2014). Additionally, sense-targeting ASO treatment reverses the pathogenic lipidomic signature in neurons, suggesting that sense RNA or DPRs, of which poly(GR) is most toxic, are driving the phospholipid saturation changes observed. The fact that similar lipid transcriptomic and lipidomic signatures were observed in both C9ALS, C9FTD and non-C9ALS and FTD in post-mortem spinal cord and brain, could suggest that TDP-43 pathology is a converging mechanism mediating this shared lipid disease signature. Alternatively, nucleocytoplasmic transport impairment may be an early common mechanism across these neurodegenerative diseases (Coyne and Rothstein, 2022). Indeed, many nuclear proteins including transcription factors are found mislocalised in the cytoplasm in post-mortem brains with ageing and across a range of age-related neurodegenerative diseases (Hutten and Dormann, 2020; Lu *et al.*, 2014; Kim and Taylor, 2017; Ramsey *et al.*, 2007; Chu *et al.*, 2007).

Mislocalisation of transcription factors could underlie the extensive transcriptomic dysregulation seen across models of C9ALS/FTD, and is an interesting hypothesis to consider. Cytoplasmic localisation of master lipid transcription factors such as SREBP or PPAR could lead to their functional impairment, causing the widespread transcriptional dysregulation of lipid metabolism with resulting effects on lipid species reported here.

6.7 Why are unsaturated lipids protective in C9ALS/FTD?

6.7.1 Unsaturated lipids increase membrane fluidity

Cell membranes are fluid mosaics of lipids and proteins, and this fluid property of membranes is influenced by temperature as well as lipid composition. The presence of double bonds in fatty acids of phospholipids creates kinks in the carbon chain, thereby reducing phospholipid packing and increasing membrane

fluidity (Ruiz *et al.*, 2023; Levental *et al.*, 2020; Ruiz *et al.*, 2019a). The biophysical state of lipid bilayers can influence the structure and activity of integral membrane proteins which make up approximately 30% of the mammalian proteome and are attractive drug targets (Overington, Al-Lazikani and Hopkins, 2006; Krogh *et al.*, 2001). Therefore, lipid membranes are more than a protective barrier, or an inert milieu in which important proteins reside, and the composition of this lipid membrane can have wide ranging effects on cellular functions (Levental and Lyman, 2023; Harayama and Riezman, 2018).

Since phospholipid PUFA levels were found to be dysregulated in *C9orf72* ALS/FTD neurons in this work, we predict that this has widespread effects on the fluidity of neuronal membranes. In a behavioural paradigm, we utilised a cold stress sensitivity assay as a proxy for membrane fluidity assessment. C9 *Drosophila* that had altered expression of desaturases were found to have a greater sensitivity to cold-stress, as expected (Brankatschk *et al.*, 2018). Desaturase overexpression in neurons of C9 flies was able to ameliorate this cold-sensitivity phenotype, possibly by fluidising membranes (Chapter 5). A contradiction arises when considering that PUFAs are susceptible to oxidative stress which can cause lipid peroxidation, which rigidifies membranes and can trigger ferroptosis (Reiter, 1998). Lipid peroxidation has been implicated in ALS patients and mouse models (Miana-Mena *et al.*, 2011; Simpson *et al.*, 2004; Shibata *et al.*, 2001). Mutations in *SOD1*, encoding the antioxidant enzyme, superoxide dismutase, is a major genetic cause of ALS, and *SOD1* mutant mice have increased spinal cord membrane rigidity, which may be due to increased lipid peroxidation (Miana-Mena *et al.*, 2011). Membrane fluidity has not yet been assessed in sporadic ALS or other genetic forms of ALS. Ferroptosis has not been explored in this study, however, it will be important to consider lipid peroxidation in future work when manipulating PUFA levels, as there may be a sweet spot that corrects disease-related deficits but does not lead to toxicity via susceptibility to peroxidation.

6.7.2 Saturated fatty acids are a toxic factor in ALS

Reactive astrocytes have been shown to promote motor neuron degeneration in ALS models, by secreting toxic factors that lead to neuronal cell death (Guttenplan *et al.*, 2020; Tripathi *et al.*, 2017; Nagai *et al.*, 2007). Saturated fatty acids have recently been identified as a key neurotoxic factor secreted by astrocytes in lipoparticles, which can subsequently be taken up by oligodendrocytes and neurons and incorporated into their membranes. In that study, saturated fatty acids were shown to lead to cell death via lipoapoptosis, rather than ferroptosis (death by lipid peroxidation), initiating the unfolded protein response (UPR) by activating PERK, with cytotoxicity occurring via PUMA and cleaved caspase-3 (Guttenplan *et al.*, 2021). Furthermore, astrocyte-specific knockout of *ELOVL1*, an enzyme responsible for producing long-chain saturated lipids, reduced astrocyte-mediated neuronal toxicity *in-vivo* (Guttenplan *et al.*, 2021). The authors of this study remark that the lipotoxic cell death is likely due to changes in membrane structure (Guttenplan *et al.*, 2021). Indeed, membrane remodelling after treatment with the saturated fatty acid palmitic acid has previously been shown to compromise endoplasmic reticulum membrane structure and integrity, triggering apoptotic cell death (Borradaile *et al.*, 2006). Other studies have shown that knocking down *stearoyl coenzyme desaturase* (*SCD1*) or treating with palmitic acid decreases membrane phospholipid unsaturation, inducing UPR via both IRE1 and PERK (Halbleib *et al.*, 2017; Volmer, van der Ploeg and Ron, 2013) or activating UPR and triggering cell death via PERK-CHOP (Ariyama *et al.*, 2010) and that this UPR activation can be suppressed by treating *SCD1* knockdown cells with monounsaturated or polyunsaturated fatty acids (Ariyama *et al.*, 2010). Therefore, loss of unsaturated lipids from neuronal membranes in ALS and FTD, as we report here, may indirectly contribute to cell type vulnerability and cell death by increasing the relative amount of saturated fatty acids in the membrane. Additionally, the decreased levels of unsaturated phospholipids reported here may also be contributed to by subcellular organellar membranes. Since membrane composition varies between organelles dependent on their unique function, global loss of unsaturated phospholipids in disease may have devastating consequences on these subcellular compartments, particularly endoplasmic

reticulum and mitochondria (Levental and Lyman, 2023; Budin *et al.*, 2018). In future, it would be informative to perform lipidomics on isolated organelles from ALS/FTD models.

6.7.3 PUFAs can influence the activity of ion channels

PUFAs have been shown to directly bind to and inactivate voltage gated potassium channels and thereby alter neuronal excitability (Moreno *et al.*, 2012; Guizy *et al.*, 2005; Vreugdenhil *et al.*, 1996). Therefore, neuronal PUFAs may be exerting neuroprotective effects through inhibitory effects on ion channels, with loss of neuronal PUFAs leading to loss of this inhibition, and as a result, contributing to excitotoxicity.

6.7.4 PUFAs can influence post-translational lipid modification of proteins with impacts on protein localisation and function

Palmitoylation is a post-translational modification of proteins involving the attachment of the saturated fatty acid palmitic acid (C16:0) at cysteine residues by thioester linkages, and this modification can be prevented by PUFAs (Webb, Hermida-Matsumoto and Resh, 2000). Palmitoylation can directly and indirectly influence the stability, localisation and clustering of ion channels at membranes (El-Husseini and Bredt, 2002). Postsynaptic density protein 95 (PSD-95) is a scaffold protein that clusters ion channels, including potassium channels and glutamate receptors AMPA and NMDA, at excitatory synapses, and this clustering is dependent on palmitoylation of PSD-95 by palmitoyl acyl transferases at dendrites (Jeyifous *et al.*, 2016; Christopherson *et al.*, 2003). Furthermore, palmitoylation of PSD-95 was found to increase levels of both PSD-95 and AMPARs at synapses (Jeyifous *et al.*, 2016). PSD-95 is transported to synaptic regions by KIF5 (Yoo *et al.*, 2019). Given that *KIF5A* mutations are a genetic cause of ALS, leading to a loss of autoinhibition, with increased microtubule binding and transport (Baron *et al.*, 2022), it is possible that PSD-95 trafficking to the synapse is enhanced, leading to increased PSD-95 palmitoylation, and increased levels of AMPARs at excitatory synapses.

Increased expression of AMPARs in motor neurons and resulting excitotoxicity have already been implicated in C9ALS/FTD (Selvaraj *et al.*, 2018). Given that PUFAs can prevent palmitoylation, PUFAs may also exert their neuroprotective effects by decreasing PSD-95 palmitoylation, and therefore decreasing AMPA receptor levels at excitatory synapses.

6.8 Conclusion

Here I have attempted to identify novel modifiers of *C9orf72* toxicity, beginning with unbiased transcriptomics approaches in *Drosophila* models of C9ALS/FTD, and confirming findings where possible in patient iPSC neurons and post-mortem brains. The Odd-skipped family were identified as modifiers of toxicity in C9 *Drosophila* in part due to their regulation of the C9 transcriptomic signature. *Trpγ* overexpression rescued sleep, motor and survival neurodegenerative phenotypes in C9 *Drosophila*, by decreasing toxic poly(GR) levels. In the main study of this thesis, I identified fatty acid metabolism, particularly phospholipid saturation, as a novel, conserved, dysregulated pathway in C9ALS/FTD. Further work will be required to determine the mechanisms by which loss of unsaturated phospholipids leads to neurodegeneration, and how desaturase overexpression ameliorates toxicity. On a broader scale, transcriptomic and lipidomic dysregulation was also found in non-*C9orf72* ALS and FTD tissues, potentially widening the applicability of our findings to a broader range of neurodegenerative diseases. Future studies correlating dietary intake of PUFAs, as well as plasma and CSF lipidomics at disease onset and throughout progression, to post-mortem brain lipidomics, and disease duration, within and between individuals, could reveal important insights for biomarker development. Given that high dietary PUFAs and elevated plasma levels of PUFAs are associated with reduced risk of ALS, our study further provides evidence that PUFA supplementation should be recommended at diagnosis and possibly as a preventative measure throughout the life course. Modulating neuronal PUFA levels genetically will be much more challenging, but this work suggests that this will be a promising approach for ameliorating C9-associated neurodegeneration.

References

Ahmed, R. M., Landin-Romero, R., Collet, T.-H., van der Klaauw, A. A., Devenney, E., Henning, E., Kiernan, M. C., Piguet, O., Farooqi, I. S. and Hodges, J. R. (2017) 'Energy expenditure in frontotemporal dementia: a behavioural and imaging study', *Brain,* 140(1), pp. 171-183.

Akbar, M., Calderon, F., Wen, Z. and Kim, H.-Y. (2005) 'Docosahexaenoic acid: a positive modulator of Akt signaling in neuronal survival', *Proceedings of the National Academy of Sciences of the United States of America,* 102(31), pp. 10858-10863.

Akitake, B., Ren, Q., Boiko, N., Ni, J., Sokabe, T., Stockand, J. D., Eaton, B. A. and Montell, C. (2015) 'Coordination and fine motor control depend on Drosophila TRPγ', *Nature Communications,* 6(1), pp. 7288.

Aladesuyi Arogundade, O., Stauffer, J. E., Saberi, S., Diaz-Garcia, S., Malik, S., Basilim, H., Rodriguez, M. J., Ohkubo, T. and Ravits, J. (2019) 'Antisense RNA foci are associated with nucleoli and TDP-43 mislocalization in C9orf72-ALS/FTD: a quantitative study', *Acta Neuropathologica,* 137(3), pp. 527-530.

Almeida, S., Gascon, E., Tran, H., Chou, H. J., Gendron, T. F., DeGroot, S., Tapper, A. R., Sellier, C., Charlet-Berguerand, N., Karydas, A., Seeley, W. W., Boxer, A. L., Petrucelli, L., Miller, B. L. and Gao, F.-B. (2013) 'Modeling key pathological features of frontotemporal dementia with C9ORF72 repeat expansion in iPSC-derived human neurons', *Acta Neuropathologica,* 126(3), pp. 385-399.

Aly, A., Laszlo, Z. I., Rajkumar, S., Demir, T., Hindley, N., Lamont, D. J., Lehmann, J., Seidel, M., Sommer, D., Franz-Wachtel, M., Barletta, F., Heumos, S., Czemmel, S., Kabashi, E., Ludolph, A., Boeckers, T. M., Henstridge, C. M. and Catanese, A. (2023) 'Integrative proteomics highlight presynaptic alterations and c-Jun misactivation as convergent pathomechanisms in ALS', *Acta Neuropathologica,* 146(3), pp. 451-475.

Amick, J., Roczniak-Ferguson, A. and Ferguson, S. M. (2016) 'C9orf72 binds SMCR8, localizes to lysosomes, and regulates mTORC1 signaling', *Molecular Biology of the Cell,* 27(20), pp. 3040-3051.

Amyotrophic Lateral Sclerosis/Riluzole Study, G., II, Lacomblez, L., Bensimon, G., Meininger, V., Leigh, P. N. and Guillet, P. (1996) 'Dose-ranging study of riluzole in amyotrophic lateral sclerosis', *The Lancet,* 347(9013), pp. 1425-1431.

Anoar, S., Woodling, N. S. and Niccoli, T. (2021) 'Mitochondria Dysfunction in Frontotemporal Dementia/Amyotrophic Lateral Sclerosis: Lessons From Drosophila Models', *Frontiers in Neuroscience,* 15.

Aoki, Y., Manzano, R., Lee, Y., Dafinca, R., Aoki, M., Douglas, A. G. L., Varela, M. A., Sathyaprakash, C., Scaber, J., Barbagallo, P., Vader, P., Mäger, I., Ezzat, K., Turner, M. R., Ito, N., Gasco, S., Ohbayashi, N., El Andaloussi, S., Takeda, S. i., Fukuda, M., Talbot, K. and Wood, M. J. A. (2017) 'C9orf72 and RAB7L1 regulate vesicle trafficking in amyotrophic lateral sclerosis and frontotemporal dementia', *Brain,* 140(4), pp. 887-897.

Arai, T., Hasegawa, M., Akiyama, H., Ikeda, K., Nonaka, T., Mori, H., Mann, D., Tsuchiya, K., Yoshida, M., Hashizume, Y. and Oda, T. (2006) 'TDP-43 is a component of ubiquitin-positive tau-negative inclusions in frontotemporal lobar degeneration and amyotrophic lateral sclerosis', *Biochemical and Biophysical Research Communications,* 351(3), pp. 602-611.

Area-Gomez, E., Larrea, D., Yun, T., Xu, Y., Hupf, J., Zandkarimi, F., Chan, R. B. and Mitsumoto, H. (2021) 'Lipidomics study of plasma from patients suggest that ALS and PLS are part of a continuum of motor neuron disorders', *Scientific Reports,* 11(1), pp. 13562.

Ariyama, H., Kono, N., Matsuda, S., Inoue, T. and Arai, H. (2010) 'Decrease in Membrane Phospholipid Unsaturation Induces Unfolded Protein Response', *Journal of Biological Chemistry,* 285(29), pp. 22027-22035.

Ash, Peter E. A., Bieniek, Kevin F., Gendron, Tania F., Caulfield, T., Lin, W.-L., DeJesus-Hernandez, M., van Blitterswijk, Marka M., Jansen-West, K., Paul, Joseph W., Rademakers, R., Boylan, Kevin B., Dickson, Dennis W. and Petrucelli, L. (2013) 'Unconventional Translation of C9ORF72 GGGGCC Expansion Generates Insoluble Polypeptides Specific to c9FTD/ALS', *Neuron,* 77(4), pp. 639-646.

Atanasio, A., Decman, V., White, D., Ramos, M., Ikiz, B., Lee, H.-C., Siao, C.-J., Brydges, S., LaRosa, E., Bai, Y., Fury, W., Burfeind, P., Zamfirova, R., Warshaw, G., Orengo, J., Oyejide, A., Fralish, M., Auerbach, W., Poueymirou, W., Freudenberg, J., Gong, G., Zambrowicz, B., Valenzuela, D., Yancopoulos, G., Murphy, A., Thurston, G. and Lai, K.-M. V. (2016) 'C9orf72 ablation causes immune dysregulation characterized by leukocyte expansion, autoantibody production and glomerulonephropathy in mice', *Scientific Reports,* 6(1), pp. 23204.

Atilano, M. L., Grönke, S., Niccoli, T., Kempthorne, L., Hahn, O., Morón-Oset, J., Hendrich, O., Dyson, M., Adams, M. L., Hull, A., Salcher-Konrad, M.-T., Monaghan, A., Bictash, M., Glaria, I., Isaacs, A. M. and Partridge, L. (2021) 'Enhanced insulin signalling ameliorates C9orf72 hexanucleotide repeat expansion toxicity in Drosophila', *eLife,* 10, pp. e58565.

Axelrod, J. (1990) 'Receptor-mediated activation of phospholipase A2 and arachidonic acid release in signal transduction', *Biochemical Society Transactions,* 18(4), pp. 503-507.

Bajar, B. T., Phi, N. T., Isaacman-Beck, J., Reichl, J., Randhawa, H. and Akin, O. (2022) 'A discrete neuronal population coordinates brain-wide developmental activity', *Nature,* 602(7898), pp. 639-646.

Baker, M., Mackenzie, I. R., Pickering-Brown, S. M., Gass, J., Rademakers, R., Lindholm, C., Snowden, J., Adamson, J., Sadovnick, A. D., Rollinson, S., Cannon, A., Dwosh, E., Neary, D., Melquist, S., Richardson, A., Dickson, D., Berger, Z., Eriksen, J., Robinson, T., Zehr, C., Dickey, C. A., Crook, R.,

McGowan, E., Mann, D., Boeve, B., Feldman, H. and Hutton, M. (2006) 'Mutations in progranulin cause tau-negative frontotemporal dementia linked to chromosome 17', *Nature,* 442(7105), pp. 916-919.

Balendra, R. and Isaacs, A. M. (2018) 'C9orf72-mediated ALS and FTD: multiple pathways to disease', *Nature reviews. Neurology,* 14(9), pp. 544-558.

Bang, J., Spina, S. and Miller, B. L. (2015) 'Frontotemporal dementia', *The Lancet,* 386(10004), pp. 1672-1682.

Baron, D. M., Fenton, A. R., Saez-Atienzar, S., Giampetruzzi, A., Sreeram, A., Shankaracharya, Keagle, P. J., Doocy, V. R., Smith, N. J., Danielson, E. W., Andresano, M., McCormack, M. C., Garcia, J., Bercier, V., Van Den Bosch, L., Brent, J. R., Fallini, C., Traynor, B. J., Holzbaur, E. L. F. and Landers, J. E. (2022) 'ALS-associated KIF5A mutations abolish autoinhibition resulting in a toxic gain of function', *Cell Reports,* 39(1), pp. 110598.

Baxi, E. G. and Thompson, T. and Li, J. and Kaye, J. A. and Lim, R. G. and Wu, J. and Ramamoorthy, D. and Lima, L. and Vaibhav, V. and Matlock, A. and Frank, A. and Coyne, A. N. and Landin, B. and Ornelas, L. and Mosmiller, E. and Thrower, S. and Farr, S. M. and Panther, L. and Gomez, E. and Galvez, E. and Perez, D. and Meepe, I. and Lei, S. and Mandefro, B. and Trost, H. and Pinedo, L. and Banuelos, M. G. and Liu, C. and Moran, R. and Garcia, V. and Workman, M. and Ho, R. and Wyman, S. and Roggenbuck, J. and Harms, M. B. and Stocksdale, J. and Miramontes, R. and Wang, K. and Venkatraman, V. and Holewenski, R. and Sundararaman, N. and Pandey, R. and Manalo, D.-M. and Donde, A. and Huynh, N. and Adam, M. and Wassie, B. T. and Vertudes, E. and Amirani, N. and Raja, K. and Thomas, R. and Hayes, L. and Lenail, A. and Cerezo, A. and Luppino, S. and Farrar, A. and Pothier, L. and Prina, C. and Morgan, T. and Jamil, A. and Heintzman, S. and Jockel-Balsarotti, J. and Karanja, E. and Markway, J. and McCallum, M. and Joslin, B. and Alibazoglu, D. and Kolb, S. and Ajroud-Driss, S. and Baloh, R. and Heitzman, D. and Miller, T. and Glass, J. D. and Patel-Murray, N. L. and Yu, H. and Sinani, E. and Vigneswaran, P. and Sherman, A. V. and Ahmad, O. and Roy, P. and Beavers,

J. C. and Zeiler, S. and Krakauer, J. W. and Agurto, C. and Cecchi, G. and Bellard, M. and Raghav, Y. and Sachs, K. and Ehrenberger, T. and Bruce, E. and Cudkowicz, M. E. and Maragakis, N. and Norel, R. and Van Eyk, J. E. and Finkbeiner, S. and Berry, J. and Sareen, D. and Thompson, L. M. and Fraenkel, E. and Svendsen, C. N. and Rothstein, J. D. (2022) 'Answer ALS, a large-scale resource for sporadic and familial ALS combining clinical and multi-omics data from induced pluripotent cell lines', *Nature Neuroscience,* 25(2), pp. 226-237.

Bazinet, R. P. and Layé, S. (2014) 'Polyunsaturated fatty acids and their metabolites in brain function and disease', *Nature Reviews Neuroscience,* 15(12), pp. 771-785.

Beck, J., Poulter, M., Hensman, D., Rohrer, Jonathan D., Mahoney, C. J., Adamson, G., Campbell, T., Uphill, J., Borg, A., Fratta, P., Orrell, Richard W., Malaspina, A., Rowe, J., Brown, J., Hodges, J., Sidle, K., Polke, James M., Houlden, H., Schott, Jonathan M., Fox, Nick C., Rossor, Martin N., Tabrizi, Sarah J., Isaacs, Adrian M., Hardy, J., Warren, J. D., Collinge, J. and Mead, S. (2013) 'Large C9orf72 Hexanucleotide Repeat Expansions Are Seen in Multiple Neurodegenerative Syndromes and Are More Frequent Than Expected in the UK Population', *The American Journal of Human Genetics,* 92(3), pp. 345-353.

Becker, E. B. E., Oliver, P. L., Glitsch, M. D., Banks, G. T., Achilli, F., Hardy, A., Nolan, P. M., Fisher, E. M. C. and Davies, K. E. (2009) 'A point mutation in TRPC3 causes abnormal Purkinje cell development and cerebellar ataxia in moonwalker mice', *Proceedings of the National Academy of Sciences,* 106(16), pp. 6706-6711.

Bellen, H. J., Levis, R. W., Liao, G., He, Y., Carlson, J. W., Tsang, G., Evans-Holm, M., Hiesinger, P. R., Schulze, K. L., Rubin, G. M., Hoskins, R. A. and Spradling, A. C. (2004) 'The BDGP Gene Disruption Project: Single Transposon Insertions Associated With 40% of Drosophila Genes', *Genetics,* 167(2), pp. 761-781.

Bellingham, M. C. (2011) 'A Review of the Neural Mechanisms of Action and Clinical Efficiency of Riluzole in Treating Amyotrophic Lateral Sclerosis: What have we Learned in the Last Decade?', *CNS Neuroscience & Therapeutics,* 17(1), pp. 4-31.

Belzil, V. V., Bauer, P. O., Prudencio, M., Gendron, T. F., Stetler, C. T., Yan, I. K., Pregent, L., Daughrity, L., Baker, M. C., Rademakers, R., Boylan, K., Patel, T. C., Dickson, D. W. and Petrucelli, L. (2013) 'Reduced C9orf72 gene expression in c9FTD/ALS is caused by histone trimethylation, an epigenetic event detectable in blood', *Acta Neuropathologica,* 126(6), pp. 895-905.

Ben Gedalya, T., Loeb, V., Israeli, E., Altschuler, Y., Selkoe, D. J. and Sharon, R. (2009) 'α-Synuclein and Polyunsaturated Fatty Acids Promote Clathrin-Mediated Endocytosis and Synaptic Vesicle Recycling', *Traffic,* 10(2), pp. 218-234.

Berger, A., Crozier, G., Bisogno, T., Cavaliere, P., Innis, S. and Di Marzo, V. (2001) 'Anandamide and diet: Inclusion of dietary arachidonate and docosahexaenoate leads to increased brain levels of the corresponding N-acylethanolamines in piglets', *Proceedings of the National Academy of Sciences,* 98(11), pp. 6402-6406.

Bischof, J., Björklund, M., Furger, E., Schertel, C., Taipale, J. and Basler, K. (2013) 'A versatile platform for creating a comprehensive UAS-ORFeome library in Drosophila', *Development,* 140(11), pp. 2434-2442.

Bjornevik, K., Cortese, M., Furtado, J., D., Paganoni, S., Schwarzschild, M., A., Cudkowicz, M., E. and Ascherio, A. (2023) 'Association of Polyunsaturated Fatty Acids and Clinical Progression in Patients With ALS', *Neurology,* 101(7), pp. e690.

Blasco, H., Veyrat-Durebex, C., Bocca, C., Patin, F., Vourc'h, P., Kouassi Nzoughet, J., Lenaers, G., Andres, C. R., Simard, G., Corcia, P. and Reynier, P.

(2017) 'Lipidomics Reveals Cerebrospinal-Fluid Signatures of ALS', *Scientific Reports,* 7(1), pp. 17652.

Bodhicharla, R., Devkota, R., Ruiz, M. and Pilon, M. (2018) 'Membrane Fluidity Is Regulated Cell Nonautonomously by Caenorhabditis elegans PAQR-2 and Its Mammalian Homolog AdipoR2', *Genetics,* 210(1), pp. 189-201.

Boeve, B. F., Boxer, A. L., Kumfor, F., Pijnenburg, Y. and Rohrer, J. D. (2022) 'Advances and controversies in frontotemporal dementia: diagnosis, biomarkers, and therapeutic considerations', *The Lancet Neurology,* 21(3), pp. 258-272.

Boeynaems, S., Bogaert, E., Michiels, E., Gijselinck, I., Sieben, A., Jovičić, A., De Baets, G., Scheveneels, W., Steyaert, J., Cuijt, I., Verstrepen, K. J., Callaerts, P., Rousseau, F., Schymkowitz, J., Cruts, M., Van Broeckhoven, C., Van Damme, P., Gitler, A. D., Robberecht, W. and Van Den Bosch, L. (2016) 'Drosophila screen connects nuclear transport genes to DPR pathology in c9ALS/FTD', *Scientific Reports,* 6(1), pp. 20877.

Borradaile, N. M., Han, X., Harp, J. D., Gale, S. E., Ory, D. S. and Schaffer, J. E. (2006) 'Disruption of endoplasmic reticulum structure and integrity in lipotoxic cell death', *Journal of Lipid Research,* 47(12), pp. 2726-2737.

Bosetti, F. (2007) 'Arachidonic acid metabolism in brain physiology and pathology: lessons from genetically altered mouse models', *Journal of Neurochemistry,* 102(3), pp. 577-586.

Bouteloup, C., Desport, J. C., Clavelou, P., Guy, N., Derumeaux-Burel, H., Ferrier, A. and Couratier, P. (2009) 'Hypermetabolism in ALS patients: an early and persistent phenomenon', *Journal of Neurology,* 256(8), pp. 1236-1242.

Bracko, O., Vinarcsik, L. K., Cruz Hernández, J. C., Ruiz-Uribe, N. E., Haft-Javaherian, M., Falkenhain, K., Ramanauskaite, E. M., Ali, M., Mohapatra, A., Swallow, M. A., Njiru, B. N., Muse, V., Michelucci, P. E., Nishimura, N. and

Schaffer, C. B. (2020) 'High fat diet worsens Alzheimer's disease-related behavioral abnormalities and neuropathology in APP/PS1 mice, but not by synergistically decreasing cerebral blood flow', *Scientific Reports,* 10(1), pp. 9884.

Brand, A. H. and Perrimon, N. (1993) 'Targeted gene expression as a means of altering cell fates and generating dominant phenotypes', *Development,* 118(2), pp. 401-415.

Brankatschk, M., Gutmann, T., Knittelfelder, O., Palladini, A., Prince, E., Grzybek, M., Brankatschk, B., Shevchenko, A., Coskun, Ü. and Eaton, S. (2018) 'A Temperature-Dependent Switch in Feeding Preference Improves Drosophila Development and Survival in the Cold', *Developmental Cell,* 46(6), pp. 781-793.e4.

Bras-Pereira, C., Bessa, J. and Casares, F. (2006) 'Odd-skipped genes specify the signaling center that triggers retinogenesis in Drosophila', *Development,* 133(21), pp. 4145.

Brayer, K. J. and Segal, D. J. (2008) 'Keep Your Fingers Off My DNA: Protein–Protein Interactions Mediated by C2H2 Zinc Finger Domains', *Cell Biochemistry and Biophysics,* 50(3), pp. 111-131.

Brenner, D., Müller, K., Wieland, T., Weydt, P., Böhm, S., Lulé, D., Hübers, A., Neuwirth, C., Weber, M., Borck, G., Wahlqvist, M., Danzer, K. M., Volk, A. E., Meitinger, T., Strom, T. M., Otto, M., Kassubek, J., Ludolph, A. C., Andersen, P. M. and Weishaupt, J. H. (2016) 'NEK1 mutations in familial amyotrophic lateral sclerosis', *Brain,* 139(5), pp. e28-e28.

Budin, I., de Rond, T., Chen, Y., Chan, L. J. G., Petzold, C. J. and Keasling, J. D. (2018) 'Viscous control of cellular respiration by membrane lipid composition', *Science,* 362(6419), pp. 1186-1189.

Burberry, A., Suzuki, N., Wang, J.-Y., Moccia, R., Mordes, D. A., Stewart, M. H., Suzuki-Uematsu, S., Ghosh, S., Singh, A., Merkle, F. T., Koszka, K., Li, Q.-Z., Zon, L., Rossi, D. J., Trowbridge, J. J., Notarangelo, L. D. and Eggan, K. (2016) 'Loss-of-function mutations in the C9ORF72 mouse ortholog cause fatal autoimmune disease', *Science translational medicine,* 8(347), pp. 347ra93-347ra93.

Burckhardt, M., Herke, M., Wustmann, T., Watzke, S., Langer, G. and Fink, A. (2016) 'Omega-3 fatty acids for the treatment of dementia', *Cochrane Database of Systematic Reviews,* (4).

Cacabelos, D., Ayala, V., Granado-Serrano, A. B., Jové, M., Torres, P., Boada, J., Cabré, R., Ramírez-Núñez, O., Gonzalo, H., Soler-Cantero, A., Serrano, J. C. E., Bellmunt, M. J., Romero, M. P., Motilva, M. J., Nonaka, T., Hasegawa, M., Ferrer, I., Pamplona, R. and Portero-Otín, M. (2016) 'Interplay between TDP-43 and docosahexaenoic acid-related processes in amyotrophic lateral sclerosis', *Neurobiology of Disease,* 88, pp. 148-160.

Cairns, N. J., Bigio, E. H., Mackenzie, I. R. A., Neumann, M., Lee, V. M. Y., Hatanpaa, K. J., White, C. L., Schneider, J. A., Grinberg, L. T., Halliday, G., Duyckaerts, C., Lowe, J. S., Holm, I. E., Tolnay, M., Okamoto, K., Yokoo, H., Murayama, S., Woulfe, J., Munoz, D. G., Dickson, D. W., Ince, P. G., Trojanowski, J. Q. and Mann, D. M. A. (2007) 'Neuropathologic diagnostic and nosologic criteria for frontotemporal lobar degeneration: consensus of the Consortium for Frontotemporal Lobar Degeneration', *Acta Neuropathologica,* 114(1), pp. 5-22.

Capolupo, L. (2023) 'Single-cell lipidomics reveals the organizing principle of cell fate decision', *Nature Reviews Molecular Cell Biology,* 24(6), pp. 377-377.

Castillo, Pablo E., Younts, Thomas J., Chávez, Andrés E. and Hashimotodani, Y. (2012) 'Endocannabinoid Signaling and Synaptic Function', *Neuron,* 76(1), pp. 70-81.

Chan, H. Y. E. and Bonini, N. M. (2000) 'Drosophila models of human neurodegenerative disease', *Cell Death & Differentiation,* 7(11), pp. 1075-1080.

Chaves-Filho, A. B., Pinto, I. F. D., Dantas, L. S., Xavier, A. M., Inague, A., Faria, R. L., Medeiros, M. H. G., Glezer, I., Yoshinaga, M. Y. and Miyamoto, S. (2019) 'Alterations in lipid metabolism of spinal cord linked to amyotrophic lateral sclerosis', *Scientific Reports,* 9(1), pp. 11642.

Chen, H. and Pugh, B. F. (2021) 'What do Transcription Factors Interact With?', *Journal of Molecular Biology,* 433(14), pp. 166883.

Chen, K.-F., Lowe, S., Lamaze, A., Krätschmer, P. and Jepson, J. (2019) 'Neurocalcin regulates nighttime sleep and arousal in Drosophila', *eLife,* 8, pp. e38114.

Chen, W., Zou, A., Zhang, H., Fu, X., Yao, F. and Yang, A. (2018) 'Odd-skipped related transcription factor 1 (OSR1) suppresses tongue squamous cell carcinoma migration and invasion through inhibiting NF-κB pathway', *European Journal of Pharmacology,* 839, pp. 33-39.

Chertemps, T., Duportets, L., Labeur, C., Ueyama, M. and Wicker-Thomas, C. (2006) 'A female-specific desaturase gene responsible for diene hydrocarbon biosynthesis and courtship behaviour in Drosophila melanogaster', *Insect Molecular Biology,* 15(4), pp. 465-473.

Chiang, P.-M., Ling, J., Jeong, Y. H., Price, D. L., Aja, S. M. and Wong, P. C. (2010) 'Deletion of TDP-43 down-regulates Tbc1d1, a gene linked to obesity, and alters body fat metabolism', *Proceedings of the National Academy of Sciences of the United States of America,* 107(37), pp. 16320-16324.

Christopherson, K. S., Sweeney, N. T., Craven, S. E., Kang, R., El-Husseini, A. E.-D. and Bredt, D. S. (2003) 'Lipid- and protein-mediated multimerization of PSD-95: implications for receptor clustering and assembly of synaptic protein networks', *Journal of Cell Science,* 116(15), pp. 3213-3219.

Chu, C. T., Plowey, E. D., Wang, Y., Patel, V. and Jordan-Sciutto, K. L. (2007) 'Location, Location, Location: Altered Transcription Factor Trafficking in Neurodegeneration', *Journal of Neuropathology & Experimental Neurology,* 66(10), pp. 873-883.

Chung, K., Wallace, J., Kim, S.-Y., Kalyanasundaram, S., Andalman, A. S., Davidson, T. J., Mirzabekov, J. J., Zalocusky, K. A., Mattis, J., Denisin, A. K., Pak, S., Bernstein, H., Ramakrishnan, C., Grosenick, L., Gradinaru, V. and Deisseroth, K. (2013) 'Structural and molecular interrogation of intact biological systems', *Nature,* 497(7449), pp. 332-337.

Chyb, S., Raghu, P. and Hardie, R. C. (1999) 'Polyunsaturated fatty acids activate the Drosophila light-sensitive channels TRP and TRPL', *Nature,* 397(6716), pp. 255-259.

Cleary, J. D., Pattamatta, A. and Ranum, L. P. W. (2018) 'Repeat-associated non-ATG (RAN) translation', *Journal of Biological Chemistry,* 293(42), pp. 16127-16141.

Coetzee, S. G., Pierce, S., Brundin, P., Brundin, L., Hazelett, D. J. and Coetzee, G. A. (2016) 'Enrichment of risk SNPs in regulatory regions implicate diverse tissues in Parkinson's disease etiology', *Scientific Reports,* 6(1), pp. 30509.

Cooper-Knock, J., Higginbottom, A., Stopford, M. J., Highley, J. R., Ince, P. G., Wharton, S. B., Pickering-Brown, S., Kirby, J., Hautbergue, G. M. and Shaw, P. J. (2015) 'Antisense RNA foci in the motor neurons of C9ORF72-ALS patients are associated with TDP-43 proteinopathy', *Acta Neuropathologica,* 130(1), pp. 63-75.

Cooper-Knock, J., Walsh, M. J., Higginbottom, A., Robin Highley, J., Dickman, M. J., Edbauer, D., Ince, P. G., Wharton, S. B., Wilson, S. A., Kirby, J., Hautbergue, G. M. and Shaw, P. J. (2014) 'Sequestration of multiple RNA recognition motif-containing proteins by C9orf72 repeat expansions', *Brain,* 137(7), pp. 2040-2051.

Coulter, D. E., Swaykus, E. A., Beran-Koehn, M. A., Goldberg, D., Wieschaus, E. and Schedl, P. (1990) 'Molecular analysis of odd-skipped, a zinc finger encoding segmentation gene with a novel pair-rule expression pattern', *The EMBO Journal,* 9(11), pp. 3795-3804.

Coyne, A. N., Baskerville, V., Zaepfel, B. L., Dickson, D. W., Rigo, F., Bennett, F., Lusk, C. P. and Rothstein, J. D. (2021) 'Nuclear accumulation of CHMP7 initiates nuclear pore complex injury and subsequent TDP-43 dysfunction in sporadic and familial ALS', *Sci Transl Med,* 13(604).

Coyne, A. N., Lorenzini, I., Chou, C.-C., Torvund, M., Rogers, R. S., Starr, A., Zaepfel, B. L., Levy, J., Johannesmeyer, J., Schwartz, J. C., Nishimune, H., Zinsmaier, K., Rossoll, W., Sattler, R. and Zarnescu, D. C. (2017) 'Post-transcriptional Inhibition of Hsc70-4/HSPA8 Expression Leads to Synaptic Vesicle Cycling Defects in Multiple Models of ALS', *Cell Reports,* 21(1), pp. 110-125.

Coyne, A. N. and Rothstein, J. D. (2022) 'Nuclear pore complexes — a doorway to neural injury in neurodegeneration', *Nature Reviews Neurology,* 18(6), pp. 348-362.

Coyne, A. N., Zaepfel, B. L., Hayes, L., Fitchman, B., Salzberg, Y., Luo, E.-C., Bowen, K., Trost, H., Aigner, S., Rigo, F., Yeo, G. W., Harel, A., Svendsen, C. N., Sareen, D. and Rothstein, J. D. (2020) 'G4C2 Repeat RNA Initiates a POM121-Mediated Reduction in Specific Nucleoporins in C9orf72 ALS/FTD', *Neuron,* 107(6), pp. 1124-1140.e11.

Cruts, M., Gijselinck, I., van der Zee, J., Engelborghs, S., Wils, H., Pirici, D., Rademakers, R., Vandenberghe, R., Dermaut, B., Martin, J.-J., van Duijn, C., Peeters, K., Sciot, R., Santens, P., De Pooter, T., Mattheijssens, M., Van den Broeck, M., Cuijt, I., Vennekens, K. l., De Deyn, P. P., Kumar-Singh, S. and Van Broeckhoven, C. (2006) 'Null mutations in progranulin cause ubiquitin-positive frontotemporal dementia linked to chromosome 17q21', *Nature,* 442(7105), pp. 920-924.

Cunningham, K. M., Maulding, K., Ruan, K., Senturk, M., Grima, J. C., Sung, H., Zuo, Z., Song, H., Gao, J., Dubey, S., Rothstein, J. D., Zhang, K., Bellen, H. J. and Lloyd, T. E. (2020) 'TFEB/Mitf links impaired nuclear import to autophagolysosomal dysfunction in C9-ALS', *eLife,* 9, pp. e59419.

Dafinca, R., Scaber, J., Ababneh, N., Lalic, T., Weir, G., Christian, H., Vowles, J., Douglas, A. G., Fletcher-Jones, A., Browne, C., Nakanishi, M., Turner, M. R., Wade-Martins, R., Cowley, S. A. and Talbot, K. (2016) 'C9orf72 Hexanucleotide Expansions Are Associated with Altered Endoplasmic Reticulum Calcium Homeostasis and Stress Granule Formation in Induced Pluripotent Stem Cell-Derived Neurons from Patients with Amyotrophic Lateral Sclerosis and Frontotemporal Dementia', *Stem Cells,* 34(8), pp. 2063-78.

Davare, M., A., Fortin Dale, A., Saneyoshi, T., Nygaard, S., Kaech, S., Banker, G., Soderling, T., R. and Wayman, G., A. (2009) 'Transient Receptor Potential Canonical 5 Channels Activate Ca2+/Calmodulin Kinase Iγ to Promote Axon Formation in Hippocampal Neurons', *The Journal of Neuroscience,* 29(31), pp. 9794.

Davie, K., Janssens, J., Koldere, D., De Waegeneer, M., Pech, U., Kreft, Ł., Aibar, S., Makhzami, S., Christiaens, V., Bravo González-Blas, C., Poovathingal, S., Hulselmans, G., Spanier, K. I., Moerman, T., Vanspauwen, B., Geurs, S., Voet, T., Lammertyn, J., Thienpont, B., Liu, S., Konstantinides, N., Fiers, M., Verstreken, P. and Aerts, S. (2018) 'A Single-Cell Transcriptome Atlas of the Aging Drosophila Brain', *Cell,* 174(4), pp. 982-998.e20.

de Celis Ibeas, J. M. and Bray, S. J. (2003) 'Bowl is required downstream of Notch for elaboration of distal limb patterning', *Development,* 130(24), pp. 5943.

de Kroon, A. I. P. M., Rijken, P. J. and De Smet, C. H. (2013) 'Checks and balances in membrane phospholipid class and acyl chain homeostasis, the yeast perspective', *Progress in Lipid Research,* 52(4), pp. 374-394.

DeJesus-Hernandez, M., Finch, N. A., Wang, X., Gendron, T. F., Bieniek, K. F., Heckman, M. G., Vasilevich, A., Murray, M. E., Rousseau, L., Weesner, R., Lucido, A., Parsons, M., Chew, J., Josephs, K. A., Parisi, J. E., Knopman, D. S., Petersen, R. C., Boeve, B. F., Graff-Radford, N. R., de Boer, J., Asmann, Y. W., Petrucelli, L., Boylan, K. B., Dickson, D. W., van Blitterswijk, M. and Rademakers, R. (2017) 'In-depth clinico-pathological examination of RNA foci in a large cohort of C9ORF72 expansion carriers', *Acta Neuropathologica,* 134(2), pp. 255-269.

DeJesus-Hernandez, M., Mackenzie, I. R., Boeve, B. F., Boxer, A. L., Baker, M., Rutherford, N. J., Nicholson, A. M., Finch, N. A., Flynn, H., Adamson, J., Kouri, N., Wojtas, A., Sengdy, P., Hsiung, G.-Y. R., Karydas, A., Seeley, W. W., Josephs, K. A., Coppola, G., Geschwind, D. H., Wszolek, Z. K., Feldman, H., Knopman, D. S., Petersen, R. C., Miller, B. L., Dickson, D. W., Boylan, K. B., Graff-Radford, N. R. and Rademakers, R. (2011) 'Expanded GGGGCC hexanucleotide repeat in noncoding region of C9ORF72 causes chromosome 9p-linked FTD and ALS', *Neuron,* 72(2), pp. 245-256.

Del Signore, S. J., Hayashi, T. and Hatini, V. (2012) 'odd-skipped genes and lines organize the notum anterior-posterior axis using autonomous and non-autonomous mechanisms', *Mechanisms of development,* 129(5-8), pp. 147-161.

Demetrius, L. A., Eckert, A. and Grimm, A. (2021) 'Sex differences in Alzheimer's disease: metabolic reprogramming and therapeutic intervention', *Trends in Endocrinology & Metabolism,* 32(12), pp. 963-979.

Deng, H.-X., Chen, W., Hong, S.-T., Boycott, K. M., Gorrie, G. H., Siddique, N., Yang, Y., Fecto, F., Shi, Y., Zhai, H., Jiang, H., Hirano, M., Rampersaud, E., Jansen, G. H., Donkervoort, S., Bigio, E. H., Brooks, B. R., Ajroud, K., Sufit, R. L., Haines, J. L., Mugnaini, E., Pericak-Vance, M. A. and Siddique, T. (2011) 'Mutations in UBQLN2 cause dominant X-linked juvenile and adult-onset ALS and ALS/dementia', *Nature,* 477(7363), pp. 211-215.

Desport, J. C., Preux, P. M., Magy, L., Boirie, Y., Vallat, J. M., Beaufrère, B. and Couratier, P. (2001) 'Factors correlated with hypermetabolism in patients with amyotrophic lateral sclerosis', *The American Journal of Clinical Nutrition,* 74(3), pp. 328-334.

Desport, J. C., Torny, F., Lacoste, M., Preux, P. M. and Couratier, P. (2005) 'Hypermetabolism in ALS: Correlations with Clinical and Paraclinical Parameters', *Neurodegenerative Diseases,* 2(3-4), pp. 202-207.

Devkota, R., Svensk, E., Ruiz, M., Ståhlman, M., Borén, J. and Pilon, M. (2017) 'The adiponectin receptor AdipoR2 and its Caenorhabditis elegans homolog PAQR-2 prevent membrane rigidification by exogenous saturated fatty acids', *PLOS Genetics,* 13(9), pp. e1007004.

Dhakal, S., Ren, Q., Liu, J., Akitake, B., Tekin, I., Montell, C. and Lee, Y. (2022) 'Drosophila TRPγ is required in neuroendocrine cells for post-ingestive food selection', *eLife,* 11, pp. e56726.

Diaz-Benjumea, F. J. and Cohen, S. M. (1995) 'Serrate signals through Notch to establish a Wingless-dependent organizer at the dorsal/ventral compartment boundary of the Drosophila wing', *Development,* 121(12), pp. 4215-4225.

Dietzl, G., Chen, D., Schnorrer, F., Su, K.-C., Barinova, Y., Fellner, M., Gasser, B., Kinsey, K., Oppel, S., Scheiblauer, S., Couto, A., Marra, V., Keleman, K. and Dickson, B. J. (2007) 'A genome-wide transgenic RNAi library for conditional gene inactivation in Drosophila', *Nature,* 448(7150), pp. 151-156.

Donnelly, Christopher J., Zhang, P.-W., Pham, Jacqueline T., Haeusler, Aaron R., Mistry, Nipun A., Vidensky, S., Daley, Elizabeth L., Poth, Erin M., Hoover, B., Fines, Daniel M., Maragakis, N., Tienari, Pentti J., Petrucelli, L., Traynor, Bryan J., Wang, J., Rigo, F., Bennett, C. F., Blackshaw, S., Sattler, R. and Rothstein, Jeffrey D. (2013) 'RNA Toxicity from the ALS/FTD C9ORF72 Expansion Is Mitigated by Antisense Intervention', *Neuron,* 80(2), pp. 415-428.

Dorst, J., Kühnlein, P., Hendrich, C., Kassubek, J., Sperfeld, A. D. and Ludolph, A. C. (2011) 'Patients with elevated triglyceride and cholesterol serum levels have a prolonged survival in amyotrophic lateral sclerosis', *Journal of Neurology,* 258(4), pp. 613-617.

Dréan, B. S.-L., Nasiadka, A., Dong, J. and Krause, H. M. (1998) 'Dynamic changes in the functions of Odd-skipped during early Drosophila embryogenesis', *Development,* 125(23), pp. 4851-4861.

Dumuis, A., Sebben, M., Haynes, L., Pin, J. P. and Bockaert, J. (1988) 'NMDA receptors activate the arachidonic acid cascade system in striatal neurons', *Nature,* 336(6194), pp. 68-70.

Dupuis, L., Corcia, P., Fergani, A., Gonzalez De Aguilar, J. L., Bonnefont-Rousselot, D., Bittar, R., Seilhean, D., Hauw, J. J., Lacomblez, L., Loeffler, J. P. and Meininger, V. (2008) 'Dyslipidemia is a protective factor in amyotrophic lateral sclerosis', *Neurology,* 70(13), pp. 1004.

Dupuis, L., Oudart, H., René, F., de Aguilar, J.-L. G. and Loeffler, J.-P. (2004) 'Evidence for defective energy homeostasis in amyotrophic lateral sclerosis: Benefit of a high-energy diet in a transgenic mouse model', *Proceedings of the National Academy of Sciences of the United States of America,* 101(30), pp. 11159.

Eady, T. N., Belayev, L., Khoutorova, L., Atkins, K. D., Zhang, C. and Bazan, N. G. (2012) 'Docosahexaenoic Acid Signaling Modulates Cell Survival in Experimental Ischemic Stroke Penumbra and Initiates Long-Term Repair in Young and Aged Rats', *PLOS ONE,* 7(10), pp. e46151.

El-Husseini, A. E.-D. and Bredt, D. S. (2002) 'Protein palmitoylation: a regulator of neuronal development and function', *Nature Reviews Neuroscience,* 3(10), pp. 791-802.

Fahy, E., Subramaniam, S., Murphy, R. C., Nishijima, M., Raetz, C. R. H., Shimizu, T., Spener, F., van Meer, G., Wakelam, M. J. O. and Dennis, E. A. (2009) 'Update of the LIPID MAPS comprehensive classification system for lipids1', *Journal of Lipid Research,* 50, pp. S9-S14.

Fang, G., Shi, B., Wu, K., Chen, S., Gao, X., Xiao, S., Kang, J. X., Li, W. and Huang, R. (2019) 'The protective role of endogenous n-3 polyunsaturated fatty acids in Tau Alzheimer's disease mouse model', *International Journal of Neuroscience,* 129(4), pp. 325-336.

Farg, M. A., Sundaramoorthy, V., Sultana, J. M., Yang, S., Atkinson, R. A. K., Levina, V., Halloran, M. A., Gleeson, P. A., Blair, I. P., Soo, K. Y., King, A. E. and Atkin, J. D. (2014) 'C9ORF72, implicated in amytrophic lateral sclerosis and frontotemporal dementia, regulates endosomal trafficking', *Human Molecular Genetics,* 23(13), pp. 3579-3595.

Fayemendy, P., Marin, B., Labrunie, A., Boirie, Y., Walrand, S., Achamrah, N., Coëffier, M., Preux, P.-M., Lautrette, G., Desport, J.-C., Couratier, P. and Jésus, P. (2021) 'Hypermetabolism is a reality in amyotrophic lateral sclerosis compared to healthy subjects', *Journal of the Neurological Sciences,* 420, pp. 117257.

Felder, C. C., Kanterman, R. Y., Ma, A. L. and Axelrod, J. (1990) 'Serotonin stimulates phospholipase A2 and the release of arachidonic acid in hippocampal neurons by a type 2 serotonin receptor that is independent of inositolphospholipid hydrolysis', *Proceedings of the National Academy of Sciences,* 87(6), pp. 2187-2191.

Fernandopulle, M. S., Prestil, R., Grunseich, C., Wang, C., Gan, L. and Ward, M. E. (2018) 'Transcription Factor–Mediated Differentiation of Human iPSCs into Neurons', *Current Protocols in Cell Biology,* 79(1), pp. e51.

FernÁndez-Eulate, G., Ruiz-Sanz, J. I., Riancho, J., ZufirÍa, M., GereÑu, G., FernÁndez-TorrÓn, R., Poza-Aldea, J. J., Ondaro, J., Espinal, J. B., GonzÁlez-

ChinchÓn, G., Zulaica, M., Ruiz-Larrea, M. B., LÓpez De Munain, A. and Gil-Bea, F. J. (2020) 'A comprehensive serum lipidome profiling of amyotrophic lateral sclerosis', *Amyotrophic Lateral Sclerosis and Frontotemporal Degeneration,* 21(3-4), pp. 252-262.

Fitzgerald, K. C., O'Reilly, É. J., Falcone, G. J., McCullough, M. L., Park, Y., Kolonel, L. N. and Ascherio, A. (2014) 'Dietary ω-3 Polyunsaturated Fatty Acid Intake and Risk for Amyotrophic Lateral Sclerosis', *JAMA Neurology,* 71(9), pp. 1102-1110.

Fitzpatrick, A. L., Kuller, L. H., Lopez, O. L., Diehr, P., O'Meara, E. S., Longstreth, W. T., Jr and Luchsinger, J. A. (2009) 'Midlife and Late-Life Obesity and the Risk of Dementia: Cardiovascular Health Study', *Archives of Neurology,* 66(3), pp. 336-342.

Fratta, P., Mizielinska, S., Nicoll, A. J., Zloh, M., Fisher, E. M. C., Parkinson, G. and Isaacs, A. M. (2012) 'C9orf72 hexanucleotide repeat associated with amyotrophic lateral sclerosis and frontotemporal dementia forms RNA G-quadruplexes', *Scientific Reports,* 2(1), pp. 1016.

Fratta, P., Polke, J. M., Newcombe, J., Mizielinska, S., Lashley, T., Poulter, M., Beck, J., Preza, E., Devoy, A., Sidle, K., Howard, R., Malaspina, A., Orrell, R. W., Clarke, J., Lu, C.-H., Mok, K., Collins, T., Shoaii, M., Nanji, T., Wray, S., Adamson, G., Pittman, A., Renton, A. E., Traynor, B. J., Sweeney, M. G., Revesz, T., Houlden, H., Mead, S., Isaacs, A. M. and Fisher, E. M. C. (2015) 'Screening a UK amyotrophic lateral sclerosis cohort provides evidence of multiple origins of the C9orf72 expansion', *Neurobiology of Aging,* 36(1), pp. 546.e1-546.e7.

Freibaum, B. D., Lu, Y., Lopez-Gonzalez, R., Kim, N. C., Almeida, S., Lee, K.-H., Badders, N., Valentine, M., Miller, B. L., Wong, P. C., Petrucelli, L., Kim, H. J., Gao, F.-B. and Taylor, J. P. (2015) 'GGGGCC repeat expansion in C9orf72 compromises nucleocytoplasmic transport', *Nature,* 525(7567), pp. 129-133.

Freischmidt, A., Wieland, T., Richter, B., Ruf, W., Schaeffer, V., Müller, K., Marroquin, N., Nordin, F., Hübers, A., Weydt, P., Pinto, S., Press, R., Millecamps, S., Molko, N., Bernard, E., Desnuelle, C., Soriani, M.-H., Dorst, J., Graf, E., Nordström, U., Feiler, M. S., Putz, S., Boeckers, T. M., Meyer, T., Winkler, A. S., Winkelman, J., de Carvalho, M., Thal, D. R., Otto, M., Brännström, T., Volk, A. E., Kursula, P., Danzer, K. M., Lichtner, P., Dikic, I., Meitinger, T., Ludolph, A. C., Strom, T. M., Andersen, P. M. and Weishaupt, J. H. (2015) 'Haploinsufficiency of TBK1 causes familial ALS and fronto-temporal dementia', *Nature Neuroscience,* 18(5), pp. 631-636.

Frick, P., Sellier, C., Mackenzie, I. R. A., Cheng, C.-Y., Tahraoui-Bories, J., Martinat, C., Pasterkamp, R. J., Prudlo, J., Edbauer, D., Oulad-Abdelghani, M., Feederle, R., Charlet-Berguerand, N. and Neumann, M. (2018) 'Novel antibodies reveal presynaptic localization of C9orf72 protein and reduced protein levels in C9orf72 mutation carriers', *Acta Neuropathologica Communications,* 6(1), pp. 72.

Gao, Y., Lan, Y., Liu, H. and Jiang, R. (2011) 'The zinc finger transcription factors Osr1 and Osr2 control synovial joint formation', *Developmental Biology,* 352(1), pp. 83-91.

Gao, Y., Lan, Y., Ovitt, C. E. and Jiang, R. (2009) 'Functional equivalence of the zinc finger transcription factors Osr1 and Osr2 in mouse development', *Developmental Biology,* 328(2), pp. 200-209.

Garrido, D., Rubin, T., Poidevin, M., Maroni, B., Le Rouzic, A., Parvy, J.-P. and Montagne, J. (2015) 'Fatty Acid Synthase Cooperates with Glyoxalase 1 to Protect against Sugar Toxicity', *PLOS Genetics,* 11(2), pp. e1004995.

Gendron, T. F., Bieniek, K. F., Zhang, Y.-J., Jansen-West, K., Ash, P. E. A., Caulfield, T., Daughrity, L., Dunmore, J. H., Castanedes-Casey, M., Chew, J., Cosio, D. M., van Blitterswijk, M., Lee, W. C., Rademakers, R., Boylan, K. B., Dickson, D. W. and Petrucelli, L. (2013) 'Antisense transcripts of the expanded C9ORF72 hexanucleotide repeat form nuclear RNA foci and undergo repeat-

associated non-ATG translation in c9FTD/ALS', *Acta Neuropathologica,* 126(6), pp. 829-844.

Gendron, T. F., van Blitterswijk, M., Bieniek, K. F., Daughrity, L. M., Jiang, J., Rush, B. K., Pedraza, O., Lucas, J. A., Murray, M. E., Desaro, P., Robertson, A., Overstreet, K., Thomas, C. S., Crook, J. E., Castanedes-Casey, M., Rousseau, L., Josephs, K. A., Parisi, J. E., Knopman, D. S., Petersen, R. C., Boeve, B. F., Graff-Radford, N. R., Rademakers, R., Lagier-Tourenne, C., Edbauer, D., Cleveland, D. W., Dickson, D. W., Petrucelli, L. and Boylan, K. B. (2015) 'Cerebellar c9RAN proteins associate with clinical and neuropathological characteristics of C9ORF72 repeat expansion carriers', *Acta Neuropathologica,* 130(4), pp. 559-573.

Ghorasaini, M., Mohammed, Y., Adamski, J., Bettcher, L., Bowden, J. A., Cabruja, M., Contrepois, K., Ellenberger, M., Gajera, B., Haid, M., Hornburg, D., Hunter, C., Jones, C. M., Klein, T., Mayboroda, O., Mirzaian, M., Moaddel, R., Ferrucci, L., Lovett, J., Nazir, K., Pearson, M., Ubhi, B. K., Raftery, D., Riols, F., Sayers, R., Sijbrands, E. J. G., Snyder, M. P., Su, B., Velagapudi, V., Williams, K. J., de Rijke, Y. B. and Giera, M. (2021) 'Cross-Laboratory Standardization of Preclinical Lipidomics Using Differential Mobility Spectrometry and Multiple Reaction Monitoring', *Analytical Chemistry,* 93(49), pp. 16369-16378.

Ghorasaini, M., Tsezou, K. I., Verhoeven, A., Mohammed, Y., Vlachoyiannopoulos, P., Mikros, E. and Giera, M. (2022) 'Congruence and Complementarity of Differential Mobility Spectrometry and NMR Spectroscopy for Plasma Lipidomics', *Metabolites*, 12(11). DOI: 10.3390/metabo12111030.

Ghosh, A., Carnahan, J. and Greenberg, M. E. (1994) 'Requirement for BDNF in Activity-Dependent Survival of Cortical Neurons', *Science,* 263(5153), pp. 1618-1623.

Gijselinck, I., Van Langenhove, T., van der Zee, J., Sleegers, K., Philtjens, S., Kleinberger, G., Janssens, J., Bettens, K., Van Cauwenberghe, C., Pereson, S., Engelborghs, S., Sieben, A., De Jonghe, P., Vandenberghe, R., Santens, P., De

Bleecker, J., Maes, G., Bäumer, V., Dillen, L., Joris, G., Cuijt, I., Corsmit, E., Elinck, E., Van Dongen, J., Vermeulen, S., Van den Broeck, M., Vaerenberg, C., Mattheijssens, M., Peeters, K., Robberecht, W., Cras, P., Martin, J.-J., De Deyn, P. P., Cruts, M. and Van Broeckhoven, C. (2012) 'A C9orf72 promoter repeat expansion in a Flanders-Belgian cohort with disorders of the frontotemporal lobar degeneration-amyotrophic lateral sclerosis spectrum: a gene identification study', *The Lancet Neurology,* 11(1), pp. 54-65.

Gijselinck, I., Van Mossevelde, S., van der Zee, J., Sieben, A., Engelborghs, S., De Bleecker, J., Ivanoiu, A., Deryck, O., Edbauer, D., Zhang, M., Heeman, B., Bäumer, V., Van den Broeck, M., Mattheijssens, M., Peeters, K., Rogaeva, E., De Jonghe, P., Cras, P., Martin, J. J., de Deyn, P. P., Cruts, M., Van Broeckhoven, C. and on behalf of the, B. C. (2016) 'The C9orf72 repeat size correlates with onset age of disease, DNA methylation and transcriptional downregulation of the promoter', *Molecular Psychiatry,* 21(8), pp. 1112-1124.

Gijselinck, I., Van Mossevelde, S., van der Zee, J., Sieben, A., Philtjens, S., Heeman, B., Engelborghs, S., Vandenbulcke, M., De Baets, G., Bäumer, V., Cuijt, I., Van den Broeck, M., Peeters, K., Mattheijssens, M., Rousseau, F., Vandenberghe, R., De Jonghe, P., Cras, P., De Deyn, P. P., Martin, J.-J., Cruts, M. and Van Broeckhoven, C. (2015) 'Loss of TBK1 is a frequent cause of frontotemporal dementia in a Belgian cohort', *Neurology,* 85(24), pp. 2116-2125.

Goodman, L. D., Prudencio, M., Kramer, N. J., Martinez-Ramirez, L. F., Srinivasan, A. R., Lan, M., Parisi, M. J., Zhu, Y., Chew, J., Cook, C. N., Berson, A., Gitler, A. D., Petrucelli, L. and Bonini, N. M. (2019a) 'Toxic expanded GGGGCC repeat transcription is mediated by the PAF1 complex in C9orf72-associated FTD', *Nature Neuroscience,* 22(6), pp. 863-874.

Goodman, L. D., Prudencio, M., Srinivasan, A. R., Rifai, O. M., Lee, V. M. Y., Petrucelli, L. and Bonini, N. M. (2019b) 'eIF4B and eIF4H mediate GR production from expanded G4C2 in a Drosophila model for C9orf72-associated ALS', *Acta Neuropathologica Communications,* 7(1), pp. 62.

Green, R. B., Hatini, V., Johansen, K. A., Liu, X.-J. and Lengyel, J. A. (2002) 'Drumstick is a zinc finger protein that antagonizes Lines to control patterning and morphogenesis of the Drosophila hindgut', *Development,* 129(15), pp. 3645.

Greenberg, L. and Hatini, V. (2009) 'Essential roles for lines in mediating leg and antennal proximodistal patterning and generating a stable Notch signaling interface at segment borders', *Developmental biology,* 330(1), pp. 93-104.

Greka, A., Navarro, B., Oancea, E., Duggan, A. and Clapham, D. E. (2003) 'TRPC5 is a regulator of hippocampal neurite length and growth cone morphology', *Nature Neuroscience,* 6(8), pp. 837-845.

Griesi-Oliveira, K., Acab, A., Gupta, A. R., Sunaga, D. Y., Chailangkarn, T., Nicol, X., Nunez, Y., Walker, M. F., Murdoch, J. D., Sanders, S. J., Fernandez, T. V., Ji, W., Lifton, R. P., Vadasz, E., Dietrich, A., Pradhan, D., Song, H., Ming, G. l., Gu, X., Haddad, G., Marchetto, M. C. N., Spitzer, N., Passos-Bueno, M. R., State, M. W. and Muotri, A. R. (2015) 'Modeling non-syndromic autism and the impact of TRPC6 disruption in human neurons', *Molecular Psychiatry,* 20(11), pp. 1350-1365.

Guizy, M., Arias, C., David, M., González, T. and Valenzuela, C. (2005) 'ω-3 and ω-6 Polyunsaturated fatty acids block HERG channels', *American Journal of Physiology-Cell Physiology,* 289(5), pp. C1251-C1260.

Guttenplan, K. A., Weigel, M. K., Adler, D. I., Couthouis, J., Liddelow, S. A., Gitler, A. D. and Barres, B. A. (2020) 'Knockout of reactive astrocyte activating factors slows disease progression in an ALS mouse model', *Nature Communications,* 11(1), pp. 3753.

Guttenplan, K. A., Weigel, M. K., Prakash, P., Wijewardhane, P. R., Hasel, P., Rufen-Blanchette, U., Münch, A. E., Blum, J. A., Fine, J., Neal, M. C., Bruce, K. D., Gitler, A. D., Chopra, G., Liddelow, S. A. and Barres, B. A. (2021)

'Neurotoxic reactive astrocytes induce cell death via saturated lipids', *Nature,* 599(7883), pp. 102-107.

Haeusler, A. R., Donnelly, C. J., Periz, G., Simko, E. A. J., Shaw, P. G., Kim, M.-S., Maragakis, N. J., Troncoso, J. C., Pandey, A., Sattler, R., Rothstein, J. D. and Wang, J. (2014) 'C9orf72 nucleotide repeat structures initiate molecular cascades of disease', *Nature,* 507(7491), pp. 195-200.

Halbleib, K., Pesek, K., Covino, R., Hofbauer, H. F., Wunnicke, D., Hänelt, I., Hummer, G. and Ernst, R. (2017) 'Activation of the unfolded protein response by lipid bilayer stress', *Molecular cell,* 67(4), pp. 673-684. e8.

Hanrieder, J. and Ewing, A. G. (2014) 'Spatial Elucidation of Spinal Cord Lipid- and Metabolite- Regulations in Amyotrophic Lateral Sclerosis', *Scientific Reports,* 4(1), pp. 5266.

Hao, I., Green, R. B., Dunaevsky, O., Lengyel, J. A. and Rauskolb, C. (2003) 'The odd-skipped family of zinc finger genes promotes Drosophila leg segmentation', *Developmental Biology,* 263(2), pp. 282-295.

Harayama, T. and Riezman, H. (2018) 'Understanding the diversity of membrane lipid composition', *Nature Reviews Molecular Cell Biology,* 19(5), pp. 281-296.

Harayama, T. and Shimizu, T. (2020) 'Roles of polyunsaturated fatty acids, from mediators to membranes', *Journal of Lipid Research,* 61(8), pp. 1150-1160.

Hart, M. C., Wang, L. and Coulter, D. E. (1996) 'Comparison of the structure and expression of odd-skipped and two related genes that encode a new family of zinc finger proteins in Drosophila', *Genetics,* 144(1), pp. 171-182.

Hartmann, J., Dragicevic, E., Adelsberger, H., Henning, H. A., Sumser, M., Abramowitz, J., Blum, R., Dietrich, A., Freichel, M., Flockerzi, V., Birnbaumer, L. and Konnerth, A. (2008) 'TRPC3 Channels Are Required for Synaptic Transmission and Motor Coordination', *Neuron,* 59(3), pp. 392-398.

Hatini, V., Green, R. B., Lengyel, J. A., Bray, S. J. and Dinardo, S. (2005) 'The Drumstick/Lines/Bowl regulatory pathway links antagonistic Hedgehog and Wingless signaling inputs to epidermal cell differentiation', *Genes & development,* 19(6), pp. 709-718.

He, C., Qu, X., Cui, L., Wang, J. and Kang, J. X. (2009) 'Improved spatial learning performance of fat-1 mice is associated with enhanced neurogenesis and neuritogenesis by docosahexaenoic acid', *Proceedings of the National Academy of Sciences,* 106(27), pp. 11370-11375.

He, J., Fu, J., Zhao, W., Ren, C., Liu, P., Chen, L., Li, D., Tang, L., Zhou, L., Zhang, Y., Ma, X., Zhang, G., Li, N. and Fan, D. (2022) 'Hypermetabolism associated with worse prognosis of amyotrophic lateral sclerosis', *Journal of Neurology,* 269(3), pp. 1447-1455.

Hendricks, E., Quihuis, A. M., Hung, S.-T., Chang, J., Dorjsuren, N., Der, B., Staats, K. A., Shi, Y., Sta Maria, N. S., Jacobs, R. E. and Ichida, J. K. (2023) 'The C9ORF72 repeat expansion alters neurodevelopment', *Cell Reports,* 42(8), pp. 112983.

Hilgers, V., Perry, M. W., Hendrix, D., Stark, A., Levine, M. and Haley, B. (2011) 'Neural-specific elongation of 3′ UTRs during Drosophila development', *Proceedings of the National Academy of Sciences,* 108(38), pp. 15864-15869.

Hnisz, D., Abraham, Brian J., Lee, Tong I., Lau, A., Saint-André, V., Sigova, Alla A., Hoke, Heather A. and Young, Richard A. (2013) 'Super-Enhancers in the Control of Cell Identity and Disease', *Cell,* 155(4), pp. 934-947.

Holthuis, J. C. M. and Menon, A. K. (2014) 'Lipid landscapes and pipelines in membrane homeostasis', *Nature,* 510(7503), pp. 48-57.

Hong, C., Jeong, B., Park, H. J., Chung, J. Y., Lee, J. E., Kim, J., Shin, Y.-C. and So, I. (2020) 'TRP Channels as Emerging Therapeutic Targets for Neurodegenerative Diseases', *Frontiers in Physiology,* 11.

Hooijmans, C. R., Pasker-de Jong, P. C. M., de Vries, R. B. M. and Ritskes-Hoitinga, M. (2012) 'The Effects of Long-Term Omega-3 Fatty Acid Supplementation on Cognition and Alzheimer's Pathology in Animal Models of Alzheimer's Disease: A Systematic Review and Meta-Analysis', *Journal of Alzheimer's Disease,* 28, pp. 191-209.

Hornburg, D., Wu, S., Moqri, M., Zhou, X., Contrepois, K., Bararpour, N., Traber, G. M., Su, B., Metwally, A. A., Avina, M., Zhou, W., Ubellacker, J. M., Mishra, T., Schüssler-Fiorenza Rose, S. M., Kavathas, P. B., Williams, K. J. and Snyder, M. P. (2023) 'Dynamic lipidome alterations associated with human health, disease and ageing', *Nature Metabolism,* 5(9), pp. 1578-1594.

Hornemann, T. (2021) 'Mini review: Lipids in Peripheral Nerve Disorders', *Neuroscience Letters,* 740, pp. 135455.

Huang, J., Du, W., Yao, H. and Wang, Y. (2011) '10 TRPC Channels in Neuronal Survival', *TRP channels*, pp. 219.

Humphrey, J., Venkatesh, S., Hasan, R., Herb, J. T., de Paiva Lopes, K., Küçükali, F., Byrska-Bishop, M., Evani, U. S., Narzisi, G., Fagegaltier, D., Sleegers, K., Phatnani, H., Knowles, D. A., Fratta, P., Raj, T. and Consortium, N. A. (2023) 'Integrative transcriptomic analysis of the amyotrophic lateral sclerosis spinal cord implicates glial activation and suggests new risk genes', *Nature Neuroscience,* 26(1), pp. 150-162.

Hutten, S. and Dormann, D. (2020) 'Nucleocytoplasmic transport defects in neurodegeneration — Cause or consequence?', *Seminars in Cell & Developmental Biology,* 99, pp. 151-162.

Hutton, M., Lendon, C. L., Rizzu, P., Baker, M., Froelich, S., Houlden, H., Pickering-Brown, S., Chakraverty, S., Isaacs, A., Grover, A., Hackett, J., Adamson, J., Lincoln, S., Dickson, D., Davies, P., Petersen, R. C., Stevens, M., de Graaff, E., Wauters, E., van Baren, J., Hillebrand, M., Joosse, M., Kwon, J. M., Nowotny, P., Che, L. K., Norton, J., Morris, J. C., Reed, L. A., Trojanowski,

J., Basun, H., Lannfelt, L., Neystat, M., Fahn, S., Dark, F., Tannenberg, T., Dodd, P. R., Hayward, N., Kwok, J. B. J., Schofield, P. R., Andreadis, A., Snowden, J., Craufurd, D., Neary, D., Owen, F., Oostra, B. A., Hardy, J., Goate, A., van Swieten, J., Mann, D., Lynch, T. and Heutink, P. (1998) 'Association of missense and 5′-splice-site mutations in tau with the inherited dementia FTDP-17', *Nature,* 393(6686), pp. 702-705.

Ilieva, E. V., Ayala, V., Jové, M., Dalfó, E., Cacabelos, D., Povedano, M., Bellmunt, M. J., Ferrer, I., Pamplona, R. and Portero-Otín, M. (2007) 'Oxidative and endoplasmic reticulum stress interplay in sporadic amyotrophic lateral sclerosis', *Brain,* 130(12), pp. 3111-3123.

Iwaki, D. D., Johansen, K. A., Singer, J. B. and Lengyel, J. A. (2001) 'drumstick, bowl, and lines Are Required for Patterning and Cell Rearrangement in the Drosophila Embryonic Hindgut', *Developmental Biology,* 240(2), pp. 611-626.

Jeon, J., Bu, F., Sun, G., Tian, J.-B., Ting, S.-M., Li, J., Aronowski, J., Birnbaumer, L., Freichel, M. and Zhu, M. X. (2021) 'Contribution of TRPC Channels in Neuronal Excitotoxicity Associated With Neurodegenerative Disease and Ischemic Stroke', *Frontiers in Cell and Developmental Biology,* 8.

Jeyifous, O., Lin, E. I., Chen, X., Antinone, S. E., Mastro, R., Drisdel, R., Reese, T. S. and Green, W. N. (2016) 'Palmitoylation regulates glutamate receptor distributions in postsynaptic densities through control of PSD95 conformation and orientation', *Proceedings of the National Academy of Sciences,* 113(52), pp. E8482-E8491.

Jia, Y., Zhou, J., Tai, Y. and Wang, Y. (2007) 'TRPC channels promote cerebellar granule neuron survival', *Nature Neuroscience,* 10(5), pp. 559-567.

Johansen, K. A., Green, R. B., Iwaki, D. D., Hernandez, J. B. and Lengyel, J. A. (2003) 'The Drm–Bowl–Lin relief-of-repression hierarchy controls fore- and hindgut patterning and morphogenesis', *Mechanisms of Development,* 120(10), pp. 1139-1151.

Johnson, J. O., Mandrioli, J., Benatar, M., Abramzon, Y., Van Deerlin, V. M., Trojanowski, J. Q., Gibbs, J. R., Brunetti, M., Gronka, S., Wuu, J., Ding, J., McCluskey, L., Martinez-Lage, M., Falcone, D., Hernandez, D. G., Arepalli, S., Chong, S., Schymick, J. C., Rothstein, J., Landi, F., Wang, Y.-D., Calvo, A., Mora, G., Sabatelli, M., Monsurrò, M. R., Battistini, S., Salvi, F., Spataro, R., Sola, P., Borghero, G., Galassi, G., Scholz, S. W., Taylor, J. P., Restagno, G., Chiò, A. and Traynor, B. J. (2010) 'Exome Sequencing Reveals VCP Mutations as a Cause of Familial ALS', *Neuron,* 68(5), pp. 857-864.

Jésus, P., Fayemendy, P., Nicol, M., Lautrette, G., Sourisseau, H., Preux, P. M., Desport, J. C., Marin, B. and Couratier, P. (2018) 'Hypermetabolism is a deleterious prognostic factor in patients with amyotrophic lateral sclerosis', *European Journal of Neurology,* 25(1), pp. 97-104.

Jörs, S., Kazanski, V., Foik, A., Krautwurst, D. and Harteneck, C. (2006) 'Receptor-induced Activation of Drosophila TRPγ by Polyunsaturated Fatty Acids*', *Journal of Biological Chemistry,* 281(40), pp. 29693-29702.

Kabashi, E., Valdmanis, P. N., Dion, P., Spiegelman, D., McConkey, B. J., Velde, C. V., Bouchard, J.-P., Lacomblez, L., Pochigaeva, K., Salachas, F., Pradat, P.-F., Camu, W., Meininger, V., Dupre, N. and Rouleau, G. A. (2008) 'TARDBP mutations in individuals with sporadic and familial amyotrophic lateral sclerosis', *Nature Genetics,* 40(5), pp. 572-574.

Kang, J. X., Wang, J., Wu, L. and Kang, Z. B. (2004) 'Fat-1 mice convert n-6 to n-3 fatty acids', *Nature,* 427(6974), pp. 504-504.

Katoh, M. (2002) 'Molecular cloning and characterization of OSR1 on human chromosome 2p24', *Int J Mol Med,* 10(2), pp. 221-5.

Kawai, S., Kato, T., Inaba, H., Okahashi, N. and Amano, A. (2005) 'Odd-skipped related 2 splicing variants show opposite transcriptional activity', *Biochemical and Biophysical Research Communications,* 328(1), pp. 306-311.

Kawai, S., Yamauchi, M., Wakisaka, S., Ooshima, T. and Amano, A. (2007) 'Zinc-Finger Transcription Factor Odd-Skipped Related 2 Is One of the Regulators in Osteoblast Proliferation and Bone Formation', *Journal of Bone and Mineral Research,* 22(9), pp. 1362-1372.

Kiernan, M. C., Vucic, S., Cheah, B. C., Turner, M. R., Eisen, A., Hardiman, O., Burrell, J. R. and Zoing, M. C. (2011) 'Amyotrophic lateral sclerosis', *The Lancet,* 377(9769), pp. 942-955.

Kim, H. J. and Taylor, J. P. (2017) 'Lost in Transportation: Nucleocytoplasmic Transport Defects in ALS and Other Neurodegenerative Diseases', *Neuron,* 96(2), pp. 285-297.

Kivipelto, M., Ngandu, T., Fratiglioni, L., Viitanen, M., Kåreholt, I., Winblad, B., Helkala, E.-L., Tuomilehto, J., Soininen, H. and Nissinen, A. (2005) 'Obesity and Vascular Risk Factors at Midlife and the Risk of Dementia and Alzheimer Disease', *Archives of Neurology,* 62(10), pp. 1556-1560.

Knight, E. M., Verkhratsky, A., Luckman, S. M., Allan, S. M. and Lawrence, C. B. (2012) 'Hypermetabolism in a triple-transgenic mouse model of Alzheimer's disease', *Neurobiology of Aging,* 33(1), pp. 187-193.

Knobloch, M. and Mansuy, I. M. (2008) 'Dendritic Spine Loss and Synaptic Alterations in Alzheimer's Disease', *Molecular Neurobiology,* 37(1), pp. 73-82.

Kostic Dedic, S. I., Stevic, Z., Dedic, V., Stojanovic, V. R., Milicev, M. and Lavrnic, D. (2012) 'Is hyperlipidemia correlated with longer survival in patients with amyotrophic lateral sclerosis?', *Neurological Research,* 34(6), pp. 576-580.

Krogh, A., Larsson, B., von Heijne, G. and Sonnhammer, E. L. L. (2001) 'Predicting transmembrane protein topology with a hidden markov model: application to complete genomes11Edited by F. Cohen', *Journal of Molecular Biology,* 305(3), pp. 567-580.

Kuersten, S. and Goodwin, E. B. (2003) 'The power of the 3′ UTR: translational control and development', *Nature Reviews Genetics,* 4(8), pp. 626-637.

Kwiatkowski, T. J., Bosco, D. A., LeClerc, A. L., Tamrazian, E., Vanderburg, C. R., Russ, C., Davis, A., Gilchrist, J., Kasarskis, E. J., Munsat, T., Valdmanis, P., Rouleau, G. A., Hosler, B. A., Cortelli, P., de Jong, P. J., Yoshinaga, Y., Haines, J. L., Pericak-Vance, M. A., Yan, J., Ticozzi, N., Siddique, T., McKenna-Yasek, D., Sapp, P. C., Horvitz, H. R., Landers, J. E. and Brown, R. H. (2009) 'Mutations in the FUS/TLS Gene on Chromosome 16 Cause Familial Amyotrophic Lateral Sclerosis', *Science,* 323(5918), pp. 1205-1208.

Laddada, L., Jagla, K. and Soler, C. (2019) 'Odd-skipped and Stripe act downstream of Notch to promote the morphogenesis of long appendicular tendons in Drosophila', *Biology Open,* 8(3).

Lafourcade, M., Elezgarai, I., Mato, S., Bakiri, Y., Grandes, P. and Manzoni, O. (2007) *Molecular Components and Functions of the Endocannabinoid System in Mouse Prefrontal Cortex.*

Lafourcade, M., Larrieu, T., Mato, S., Duffaud, A., Sepers, M., Matias, I., De Smedt-Peyrusse, V., Labrousse, V. F., Bretillon, L., Matute, C., Rodríguez-Puertas, R., Layé, S. and Manzoni, O. J. (2011) 'Nutritional omega-3 deficiency abolishes endocannabinoid-mediated neuronal functions', *Nature Neuroscience,* 14(3), pp. 345-350.

Lagier-Tourenne, C., Baughn, M., Rigo, F., Sun, S., Liu, P., Li, H.-R., Jiang, J., Watt, A. T., Chun, S., Katz, M., Qiu, J., Sun, Y., Ling, S.-C., Zhu, Q., Polymenidou, M., Drenner, K., Artates, J. W., McAlonis-Downes, M., Markmiller, S., Hutt, K. R., Pizzo, D. P., Cady, J., Harms, M. B., Baloh, R. H., Vandenberg, S. R., Yeo, G. W., Fu, X.-D., Bennett, C. F., Cleveland, D. W. and Ravits, J. (2013) 'Targeted degradation of sense and antisense C9orf72 RNA foci as therapy for ALS and frontotemporal degeneration', *Proceedings of the National Academy of Sciences,* 110(47), pp. E4530-E4539.

Lagier-Tourenne, C., Polymenidou, M. and Cleveland, D. W. (2010) 'TDP-43 and FUS/TLS: emerging roles in RNA processing and neurodegeneration', *Human Molecular Genetics,* 19(R1), pp. R46-R64.

Lan, Y., Kingsley, P. D., Cho, E.-S. and Jiang, R. (2001) 'Osr2, a new mouse gene related to Drosophila odd-skipped, exhibits dynamic expression patterns during craniofacial, limb, and kidney development', *Mechanisms of Development,* 107(1), pp. 175-179.

Lan, Y., Ovitt, C. E., Cho, E. S., Maltby, K. M., Wang, Q. and Jiang, R. (2004) 'Odd-skipped related 2 (Osr2) encodes a key intrinsic regulator of secondary palate growth and morphogenesis', *Development,* 131(13), pp. 3207-16.

Larrieu, T., Madore, C., Joffre, C. and Layé, S. (2012) 'Nutritional n-3 polyunsaturated fatty acids deficiency alters cannabinoid receptor signaling pathway in the brain and associated anxiety-like behavior in mice', *Journal of Physiology and Biochemistry,* 68(4), pp. 671-681.

Latchman, D. S. (1997) 'Transcription factors: An overview', *The International Journal of Biochemistry & Cell Biology,* 29(12), pp. 1305-1312.

Latouche, M., Lasbleiz, C., Martin, E., Monnier, V., Debeir, T., Mouatt-Prigent, A., Muriel, M., Morel, L., Ruberg, M., Brice, A., Stevanin, G. and Tricoire, H. (2007) 'A Conditional Pan-Neuronal Drosophila Model of Spinocerebellar Ataxia 7 with a Reversible Adult Phenotype Suitable for Identifying Modifier Genes', *The Journal of Neuroscience,* 27(10), pp. 2483-2492.

Lee, H., Lee, J. J., Park, N. Y., Dubey, S. K., Kim, T., Ruan, K., Lim, S. B., Park, S.-H., Ha, S., Kovlyagina, I., Kim, K.-t., Kim, S., Oh, Y., Kim, H., Kang, S.-U., Song, M.-R., Lloyd, T. E., Maragakis, N. J., Hong, Y. B., Eoh, H. and Lee, G. (2021) 'Multi-omic analysis of selectively vulnerable motor neuron subtypes implicates altered lipid metabolism in ALS', *Nature Neuroscience*.

Lee, T. and Luo, L. (1999) 'Mosaic Analysis with a Repressible Cell Marker for Studies of Gene Function in Neuronal Morphogenesis', *Neuron,* 22(3), pp. 451-461.

Lee, Y.-B., Chen, H.-J., Peres, João N., Gomez-Deza, J., Attig, J., Štalekar, M., Troakes, C., Nishimura, Agnes L., Scotter, Emma L., Vance, C., Adachi, Y., Sardone, V., Miller, Jack W., Smith, Bradley N., Gallo, J.-M., Ule, J., Hirth, F., Rogelj, B., Houart, C. and Shaw, Christopher E. (2013) 'Hexanucleotide Repeats in ALS/FTD Form Length-Dependent RNA Foci, Sequester RNA Binding Proteins, and Are Neurotoxic', *Cell Reports,* 5(5), pp. 1178-1186.

Levental, I. and Lyman, E. (2023) 'Regulation of membrane protein structure and function by their lipid nano-environment', *Nature Reviews Molecular Cell Biology,* 24(2), pp. 107-122.

Levental, Kandice R., Lorent, Joseph H., Lin, X., Skinkle, Allison D., Surma, Michal A., Stockenbojer, Emily A., Gorfe, Alemayehu A. and Levental, I. (2016) 'Polyunsaturated Lipids Regulate Membrane Domain Stability by Tuning Membrane Order', *Biophysical Journal,* 110(8), pp. 1800-1810.

Levental, K. R., Malmberg, E., Symons, J. L., Fan, Y.-Y., Chapkin, R. S., Ernst, R. and Levental, I. (2020) 'Lipidomic and biophysical homeostasis of mammalian membranes counteracts dietary lipid perturbations to maintain cellular fitness', *Nature Communications,* 11(1), pp. 1339.

Levine, T. P., Daniels, R. D., Gatta, A. T., Wong, L. H. and Hayes, M. J. (2013) 'The product of C9orf72, a gene strongly implicated in neurodegeneration, is structurally related to DENN Rab-GEFs', *Bioinformatics,* 29(4), pp. 499-503.

Levy, P. and Larsen, C. (2013) 'Odd-skipped labels a group of distinct neurons associated with the mushroom body and optic lobe in the adult Drosophila brain', *Journal of Comparative Neurology,* 521(16), pp. 3716-3740.

Leyva-Díaz, E. and Hobert, O. (2019) 'Transcription factor autoregulation is required for acquisition and maintenance of neuronal identity', *Development,* 146(13), pp. dev177378.

Li, H., Handsaker, B., Wysoker, A., Fennell, T., Ruan, J., Homer, N., Marth, G., Abecasis, G., Durbin, R. and Genome Project Data Processing, S. (2009) 'The Sequence Alignment/Map format and SAMtools', *Bioinformatics (Oxford, England),* 25(16), pp. 2078-2079.

Li, J., Jaiswal, M. K., Chien, J.-F., Kozlenkov, A., Jung, J., Zhou, P., Gardashli, M., Pregent, L. J., Engelberg-Cook, E., Dickson, D. W., Belzil, V. V., Mukamel, E. A. and Dracheva, S. (2023) 'Divergent single cell transcriptome and epigenome alterations in ALS and FTD patients with C9orf72 mutation', *Nature Communications,* 14(1), pp. 5714.

Ling, S.-C., Polymenidou, M. and Cleveland, Don W. (2013) 'Converging Mechanisms in ALS and FTD: Disrupted RNA and Protein Homeostasis', *Neuron,* 79(3), pp. 416-438.

Lingwood, D. and Simons, K. (2010) 'Lipid Rafts As a Membrane-Organizing Principle', *Science,* 327(5961), pp. 46-50.

Liu, Y., Wang, T., Ji, Y. J., Johnson, K., Liu, H., Johnson, K., Bailey, S., Suk, Y., Lu, Y.-N., Liu, M. and Wang, J. (2018) 'A C9orf72-CARM1 axis regulates lipid metabolism under glucose starvation-induced nutrient stress', *Genes & development,* 32(21-22), pp. 1380-1397.

Lomen-Hoerth, C., Anderson, T. and Miller, B. (2002) 'The overlap of amyotrophic lateral sclerosis and frontotemporal dementia', *Neurology,* 59(7), pp. 1077-1079.

Lopez-Gonzalez, R., Yang, D., Pribadi, M., Kim, T. S., Krishnan, G., Choi, S. Y., Lee, S., Coppola, G. and Gao, F.-B. (2019) 'Partial inhibition of the overactivated Ku80-dependent DNA repair pathway rescues neurodegeneration

in C9ORF72-ALS/FTD', *Proceedings of the National Academy of Sciences,* 116(19), pp. 9628-9633.

Love, M. I., Huber, W. and Anders, S. (2014) 'Moderated estimation of fold change and dispersion for RNA-seq data with DESeq2', *Genome Biology,* 15(12), pp. 550.

Lu, T., Aron, L., Zullo, J., Pan, Y., Kim, H., Chen, Y., Yang, T.-H., Kim, H.-M., Drake, D., Liu, X. S., Bennett, D. A., Colaiácovo, M. P. and Yankner, B. A. (2014) 'REST and stress resistance in ageing and Alzheimer's disease', *Nature,* 507(7493), pp. 448-454.

Ludolph, A. C., Dorst, J., Dreyhaupt, J., Weishaupt, J. H., Kassubek, J., Weiland, U., Meyer, T., Petri, S., Hermann, A., Emmer, A., Grosskreutz, J., Grehl, T., Zeller, D., Boentert, M., Schrank, B., Prudlo, J., Winkler, A. S., Gorbulev, S., Roselli, F., Schuster, J., Dupuis, L. and for the, L.-A. L. S. S. G. (2020) 'Effect of High-Caloric Nutrition on Survival in Amyotrophic Lateral Sclerosis', *Annals of Neurology,* 87(2), pp. 206-216.

Lynn, Y. S., Letzel, A., Somerfield, C. B. H., Kyser, K., Lin, E. L., Roper, A., Yuan, Y., Saunders, C., Farag, M., Colourous, S. and Larsen, C. (2020) 'Odd-skipped controls neurite morphology and affect cell survival in Drosophila Melanogaster CNS', *bioRxiv*.

Mackenzie, I. R., Arzberger, T., Kremmer, E., Troost, D., Lorenzl, S., Mori, K., Weng, S.-M., Haass, C., Kretzschmar, H. A., Edbauer, D. and Neumann, M. (2013) 'Dipeptide repeat protein pathology in C9ORF72 mutation cases: clinico-pathological correlations', *Acta Neuropathologica,* 126(6), pp. 859-879.

Mackenzie, I. R. A., Frick, P., Grässer, F. A., Gendron, T. F., Petrucelli, L., Cashman, N. R., Edbauer, D., Kremmer, E., Prudlo, J., Troost, D. and Neumann, M. (2015) 'Quantitative analysis and clinico-pathological correlations of different dipeptide repeat protein pathologies in C9ORF72 mutation carriers', *Acta Neuropathologica,* 130(6), pp. 845-861.

Mackenzie, I. R. A., Neumann, M., Baborie, A., Sampathu, D. M., Du Plessis, D., Jaros, E., Perry, R. H., Trojanowski, J. Q., Mann, D. M. A. and Lee, V. M. Y. (2011) 'A harmonized classification system for FTLD-TDP pathology', *Acta Neuropathologica,* 122(1), pp. 111-113.

Mackenzie, I. R. A., Rademakers, R. and Neumann, M. (2010) 'TDP-43 and FUS in amyotrophic lateral sclerosis and frontotemporal dementia', *The Lancet Neurology,* 9(10), pp. 995-1007.

Majounie, E., Renton, A. E., Mok, K., Dopper, E. G. P., Waite, A., Rollinson, S., Chiò, A., Restagno, G., Nicolaou, N., Simon-Sanchez, J., van Swieten, J. C., Abramzon, Y., Johnson, J. O., Sendtner, M., Pamphlett, R., Orrell, R. W., Mead, S., Sidle, K. C., Houlden, H., Rohrer, J. D., Morrison, K. E., Pall, H., Talbot, K., Ansorge, O., Hernandez, D. G., Arepalli, S., Sabatelli, M., Mora, G., Corbo, M., Giannini, F., Calvo, A., Englund, E., Borghero, G., Floris, G. L., Remes, A. M., Laaksovirta, H., McCluskey, L., Trojanowski, J. Q., Van Deerlin, V. M., Schellenberg, G. D., Nalls, M. A., Drory, V. E., Lu, C.-S., Yeh, T.-H., Ishiura, H., Takahashi, Y., Tsuji, S., Le Ber, I., Brice, A., Drepper, C., Williams, N., Kirby, J., Shaw, P., Hardy, J., Tienari, P. J., Heutink, P., Morris, H. R., Pickering-Brown, S. and Traynor, B. J. (2012) 'Frequency of the C9orf72 hexanucleotide repeat expansion in patients with amyotrophic lateral sclerosis and frontotemporal dementia: a cross-sectional study', *The Lancet Neurology,* 11(4), pp. 323-330.

Mann, D. M. A., Rollinson, S., Robinson, A., Bennion Callister, J., Thompson, J. C., Snowden, J. S., Gendron, T., Petrucelli, L., Masuda-Suzukake, M., Hasegawa, M., Davidson, Y. and Pickering-Brown, S. (2013) 'Dipeptide repeat proteins are present in the p62 positive inclusions in patients with frontotemporal lobar degeneration and motor neurone disease associated with expansions in C9ORF72', *Acta Neuropathologica Communications,* 1(1), pp. 68.

Maor-Nof, M., Shipony, Z., Lopez-Gonzalez, R., Nakayama, L., Zhang, Y.-J., Couthouis, J., Blum, J. A., Castruita, P. A., Linares, G. R., Ruan, K., Ramaswami, G., Simon, D. J., Nof, A., Santana, M., Han, K., Sinnott-Armstrong, N., Bassik, M. C., Geschwind, D. H., Tessier-Lavigne, M., Attardi, L.

D., Lloyd, T. E., Ichida, J. K., Gao, F.-B., Greenleaf, W. J., Yokoyama, J. S., Petrucelli, L. and Gitler, A. D. (2021) 'p53 is a central regulator driving neurodegeneration caused by C9orf72 poly(PR)', *Cell,* 184(3), pp. 689-708.e20.

Mariosa, D., Hammar, N., Malmström, H., Ingre, C., Jungner, I., Ye, W., Fang, F. and Walldius, G. (2017) 'Blood biomarkers of carbohydrate, lipid, and apolipoprotein metabolisms and risk of amyotrophic lateral sclerosis: A more than 20-year follow-up of the Swedish AMORIS cohort', *Annals of Neurology,* 81(5), pp. 718-728.

Markstein, M., Pitsouli, C., Villalta, C., Celniker, S. E. and Perrimon, N. (2008) 'Exploiting position effects and the gypsy retrovirus insulator to engineer precisely expressed transgenes', *Nature Genetics,* 40(4), pp. 476-483.

Maruyama, H., Morino, H., Ito, H., Izumi, Y., Kato, H., Watanabe, Y., Kinoshita, Y., Kamada, M., Nodera, H., Suzuki, H., Komure, O., Matsuura, S., Kobatake, K., Morimoto, N., Abe, K., Suzuki, N., Aoki, M., Kawata, A., Hirai, T., Kato, T., Ogasawara, K., Hirano, A., Takumi, T., Kusaka, H., Hagiwara, K., Kaji, R. and Kawakami, H. (2010) 'Mutations of optineurin in amyotrophic lateral sclerosis', *Nature,* 465(7295), pp. 223-226.

Marza, E., Long, T., Saiardi, A., Sumakovic, M., Eimer, S., Hall, D. H. and Lesa, G. M. (2007) 'Polyunsaturated Fatty Acids Influence Synaptojanin Localization to Regulate Synaptic Vesicle Recycling', *Molecular Biology of the Cell,* 19(3), pp. 833-842.

Masrori, P. and Van Damme, P. (2020) 'Amyotrophic lateral sclerosis: a clinical review', *European Journal of Neurology,* 27(10), pp. 1918-1929.

Mayr, C. (2019) 'What are 3′ UTRs doing?', *Cold Spring Harbor perspectives in biology,* 11(10), pp. a034728.

Mead, R. J., Shan, N., Reiser, H. J., Marshall, F. and Shaw, P. J. (2023) 'Amyotrophic lateral sclerosis: a neurodegenerative disorder poised for

successful therapeutic translation', *Nature Reviews Drug Discovery,* 22(3), pp. 185-212.

Mehta, A. R., Gregory, J. M., Dando, O., Carter, R. N., Burr, K., Nanda, J., Story, D., McDade, K., Smith, C., Morton, N. M., Mahad, D. J., Hardingham, G. E., Chandran, S. and Selvaraj, B. T. (2021) 'Mitochondrial bioenergetic deficits in C9orf72 amyotrophic lateral sclerosis motor neurons cause dysfunctional axonal homeostasis', *Acta Neuropathologica*.

Mehta, A. R., Selvaraj, B. T., Barton, S. K., McDade, K., Abrahams, S., Chandran, S., Smith, C. and Gregory, J. M. (2020) 'Improved detection of RNA foci in C9orf72 amyotrophic lateral sclerosis post-mortem tissue using BaseScope™ shows a lack of association with cognitive dysfunction', *Brain Communications,* 2(1), pp. fcaa009.

Meng, X., Brodsky, M. H. and Wolfe, S. A. (2005) 'A bacterial one-hybrid system for determining the DNA-binding specificity of transcription factors', *Nature Biotechnology,* 23(8), pp. 988-994.

Miana-Mena, F. J., Piedrafita, E., González-Mingot, C., Larrodé, P., Muñoz, M. J., Martínez-Ballarín, E., Reiter, R. J., Osta, R. and García, J. J. (2011) 'Levels of membrane fluidity in the spinal cord and the brain in an animal model of amyotrophic lateral sclerosis', *Journal of Bioenergetics and Biomembranes,* 43(2), pp. 181.

Miller, R. G., Mitchell, J. D. and Moore, D. H. (2012) 'Riluzole for amyotrophic lateral sclerosis (ALS)/motor neuron disease (MND)', *Cochrane Database of Systematic Reviews,* (3).

Miura, P., Shenker, S., Andreu-Agullo, C., Westholm, J. O. and Lai, E. C. (2013) 'Widespread and extensive lengthening of 3′ UTRs in the mammalian brain', *Genome research,* 23(5), pp. 812-825.

Mizielinska, S., Grönke, S., Niccoli, T., Ridler, C. E., Clayton, E. L., Devoy, A., Moens, T., Norona, F. E., Woollacott, I. O. C., Pietrzyk, J., Cleverley, K., Nicoll, A. J., Pickering-Brown, S., Dols, J., Cabecinha, M., Hendrich, O., Fratta, P., Fisher, E. M. C., Partridge, L. and Isaacs, A. M. (2014) 'C9orf72 repeat expansions cause neurodegeneration in Drosophila through arginine-rich proteins', *Science (New York, N.Y.),* 345(6201), pp. 1192-1194.

Mizielinska, S., Lashley, T., Norona, F. E., Clayton, E. L., Ridler, C. E., Fratta, P. and Isaacs, A. M. (2013) 'C9orf72 frontotemporal lobar degeneration is characterised by frequent neuronal sense and antisense RNA foci', *Acta Neuropathologica,* 126(6), pp. 845-857.

Mochel, F., Charles, P., Seguin, F., Barritault, J., Coussieu, C., Perin, L., Le Bouc, Y., Gervais, C., Carcelain, G., Vassault, A., Feingold, J., Rabier, D. and Durr, A. (2007) 'Early Energy Deficit in Huntington Disease: Identification of a Plasma Biomarker Traceable during Disease Progression', *PLOS ONE,* 2(7), pp. e647.

Moens, T. G., Mizielinska, S., Niccoli, T., Mitchell, J. S., Thoeng, A., Ridler, C. E., Grönke, S., Esser, J., Heslegrave, A., Zetterberg, H., Partridge, L. and Isaacs, A. M. (2018) 'Sense and antisense RNA are not toxic in Drosophila models of C9orf72-associated ALS/FTD', *Acta Neuropathologica,* 135(3), pp. 445-457.

Moens, T. G., Partridge, L. and Isaacs, A. M. (2017) 'Genetic models of C9orf72: what is toxic?', *Current Opinion in Genetics & Development,* 44, pp. 92-101.

Moraru, A., Cakan-Akdogan, G., Strassburger, K., Males, M., Mueller, S., Jabs, M., Muelleder, M., Frejno, M., Braeckman, B. P., Ralser, M. and Teleman, A. A. (2017) 'THADA Regulates the Organismal Balance between Energy Storage and Heat Production', *Developmental Cell,* 41(1), pp. 72-81.e6.

Moreno, C., Macias, A., Prieto, A., De La Cruz, A. and Valenzuela, C. (2012) 'Polyunsaturated fatty acids modify the gating of Kv channels', *Frontiers in Pharmacology,* 3, pp. 163.

Mori, A., Hatano, T., Inoshita, T., Shiba-Fukushima, K., Koinuma, T., Meng, H., Kubo, S.-i., Spratt, S., Cui, C., Yamashita, C., Miki, Y., Yamamoto, K., Hirabayashi, T., Murakami, M., Takahashi, Y., Shindou, H., Nonaka, T., Hasegawa, M., Okuzumi, A., Imai, Y. and Hattori, N. (2019) 'Parkinson's disease-associated iPLA2-VIA/PLA2G6 regulates neuronal functions and α-synuclein stability through membrane remodeling', *Proceedings of the National Academy of Sciences,* 116(41), pp. 20689-20699.

Mori, K., Weng, S.-M., Arzberger, T., May, S., Rentzsch, K., Kremmer, E., Schmid, B., Kretzschmar, H. A., Cruts, M., Van Broeckhoven, C., Haass, C. and Edbauer, D. (2013) 'The C9orf72 GGGGCC Repeat Is Translated into Aggregating Dipeptide-Repeat Proteins in FTLD/ALS', *Science,* 339(6125), pp. 1335-1338.

Murphy, R. C. (2018) 'Challenges in mass spectrometry-based lipidomics of neutral lipids', *TrAC Trends in Analytical Chemistry,* 107, pp. 91-98.

Nagai, M., Re, D. B., Nagata, T., Chalazonitis, A., Jessell, T. M., Wichterle, H. and Przedborski, S. (2007) 'Astrocytes expressing ALS-linked mutated SOD1 release factors selectively toxic to motor neurons', *Nature Neuroscience,* 10(5), pp. 615-622.

Narayanan, K. L., Irmady, K., Subramaniam, S., Unsicker, K. and von Bohlen und Halbach, O. (2008) 'Evidence that TRPC1 is involved in hippocampal glutamate-induced cell death', *Neuroscience Letters,* 446(2), pp. 117-122.

Nativio, R., Donahue, G., Berson, A., Lan, Y., Amlie-Wolf, A., Tuzer, F., Toledo, J. B., Gosai, S. J., Gregory, B. D., Torres, C., Trojanowski, J. Q., Wang, L.-S., Johnson, F. B., Bonini, N. M. and Berger, S. L. (2018) 'Dysregulation of the

epigenetic landscape of normal aging in Alzheimer's disease', *Nature Neuroscience,* 21(4), pp. 497-505.

Neumann, M., Rademakers, R., Roeber, S., Baker, M., Kretzschmar, H. A. and Mackenzie, I. R. A. (2009) 'A new subtype of frontotemporal lobar degeneration with FUS pathology', *Brain,* 132(11), pp. 2922-2931.

Neumann, M., Sampathu, D. M., Kwong, L. K., Truax, A. C., Micsenyi, M. C., Chou, T. T., Bruce, J., Schuck, T., Grossman, M., Clark, C. M., McCluskey, L. F., Miller, B. L., Masliah, E., Mackenzie, I. R., Feldman, H., Feiden, W., Kretzschmar, H. A., Trojanowski, J. Q. and Lee, V. M.-Y. (2006) 'Ubiquitinated TDP-43 in Frontotemporal Lobar Degeneration and Amyotrophic Lateral Sclerosis', *Science,* 314(5796), pp. 130-133.

Nicolas, A. and Kenna, K. P. and Renton, A. E. and Ticozzi, N. and Faghri, F. and Chia, R. and Dominov, J. A. and Kenna, B. J. and Nalls, M. A. and Keagle, P. and Rivera, A. M. and van Rheenen, W. and Murphy, N. A. and van Vugt, J. J. F. A. and Geiger, J. T. and Van der Spek, R. A. and Pliner, H. A. and Shankaracharya and Smith, B. N. and Marangi, G. and Topp, S. D. and Abramzon, Y. and Gkazi, A. S. and Eicher, J. D. and Kenna, A. and Logullo, F. O. and Simone, I. and Logroscino, G. and Salvi, F. and Bartolomei, I. and Borghero, G. and Murru, M. R. and Costantino, E. and Pani, C. and Puddu, R. and Caredda, C. and Piras, V. and Tranquilli, S. and Cuccu, S. and Corongiu, D. and Melis, M. and Milia, A. and Marrosu, F. and Marrosu, M. G. and Floris, G. and Cannas, A. and Capasso, M. and Caponnetto, C. and Mancardi, G. and Origone, P. and Mandich, P. and Conforti, F. L. and Cavallaro, S. and Mora, G. and Marinou, K. and Sideri, R. and Penco, S. and Mosca, L. and Lunetta, C. and Pinter, G. L. and Corbo, M. and Riva, N. and Carrera, P. and Volanti, P. and Mandrioli, J. and Fini, N. and Fasano, A. and Tremolizzo, L. and Arosio, A. and Ferrarese, C. and Trojsi, F. and Tedeschi, G. and Monsurrò, M. R. and Piccirillo, G. and Femiano, C. and Ticca, A. and Ortu, E. and La Bella, V. and Spataro, R. and Colletti, T. and Sabatelli, M. and Zollino, M. and Conte, A. and Luigetti, M. and Lattante, S. and Santarelli, M. and Petrucci, A. and Pugliatti, M. and Pirisi, A. and Parish, L. D. and Occhineri, P. and Giannini, F. and Battistini,

S. and Ricci, C. and Benigni, M. and Cau, T. B. and Loi, D. and Calvo, A. and Moglia, C. and Brunetti, M. and Barberis, M. and Restagno, G. and Casale, F. and Marrali, G. and Fuda, G. and Ossola, I. and Cammarosano, S. and Canosa, A. and Ilardi, A. and Manera, U. and Grassano, M. and Tanel, R. and Pisano, F. and Mazzini, L. and Messina, S. and Simone, I. L. and D'Alfonso, S. and Corrado, L. and Ferrucci, L. and Harms, M. B. and Goldstein, D. B. and Shneider, N. A. and Goutman, S. and Simmons, Z. and Miller, T. M. and Chandran, S. and Pal, S. and Manousakis, G. and Appel, S. H. and Simpson, E. and Wang, L. and Baloh, R. H. and Gibson, S. and Bedlack, R. and Lacomis, D. and Sareen, D. and Sherman, A. and Bruijn, L. and Penny, M. and Moreno, C. d. A. M. and Kamalakaran, S. and Allen, A. S. and Appel, S. and Bedlack, R. S. and Boone, B. E. and Brown, R. and Carulli, J. P. and Chesi, A. and Chung, W. K. and Cirulli, E. T. and Cooper, G. M. and Couthouis, J. and Day-Williams, A. G. and Dion, P. A. and Gitler, A. D. and Glass, J. D. and Han, Y. and Harris, T. and Hayes, S. D. and Jones, A. L. and Keebler, J. and Krueger, B. J. and Lasseigne, B. N. and Levy, S. E. and Lu, Y.-F. and Maniatis, T. and McKenna-Yasek, D. and Myers, R. M. and Petrovski, S. and Pulst, S. M. and Raphael, A. R. and Ravits, J. M. and Ren, Z. and Rouleau, G. A. and Sapp, P. C. and Sims, K. B. and Staropoli, J. F. and Waite, L. L. and Wang, Q. and Wimbish, J. R. and Xin, W. W. and Phatnani, H. and Kwan, J. and Broach, J. R. and Arcila-Londono, X. and Lee, E. B. and Van Deerlin, V. M. and Fraenkel, E. and Ostrow, L. W. and Baas, F. and Zaitlen, N. and Berry, J. D. and Malaspina, A. and Fratta, P. and Cox, G. A. and Thompson, L. M. and Finkbeiner, S. and Dardiotis, E. and Hornstein, E. and MacGowan, D. J. and Heiman-Patterson, T. and Hammell, M. G. and Patsopoulos, N. A. and Dubnau, J. and Nath, A. and Musunuri, R. L. and Evani, U. S. and Abhyankar, A. and Zody, M. C. and Kaye, J. and Finkbeiner, S. and Wyman, S. and LeNail, A. and Lima, L. and Rothstein, J. D. and Svendsen, C. N. and Van Eyk, J. and Maragakis, N. J. and Kolb, S. J. and Cudkowicz, M. and Baxi, E. and Wyman, S. K. and LeNail, A. and Van Eyk, J. E. and Benatar, M. and Taylor, J. P. and Wu, G. and Rampersaud, E. and Wuu, J. and Rademakers, R. and Züchner, S. and Schule, R. and McCauley, J. and Hussain, S. and Cooley, A. and Wallace, M. and Clayman, C. and Barohn, R. and Statland, J. and Ravits, J. and Swenson, A. and Jackson, C. and Trivedi, J. and Khan, S. and Katz, J. and Jenkins, L. and Burns, T. and Gwathmey, K.

and Caress, J. and McMillan, C. and Elman, L. and Pioro, E. and Heckmann, J. and So, Y. and Walk, D. and Maiser, S. and Zhang, J. and Silani, V. and Gellera, C. and Ratti, A. and Taroni, F. and Lauria, G. and Verde, F. and Fogh, I. and Tiloca, C. and Comi, G. P. and Sorarù, G. and Cereda, C. and De Marchi, F. and Corti, S. and Ceroni, M. and Siciliano, G. and Filosto, M. and Inghilleri, M. and Peverelli, S. and Colombrita, C. and Poletti, B. and Maderna, L. and Del Bo, R. and Gagliardi, S. and Querin, G. and Bertolin, C. and Pensato, V. and Castellotti, B. and Camu, W. and Mouzat, K. and Lumbroso, S. and Corcia, P. and Meininger, V. and Besson, G. and Lagrange, E. and Clavelou, P. and Guy, N. and Couratier, P. and Vourch, P. and Danel, V. and Bernard, E. and Lemasson, G. and Laaksovirta, H. and Myllykangas, L. and Jansson, L. and Valori, M. and Ealing, J. and Hamdalla, H. and Rollinson, S. and Pickering-Brown, S. and Orrell, R. W. and Sidle, K. C. and Hardy, J. and Singleton, A. B. and Johnson, J. O. and Arepalli, S. and Polak, M. and Asress, S. and Al-Sarraj, S. and King, A. and Troakes, C. and Vance, C. and de Belleroche, J. and ten Asbroek, A. L. M. A. and Muñoz-Blanco, J. L. and Hernandez, D. G. and Ding, J. and Gibbs, J. R. and Scholz, S. W. and Floeter, M. K. and Campbell, R. H. and Landi, F. and Bowser, R. and MacGowan, D. J. L. and Kirby, J. and Pioro, E. P. and Pamphlett, R. and Broach, J. and Gerhard, G. and Dunckley, T. L. and Brady, C. B. and Kowall, N. W. and Troncoso, J. C. and Le Ber, I. and Heiman-Patterson, T. D. and Kamel, F. and Van Den Bosch, L. and Strom, T. M. and Meitinger, T. and Shatunov, A. and Van Eijk, K. R. and de Carvalho, M. and Kooyman, M. and Middelkoop, B. and Moisse, M. and McLaughlin, R. L. and Van Es, M. A. and Weber, M. and Boylan, K. B. and Van Blitterswijk, M. and Morrison, K. E. and Basak, A. N. and Mora, J. S. and Drory, V. E. and Shaw, P. J. and Turner, M. R. and Talbot, K. and Hardiman, O. and Williams, K. L. and Fifita, J. A. and Nicholson, G. A. and Blair, I. P. and Esteban-Pérez, J. and García-Redondo, A. and Al-Chalabi, A. and Al Kheifat, A. and Andersen, P. and Chio, A. and Cooper-Knock, J. and Dekker, A. and Drory, V. and Redondo, A. G. and Gotkine, M. and Hide, W. and Iacoangeli, A. and Glass, J. and Kenna, K. and Kiernan, M. and Landers, J. and McLaughlin, R. and Mill, J. and Neto, M. M. and Moisse, M. and Pardina, J. M. and Morrison, K. and Newhouse, S. and Pinto, S. and Pulit, S. and Robberecht, W. and Shaw, P. and Shaw, C. and Sproviero, W. and Tazelaar, G. and van Damme, P. and van den

Berg, L. and van der Spek, R. and van Eijk, K. and van Es, M. and van Vugt, J. and Veldink, J. and Zatz, M. and Bauer, D. C. and Twine, N. A. and Rogaeva, E. and Zinman, L. and Cooper-Knock, J. and Brice, A. and Goutman, S. A. and Feldman, E. L. and Gibson, S. B. and Van Damme, P. and Ludolph, A. C. and Andersen, P. M. and Weishaupt, J. H. and Trojanowski, J. Q. and Brown, R. H., Jr. and van den Berg, L. H. and Veldink, J. H. and Stone, D. J. and Tienari, P. and Chiò, A. and Shaw, C. E. and Traynor, B. J. and Landers, J. E. (2018) 'Genome-wide Analyses Identify KIF5A as a Novel ALS Gene', *Neuron,* 97(6), pp. 1268-1283.e6.

Nordin, A., Akimoto, C., Wuolikainen, A., Alstermark, H., Jonsson, P., Birve, A., Marklund, S. L., Graffmo, K. S., Forsberg, K., Brännström, T. and Andersen, P. M. (2015) 'Extensive size variability of the GGGGCC expansion in C9orf72 in both neuronal and non-neuronal tissues in 18 patients with ALS or FTD', *Human Molecular Genetics,* 24(11), pp. 3133-3142.

Nott, A., Holtman, I. R., Coufal, N. G., Schlachetzki, J. C. M., Yu, M., Hu, R., Han, C. Z., Pena, M., Xiao, J., Wu, Y., Keulen, Z., Pasillas, M. P., O'Connor, C., Nickl, C. K., Schafer, S. T., Shen, Z., Rissman, R. A., Brewer, J. B., Gosselin, D., Gonda, D. D., Levy, M. L., Rosenfeld, M. G., McVicker, G., Gage, F. H., Ren, B. and Glass, C. K. (2019) 'Brain cell type–specific enhancer–promoter interactome maps and disease-risk association', *Science,* 366(6469), pp. 1134-1139.

Noyes, M. B., Meng, X., Wakabayashi, A., Sinha, S., Brodsky, M. H. and Wolfe, S. A. (2008) 'A systematic characterization of factors that regulate Drosophila segmentation via a bacterial one-hybrid system', *Nucleic Acids Research,* 36(8), pp. 2547-2560.

Nusinow, D., Greenberg, L. and Hatini, V. (2008) 'Reciprocal roles for bowl and lines in specifying the peripodial epithelium and the disc proper of the Drosophila wing primordium', *Development (Cambridge, England),* 135(18), pp. 3031-3041.

Nüsslein-Volhard, C. and Wieschaus, E. (1980) 'Mutations affecting segment number and polarity in Drosophila', *Nature,* 287(5785), pp. 795-801.

Okamoto, K., Kihira, T., Kondo, T., Kobashi, G., Washio, M., Sasaki, S., Yokoyama, T., Miyake, Y., Sakamoto, N., Inaba, Y. and Nagai, M. (2007) 'Nutritional status and risk of amyotrophic lateral sclerosis in Japan', *Amyotrophic Lateral Sclerosis,* 8(5), pp. 300-304.

Orr, S. K., Palumbo, S., Bosetti, F., Mount, H. T., Kang, J. X., Greenwood, C. E., Ma, D. W. L., Serhan, C. N. and Bazinet, R. P. (2013) 'Unesterified docosahexaenoic acid is protective in neuroinflammation', *Journal of Neurochemistry,* 127(3), pp. 378-393.

Osterwalder, T., Yoon, K. S., White, B. H. and Keshishian, H. (2001) 'A conditional tissue-specific transgene expression system using inducible GAL4', *Proceedings of the National Academy of Sciences,* 98(22), pp. 12596.

Otani, K., Dong, Y., Li, X., Lu, J., Zhang, N., Xu, L., Go, M. Y. Y., Ng, E. K. W., Arakawa, T., Chan, F. K. L., Sung, J. J. Y. and Yu, J. (2014) 'Odd-skipped related 1 is a novel tumour suppressor gene and a potential prognostic biomarker in gastric cancer', *The Journal of pathology,* 234(3), pp. 302-315.

Overington, J. P., Al-Lazikani, B. and Hopkins, A. L. (2006) 'How many drug targets are there?', *Nature Reviews Drug Discovery,* 5(12), pp. 993-996.

O'Rourke, J. G., Bogdanik, L., Yáñez, A., Lall, D., Wolf, A. J., Muhammad, A. K. M. G., Ho, R., Carmona, S., Vit, J. P., Zarrow, J., Kim, K. J., Bell, S., Harms, M. B., Miller, T. M., Dangler, C. A., Underhill, D. M., Goodridge, H. S., Lutz, C. M. and Baloh, R. H. (2016) 'C9orf72 is required for proper macrophage and microglial function in mice', *Science,* 351(6279), pp. 1324-1329.

Paganoni, S., Deng, J., Jaffa, M., Cudkowicz, M. E. and Wills, A.-M. (2011) 'Body mass index, not dyslipidemia, is an independent predictor of survival in amyotrophic lateral sclerosis', *Muscle & Nerve,* 44(1), pp. 20-24.

Palacios-Muñoz, A., de Paula Moreira, D., Silva, V., García, I. E., Aboitiz, F., Zarrei, M., Campos, G., Rennie, O., Howe, J. L., Anagnostou, E., Ambrozewic, P., Scherer, S. W., Passos-Bueno, M. R. and Ewer, J. (2022) 'Mutations in trpγ, the homologue of TRPC6 autism candidate gene, causes autism-like behavioral deficits in Drosophila', *Molecular Psychiatry,* 27(8), pp. 3328-3342.

Pantazis, C. B., Yang, A., Lara, E., McDonough, J. A., Blauwendraat, C., Peng, L., Oguro, H., Kanaujiya, J., Zou, J., Sebesta, D., Pratt, G., Cross, E., Blockwick, J., Buxton, P., Kinner-Bibeau, L., Medura, C., Tompkins, C., Hughes, S., Santiana, M., Faghri, F., Nalls, M. A., Vitale, D., Ballard, S., Qi, Y. A., Ramos, D. M., Anderson, K. M., Stadler, J., Narayan, P., Papademetriou, J., Reilly, L., Nelson, M. P., Aggarwal, S., Rosen, L. U., Kirwan, P., Pisupati, V., Coon, S. L., Scholz, S. W., Priebe, T., Öttl, M., Dong, J., Meijer, M., Janssen, L. J. M., Lourenco, V. S., van der Kant, R., Crusius, D., Paquet, D., Raulin, A.-C., Bu, G., Held, A., Wainger, B. J., Gabriele, R. M. C., Casey, J. M., Wray, S., Abu-Bonsrah, D., Parish, C. L., Beccari, M. S., Cleveland, D. W., Li, E., Rose, I. V. L., Kampmann, M., Calatayud Aristoy, C., Verstreken, P., Heinrich, L., Chen, M. Y., Schüle, B., Dou, D., Holzbaur, E. L. F., Zanellati, M. C., Basundra, R., Deshmukh, M., Cohen, S., Khanna, R., Raman, M., Nevin, Z. S., Matia, M., Van Lent, J., Timmerman, V., Conklin, B. R., Johnson Chase, K., Zhang, K., Funes, S., Bosco, D. A., Erlebach, L., Welzer, M., Kronenberg-Versteeg, D., Lyu, G., Arenas, E., Coccia, E., Sarrafha, L., Ahfeldt, T., Marioni, J. C., Skarnes, W. C., Cookson, M. R., Ward, M. E. and Merkle, F. T. (2022) 'A reference human induced pluripotent stem cell line for large-scale collaborative studies', *Cell Stem Cell,* 29(12), pp. 1685-1702.e22.

Penney, J., Ralvenius, W. T. and Tsai, L.-H. (2020) 'Modeling Alzheimer's disease with iPSC-derived brain cells', *Molecular Psychiatry,* 25(1), pp. 148-167.

Perkins, E. M., Burr, K., Banerjee, P., Mehta, A. R., Dando, O., Selvaraj, B. T., Suminaite, D., Nanda, J., Henstridge, C. M., Gillingwater, T. H., Hardingham, G. E., Wyllie, D. J. A., Chandran, S. and Livesey, M. R. (2021) 'Altered network

properties in C9ORF72 repeat expansion cortical neurons are due to synaptic dysfunction', *Molecular Neurodegeneration,* 16(1), pp. 13.

Perkins, L. A., Holderbaum, L., Tao, R., Hu, Y., Sopko, R., McCall, K., Yang-Zhou, D., Flockhart, I., Binari, R., Shim, H.-S., Miller, A., Housden, A., Foos, M., Randkelv, S., Kelley, C., Namgyal, P., Villalta, C., Liu, L.-P., Jiang, X., Huan-Huan, Q., Wang, X., Fujiyama, A., Toyoda, A., Ayers, K., Blum, A., Czech, B., Neumuller, R., Yan, D., Cavallaro, A., Hibbard, K., Hall, D., Cooley, L., Hannon, G. J., Lehmann, R., Parks, A., Mohr, S. E., Ueda, R., Kondo, S., Ni, J.-Q. and Perrimon, N. (2015) 'The Transgenic RNAi Project at Harvard Medical School: Resources and Validation', *Genetics,* 201(3), pp. 843-852.

Phukan, J., Elamin, M., Bede, P., Jordan, N., Gallagher, L., Byrne, S., Lynch, C., Pender, N. and Hardiman, O. (2012) 'The syndrome of cognitive impairment in amyotrophic lateral sclerosis: a population-based study', *Journal of Neurology, Neurosurgery & Psychiatry,* 83(1), pp. 102.

Piomelli, D., Astarita, G. and Rapaka, R. (2007) 'A neuroscientist's guide to lipidomics', *Nature Reviews Neuroscience,* 8(10), pp. 743-754.

Piper, M. D. W. and Partridge, L. (2016) 'Protocols to Study Aging in Drosophila', in Dahmann, C. (ed.) *Drosophila: Methods and Protocols*. New York, NY: Springer New York, pp. 291-302.

Piper, M. D. W. and Partridge, L. (2018) 'Drosophila as a model for ageing', *Biochimica et Biophysica Acta (BBA) - Molecular Basis of Disease,* 1864(9, Part A), pp. 2707-2717.

Piscitelli, F., Carta, G., Bisogno, T., Murru, E., Cordeddu, L., Berge, K., Tandy, S., Cohn, J. S., Griinari, M., Banni, S. and Di Marzo, V. (2011) 'Effect of dietary krill oil supplementation on the endocannabinoidome of metabolically relevant tissues from high-fat-fed mice', *Nutrition & Metabolism,* 8(1), pp. 51.

Popugaeva, E., Chernyuk, D., Zhang, H., Postnikova, T. Y., Pats, K., Fedorova, E., Poroikov, V., Zaitsev, A. V. and Bezprozvanny, I. (2019) 'Derivatives of Piperazines as Potential Therapeutic Agents for Alzheimer's Disease', *Molecular Pharmacology,* 95(4), pp. 337-348.

Pratley, R. E., Salbe, A. D., Ravussin, E. and Caviness, J. N. (2000) 'Higher sedentary energy expenditure in patients with Huntington's disease', *Annals of Neurology,* 47(1), pp. 64-70.

Puram, S. V., Riccio, A., Koirala, S., Ikeuchi, Y., Kim, A. H., Corfas, G. and Bonni, A. (2011) 'A TRPC5-regulated calcium signaling pathway controls dendrite patterning in the mammalian brain', *Genes Dev,* 25(24), pp. 2659-73.

Qu, Y., Chen, X., Xu, M.-M. and Sun, Q. (2019) 'Relationship between high dietary fat intake and Parkinson's disease risk: a meta-analysis', *Neural Regeneration Research,* 14(12).

Quaegebeur, A., Glaria, I., Lashley, T. and Isaacs, A. M. (2020) 'Soluble and insoluble dipeptide repeat protein measurements in C9orf72-frontotemporal dementia brains show regional differential solubility and correlation of poly-GR with clinical severity', *Acta Neuropathologica Communications,* 8(1), pp. 184.

Ramos, D. M., Skarnes, W. C., Singleton, A. B., Cookson, M. R. and Ward, M. E. (2021) 'Tackling neurodegenerative diseases with genomic engineering: A new stem cell initiative from the NIH', *Neuron,* 109(7), pp. 1080-1083.

Ramsey, C. P., Glass, C. A., Montgomery, M. B., Lindl, K. A., Ritson, G. P., Chia, L. A., Hamilton, R. L., Chu, C. T. and Jordan-Sciutto, K. L. (2007) 'Expression of Nrf2 in Neurodegenerative Diseases', *Journal of Neuropathology & Experimental Neurology,* 66(1), pp. 75-85.

Randall, A. S., Liu, C.-H., Chu, B., Zhang, Q., Dongre, S. A., Juusola, M., Franze, K., Wakelam, M. J. O. and Hardie, R. C. (2015) 'Speed and Sensitivity

of Phototransduction in Drosophila Depend on Degree of Saturation of Membrane Phospholipids', *The Journal of Neuroscience,* 35(6), pp. 2731.

Rawicz, W., Olbrich, K. C., McIntosh, T., Needham, D. and Evans, E. (2000) 'Effect of Chain Length and Unsaturation on Elasticity of Lipid Bilayers', *Biophysical Journal,* 79(1), pp. 328-339.

Reiter, L. T., Potocki, L., Chien, S., Gribskov, M. and Bier, E. (2001) 'A Systematic Analysis of Human Disease-Associated Gene Sequences In Drosophila melanogaster', *Genome Research,* 11(6), pp. 1114-1125.

Reiter, R. J. (1998) 'Oxidative damage in the central nervous system: protection by melatonin', *Progress in Neurobiology,* 56(3), pp. 359-384.

Renton, A. E., Majounie, E., Waite, A., Simón-Sánchez, J., Rollinson, S., Gibbs, J. R., Schymick, J. C., Laaksovirta, H., van Swieten, J. C., Myllykangas, L., Kalimo, H., Paetau, A., Abramzon, Y., Remes, A. M., Kaganovich, A., Scholz, S. W., Duckworth, J., Ding, J., Harmer, D. W., Hernandez, D. G., Johnson, J. O., Mok, K., Ryten, M., Trabzuni, D., Guerreiro, R. J., Orrell, R. W., Neal, J., Murray, A., Pearson, J., Jansen, I. E., Sondervan, D., Seelaar, H., Blake, D., Young, K., Halliwell, N., Callister, J. B., Toulson, G., Richardson, A., Gerhard, A., Snowden, J., Mann, D., Neary, D., Nalls, M. A., Peuralinna, T., Jansson, L., Isoviita, V.-M., Kaivorinne, A.-L., Hölttä-Vuori, M., Ikonen, E., Sulkava, R., Benatar, M., Wuu, J., Chiò, A., Restagno, G., Borghero, G., Sabatelli, M., Consortium, I., Heckerman, D., Rogaeva, E., Zinman, L., Rothstein, J. D., Sendtner, M., Drepper, C., Eichler, E. E., Alkan, C., Abdullaev, Z., Pack, S. D., Dutra, A., Pak, E., Hardy, J., Singleton, A., Williams, N. M., Heutink, P., Pickering-Brown, S., Morris, H. R., Tienari, P. J. and Traynor, B. J. (2011) 'A hexanucleotide repeat expansion in C9ORF72 is the cause of chromosome 9p21-linked ALS-FTD', *Neuron,* 72(2), pp. 257-268.

Richter, J. M., Schaefer, M. and Hill, K. (2014) 'Riluzole activates TRPC5 channels independently of PLC activity', *British Journal of Pharmacology,* 171(1), pp. 158-170.

Riehle, M., Tsvetkov, D., Gohlke, B.-O., Preissner, R., Harteneck, C., Gollasch, M. and Nürnberg, B. (2018) 'Molecular basis for the sensitivity of TRP channels to polyunsaturated fatty acids', *Naunyn-Schmiedeberg's archives of pharmacology,* 391(8), pp. 833-846.

Ringholz, G. M., Appel, S. H., Bradshaw, M., Cooke, N. A., Mosnik, D. M. and Schulz, P. E. (2005) 'Prevalence and patterns of cognitive impairment in sporadic ALS', *Neurology,* 65(4), pp. 586.

Rizzu, P., Blauwendraat, C., Heetveld, S., Lynes, E. M., Castillo-Lizardo, M., Dhingra, A., Pyz, E., Hobert, M., Synofzik, M., Simón-Sánchez, J., Francescatto, M. and Heutink, P. (2016) 'C9orf72 is differentially expressed in the central nervous system and myeloid cells and consistently reduced in C9orf72, MAPT and GRN mutation carriers', *Acta Neuropathologica Communications,* 4(1), pp. 37.

Rosen, D. R., Siddique, T., Patterson, D., Figlewicz, D. A., Sapp, P., Hentati, A., Donaldson, D., Goto, J., O'Regan, J. P., Deng, H.-X., Rahmani, Z., Krizus, A., McKenna-Yasek, D., Cayabyab, A., Gaston, S. M., Berger, R., Tanzi, R. E., Halperin, J. J., Herzfeldt, B., Van den Bergh, R., Hung, W.-Y., Bird, T., Deng, G., Mulder, D. W., Smyth, C., Laing, N. G., Soriano, E., Pericak–Vance, M. A., Haines, J., Rouleau, G. A., Gusella, J. S., Horvitz, H. R. and Brown, R. H. (1993) 'Mutations in Cu/Zn superoxide dismutase gene are associated with familial amyotrophic lateral sclerosis', *Nature,* 362(6415), pp. 59-62.

Rubino, E., Rainero, I., Chiò, A., Rogaeva, E., Galimberti, D., Fenoglio, P., Grinberg, Y., Isaia, G., Calvo, A., Gentile, S., Bruni, A. C., George-Hyslop, P. H. S., Scarpini, E., Gallone, S. and Pinessi, L. (2012) 'SQSTM1 mutations in frontotemporal lobar degeneration and amyotrophic lateral sclerosis', *Neurology,* 79(15), pp. 1556.

Ruiz, M., Bodhicharla, R., Ståhlman, M., Svensk, E., Busayavalasa, K., Palmgren, H., Ruhanen, H., Boren, J. and Pilon, M. (2019a) 'Evolutionarily

conserved long-chain Acyl-CoA synthetases regulate membrane composition and fluidity', *eLife,* 8, pp. e47733.

Ruiz, M., Devkota, R., Kaper, D., Ruhanen, H., Busayavalasa, K., Radović, U., Henricsson, M., Käkelä, R., Borén, J. and Pilon, M. (2023) 'AdipoR2 recruits protein interactors to promote fatty acid elongation and membrane fluidity', *Journal of Biological Chemistry,* 299(6).

Ruiz, M., Devkota, R., Panagaki, D., Bergh, P.-O., Kaper, D., Henricsson, M., Nik, A., Petkevicius, K., Höög, J. L., Bohlooly-Y, M., Carlsson, P., Borén, J. and Pilon, M. (2022) 'Sphingosine 1-phosphate mediates adiponectin receptor signaling essential for lipid homeostasis and embryogenesis', *Nature Communications,* 13(1), pp. 7162.

Ruiz, M., Palmgren, H., Henricsson, M., Devkota, R., Jaiswal, H., Maresca, M., Bohlooly-Y, M., Peng, X.-R., Borén, J. and Pilon, M. (2021) 'Extensive transcription mis-regulation and membrane defects in AdipoR2-deficient cells challenged with saturated fatty acids', *Biochimica et Biophysica Acta (BBA) - Molecular and Cell Biology of Lipids,* 1866(4), pp. 158884.

Ruiz, M., Ståhlman, M., Borén, J. and Pilon, M. (2019b) 'AdipoR1 and AdipoR2 maintain membrane fluidity in most human cell types and independently of adiponectin', *Journal of Lipid Research,* 60(5), pp. 995-1004.

Ryan, M., Heverin, M., McLaughlin, R. L. and Hardiman, O. (2019) 'Lifetime Risk and Heritability of Amyotrophic Lateral Sclerosis', *JAMA Neurology,* 76(11), pp. 1367-1374.

Saberi, S., Stauffer, J. E., Jiang, J., Garcia, S. D., Taylor, A. E., Schulte, D., Ohkubo, T., Schloffman, C. L., Maldonado, M., Baughn, M., Rodriguez, M. J., Pizzo, D., Cleveland, D. and Ravits, J. (2018) 'Sense-encoded poly-GR dipeptide repeat proteins correlate to neurodegeneration and uniquely co-localize with TDP-43 in dendrites of repeat-expanded C9orf72 amyotrophic lateral sclerosis', *Acta Neuropathologica,* 135(3), pp. 459-474.

Sareen, D., O'Rourke, J. G., Meera, P., Muhammad, A. K. M. G., Grant, S., Simpkinson, M., Bell, S., Carmona, S., Ornelas, L., Sahabian, A., Gendron, T., Petrucelli, L., Baughn, M., Ravits, J., Harms, M. B., Rigo, F., Bennett, C. F., Otis, T. S., Svendsen, C. N. and Baloh, R. H. (2013) 'Targeting RNA Foci in iPSC-Derived Motor Neurons from ALS Patients with a C9ORF72 Repeat Expansion', *Science Translational Medicine,* 5(208), pp. 208ra149-208ra149.

Sattler, R. and Tymianski, M. (2000) 'Molecular mechanisms of calcium-dependent excitotoxicity', *Journal of Molecular Medicine,* 78(1), pp. 3-13.

Schludi, M. H., May, S., Grässer, F. A., Rentzsch, K., Kremmer, E., Küpper, C., Klopstock, T., Arzberger, T., Edbauer, D., German Consortium for Frontotemporal Lobar, D. and Bavarian Brain Banking, A. (2015) 'Distribution of dipeptide repeat proteins in cellular models and C9orf72 mutation cases suggests link to transcriptional silencing', *Acta Neuropathologica,* 130(4), pp. 537-555.

Schmelzer, K., Fahy, E., Subramaniam, S. and Dennis, E. A. (2007) 'The Lipid Maps Initiative in Lipidomics', *Methods in Enzymology*: Academic Press, pp. 171-183.

Schmitt, F., Hussain, G., Dupuis, L., Loeffler, J.-P. and Henriques, A. (2014) 'A plural role for lipids in motor neuron diseases: energy, signaling and structure', *Frontiers in Cellular Neuroscience,* 8, pp. 25.

Schneider, C. A., Rasband, W. S. and Eliceiri, K. W. (2012) 'NIH Image to ImageJ: 25 years of image analysis', *Nature Methods,* 9(7), pp. 671-675.

Schwarz, Y., Oleinikov, K., Schindeldecker, B., Wyatt, A., Weißgerber, P., Flockerzi, V., Boehm, U., Freichel, M. and Bruns, D. (2019) 'TRPC channels regulate Ca2+-signaling and short-term plasticity of fast glutamatergic synapses', *PLOS Biology,* 17(9), pp. e3000445.

Sellier, C., Campanari, M.-L., Julie Corbier, C., Gaucherot, A., Kolb-Cheynel, I., Oulad-Abdelghani, M., Ruffenach, F., Page, A., Ciura, S., Kabashi, E. and Charlet-Berguerand, N. (2016) 'Loss of C9ORF72 impairs autophagy and synergizes with polyQ Ataxin-2 to induce motor neuron dysfunction and cell death', *The EMBO Journal,* 35(12), pp. 1276-1297.

Selvaraj, B. T., Livesey, M. R. and Chandran, S. (2017) 'Modeling the C9ORF72 repeat expansion mutation using human induced pluripotent stem cells', *Brain Pathology,* 27(4), pp. 518-524.

Selvaraj, B. T., Livesey, M. R., Zhao, C., Gregory, J. M., James, O. T., Cleary, E. M., Chouhan, A. K., Gane, A. B., Perkins, E. M., Dando, O., Lillico, S. G., Lee, Y.-B., Nishimura, A. L., Poreci, U., Thankamony, S., Pray, M., Vasistha, N. A., Magnani, D., Borooah, S., Burr, K., Story, D., McCampbell, A., Shaw, C. E., Kind, P. C., Aitman, T. J., Whitelaw, C. B. A., Wilmut, I., Smith, C., Miles, G. B., Hardingham, G. E., Wyllie, D. J. A. and Chandran, S. (2018) 'C9ORF72 repeat expansion causes vulnerability of motor neurons to Ca2+-permeable AMPA receptor-mediated excitotoxicity', *Nature Communications,* 9(1), pp. 347.

Serhan, C. N. (2014) 'Pro-resolving lipid mediators are leads for resolution physiology', *Nature,* 510(7503), pp. 92-101.

Shen, L. R., Lai, C. Q., Feng, X., Parnell, L. D., Wan, J. B., Wang, J. D., Li, D., Ordovas, J. M. and Kang, J. X. (2010) 'Drosophila lacks C20 and C22 PUFAs', *Journal of lipid research,* 51(10), pp. 2985-2992.

Shibata, N., Nagai, R., Uchida, K., Horiuchi, S., Yamada, S., Hirano, A., Kawaguchi, M., Yamamoto, T., Sasaki, S. and Kobayashi, M. (2001) 'Morphological evidence for lipid peroxidation and protein glycoxidation in spinal cords from sporadic amyotrophic lateral sclerosis patients', *Brain Res,* 917(1), pp. 97-104.

Shirangi, T. R., Dufour, H. D., Williams, T. M. and Carroll, S. B. (2009) 'Rapid Evolution of Sex Pheromone-Producing Enzyme Expression in Drosophila', *PLOS Biology,* 7(8), pp. e1000168.

Shokri, L., Inukai, S., Hafner, A., Weinand, K., Hens, K., Vedenko, A., Gisselbrecht, S. S., Dainese, R., Bischof, J., Furger, E., Feuz, J.-D., Basler, K., Deplancke, B. and Bulyk, M. L. (2019) 'A Comprehensive Drosophila melanogaster Transcription Factor Interactome', *Cell Reports,* 27(3), pp. 955-970.e7.

Simpson, E. P., Henry, Y. K., Henkel, J. S., Smith, R. G. and Appel, S. H. (2004) 'Increased lipid peroxidation in sera of ALS patients', *Neurology,* 62(10), pp. 1758.

Skibinski, G., Parkinson, N. J., Brown, J. M., Chakrabarti, L., Lloyd, S. L., Hummerich, H., Nielsen, J. E., Hodges, J. R., Spillantini, M. G., Thusgaard, T., Brandner, S., Brun, A., Rossor, M. N., Gade, A., Johannsen, P., Sørensen, S. A., Gydesen, S., Fisher, E. M. C. and Collinge, J. (2005) 'Mutations in the endosomal ESCRTIII-complex subunit CHMP2B in frontotemporal dementia', *Nature Genetics,* 37(8), pp. 806-808.

Slater, G., Levy, P., Chan, K. L. A. and Larsen, C. (2015) 'A central neural pathway controlling odor tracking in Drosophila', *The Journal of neuroscience : the official journal of the Society for Neuroscience,* 35(5), pp. 1831-1848.

Slotsbo, S., Sørensen, J. G., Holmstrup, M., Kostal, V., Kellermann, V. and Overgaard, J. (2016) 'Tropical to subpolar gradient in phospholipid composition suggests adaptive tuning of biological membrane function in drosophilids', *Functional Ecology,* 30(5), pp. 759-768.

So, P. L. and Danielian, P. S. (1999) 'Cloning and expression analysis of a mouse gene related to Drosophila odd-skipped', *Mechanisms of Development,* 84(1), pp. 157-160.

Sogorb-Esteve, A., Colas, R. A., Dalli, J. and Rohrer, J. D. (2021) 'Differential Lipid Mediator Involvement in the Different Forms of Genetic Frontotemporal Dementia: Novel Insights into Neuroinflammation', *Journal of Alzheimer's Disease,* 84, pp. 283-289.

Sol, J., Jové, M., Povedano, M., Sproviero, W., Domínguez, R., Piñol-Ripoll, G., Romero-Guevara, R., Hye, A., Al-Chalabi, A., Torres, P., Andres-Benito, P., Area-Gómez, E., Pamplona, R., Ferrer, I., Ayala, V. and Portero-Otín, M. (2021) 'Lipidomic traits of plasma and cerebrospinal fluid in amyotrophic lateral sclerosis correlate with disease progression', *Brain Communications,* 3(3), pp. fcab143.

Soldner, F., Stelzer, Y., Shivalila, C. S., Abraham, B. J., Latourelle, J. C., Barrasa, M. I., Goldmann, J., Myers, R. H., Young, R. A. and Jaenisch, R. (2016) 'Parkinson-associated risk variant in distal enhancer of α-synuclein modulates target gene expression', *Nature,* 533(7601), pp. 95-99.

Sommer, D., Rajkumar, S., Seidel, M., Aly, A., Ludolph, A., Ho, R., Boeckers, T. M. and Catanese, A. (2022) 'Aging-Dependent Altered Transcriptional Programs Underlie Activity Impairments in Human C9orf72-Mutant Motor Neurons', *Frontiers in Molecular Neuroscience,* 15.

Sousa, B. C., Klein, Z. G., Taylor, D., West, G., Huipeng, A. N., Wakelam, M. J. O. and Lopez-Clavijo, A. F. (2023) 'Comprehensive lipidome of human plasma using minimal sample manipulation by liquid chromatography coupled with mass spectrometry', *Rapid Communications in Mass Spectrometry,* n/a(n/a), pp. e9472.

Sreedharan, J., Blair, I. P., Tripathi, V. B., Hu, X., Vance, C., Rogelj, B., Ackerley, S., Durnall, J. C., Williams, K. L., Buratti, E., Baralle, F., de Belleroche, J., Mitchell, J. D., Leigh, P. N., Al-Chalabi, A., Miller, C. C., Nicholson, G. and Shaw, C. E. (2008) 'TDP-43 Mutations in Familial and Sporadic Amyotrophic Lateral Sclerosis', *Science,* 319(5870), pp. 1668-1672.

Steyn, F. J., Ioannides, Z. A., van Eijk, R. P. A., Heggie, S., Thorpe, K. A., Ceslis, A., Heshmat, S., Henders, A. K., Wray, N. R., van den Berg, L. H., Henderson, R. D., McCombe, P. A. and Ngo, S. T. (2018) 'Hypermetabolism in ALS is associated with greater functional decline and shorter survival', *Journal of neurology, neurosurgery, and psychiatry,* 89(10), pp. 1016-1023.

Strong, M. J., Abrahams, S., Goldstein, L. H., Woolley, S., McLaughlin, P., Snowden, J., Mioshi, E., Roberts-South, A., Benatar, M., HortobáGyi, T., Rosenfeld, J., Silani, V., Ince, P. G. and Turner, M. R. (2017) 'Amyotrophic lateral sclerosis - frontotemporal spectrum disorder (ALS-FTSD): Revised diagnostic criteria', *Amyotrophic Lateral Sclerosis and Frontotemporal Degeneration,* 18(3-4), pp. 153-174.

Su, B., Bettcher, L. F., Hsieh, W.-Y., Hornburg, D., Pearson, M. J., Blomberg, N., Giera, M., Snyder, M. P., Raftery, D., Bensinger, S. J. and Williams, K. J. (2021) 'A DMS Shotgun Lipidomics Workflow Application to Facilitate High-Throughput, Comprehensive Lipidomics', *Journal of the American Society for Mass Spectrometry,* 32(11), pp. 2655-2663.

Suh, E., Lee, E. B., Neal, D., Wood, E. M., Toledo, J. B., Rennert, L., Irwin, D. J., McMillan, C. T., Krock, B., Elman, L. B., McCluskey, L. F., Grossman, M., Xie, S. X., Trojanowski, J. Q. and Van Deerlin, V. M. (2015) 'Semi-automated quantification of C9orf72 expansion size reveals inverse correlation between hexanucleotide repeat number and disease duration in frontotemporal degeneration', *Acta Neuropathologica,* 130(3), pp. 363-372.

Suito, T., Nagao, K., Takeuchi, K., Juni, N., Hara, Y. and Umeda, M. (2020) 'Functional expression of Δ12 fatty acid desaturase modulates thermoregulatory behaviour in Drosophila', *Scientific Reports,* 10(1), pp. 11798.

Szebényi, K., Wenger, L. M. D., Sun, Y., Dunn, A. W. E., Limegrover, C. A., Gibbons, G. M., Conci, E., Paulsen, O., Mierau, S. B., Balmus, G. and Lakatos, A. (2021) 'Human ALS/FTD brain organoid slice cultures display distinct early

astrocyte and targetable neuronal pathology', *Nature Neuroscience,* 24(11), pp. 1542-1554.

Takahashi, K., Tanabe, K., Ohnuki, M., Narita, M., Ichisaka, T., Tomoda, K. and Yamanaka, S. (2007) 'Induction of Pluripotent Stem Cells from Adult Human Fibroblasts by Defined Factors', *Cell,* 131(5), pp. 861-872.

Tena, J. J., Neto, A., de la Calle-Mustienes, E., Bras-Pereira, C., Casares, F. and Gómez-Skarmeta, J. L. (2007) 'Odd-skipped genes encode repressors that control kidney development', *Developmental Biology,* 301(2), pp. 518-531.

Thompson, A. G., Marsden, R., Talbot, K. and Turner, M. R. (2023) 'Primary care blood tests show lipid profile changes in pre-symptomatic amyotrophic lateral sclerosis', *Brain Communications,* 5(4).

Thompson, A. G., Talbot, K. and Turner, M. R. (2022) 'Higher blood high density lipoprotein and apolipoprotein A1 levels are associated with reduced risk of developing amyotrophic lateral sclerosis', *Journal of Neurology, Neurosurgery & Psychiatry,* 93(1), pp. 75.

Todd, T. W. and Petrucelli, L. (2016) 'Insights into the pathogenic mechanisms of Chromosome 9 open reading frame 72 (C9orf72) repeat expansions', *Journal of Neurochemistry,* 138(S1), pp. 145-162.

Tracey, T. J., Kirk, S. E., Steyn, F. J. and Ngo, S. T. (2021) 'The role of lipids in the central nervous system and their pathological implications in amyotrophic lateral sclerosis', *Seminars in Cell & Developmental Biology,* 112, pp. 69-81.

Tracey, T. J., Steyn, F. J., Wolvetang, E. J. and Ngo, S. T. (2018) 'Neuronal Lipid Metabolism: Multiple Pathways Driving Functional Outcomes in Health and Disease', *Frontiers in Molecular Neuroscience,* 11, pp. 10.

Tran, H., Almeida, S., Moore, J., Gendron, Tania F., Chalasani, U., Lu, Y., Du, X., Nickerson, Jeffrey A., Petrucelli, L., Weng, Z. and Gao, F.-B. (2015)

'Differential Toxicity of Nuclear RNA Foci versus Dipeptide Repeat Proteins in a Drosophila Model of C9ORF72 FTD/ALS', *Neuron,* 87(6), pp. 1207-1214.

Tricoire, H., Battisti, V., Trannoy, S., Lasbleiz, C., Pret, A.-M. and Monnier, V. (2009) 'The steroid hormone receptor EcR finely modulates Drosophila lifespan during adulthood in a sex-specific manner', *Mechanisms of Ageing and Development,* 130(8), pp. 547-552.

Tripathi, P., Rodriguez-Muela, N., Klim, J. R., de Boer, A. S., Agrawal, S., Sandoe, J., Lopes, C. S., Ogliari, K. S., Williams, L. A., Shear, M., Rubin, L. L., Eggan, K. and Zhou, Q. (2017) 'Reactive Astrocytes Promote ALS-like Degeneration and Intracellular Protein Aggregation in Human Motor Neurons by Disrupting Autophagy through TGF-β1', *Stem Cell Reports,* 9(2), pp. 667-680.

Ugur, B., Chen, K. and Bellen, H. J. (2016) 'Drosophila tools and assays for the study of human diseases', *Disease Models & Mechanisms,* 9(3), pp. 235-244.

Urwin, H., Josephs, K. A., Rohrer, J. D., Mackenzie, I. R., Neumann, M., Authier, A., Seelaar, H., Van Swieten, J. C., Brown, J. M., Johannsen, P., Nielsen, J. E., Holm, I. E., Dickson, D. W., Rademakers, R., Graff-Radford, N. R., Parisi, J. E., Petersen, R. C., Hatanpaa, K. J., White Iii, C. L., Weiner, M. F., Geser, F., Van Deerlin, V. M., Trojanowski, J. Q., Miller, B. L., Seeley, W. W., van der Zee, J., Kumar-Singh, S., Engelborghs, S., De Deyn, P. P., Van Broeckhoven, C., Bigio, E. H., Deng, H.-X., Halliday, G. M., Kril, J. J., Munoz, D. G., Mann, D. M., Pickering-Brown, S. M., Doodeman, V., Adamson, G., Ghazi-Noori, S., Fisher, E. M. C., Holton, J. L., Revesz, T., Rossor, M. N., Collinge, J., Mead, S., Isaacs, A. M. and The, F. C. (2010) 'FUS pathology defines the majority of tau- and TDP-43-negative frontotemporal lobar degeneration', *Acta Neuropathologica,* 120(1), pp. 33-41.

Vahsen, B. F., Gray, E., Candalija, A., Cramb, K. M. L., Scaber, J., Dafinca, R., Katsikoudi, A., Xu, Y., Farrimond, L., Wade-Martins, R., James, W. S., Turner, M. R., Cowley, S. A. and Talbot, K. (2022) 'Human iPSC co-culture model to

investigate the interaction between microglia and motor neurons', *Scientific Reports,* 12(1), pp. 12606.

Vahsen, B. F., Gray, E., Thompson, A. G., Ansorge, O., Anthony, D. C., Cowley, S. A., Talbot, K. and Turner, M. R. (2021) 'Non-neuronal cells in amyotrophic lateral sclerosis—from pathogenesis to biomarkers', *Nature Reviews Neurology,* 17(6), pp. 333-348.

van Blitterswijk, M., DeJesus-Hernandez, M., Niemantsverdriet, E., Murray, M. E., Heckman, M. G., Diehl, N. N., Brown, P. H., Baker, M. C., Finch, N. A., Bauer, P. O., Serrano, G., Beach, T. G., Josephs, K. A., Knopman, D. S., Petersen, R. C., Boeve, B. F., Graff-Radford, N. R., Boylan, K. B., Petrucelli, L., Dickson, D. W. and Rademakers, R. (2013) 'Association between repeat sizes and clinical and pathological characteristics in carriers of C9ORF72 repeat expansions (Xpansize-72): a cross-sectional cohort study', *The Lancet Neurology,* 12(10), pp. 978-988.

Van Deerlin, V. M., Leverenz, J. B., Bekris, L. M., Bird, T. D., Yuan, W., Elman, L. B., Clay, D., Wood, E. M., Chen-Plotkin, A. S., Martinez-Lage, M., Steinbart, E., McCluskey, L., Grossman, M., Neumann, M., Wu, I. L., Yang, W.-S., Kalb, R., Galasko, D. R., Montine, T. J., Trojanowski, J. Q., Lee, V. M. Y., Schellenberg, G. D. and Yu, C.-E. (2008) 'TARDBP mutations in amyotrophic lateral sclerosis with TDP-43 neuropathology: a genetic and histopathological analysis', *The Lancet Neurology,* 7(5), pp. 409-416.

van Langenhove, T., van der Zee, J. and van Broeckhoven, C. (2012) 'The molecular basis of the frontotemporal lobar degeneration–amyotrophic lateral sclerosis spectrum', *Annals of Medicine,* 44(8), pp. 817-828.

van Meer, G. (2005) 'Cellular lipidomics', *The EMBO Journal,* 24(18), pp. 3159-3165.

van Meer, G., Voelker, D. R. and Feigenson, G. W. (2008) 'Membrane lipids: where they are and how they behave', *Nature Reviews Molecular Cell Biology,* 9(2), pp. 112-124.

van Rheenen, W. and van der Spek, R. A. A. and Bakker, M. K. and van Vugt, J. J. F. A. and Hop, P. J. and Zwamborn, R. A. J. and de Klein, N. and Westra, H.-J. and Bakker, O. B. and Deelen, P. and Shireby, G. and Hannon, E. and Moisse, M. and Baird, D. and Restuadi, R. and Dolzhenko, E. and Dekker, A. M. and Gawor, K. and Westeneng, H.-J. and Tazelaar, G. H. P. and van Eijk, K. R. and Kooyman, M. and Byrne, R. P. and Doherty, M. and Heverin, M. and Al Khleifat, A. and Iacoangeli, A. and Shatunov, A. and Ticozzi, N. and Cooper-Knock, J. and Smith, B. N. and Gromicho, M. and Chandran, S. and Pal, S. and Morrison, K. E. and Shaw, P. J. and Hardy, J. and Orrell, R. W. and Sendtner, M. and Meyer, T. and Başak, N. and van der Kooi, A. J. and Ratti, A. and Fogh, I. and Gellera, C. and Lauria, G. and Corti, S. and Cereda, C. and Sproviero, D. and D'Alfonso, S. and Sorarù, G. and Siciliano, G. and Filosto, M. and Padovani, A. and Chiò, A. and Calvo, A. and Moglia, C. and Brunetti, M. and Canosa, A. and Grassano, M. and Beghi, E. and Pupillo, E. and Logroscino, G. and Nefussy, B. and Osmanovic, A. and Nordin, A. and Lerner, Y. and Zabari, M. and Gotkine, M. and Baloh, R. H. and Bell, S. and Vourc'h, P. and Corcia, P. and Couratier, P. and Millecamps, S. and Meininger, V. and Salachas, F. and Mora Pardina, J. S. and Assialioui, A. and Rojas-García, R. and Dion, P. A. and Ross, J. P. and Ludolph, A. C. and Weishaupt, J. H. and Brenner, D. and Freischmidt, A. and Bensimon, G. and Brice, A. and Durr, A. and Payan, C. A. M. and Saker-Delye, S. and Wood, N. W. and Topp, S. and Rademakers, R. and Tittmann, L. and Lieb, W. and Franke, A. and Ripke, S. and Braun, A. and Kraft, J. and Whiteman, D. C. and Olsen, C. M. and Uitterlinden, A. G. and Hofman, A. and Rietschel, M. and Cichon, S. and Nöthen, M. M. and Amouyel, P. and Comi, G. and Riva, N. and Lunetta, C. and Gerardi, F. and Cotelli, M. S. and Rinaldi, F. and Chiveri, L. and Guaita, M. C. and Perrone, P. and Ceroni, M. and Diamanti, L. and Ferrarese, C. and Tremolizzo, L. and Delodovici, M. L. and Bono, G. and Manera, U. and Vasta, R. and Bombaci, A. and Casale, F. and Fuda, G. and Salamone, P. and Iazzolino, B. and Peotta, L. and Cugnasco, P. and De Marco, G. and Torrieri, M. C. and Palumbo, F. and Gallone, S. and

Barberis, M. and Sbaiz, L. and Gentile, S. and Mauro, A. and Mazzini, L. and De Marchi, F. and Corrado, L. and Bertolotto, A. and Gionco, M. and Leotta, D. and Odddenino, E. and Imperiale, D. and Cavallo, R. and Pignatta, P. and De Mattei, M. and Geda, C. and Papurello, D. M. and Gusmaroli, G. and Comi, C. and Labate, C. and Ruiz, L. and Ferrandi, D. and Rota, E. and Aguggia, M. and Di Vito, N. and Meineri, P. and Ghiglione, P. and Launaro, N. and Dotta, M. and Di Sapio, A. and Giardini, G. and Tiloca, C. and Peverelli, S. and Taroni, F. and Pensato, V. and Castellotti, B. and Comi, G. P. and Del Bo, R. and Gagliardi, S. and Raggi, F. and Simoncini, C. and Lo Gerfo, A. and Inghilleri, M. and Ferlini, A. and Simone, I. L. and Passarella, B. and Guerra, V. and Zoccolella, S. and Nozzoli, C. and Mundi, C. and Leone, M. and Zarrelli, M. and Tamma, F. and Valluzzi, F. and Calabrese, G. and Boero, G. and Rini, A. and Traynor, B. J. and Singleton, A. B. and Mitne Neto, M. and Cauchi, R. J. and Ophoff, R. A. and Wiedau-Pazos, M. and Lomen-Hoerth, C. and van Deerlin, V. M. and Grosskreutz, J. and Roediger, A. and Gaur, N. and Jörk, A. and Barthel, T. and Theele, E. and Ilse, B. and Stubendorff, B. and Witte, O. W. and Steinbach, R. and Hübner, C. A. and Graff, C. and Brylev, L. and Fominykh, V. and Demeshonok, V. and Ataulina, A. and Rogelj, B. and Koritnik, B. and Zidar, J. and Ravnik-Glavač, M. and Glavač, D. and Stević, Z. and Drory, V. and Povedano, M. and Blair, I. P. and Kiernan, M. C. and Benyamin, B. and Henderson, R. D. and Furlong, S. and Mathers, S. and McCombe, P. A. and Needham, M. and Ngo, S. T. and Nicholson, G. A. and Pamphlett, R. and Rowe, D. B. and Steyn, F. J. and Williams, K. L. and Mather, K. A. and Sachdev, P. S. and Henders, A. K. and Wallace, L. and de Carvalho, M. and Pinto, S. and Petri, S. and Weber, M. and Rouleau, G. A. and Silani, V. and Curtis, C. J. and Breen, G. and Glass, J. D. and Brown, R. H. and Landers, J. E. and Shaw, C. E. and Andersen, P. M. and Groen, E. J. N. and van Es, M. A. and Pasterkamp, R. J. and Fan, D. and Garton, F. C. and McRae, A. F. and Davey Smith, G. and Gaunt, T. R. and Eberle, M. A. and Mill, J. and McLaughlin, R. L. and Hardiman, O. and Kenna, K. P. and Wray, N. R. and Tsai, E. and Runz, H. and Franke, L. and Al-Chalabi, A. and Van Damme, P. and van den Berg, L. H. and Veldink, J. H. and Consortium, S. and Consortium, P. and Consortium, S. and Consortium, S. (2021) 'Common and rare variant association analyses in amyotrophic lateral sclerosis identify 15 risk loci with

distinct genetic architectures and neuron-specific biology', *Nature Genetics,* 53(12), pp. 1636-1648.

Vance, C., Rogelj, B., Hortobágyi, T., De Vos, K. J., Nishimura, A. L., Sreedharan, J., Hu, X., Smith, B., Ruddy, D., Wright, P., Ganesalingam, J., Williams, K. L., Tripathi, V., Al-Saraj, S., Al-Chalabi, A., Leigh, P. N., Blair, I. P., Nicholson, G., de Belleroche, J., Gallo, J.-M., Miller, C. C. and Shaw, C. E. (2009) 'Mutations in FUS, an RNA Processing Protein, Cause Familial Amyotrophic Lateral Sclerosis Type 6', *Science,* 323(5918), pp. 1208-1211.

Vasiliauskaité-Brooks, I., Sounier, R., Rochaix, P., Bellot, G., Fortier, M., Hoh, F., De Colibus, L., Bechara, C., Saied, E. M., Arenz, C., Leyrat, C. and Granier, S. (2017) 'Structural insights into adiponectin receptors suggest ceramidase activity', *Nature,* 544(7648), pp. 120-123.

Veldink, J. H., Kalmijn, S., Groeneveld, G.-J., Wunderink, W., Koster, A., de Vries, J. H. M., van der Luyt, J., Wokke, J. H. J. and Van den Berg, L. H. (2007) 'Intake of polyunsaturated fatty acids and vitamin E reduces the risk of developing amyotrophic lateral sclerosis', *Journal of Neurology, Neurosurgery & Psychiatry,* 78(4), pp. 367-371.

Vial, D. and Piomelli, D. (1995) 'Dopamine D2 Receptors Potentiate Arachidonate Release via Activation of Cytosolic, Arachidonate-Specific Phospholipase A2', *Journal of Neurochemistry,* 64(6), pp. 2765-2772.

Volmer, R., van der Ploeg, K. and Ron, D. (2013) 'Membrane lipid saturation activates endoplasmic reticulum unfolded protein response transducers through their transmembrane domains', *Proceedings of the National Academy of Sciences,* 110(12), pp. 4628-4633.

Vreugdenhil, M., Bruehl, C., Voskuyl, R. A., Kang, J. X., Leaf, A. and Wadman, W. J. (1996) 'Polyunsaturated fatty acids modulate sodium and calcium currents in CA1 neurons', *Proceedings of the National Academy of Sciences,* 93(22), pp. 12559-12563.

Waite, A. J., Bäumer, D., East, S., Neal, J., Morris, H. R., Ansorge, O. and Blake, D. J. (2014) 'Reduced C9orf72 protein levels in frontal cortex of amyotrophic lateral sclerosis and frontotemporal degeneration brain with the C9ORF72 hexanucleotide repeat expansion', *Neurobiology of Aging,* 35(7), pp. 1779.e5-1779.e13.

Wang, Q., Lan, Y., Cho, E.-S., Maltby, K. M. and Jiang, R. (2005) 'Odd-skipped related 1 (Odd1) is an essential regulator of heart and urogenital development', *Developmental Biology,* 288(2), pp. 582-594.

Wang, Y., Lei, L., Xu, F. and Xu, H. T. (2020) 'Reduced expression of odd-skipped related transcription factor 1 promotes proliferation and invasion of breast cancer cells and indicates poor patient prognosis', *Oncol Lett,* 20(3), pp. 2946-2954.

Wang, Y., Lei, L., Zheng, Y.-W., Zhang, L., Li, Z.-H., Shen, H.-Y., Jiang, G.-Y., Zhang, X.-P., Wang, E.-H. and Xu, H.-T. (2018) 'Odd-skipped related 1 inhibits lung cancer proliferation and invasion by reducing Wnt signaling through the suppression of SOX9 and β-catenin', *Cancer science,* 109(6), pp. 1799-1810.

Watkins, P. A. (1997) 'Fatty acid activation', *Progress in Lipid Research,* 36(1), pp. 55-83.

Watts, G. D. J., Thomasova, D., Ramdeen, S. K., Fulchiero, E. C., Mehta, S. G., Drachman, D. A., Weihl, C. C., Jamrozik, Z., Kwiecinski, H., Kaminska, A. and Kimonis, V. E. (2007) 'Novel VCP mutations in inclusion body myopathy associated with Paget disease of bone and frontotemporal dementia', *Clinical Genetics,* 72(5), pp. 420-426.

Webb, A. E. and Brunet, A. (2014) 'FOXO transcription factors: key regulators of cellular quality control', *Trends in Biochemical Sciences,* 39(4), pp. 159-169.

Webb, Y., Hermida-Matsumoto, L. and Resh, M. D. (2000) 'Inhibition of protein palmitoylation, raft localization, and T cell signaling by 2-bromopalmitate and

polyunsaturated fatty acids', *Journal of Biological Chemistry,* 275(1), pp. 261-270.

Webster, C. P., Smith, E. F., Bauer, C. S., Moller, A., Hautbergue, G. M., Ferraiuolo, L., Myszczynska, M. A., Higginbottom, A., Walsh, M. J., Whitworth, A. J., Kaspar, B. K., Meyer, K., Shaw, P. J., Grierson, A. J. and De Vos, K. J. (2016) 'The C9orf72 protein interacts with Rab1a and the ULK1 complex to regulate initiation of autophagy', *The EMBO Journal,* 35(15), pp. 1656-1676.

Wehrspaun, C., Ponting, C. and Marques, A. (2014) 'Brain-expressed 3′UTR extensions strengthen miRNA cross-talk between ion channel/transporter encoding mRNAs', *Frontiers in Genetics,* 5.

Weick, J. P., Austin Johnson, M. and Zhang, S.-C. (2009) 'Developmental Regulation of Human Embryonic Stem Cell-Derived Neurons by Calcium Entry via Transient Receptor Potential Channels', *Stem Cells,* 27(12), pp. 2906-2916.

Wenk, M. R. (2005) 'The emerging field of lipidomics', *Nature Reviews Drug Discovery,* 4(7), pp. 594-610.

Westeneng, H.-J., Debray, T. P. A., Visser, A. E., van Eijk, R. P. A., Rooney, J. P. K., Calvo, A., Martin, S., McDermott, C. J., Thompson, A. G., Pinto, S., Kobeleva, X., Rosenbohm, A., Stubendorff, B., Sommer, H., Middelkoop, B. M., Dekker, A. M., van Vugt, J. J. F. A., van Rheenen, W., Vajda, A., Heverin, M., Kazoka, M., Hollinger, H., Gromicho, M., Körner, S., Ringer, T. M., Rödiger, A., Gunkel, A., Shaw, C. E., Bredenoord, A. L., van Es, M. A., Corcia, P., Couratier, P., Weber, M., Grosskreutz, J., Ludolph, A. C., Petri, S., de Carvalho, M., Van Damme, P., Talbot, K., Turner, M. R., Shaw, P. J., Al-Chalabi, A., Chiò, A., Hardiman, O., Moons, K. G. M., Veldink, J. H. and van den Berg, L. H. (2018) 'Prognosis for patients with amyotrophic lateral sclerosis: development and validation of a personalised prediction model', *The Lancet Neurology,* 17(5), pp. 423-433.

Wojciechowska, M. and Krzyzosiak, W. J. (2011) 'Cellular toxicity of expanded RNA repeats: focus on RNA foci', *Human Molecular Genetics,* 20(19), pp. 3811-3821.

Wong, R., Piper, M. D. W., Wertheim, B. and Partridge, L. (2009) 'Quantification of Food Intake in Drosophila', *PLOS ONE,* 4(6), pp. e6063.

Woollacott, I. O. C. and Mead, S. (2014) 'The C9ORF72 expansion mutation: gene structure, phenotypic and diagnostic issues', *Acta Neuropathologica,* 127(3), pp. 319-332.

Wu, D., Huang, W., Richardson, P. M., Priestley, J. V. and Liu, M. (2008) 'TRPC4 in Rat Dorsal Root Ganglion Neurons Is Increased after Nerve Injury and Is Necessary for Neurite Outgrowth*', *Journal of Biological Chemistry,* 283(1), pp. 416-426.

Wu, K., Gao, X., Shi, B., Chen, S., Zhou, X., Li, Z., Gan, Y., Cui, L., Kang, J. x., Li, W. and Huang, R. (2016) 'Enriched endogenous n-3 polyunsaturated fatty acids alleviate cognitive and behavioral deficits in a mice model of Alzheimer's disease', *Neuroscience,* 333, pp. 345-355.

Xiao, S., MacNair, L., McGoldrick, P., McKeever, P. M., McLean, J. R., Zhang, M., Keith, J., Zinman, L., Rogaeva, E. and Robertson, J. (2015) 'Isoform-specific antibodies reveal distinct subcellular localizations of C9orf72 in amyotrophic lateral sclerosis', *Annals of Neurology,* 78(4), pp. 568-583.

Xu, D., Vincent, A., González-Gutiérrez, A., Aleyakpo, B., Anoar, S., Giblin, A., Atilano, M. L., Adams, M., Shen, D., Thoeng, A., Tsintzas, E., Maeland, M., Isaacs, A. M., Sierralta, J. and Niccoli, T. (2023) 'A monocarboxylate transporter rescues frontotemporal dementia and Alzheimer's disease models', *PLOS Genetics,* 19(9), pp. e1010893.

Yang, D., Abdallah, A., Li, Z., Lu, Y., Almeida, S. and Gao, F.-B. (2015) 'FTD/ALS-associated poly(GR) protein impairs the Notch pathway and is

recruited by poly(GA) into cytoplasmic inclusions', *Acta Neuropathologica,* 130(4), pp. 525-535.

Yang, Y., Wei, M. and Chen, L. (2022) 'Structural identification of riluzole-binding site on human TRPC5', *Cell Discovery,* 8(1), pp. 67.

Yoo, K.-S., Lee, K., Oh, J.-Y., Lee, H., Park, H., Park, Y. S. and Kim, H. K. (2019) 'Postsynaptic density protein 95 (PSD-95) is transported by KIF5 to dendritic regions', *Molecular Brain,* 12(1), pp. 97.

Young, J. J., Lavakumar, M., Tampi, D., Balachandran, S. and Tampi, R. R. (2017) 'Frontotemporal dementia: latest evidence and clinical implications', *Therapeutic Advances in Psychopharmacology,* 8(1), pp. 33-48.

Yuva-Aydemir, Y., Almeida, S. and Gao, F.-B. (2018) 'Insights into C9ORF72-Related ALS/FTD from Drosophila and iPSC Models', *Trends in Neurosciences,* 41(7), pp. 457-469.

Yuva-Aydemir, Y., Almeida, S., Krishnan, G., Gendron, T. F. and Gao, F.-B. (2019) 'Transcription elongation factor AFF2/FMR2 regulates expression of expanded GGGGCC repeat-containing C9ORF72 allele in ALS/FTD', *Nature Communications,* 10(1), pp. 5466.

Zhang, H., SuN, S., Wu, L., Pchitskaya, E., Zakharova, O., Tacer, K. and Bezprozvanny, I. (2016a) 'Store-Operated Calcium Channel Complex in Postsynaptic Spines: A New Therapeutic Target for Alzheimer's Disease Treatment', *The Journal of Neuroscience,* 36(47), pp. 11837.

Zhang, K., Donnelly, C. J., Haeusler, A. R., Grima, J. C., Machamer, J. B., Steinwald, P., Daley, E. L., Miller, S. J., Cunningham, K. M., Vidensky, S., Gupta, S., Thomas, M. A., Hong, I., Chiu, S.-L., Huganir, R. L., Ostrow, L. W., Matunis, M. J., Wang, J., Sattler, R., Lloyd, T. E. and Rothstein, J. D. (2015a) 'The C9orf72 repeat expansion disrupts nucleocytoplasmic transport', *Nature,* 525(7567), pp. 56-61.

Zhang, L., Dai, F., Cui, L., Jing, H., Fan, P., Tan, X., Guo, Y. and Zhou, G. (2015b) 'Novel role for TRPC4 in regulation of macroautophagy by a small molecule in vascular endothelial cells', *Biochimica et Biophysica Acta (BBA) - Molecular Cell Research,* 1853(2), pp. 377-387.

Zhang, Y., Chen, J., Qiu, J., Li, Y., Wang, J. and Jiao, J. (2016b) 'Intakes of fish and polyunsaturated fatty acids and mild-to-severe cognitive impairment risks: a dose-response meta-analysis of 21 cohort studies123', *The American Journal of Clinical Nutrition,* 103(2), pp. 330-340.

Zhang, Y., Yuan, Y., Liang, P., Guo, X., Ying, Y., Shu, X.-S., Gao, M., Jr. and Cheng, Y. (2017) 'OSR1 is a novel epigenetic silenced tumor suppressor regulating invasion and proliferation in renal cell carcinoma', *Oncotarget,* 8(18), pp. 30008-30018.

Zhang, Y.-J., Guo, L., Gonzales, P. K., Gendron, T. F., Wu, Y., Jansen-West, K., O'Raw, A. D., Pickles, S. R., Prudencio, M., Carlomagno, Y., Gachechiladze, M. A., Ludwig, C., Tian, R., Chew, J., DeTure, M., Lin, W.-L., Tong, J., Daughrity, L. M., Yue, M., Song, Y., Andersen, J. W., Castanedes-Casey, M., Kurti, A., Datta, A., Antognetti, G., McCampbell, A., Rademakers, R., Oskarsson, B., Dickson, D. W., Kampmann, M., Ward, M. E., Fryer, J. D., Link, C. D., Shorter, J. and Petrucelli, L. (2019) 'Heterochromatin anomalies and double-stranded RNA accumulation underlie C9orf72 poly(PR) toxicity', *Science,* 363(6428), pp. eaav2606.

Zhou, J., Du, W., Zhou, K., Tai, Y., Yao, H., Jia, Y., Ding, Y. and Wang, Y. (2008) 'Critical role of TRPC6 channels in the formation of excitatory synapses', *Nature Neuroscience,* 11(7), pp. 741-743.

Zhou, Z., Ryan, J., Tonkin, A. M., Zoungas, S., Lacaze, P., Wolfe, R., Orchard, S. G., Murray, A. M., Mcneil, J. J., Yu, C., Watts, G. F., Hussain, S. M., Beilin, L. J., Ernst, M., Stocks, N., Woods, R. L., Zhu, C., Reid, C., Shah, R. C., Chong, T. T., Sood, A., Sheets, K. M. and Nelson, M. (2023) 'Association Between

Triglycerides and Risk of Dementia in Community-Dwelling Older Adults: A Prospective Cohort Study', *Neurology*, pp. 10.1212/WNL.0000000000207923.

Zhu, Q., Jiang, J., Gendron, T. F., McAlonis-Downes, M., Jiang, L., Taylor, A., Diaz Garcia, S., Ghosh Dastidar, S., Rodriguez, M. J., King, P., Zhang, Y., La Spada, A. R., Xu, H., Petrucelli, L., Ravits, J., Da Cruz, S., Lagier-Tourenne, C. and Cleveland, D. W. (2020) 'Reduced C9ORF72 function exacerbates gain of toxicity from ALS/FTD-causing repeat expansion in C9orf72', *Nature Neuroscience,* 23(5), pp. 615-624.

Zhu, Y., Gao, M., Zhou, T., Xie, M., Mao, A., Feng, L., Yao, X., Wong, W. T. and Ma, X. (2019) 'The TRPC5 channel regulates angiogenesis and promotes recovery from ischemic injury in mice', *Journal of Biological Chemistry,* 294(1), pp. 28-37.

Zu, T., Gibbens, B., Doty, N. S., Gomes-Pereira, M., Huguet, A., Stone, M. D., Margolis, J., Peterson, M., Markowski, T. W., Ingram, M. A. C., Nan, Z., Forster, C., Low, W. C., Schoser, B., Somia, N. V., Clark, H. B., Schmechel, S., Bitterman, P. B., Gourdon, G., Swanson, M. S., Moseley, M. and Ranum, L. P. W. (2011) 'Non-ATG–initiated translation directed by microsatellite expansions', *Proceedings of the National Academy of Sciences,* 108(1), pp. 260-265.

Zu, T., Liu, Y., Bañez-Coronel, M., Reid, T., Pletnikova, O., Lewis, J., Miller, T. M., Harms, M. B., Falchook, A. E., Subramony, S. H., Ostrow, L. W., Rothstein, J. D., Troncoso, J. C. and Ranum, L. P. W. (2013) 'RAN proteins and RNA foci from antisense transcripts in C9ORF72 ALS and frontotemporal dementia', *Proceedings of the National Academy of Sciences,* 110(51), pp. E4968-E4977.